Surface Temperature Pattern Characterization and Analysis: An Investigation of Urban Effects on Surface Warming

XUE, Yucai

A Thesis Submitted in Partial Fulfillment

of the Requirements for the Degree of

Doctor of Philosophy

in

Geography and Resource Management

September 2008

Committee Members Approved:

Prof. LIN Hui, Chairmen

Prof. SHI Wenzhong

Prof. CHEN Yongqin

Prof. FUNG Tung, Supervisor

Prof. TSOU Jinyeu, Co-supervisor

ABSTRACT

of thesis entitled:

Surface Temperature Pattern Characterization and Analysis: An Investigation of Urban Effects on Surface Warming

Submitted by XUE, Yucai
for the degree of Doctor of Philosophy
at The Chinese University of Hong Kong
in September 2008

During the process of worldwide urbanization along with high rise and high density housing development in large cities, urban warming has received growing concern among many environmental issues related to urban landscape change. Due to the complicated interplay between urban environment and local climate, it is far from certain about the urban effects on local warming. In this literature, a systematic monitoring and analysis of the spatial dependency and heterogeneity of urban thermal landscape at city scale remains inadequate. The goal of this doctoral research is to develop a research framework incorporating geospatial statistics, thermal infrared remote sensing and landscape ecology to study the urban effect on local surface thermal landscape regarding both the pattern and process.

Located in a subtropical region, Hong Kong's development with high rise and high density housing made it a suitable site for studying urban effect on local warming. This research chose Hong Kong as the case study which hopes to enrich our knowledge regarding urban local thermal performance and add to our understanding of urban microclimate in hot-humid weather area.

Contrasting the day-night variation in thermal landscape, the higher local variation and irregularity on urban surface temperature pattern during daytime was observed and identified by landscape metrics compared with those of nighttime pattern. The diversity and fragmentation metrics had revealed the influence of urban development on the overall urban landscape pattern. Along with urban development, daytime

pattern of urban thermal landscape presented more fragmentation, less diversity and uneven texture distribution within daytime observations.

In summary, global regression analysis confirmed the relationship between environmental factors and surface temperature and gave a general overview of urban effect on local surface warming. The distinctive mechanism of dominating day-night surface warming was uncovered by regression analysis. Vegetation played the most important role which could be referred as surface cooling in average to local surface temperature variation as compared with other measures of local environment during both daytime and nighttime. Besides the dominant role of local solar radiation on surface warming, building square footage demonstrated the second important influence on local surface temperature elevation during daytime. During nighttime, population density played a dominant role on nighttime surface warming among different parameters, with the second important contribution of nighttime surface warming coming from road density. While elevation and distance from coast demonstrated obvious cooling effect on surface temperature within most nighttime models.

GWR analysis offered an in-depth investigation of local effect on surface temperature variation which had been proven to be spatially varying and influenced by local weather condition with local environmental setting quantified with the referred site specific environmental factors. The local dominant factor accounted for most to the site specific surface temperature variation which varied significantly in space and time and prevented a general delineation of the relative association among environmental factors to surface temperature disparities. The effective adaptive measures could be devised locally with reference to day-night needs in the identification of this feature.

摘　要

伴隨著全球城市化進程的進一步加強，尤其是大中城市趨於高密度高空發展，地表面從自然下墊面綠地、水面等到混凝土、柏油路面及各種建築牆面爲主的人工構築物的轉換使得表面熱力屬性發生了很大改變，城市熱環境逐步惡化特別是城市熱島現象更爲突出。由於城市環境與區域氣候的相互作用關係複雜，城市環境對於區域變暖的影響與作用有待進一步研究，尤其是從時空變化的角度集合城市表面與結構量化從城市尺度去系統研究城市熱力景觀的空間異質與依賴。本文研究的主要目的就是集合热红外遥感，景觀生態學以及地理空間統計分析方法系統研究分析城市環境對於區域表面升溫的影響。

香港的亞熱帶氣候及其城市空間的高密度高空發展，爲研究城市環境對於城市變暖的影響和作用提供很好的參考。其景觀指數分析結果表明就日夜變化來說，相對於夜間分佈模式日間地表溫度分佈的區域變化和不規則性明顯加劇。同時景觀多樣性和破碎度指數表明隨著城市發展，對比日間表面溫度分佈指數在對應時間序列上的變化，城市日間熱力景觀呈現進一步破碎化，多樣性逐步減小及紋理分佈越發不規則的趨勢。

線性回歸分析證實了以有關環境參數量化表示的城市區域環境和表面溫度差異存在相關聯繫，同時對於研究城市環境對於城市表面溫度變化的作用影響提供了一個總體量化評估。並進一步揭示出相關環境參數影響日夜表面溫度變化的不同機制。該分析表明相對於其他環境參數植被是控制日夜區域表面溫度變化的一個最重要的參數。除了太陽輻射，表面建築覆蓋率對於日間表面升溫的作用位居第二。人口密度被認爲是夜間表面升溫的最重要因素，道路密度的作用次之。大部分夜間模型分析表明海拔高度以及近海距離的夜間降溫作用比

較明顯。

地理加權回歸分析爲進一步研究區域環境對於實地表面溫度變化的影響作用提供了參考依據，該分析表明用相關參數表徵量化的區域環境對於實地表面溫度變化的作用在空間上是變化的，隨著區域氣候條件的不同具有空間不平穩性。這種變化體現在對於研究區內定位不同的地理空間，主導實地表面溫度變化的環境參數時空變化明顯，這也對於統一探討各種環境因素對於城市表面升溫及溫度分佈不均的相對作用造成了困難。同時也說明有關適應與應對城市變暖的措施應該針對日夜需要是具有區域有效性的。

TABLE OF CONTENTS

ABSTRACT I

TABLE OF CONTENTS V

LIST OF TABLES VII

LIST OF FIGURES VIII

ABBREVIATIONS XI

ACKNOWLEDGEMENT XII

CHAPTER 1: INTRODUCTION 1

1.1. BACKGROUND 1

1.1.1. Urban Warming *1*

1.1.2. Urban Sprawl *4*

1.2. RESEARCH QUESTIONS 6

1.3. RESEARCH SCOPE AND OBJECTIVES 8

1.4. THESIS STRUCTURE 10

CHAPTER 2: URBAN THERMAL ENVIRONMENT 11

2.1. THE COMPLEXITY OF URBAN THERMAL ENVIRONMENT 11

2.1.1. Urban Heat Islands (UHIs) *12*

2.1.2. The Heterogeneity of Spatial Pattern *14*

2.1.3. Intensive Variation of Temporal Pattern *17*

2.1.4. The Impacts of UHI *21*

2.2. UHI STUDIES 22

2.3. BASIC THEORY OF THERMAL REMOTE SENSING 29

2.3.1. The Physics of Radiation *29*

2.3.2. Land Surface Temperature (LST) Algorithms *30*

2.3.3. Advantages and Limitations of Thermal Infrared Remote Sensing *33*

2.4. GEOGRAPHICALLY WEIGHTED REGRESSION (GWR) 36

2.5. SUMMARY 40

CHAPTER 3: METHODOLOGY AND DATA 41

3.1. INTRODUCTION 41

3.2. STUDY AREA AND DATA SOURCE 44

3.3. RESEARCH ASSUMPTIONS 57

3.4. FRAMEWORK OF THE RESEARCH 65

3.5. URBAN THERMAL LANDSCAPE CHARACTERIZATION AND ANALYSIS 70

3.5.1. Landscape Metrics *70*

3.5.2. Regression Analysis *74*

3.6. SUMMARY 78

CHAPTER 4: DATA PREPARATION **80**

4.1. IMAGE PRE-PROCESSING 80
4.2. EXPLANATORY VARIABLES 82
4.3. SUMMARY 90

CHAPTER 5: RESULTS AND DISCUSSIONS **91**

5.1. INTRODUCTION 91
5.2. URBAN THERMAL LANDSCAPE CHARACTERIZATION 92
5.2.1. Spatial-Temporal Variation *92*
5.2.2. Landscape Metrics *101*
5.3. EXPLANATORY ANALYSIS 105
5.3.1. Global Analysis *106*
5.3.2. Urban and Rural Pattern *113*
5.4. GEOGRAPHICALLY WEIGHTED REGRESSION 118
5.5. SUMMARY 133

CHAPTER 6: CONCLUSIONS **148**

6.1. SUMMARY 148
6.2. IMPLICATIONS 151
6.3. LIMITATIONS AND FUTURE WORK 153

APPENDIX 1: RESIDUAL ERROR REPORT OF ORTHO-RECTIFICATION OF ASTER IMAGES 157

APPENDIX 2: MAPS OF URBAN ENVIRONMENTAL VARIABLES 169

APPENDIX 3: STATISTICAL DESCRIPTIONS OF LOCAL SURFACE TEMPERATURE VARIATION ALONG WITH LAND USE LAND COVER 176

APPENDIX 4A: COLLINEARITY DIAGNOSTICS OF THE VARIABLES 178

APPENDIX 4B: STATISTICAL DESCRIPTIONS OF THE VARIABLES 182

APPENDIX 5: LOCATION OF 276 URBAN AND RURAL SAMPLE POINTS 187

APPENDIX 6: COEFFICIENTS DISTRIBUTION OF ENVIRONMENTAL VARIABLES 188

REFERENCES 201

LIST OF TABLES

Table 2.1 Impacts of UHIs classified by climate region 21
Table 2.2 Global v.s. local statistics 37
Table 3.1 Summary of climate change in HKSAR 41
Table 3.2 The reported dominant land use classification (%) in 2003 and 2006 46
Table 3.3 Spectral and spatial characteristics of the ASTER Bands 46
Table 3.4 Descriptive statistics of surface temperature for the images used in this research 48
Table 3. 5 Meteorological background for urban thermal landscape study 50
Table 3.6 Landscape pattern metrics used in analysis 72
Table 4.1 Overall RMS errors of ortho-rectification 81
Table 4.2 Variables list for regression analysis 82
Table 4.3 List of solar angle information 83
Table 4.4 ASTER unit conversion coefficients (watts/meter2/steradian/micrometer) /DN 85
Table 4.5 List of parameters information for diffuse radiation calculation 88
Table 5.1 Land use classification Scheme 93
Table 5.2 Landscape metrics indices during the study period 104
Table 5.3 Variables list for regression modelling 107
Table 5.4 Parameter coefficient estimation and the model evaluation for global linear regression analysis 112
Table 5.5 Discrepancy of global linear regression model between urban and rural .117
Table 5.6 Geographically weighted regression diagnosis 120
Table 5.7 Statistical descriptions of CC value of 1070 sample points 122

LIST OF FIGURES

Figure 2.1 Three main types of Urban Heat Islands (UHIs). 13
Figure 2.2 Urban heat island characteristics 15
Figure 2.3 Typical temporal variation of urban and rural air temperature (thin lines), and heat island magnitude (thick line) under clear skies and weak airflow, which is produced by the cooling rates and vary depending on the climate region and season 18
Figure 2.4 Measurement approaches of various types of UHI 23
Figure 2.5 Process of UHI at micro-scale 24
Figure 2.6 Relationship between AVHRR channels 4 and 5 (dashed lines) and the atmospheric window in the thermal infrared part of the spectrum (solid line)... 29
Figure 2.7 Basic design of TES algorithm 32
Figure 2.8 Conceptual diagram of the urban surface and biases in the surface viewed by nadir and off-nadir remote sensors. The 'complete' surface (a) is the full urban-atmosphere interface; remote sensors viewing from (b) nadir, and (C) off-nadir viewing directions see only a subset of the complete surface. With inclusion of shading effects (d) off-nadir views from different directions view different amount of sunlit and shaded surfaces 34
Figure 3.1 Study area with weather stations 45
Figure 3.2 ASTER spectrum bandwidth comparison with Landsat ETM+ 46
Figure 3.3 Land surface temperature image during nighttime 10.28.2003 51
Figure 3.4 Land surface temperature image during daytime 11.03.2003 51
Figure 3.5 Land surface temperature image during nighttime 10.05.2004 52
Figure 3.6 Land surface temperature image during daytime 11.21.2004 52
Figure 3.7 Land surface temperature image during nighttime 10.01.2005 53
Figure 3.8 Land surface temperature image during daytime 10.23.2005 53
Figure 3.9 Land surface temperature image during daytime 04.17.2006 54
Figure 3.10 VNIR image in 11.03.2003 55

Figure 3.11 VNIR image in 11.21.2004 55
Figure 3.12 VNIR image in 10.23.2005 56
Figure 3.13 VNIR image in 04.17.2006 56
Figure 3.14 Factors affecting Urban Heat Islands (UHIs) 59
Figure 3.15 Proposed research framework 68
Figure 3.16 Conceptual design of thermal landscape correlation analysis 69
Figure 5.1 Land use map of study area in Hong Kong 92
Figure 5.2 Diurnal and seasonal variations of surface temperature along with land use 96
Figure 5.3 Nighttime surface temperature categorization based on land use in 10/28/2003 96
Figure 5.4 Daytime surface temperature categorization based on land use in 11/03/2003 97
Figure 5.5 Daytime surface temperature categorization based on land use in 04/17/2006 97
Figure 5.6 Local variations of nighttime surface temperature in 10/28/2003 99
Figure 5.7 Local variations of daytime surface temperature in 11/03/2003 99
Figure 5.8 Local variations of daytime surface temperature in 04/17/2006 100
Figure 5.9 Local variations of surface temperature within each land use category. 100
Figure 5.10 Strategically located sample points over study area 106
Figure 5.11 Coefficients contribution of Intercept in nighttime model 10/28/03 135
Figure 5.12 Coefficients contribution of Intercept in daytime model 11/03/03 135
Figure 5.13 Coefficients contribution of Intercept in daytime model 04/17/06 136
Figure 5.14 Coefficients contribution for Solar Radiation in daytime model 11/03/03 136
Figure 5.15 Coefficients contribution of Vegetation NDVI in nighttime model 10/28/03 137
Figure 5.16 Coefficients contribution of Vegetation NDVI in daytime model 11/03/03 137
Figure 5.17 Coefficients contribution of Vegetation NDVI in daytime model

04/17/06 138
Figure 5.18 Coefficients contribution of Road Density in daytime model 11/03/03138
Figure 5.19 Coefficients contribution of Population Density in nighttime model 10/28/03 139
Figure 5.20 Coefficients contribution of Population Density in daytime model 11/03/03 139
Figure 5.21 Coefficients contribution of Population Density in daytime model 04/17/06 140
Figure 5.22 Coefficients contribution of Distance from coast in nighttime model 10/28/03 140
Figure 5.23 Coefficients contribution of Distance from coast in daytime model 11/03/03 141
Figure 5.24 Coefficients contribution of Distance from coast in daytime model 04/17/06 141
Figure 5.25 Coefficients contribution of Building footsq_a in daytime model 11/03/03 142
Figure 5.26 Coefficients contribution of Building footsq_a of daytime in model 04/17/06 142
Figure 5.27 Coefficients contribution of Elevation in nighttime model 10/28/03... 143
Figure 5.28 Coefficients contribution of Elevation in daytime model 11/03/03 143
Figure 5.29 Coefficients contribution of Elevation in daytime model 04/17/06 144
Figure 5.30 Coefficients contribution of Site Openness in nighttime model 10/28/03 144
Figure 5.31 Coefficients contribution of Site Openness in daytime model 11/03/03 145
Figure 5.32 Coefficients contribution of Site Openness in daytime model 04/17/06 145
Figure 5.33 Local dominant factor to LST variation in nighttime model 10/28/03 146
Figure 5.34 Local dominant factor to LST variation in daytime model 11/03/03... 146
Figure 5.35 Local dominant factor to LST variation in daytime model 04/17/06... 147

ABBREVIATIONS

UHI:	Urban Heat Island
IPCC:	The Intergovernmental Panel on Climate Change
GHG:	Greenhouse Gases
PLEA:	Passive and Low Energy Architecture
GWR:	Geographically Weighted Regression
LST:	Land Surface Temperature
CLHI:	Canopy Layer Heat Island
BLHI:	Boundary Layer Heat Island
SHI:	Surface Heat Island
UCL:	Urban Canopy Layer
TES:	Temperature Emissivity Separation
ASTER:	Advanced Spaceborne Thermal Emission and Reflection Radiometer
VNIR:	Visible and Near Infrared
SWIR:	Short Wave Infrared
TIR:	Thermal Infrared
NP:	Number of Patches
AREA_MN:	Mean Patch Area
LPI:	Largest Patch Index
LSI:	Landscape Shape Index
MSIDI:	Modified Simpson's Diversity Index
FRAC_AM:	Area-weighted Mean Fractal Dimension Index
IJI:	Interspersion & Juxtaposition Index
AIC:	Akaike Information Criterion
GCPs:	Ground Control Points
NDVI:	Normalized Difference Vegetation Index
CI:	Condition Indices
OLS:	Ordinary Least Squares
CC:	Component Contribution

ACKNOWLEDGEMENT

I owe gratitude to many people whose accompany, support and assistance was indispensable during the whole study period. First among them are my supervisors, Professor FUNG Tung and Professor TSOU Jinyeu, who have given me invaluable guidance, insightful comments and advice, and unfailing support during this research endeavor. I will always be grateful for their support and guidance. I am obliged to Prof. FUNG Tung, who had contributed a lot of efforts and time for proofreading and revising my thesis, which is especially valuable to me. I would like to express my heartfelt gratitude to him for showing me the way of doing research and scientific writing which is not only crucial to the completion of this research but also to my career in the future.

My sincere thanks also go to, Prof. LIN Hui, Prof. CHEN Yongqin, and Prof. LEUNG Yee, Prof. ZHANG Li, Prof. SHEN Jianfa at the department, studying and working with them is a pleasure experience, their comment, concern and encouragement about my study is valuable to me. I would also like to thank the members of my PhD committee who took efforts in reading and providing me with valuable comments of this thesis. Special thanks to Dr. YANG Limin, for his friendly assistance and inspiring opinions sharing with me during the very beginning stages of this research, which was definitely encouraging to a PhD beginner.

I am also grateful to my friends and colleagues in CUHK during the past years of my study. I also want to thank, ZHANG Yongjun, Li Wenjing, WONG Kwankit Frankie, and He Jie for their technical assistance and invaluable discussion; SHI jingjing, SANG Huiyong, JIANG Yihong, YANG Ping, WANG Dan, LUO Xiaolong, and LI Xiang, ZHAO Yibin, ZHENG Hailong, LIU Jianbo from the Department of GRM; MEI Qing, ZHANG Hui, XIONG Yan and REN Chao from the Department of Architecture for their cheerful encouragements and valuable discussions.

My gratitude also extends to my previous advisors from my graduate studies at WUHAN University, Professor ZHANG Zuxun and ZhANG Jianqing, for your continued support and for setting such fine examples of developing research expertise.

Finally, I would like to thank my families who have contributed the most to my life, in particular my parents, my husband and my brother for their endless encouragement, sacrifice, and patience.

CHAPTER 1: INTRODUCTION

1.1. Background

1.1.1. Urban Warming

During the process of urbanization world wide, corresponding to this alteration process from vegetated area to impervious concrete artificial surface, its effect on urban environment turns out to be one big problem during this process and appeals to a lot of concerns. Apart from the change on surface material, as a result of urban geometry together with high rise and high density housing development, the urban "roughness" has increased, which leads to a reduction of about 25% in wind speeds, and a lesser albedo of urban surfaces (Landsberg, 1970). Craig and Lowry's model (1972) found that the trapping of insolation by tall buildings may cause an average daily decrease in albedo of 20%. The resultant modification on urban thermal environment is the increased thermal anomalies, which is widely observed and termed urban heat island. The urban rural temperature difference has been recognized and has even been detected in cities with populations less than 10,000 (Karl et al., 1988), which usually refers to urban heat island.

Urbanization favors the development of urban warming which has been observed through long term climatic records (Karl et al., 1988) and thermal infrared remote sensing (Rao, 1972; Roth et al., 1989). Urban warming is a manifestation of the direct and indirect alteration of the energy budget in the urban boundary layer (Hinkel et al., 2003). At the global scale, Jones et al. (1990) concluded that the global urban warming bias is between 0.01 C° and 0.10 C°. If the high-end estimate is correct, the UHI bias represents nearly 25 percent of the global warming of the past century (Balling, 1992). Among the impacts of urbanization on local environment, urban warming still remains an area where further research is needed to study the impacts and causality of its formation. "The impacts of urban warming events where local

weather patterns are affected are over and above the urban warming itself, which has energy, comfort and livability affects besides serious health impositions on urban populations" (Samuels, p.1).

Apart from urban surface and geometry, the study of Bornstein (1968) also confirmed the contribution of elevated layers of smoke, water vapor, carbon dioxide and sulfur dioxide to the development of nocturnal heat islands. In a global environment background, recently released The Intergovernmental Panel on Climate Change (IPCC) Fourth Assessment Report (2007a) concludes that "warming of the climate system is unequivocal". And "most of the observed increase in globally averaged temperatures since the mid-20th century is very likely due to the observed increase in anthropogenic greenhouse gas concentrations" (IPCC, 2007a, p.10). According to the report (2007b), "the largest growth in global GHG (Greenhouse Gases) emissions between 1970 and 2004 has come from the energy supply sector (an increase of 145%). The growth in direct emissions in this period from transport was 120%, industry 65% and land use, land use change, and forestry (LULUCF) 40%. Between 1970 and 1990 direct emissions from agriculture grew by 27% and from buildings by 26%, and the latter remained at approximately at 1990 levels thereafter. However, the buildings sector has a high level of electricity use and hence the total of direct and indirect emissions in this sector is much higher (75%) than direct emissions" (IPCC, 2007b, p.3~4).

This phenomenon has been observed in Hong Kong SAR, as well as in China. According to the Hong Kong Observatory (2004) report of Technical Note No.107, "the analysis of temperature records shows that Hong Kong has been warming up during the past 118 years, in line with the global warming trend. This is also consistent with the warming trend in China mainland in the past 50 years. In the period 1989 to 2002, the rural areas of Hong Kong have been warming up at a rate of about 0.2℃ per decade. At the Hong Kong Observatory Headquarters in the heart of urban Hong Kong, the corresponding rise was about 0.6℃ per decade. The

difference of 0.4℃ per decade between temperatures in urban and rural areas may be attributed to the effects of high density urban development" (Hong Kong Observatory, 2004).

Since urban buildings play a dominant role on urban warming in direct and indirect way and account for a large single fraction of energy use. Regarding the mitigation strategies from building sector through urban planning and design, in the literature many researches have been carried out by Passive and Low Energy Architecture (PLEA) from architecture community to study how to effectively mitigate the effect of urban warming. However, urban building thermal performance is confined with local climate and the impacts of urban warming is magnified with high rise high density urban buildings as well. This complicated interactive correlation between urban building and local climate limits and obscures the effect of these thermal efficiency and mitigation strategies. Currently only scant knowledge on environmental performance of the different land uses is available (Pauleit and Duhume, 2000). An assessment of the local thermal response to the urban surface and geometry impact has not been fully addressed with the estimates based on urban rural comparison (e.g. UHI) which may vary with the method of classifying urban and rural areas (Lim et al., 2005). The IPCC Fourth Assessment Report (2007b, p.35) also pointed out, "there are still relevant gaps in currently available knowledge regarding some aspects of mitigation of climate change. Additional research addressing those gaps would further reduce uncertainties and thus facilitate decision-making related to mitigation of climate change".

From the perspective of urban planning and design for urban warming effects mitigation, the questions regarding in which way and how much efficient use of land can contribute to enhance urban living as well as mitigate urban warming remain central issues related to the functionality of urban planning and design in the mitigation efforts. Before going further into this, the characteristics of urban thermal performance in spatial and temporal dimension are essential and must be examined

in depth. And how the relationship between local environmental factors and thermal performance would vary across space and time still need further investigation. The knowledge regarding the urban effects on local warming is limited in the literature and is fundamental for bridging the application gap of transferring urban thermal environment knowledge into urban planning and design application through passive cooling urban planning and design application. A systematic investigation of urban thermal landscape characteristics and local effects on urban surface warming is necessary for the input and in pursuit of the understanding of urban thermal process.

1.1.2. Urban Sprawl

Rapid urbanization which is transforming natural vegetation to man-made heat absorbing surfaces is taking place on a global scale. In 1950 approximately 30% of the world population lived in urban areas and, by 2030 almost 60% will live in urban areas (Golden, 2005). Global urbanization is the inevitable trend in the world, the metabolism of urban activities, however, has become a threat to global environment (Pauleit and Duhume, 2000). During this global process of urbanization, how to balance the urban population growth and urban environment sustainable development is an urgent issue. How to accommodate the vast amount of people surging into the city with the minimized adverse impacts on local, regional even global environment remains one tough challenge for the decision makers. During the procedure of urban sprawl, informed and scientific acknowledge is crucial to form and speculate effective strategies in order to alleviate the stress that urban development brought to environment.

It is well recognized that urbanization has a strong influence on the diurnal temperature range (Easterling et al., 1997). Urban form including urban surface and geometry has direct impact on urban warming, with urban change of thermal properties in terms of urban roughness, radioactive, conductivity and heat capacity, and evapotranspiration efficiency etc. The urban landscape forms the urban canopy layer, its properties directly determine the urban thermal behavior through urban

canopy layer. On the other hand, since urban buildings contribute a great portion in GHG (Greenhouse Gases) emission and thus could play a crucial role in this mitigation progress, regarding urban thermal environment management there something must be done to efficiently reduce the GHG emission from passive urban cooling by reducing the usage of electricity consumed in urban living. The urban landscape can be designed and managed in the practices of urban planning. Under the same spatial capacity, different layout plans may present thermal behavior diversely. "The mechanisms that drive urban warming are regional in scale and highly sensitive to the total area occupied by the city and its suburbs. The intensification of these changes and their ultimate harm to the environment can be significantly reduced through informed and efficient uses of land" (Stone and Rodgers, 2001). To this end, efficient planning and design within urban space can be taken as one potential solution to reduce the negative effect of urbanization on urban microclimate.

It has been proved and well documented that urban land use and land cover has a direct effect on urban thermal environment (Eliasson and Svensson, 2003), from this aspect the urban thermal environment can be enhanced through efficient use of land and informed management. Moreover the electricity for urban living can be greatly reduced through improving urban outdoor thermal environment in order to reduce GHG emissions for urban living. The subsequent effect it achieves would include not only enhancing urban living but also sustaining urban as far as global environment.

Focusing on urban thermal environment, most of work on sustainable landscape design is demonstrated showing the potential thermal performance efficiency and benefit for urban environment improvement (Steemers, 2003). In this context, to study the relationship between the urban form and urban thermal pattern has significant meaning for these endeavors. Urban thermal landscape monitoring and analysis may add to our understanding of the complex of urban thermal environment with primary knowledge regarding the thermal performance of urban surface.

1.2. Research Questions

Transferring ecological knowledge into urban planning and design is widely accepted to achieve environment sustainability. Before doing this, the first step is to critically examine the urban environment in a holistic way. Regarding urban thermal environment study, "quantitative information on the types and distribution of urban thermal environment can be of value in the design of cities, in engineering urban hydrologic systems, in planning for the efficient removal of air pollutants, and in assuring the success of studies of inadvertent weather modification by urbanization" (Morgan et al., 1977, p.55). Urban warming is sensitive to the nature (thermal properties, including albedo, water content, heat capacity and thermal conductivity) and the placement (surface geometry or urban topography) of urban surface.

How the land use and land cover affect the urban thermal landscape; in which way the urban was formed can improve the urban thermal environment as well as accommodating the same amount of population; Is there any methodology that can be drawn to carry out monitoring and analysis of the urban thermal landscape; whether the knowledge obtained through these analysis can be of practical use for urban planning and design. The informed knowledge about the characteristics of urban thermal landscape in spatial and temporal dimension and urban effects of local warming is pivotal in the practice of passive cooling urban planning and design and urban thermal environment sustainability. This made the characterization and analysis of the spatial heterogeneity and dependence of urban thermal landscape necessary and essential for advancing our knowledge of urban thermal environment.

In this literature, a systematic monitoring and analysis of the spatial dependency and heterogeneity of urban thermal landscape at city scale remains inadequate due to: 1) the climate observation recording in isolated observation stations in coarse grid or with incomplete cover comparing with highly varying urban surface and topography, made it difficult to systematically investigate correlations between local thermal abnormalities and local environmental setting at micro-scale. 2) Limited attention has

been paid to the differentiation of local influence of urban settings on local warming, as well as local surface warming combining urban surface and urban geometry measures whilst local surface thermal disparities are highly sensitive to the local landscape composition and configuration. 3) The effort to develop a systematic methodology for urban thermal landscape monitoring and analysis aiming at delimitation of local effects on urban surface warming is inadequate at city scale.

With the advancement of remote sensing techniques with high spatial and spectral resolution, urban applications of thermal infrared remote sensing are possible, which provide a platform for the in-depth study of urban thermal landscape based on the continued surface of satellite derived surface temperatures. It presents a potential opportunity for urban thermal landscape characterization and analysis from the distribution of satellite derived surface temperatures. At the same time it enables the correlations to be established with local environmental factors for studying urban effects on local surface thermal abnormalities. Combining with geosciences and geospatial statistics, a systematic investigation of urban effect on local thermal landscape can be implemented through monitoring and analyzing the urban surface temperature pattern in detail based on thermal infrared remote sensing. This thesis tries to figure out environmental indicators and their influences on urban thermal disparities based on a systematic investigation framework, during which Hong Kong is chosen as the case study. Hong Kong is a highly developed city in Asia, the high rise and high density housing development due to scarce land suitable for urban development made urban environment especially urban thermal environment critical for urban settlement under a sub-tropical climate. The highly varied urban surface and geometry along with a hilly topography magnify the local effect of urban environmental setting on urban thermal abnormalities which made the heterogeneity of urban thermal landscape in spatial-temporal dimension. The systematic investigation of urban thermal landscape in Hong Kong may help enrich our understanding of local effects on urban surface warming.

1.3. Research Scope and Objectives

In the subtropical city with high-rise building development, Hong Kong, nearly 60% of electrical energy use is for space conditioning during summer months (Giridharan et al., 2004). Climate control is of paramount importance to reduce negative effect brought by urban warming. In the literature the spatial dependence and heterogeneity of urban thermal landscape is widely observed based on thermal infrared remote sensing within the urban environment. Urban surface warming is conceived as a big contribution to urban warming, the study of urban surface warming possesses significant meaning for probing into the problem of urban warming. Moreover the importance of urban thermal performance can be acknowledged in a wider context of urban landscape as one component towards sustainable development.

For any mitigating measures to be effective, it is important that the underlying processes are properly understood (Sturman, 1998). It seems that the heterogeneity of the city landscape makes the complexity of urban thermal environment induced by the intensive variation in spatial and temporal dimension across the city. In doing this, environmental indicator identification is necessary based on investigating urban thermal performance relating to urban landscape pattern. "Surface temperature data of urban areas derived from satellite thermal sensors are under-utilized in planning applications because of the inability to demonstrate meaningful relationships between the satellite-derived data and urban microclimate" (Nichol, 1994). With the remote sensing technology development, high spatial and temporal resolution imagery available provides the potential to monitor and analyze the urban surface thermal landscape with more detail.

A major theme of this research is to investigate urban surface warming through the monitoring and analysis of urban thermal landscape based on thermal remote sensing. The intention is to exploit the capabilities of thermal remote sensing application on urban warming studies through obtaining information regarding surface temperature disparities which might not be accessed in other ways. In this sense, the study builds

on recent pioneering studies that attempt to apply thermal remote sensing into urban climate studies. Introducing urban thermal remote sensing to the study of urban thermal landscape provides a meeting point for the investigation of urban effect on local climate, and it also shows that urban applications of remote sensing can inform the research of urban warming. The goal of this doctoral research is to develop a research framework incorporating geospatial statistics, thermal infrared remote sensing and landscape ecology to study the urban effect on local surface thermal landscape regarding both the pattern and process. In this context, this research effort mainly contributes to achieve the objectives of this study as following:

- To develop research framework and methodology for a systematic investigation of urban thermal landscape combining with remote sensing, geospatial statistics technique and landscape ecology.

- To characterize the dynamics of urban thermal landscape across space and time at the landscape scale in order to obtain an overview of the spatial dependency and heterogeneity of urban surface warming.

- To analyze the relationship between urban form and surface temperature variation in order to clarify the local effects on surface warming.

- To reveal the possible dynamics in the local influences of environmental indicators on the variation of local surface temperature across space and time.

- To investigate and identify the environmental indicators which have more obvious influences to the increase of local surface temperature in site study of Hong Kong.

In this study the ASTER data covering part of Hong Kong area during 2003~2006 will be used to conduct the integrated investigation of urban thermal landscape based on thermal infrared remote sensing. Moreover the GIS data layers of urban infrastructure and population census data archived at the Department of Geography and Resource

Management, the Chinese University of Hong Kong (CUHK), and the local background meteorology data from Hong Kong Observatory have been collected to facilitate the validation and interpretation of this analysis.

1.4. Thesis Structure

This thesis is organized in the following way, with this chapter as the introductory chapter, and is divided into six chapters. Chapter 2 reviews the literature on urban thermal environment. The chapter begins with the discrimination of the characteristics of Urban Heat Island (UHI) with spatial and temporal heterogeneity, in particular the UHI studies based on thermal infrared remote sensing is reviewed. Then it is followed by the review of the techniques and practices of remote sensing of UHIs, with advantages and limitations of thermal infrared remote sensing discussed. The local statistical technique of Geographically Weighted Regression (GWR) is introduced for local relationship identification between local environmental setting and surface temperature elevation.

Chapter 3 elaborates the methodological framework of this study. This chapter begins with study site description and data used, and then is followed by the construction of assumption on which the subsequent analyses based. The next section discusses urban thermal landscape characterization and analysis techniques employed in the study, the landscape metrics and regression analysis is elaborated in detail.

With the data preparation of image preprocessing and environmental variables calculation is demonstrated in Chapter 4. The thermal landscape characterization and analysis based on thermal infrared remote sensing are summarized and discussed in Chapter 5. The statistical results of regression analysis are shown and deliberated in detail. This thesis ends with a concluding chapter, Chapter 6 in which the findings of the study is summarized. This is followed by the discussion on limitation of the study and recommendations on future work are provided for further studies.

CHAPTER 2: URBAN THERMAL ENVIRONMENT

This chapter provides the background and basic concepts of urban thermal environment upon which the study of urban thermal landscape is based. First, the complexity of urban thermal environment is introduced and the feature of study at different scales is addressed in detail. It helps to give a holistic review of urban thermal environment study, from which urban thermal landscape monitoring and analysis extends. It also contributes to the development of conceptual framework of this thesis study for a systematic investigation of urban effects on surface warming. In the second section current practices in Urban Heat Island (UHI) studies based on thermal infrared remote sensing are reviewed. Moreover the theoretical foundation of thermal infrared remote sensing for urban thermal environment study is illustrated, with the various algorithms of Land Surface Temperature (LST) generation reviewed. In the last part the local exploratory technique of Geographically Weighted Regression (GWR) is introduced and reviewed which can be used to investigate local effects on urban surface warming.

2.1. The Complexity of Urban Thermal Environment

During the process of urbanization, together with high rise and high density housing development, the climate has been modified, in particular the incurred change in urban thermal environment reflected by the development of urban heat islands has received growing concern corresponding to this alteration process from natural surfaces to impervious concrete man-made surface with heat absorbing materials. Among the pressures which urbanization brought to the environment, the intensification of these pressures from sensible heat flux is observed, represented by the phenomenon of urban areas becoming warmer compared with the surrounding rural areas. Urban warming is a manifestation of the direct and indirect alteration of the energy budget in the urban boundary layer (Hinkel et al., 2003). Urban micro-climate exhibits a high variability and is observed generally warmer and less

windy than rural areas, which depends on many characteristics such as topography, regional wind speed, urban morphology (Souza et al., 2004). Urban microclimate is regarded as the interactive result of regional climate and local environment, urbanization has been considered as one important factor contributing to the observed significant change of urban warming.

Urban Heat Island (UHI) effect is among the best expressions of the impact of human activity on local climate (Hinkel et al., 2003). The development of UHI is attributed to various causes (Oke, 1987): trapping of both incoming solar and outgoing long-wave radiation, reduction of turbulent heat transport due to the geometry of the street canyons, decreased evapotranspiration and increased sensible heat storage due to construction materials, building and traffic heat losses as well as air pollution leading to increased long-wave radiation from sky. Moreover, its pattern in spatial and temporal dimension is varied with the local composition and configuration of urban environmental setting. The exact extent of the UHI depends on time and space as a function of meteorological, locational and urban characteristic (Emmanuel, 1997). The intensity of UHI depends on the size, population and industrial development of the city, together with the topography, physical layout, regional climate and meteorological conditions (Oke et al., 1991). Owing to cities with highly variable physical composition and spatial configuration, together with high density population concentration and discontinuous artificial surface canopy, within which quantity of human interference activities take place, the urban thermal environment exhibits great complexity formulated with the intensive variability at micro-scale in spatial-temporal dimension.

2.1.1. Urban Heat Islands (UHIs)

According to Voogt (2004), "an urban heat island is the name given to describe the characteristic warmth of both the atmosphere and surfaces in cities (urban areas) compared to their (nonurbanized) surroundings, it is an example of unintentional climate modification when urbanization changes the characteristics of the Earth's

surface and atmosphere". The UHI is maximized under conditions of minimal cloud cover (increase solar input), low wind speeds (reduced mixing of air) and high vertical stability (thermal inversions) (Oke, 1987). A comprehensive review given by Voogt (2004) about urban heat island in the literature has differentiated UHIs studies at different scales. There are three types of heat islands in Voogt's definition: canopy layer heat island (CLHI); boundary layer heat island (BLHI); surface heat island (SHI). As shown in Figure 2.1, "The first two refer to a warming of the urban atmosphere; the last refers to the relative warmth of urban surfaces. The urban canopy layer (UCL) is the layer of air closest to the surface in cities, extending upwards to approximately the mean building height; Above the urban canopy layer lies the urban boundary layer, which may be 1 kilometer (km) or more in thickness by day, shrinking to hundreds of meters or less at night (Oke, 1995)" (Voogt, 2004).

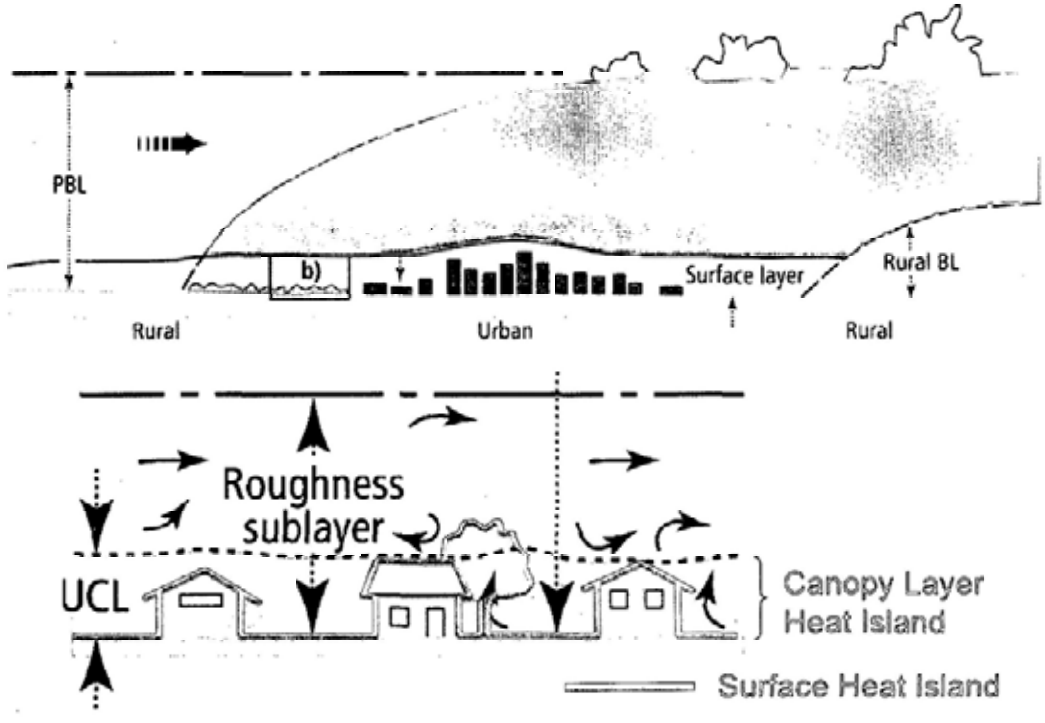

Figure 2.1 Three main types of Urban Heat Islands (UHIs).

Source: Voogt (EPA presentation, revised by Voogt after a figure in Oke, 1997)

Voogt (2004) has discriminated that the feature of urban heat island at various scale

possessed also is diversified from each other: "Heat island types vary in their spatial form (shape), temporal (related to time) characteristics, and some of the underlying physical processes contribute to their development, the boundary layer heat island shows much less variability than the other heat island types and a cross-section shows its shape resembles a simple dome or plume with warmer air transported downwind of the city". In the practices of past UHI studies, thermometers are usually used to measure air temperatures for CLHI or BLHI study, whereas the SHI is measured by thermal infrared remote sensors mounted on satellites or aircraft.

2.1.2. The Heterogeneity of Spatial Pattern

Due to urban sprawl, the urban morphology has been modified significantly from evaporative and porous continuous natural surface into concrete isolated man-made surface. This alteration has significantly changed the thermal properties of urban environment setting in terms of surface roughness, emissive and evaporative properties, and thermal inertia, moisture content, etc. The thermal behavior of urban surface resulted from this change makes the warmth of urban surface obvious and further signifies urban rural temperature difference (i.e. UHI).

The diversity of temperature distribution across city also increased correspondingly along with different land use upon urban topography. The high rise high density housing development contributes to the development of UHI through the formation of street canyon effect, which traps heat and distorts air movement. With the housing development with different height and various densities, the urban microclimate shows high heterogeneity of thermal distribution across city which is highly sensitive to local environmental setting. Besides urban rural temperature difference, the local thermal environment within urban area is varying as well under distinctive local environmental setting. For example, the air temperature of urban park with intense vegetation will be a few degrees lower than high density built-up area especially in downtown area as illustrated in Figure 2.2.

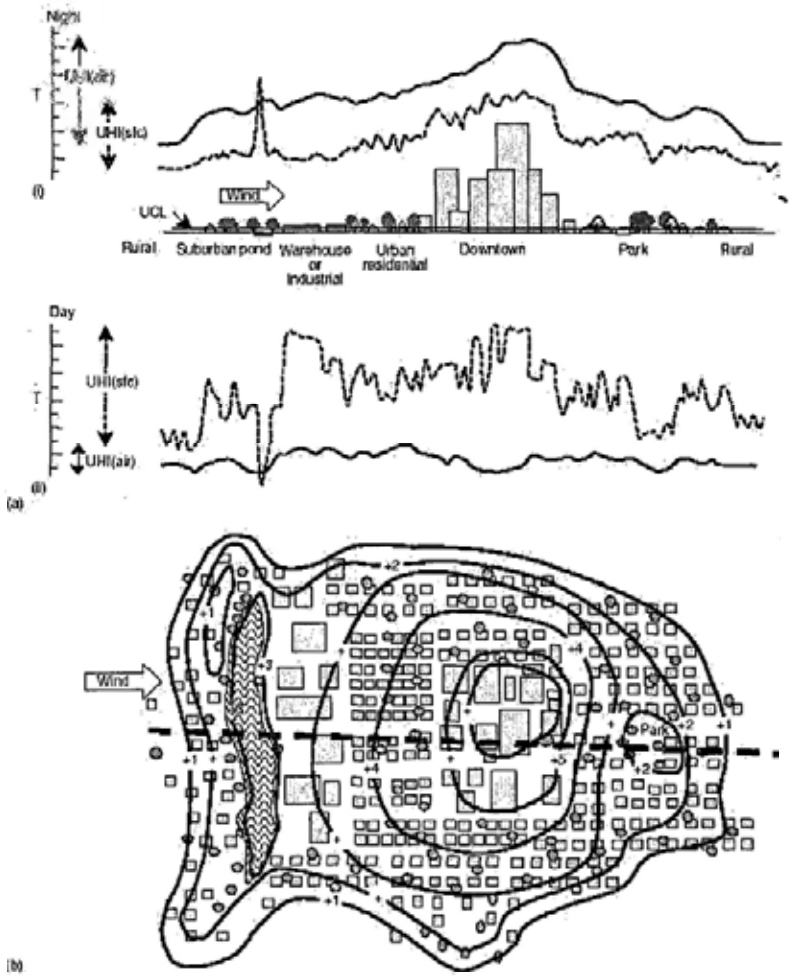

Figure 2.2 Urban heat island characteristics

Source: Voogt (2002)

Urban form is considered as one important cause to UHI formation and intensification. "City form comprises the materials used in construction, the surface characteristics of the city such as the building dimensions and spacing, thermal properties, and amount of greenspace" (Voogt, 2004). In the exploration of urban effect on local thermal environment, in particular intra-urban temperature disparities, urban form is the main interest of this research which can be changed through urban design. "Within a city there is substantial variation in temperature related to topography, proximity to lakes, rivers, and oceans, the density of development, the amount of vegetated cover, and type of building materials" (Bonan, 2008, p.4).The mechanism driving the urban rural and intra-urban temperature difference is

complicated as the integrated functioning of urban surface and geometry, regional climate, anthropogenic heat and the concentrations of urban pollutions. The deliberation in the following mainly focuses on the influence of the factors that are closely related with urban form on local temperature enhancement.

The nature of the surface is an important factor on the spatial patterns of surface and canopy layer air temperature in the city (Voogt, 2004). Urbanization featured increasing man made surfaces and lack of vegetation compared with rural area, the modified surface characteristics including albedo, heat capacity, thermal conductivity, and wetness may subsequently alter the radiation balance at the surface, the storage of heat in the urban fabric, and the partitioning of energy into latent and sensible heat (Landsberg 1981; Oke 1982, 1987, 1988a, 1995). Regarding the thermal performance, impervious built surfaces generally absorb more solar radiation than vegetation covering the soil and preventing heat dissipation from evapotranspiration (Bonan, 2008). Moreover, "surface temperatures are particularly sensitive to surface conditions: during daytime, dry, dark surfaces that strongly absorb sunlight become very hot, while lighter and/or moist surfaces are much cooler" (Roth et al., 1989; Voogt and Oke, 2003). A study of summer and autumn air temperature in Lawrence, Kansas, found land use (e.g., residential, commercial, industrial, park) and the type of surface material (e.g., asphalt, concrete, brick, gravel, grass) accounted for 17-25% of the variance in measured air temperature (Henry et al., 1985; Henry and Dicks,1987).

Apart from surface physical materials, the spatial configuration of urban surfaces, especially the placement of buildings including orientation and spacing, is considered as the important contribution to the development of urban heat island. Urban buildings absorb energy with high heat capacity construction materials, and trap energy through reducing the urban long wave heat loss and absorption and reflection of solar radiation with buildings multiple surfaces when deep street canyons formed in high rise high density urban area. Moreover the buildings especially in high rise high density slow down the wind and weaken the convection of mixing heat. "The less a surface opens to

the sky, the slower its cooling ability" (Souza et al., 2004). The urban geometry demonstrates a significant relationship with temperature variations in most findings through quantifying with height-width ratio and sky view factor (Goh and Chang, 1999; Eliasson, 1996; Nunez et al., 2001).

The formation and magnitude of UHI also depends on the regional or local weather condition, especially atmospheric humidity and wind. The wind speed limits heat island development with improving the convection of mixing heat throughout the atmosphere which increases with population size (Bonan, 2008). "For example, coastal cities may experience cooling of urban temperatures in the summer when sea surface temperatures are cooler than the land and winds blow onshore" (Voogt, 2004). Moreover regional or local climate is closely related with geographic location. Where cities are surrounded by wet rural surfaces, a slower cooling process by these surfaces can reduce the heat island magnitude, especially in warm humid climates (Oke et al., 1991). Therefore the influence of geographic location and population density on local temperature variation is noticeable which can be considered as important factors contributing to the development of local temperature variation.

2.1.3. Intensive Variation of Temporal Pattern

The difference of urban-rural air temperature is highly variable in temporal dimension owing to the difference in the cooling rates between urban and rural area (Figure 2.3). The temporal dynamics of UHI at various scales are distinctive in Voogt (2004) description:

- CLHI: the heat island intensity increases with time from sunset to a maximum somewhere between a few hours after sunset to the predawn hours. During the day the CLHI intensity is typically fairly weak or sometimes negative (a cool island) in some parts of the city where there is extensive shading by tall buildings or other structures and a lag in warming due to storage of heat by building materials.

- SHI: is strongly positive in both day and night time due to warmer urban surfaces. Daytime SHI is usually the largest because solar radiation affects surface temperatures.
- BLHI: is generally positive both day and night but much smaller in magnitude than CLHI or SHI.

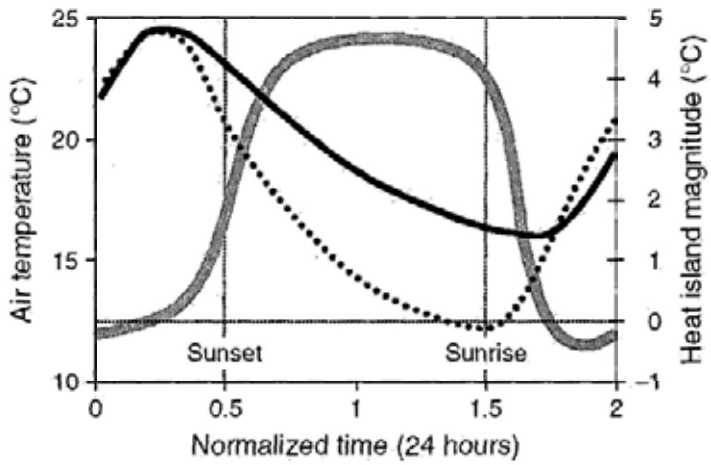

Figure 2.3 Typical temporal variation of urban and rural air temperature (thin lines), and heat island magnitude (thick line) under clear skies and weak airflow, which is produced by the cooling rates and vary depending on the climate region and season

Source: Voogt (2002)

The regional or local weather condition, particularly wind and cloud may influence the magnitude and frequency of heat islands: "Increasing winds mix the air and reduce the heat island; Increasing clouds reduce radiative cooling at night and also reduce the heat island" (Voogt, 2004). The magnitude of the UHI usually observed greatest during the night, under clear skies and weak winds. The temporal dynamics of urban heat island may be diversified along with the seasonal variations of wind and cloud. As Voogt (2004) pointed out, "seasonal variations in weather patterns affect heat island frequency and magnitude, heat islands of cities located in the mid latitudes usually are strongest in the summer or winter seasons, in tropical climates, the dry season may favor large heat island magnitudes". Therefore in a systematic

investigation of local thermal environment, information regarding the regional or local weather condition is necessary to discuss the observed local pattern.

Given that increased heat storage within the urban fabric may be driven mainly by enhanced daytime surface heating, which occurs because of surface dryness (Carlson et al., 1981). Then the warmth of urban surface can be considered as an important contribution to the magnification of urban warming, the study of urban surface warming possesses significant meaning for the study of urban effect on local thermal environment. "Understanding how thermal energy is portioned across a landscape, and the magnitude or variations in surface temperatures emanating from various landscape elements, is essential to defining the overall mechanisms that govern land-atmosphere interactions" (Quattrochi and Luvall, 1999b). Based on thermal infrared remote sensing, surface temperature pattern can be characterized and analyzed in detail. "Because radiant emissions from surfaces can be measured from airborne or satellite platforms, this larger number of observations enables the thermal properties of small surface features to be measured, allowing for a high-resolution investigation of urban microclimates" (Hardegree, 2006). However, "a number of investigators have provided evidence using thermal infrared remote sensor data that urban areas are strong daytime long wave radiators, but they have provided limited knowledge on the thermal energy responses contributed by discrete surfaces common to the urban landscape" (Quattrochi and Ridd, 1998). There is an urgent need to carry out a systematic investigation of surface thermal pattern represented by urban surface temperature distribution and variation with urban thermal landscape characterization and analysis aiming at delimitating its spatial heterogeneity and dependence in order to acknowledge the development of urban surface warming.

Besides the study of UHI at various scales, a Stewart's review (2007) of observational urban heat island (UHI) literature "uncovers widespread discrepancies in the representation and classification of so-called urban and rural measurement sites defining heat island magnitude, while the apparent simplicity behind urban-rural site

classification is obscuring the complex array of surfaces and near-surface climates that actually define UHI magnitude, therefore the movement toward a multidimensional, local-scale landscape-classification scheme which is regarded as better suited to the complexity of surface climates characterizing UHI in cities and regions worldwide is initiated." In the view of Nichol (1996), "for daytime studies based on satellite image data, the term surface temperature patterns may be more meaningful than surface heat island, since due to the heterogeneous nature of the urban environment, surface temperatures are discontinuous between urban structures and are influenced by building geometry" (p.145). Due to such consideration, the continuous surface temperature pattern derived from thermal infrared remote sensing can be regarded as one kind of landscape, i.e. urban thermal landscape, which the landscape ecology methodology can be introduced to study the pattern variations in spatial and temporal dimensions. Landscape ecology is one field of science mainly focusing on studying the underlying process from the observed patterns with various metrics developed to measure the structure of the observed pattern. In this research context, the main objective utilizing landscape metrics is to characterize the urban thermal landscape pattern in order to acknowledge the structure and dynamics of local thermal anomalies in spatial-temporal dimension. The overall structure of urban surface temperature distribution at the landscape scale can be measured with the descriptive landscape ecology metrics and the comparison can be made in temporal dimension in order to characterize the dynamics of urban surface thermal landscape pattern. This overall landscape scale study of urban thermal landscape may help avoid the possible bias introduced with urban rural delimitation and emphasize on the local pattern and process regarding local effect of urban environment on surface thermal environment.

Compared with the UHI studies at various scales within the previous review, it can be found that the scope of this study may be quite different from traditional urban heat island study based on urban rural difference, which focus on the study of urban thermal landscape at landscape scale represented by the mapped surface temperature distribution. It also hopes to enrich our knowledge regarding the local effects on

urban surface warming with the study of urban surface thermal environment in subtropical region with high density high rise development as well.

2.1.4. The Impacts of UHI

The UHI has important implications for human habitation comfort and public health, urban air pollution, energy management and urban planning, as summarized in Table 2.1. The impact may range from favorable to unfavorable and vary with time and location under site-specific local weather conditions. In Oke's (1997) view, "In temperate and cold climates heat islands may provide some benefits, especially in the cold season because of reduced heating loads; In these cases impacts of the UHI may be mostly beneficial in the winter, and undesirable in the summer". However, UHIs of cities in hot climates are generally non-beneficial as they lead to larger cooling loads and energy use, increased human discomfort and higher air pollution concentrations (Voogt, 2002).

Table 2.1 Impacts of UHIs classified by climate region

Impact	Cold climate region	Hot climate region
Human comfort	Positive (winter season) Negative (summer season)	Negative (all seasons)
Energy use	Positive (winter) Negative (summer)	Negative
Air pollution	Negative	Negative
Water use	Negative	Negative
Biological activity	Positive	? but probably neutral
Ice and snow	Positive	NA

Source: Voogt (2002)

The impacts of UHI vary from negative to positive under different location and seasonal climate condition. Therefore the impact of UHI should be critically examined before conducting any suitable strategies towards urban thermal environment

improvement. Cities with different location under different climate condition should be prudent in taking measures to mitigate UHI negative effect depending on its specific characteristic of urban environment.

Human activities can result in both intentional and inadvertent modifications of climate, and these are strongly evident in the artificial landscape represented large cities (Sturman, 1998). The negative impacts of local climate modification like UHI induced by the artificial landscape can be mitigated through landscape management in the practices of environmental responsible urban planning and design. Urban landscape also provides numerous challenges for urban planners, civil engineers, environmentalists, sociologists, economists, and even remote sensing scientists (Mesev, 2003). The increasing awareness of the importance of sustainability in natural resources is stimulating the improvement of current methods to better understand and quantify the causes and consequences of urban landscape evolution (Turner, 1987). It seems that the intense variations of the artificial urban landscape made the diversity and complexity of urban thermal environment across the city. To analyze the structure, function, and dynamics of urban systems, we need to link the landscape pattern with its processes (Geoghegan et al., 1998). In the context of urban thermal environment analysis along with the complexity of urban thermal landscape in spatial and temporal pattern, the efforts can be made to understand the relationship between urban landscape pattern and urban warming.

2.2. UHI Studies

In the literature, numerous researches have been conducted to study UHI using various measurement approaches in the past. With reference to different types of UHIs at various scales, the approaches used for UHI measurement are different depending on observation methods and definition of the observed surface in Voogt's summary (Figure 2.4). Since the structure of UHI "is complicated by the presence of parks, forested areas, rivers and streams, and other "non-urban" features that exist in the urban landscape. Thus detailed spatial investigations of the UHI can reveal

micro-climate details that explain how various surface features enhance or mitigate the UHI effect" (George and Becker, 2003). In this research, the main interest is the surface temperature variation or local surface warming at micro-scale, which is considered as the important contribution to urban warming and can be measured with thermal infrared remote sensing in detail at the landscape scale.

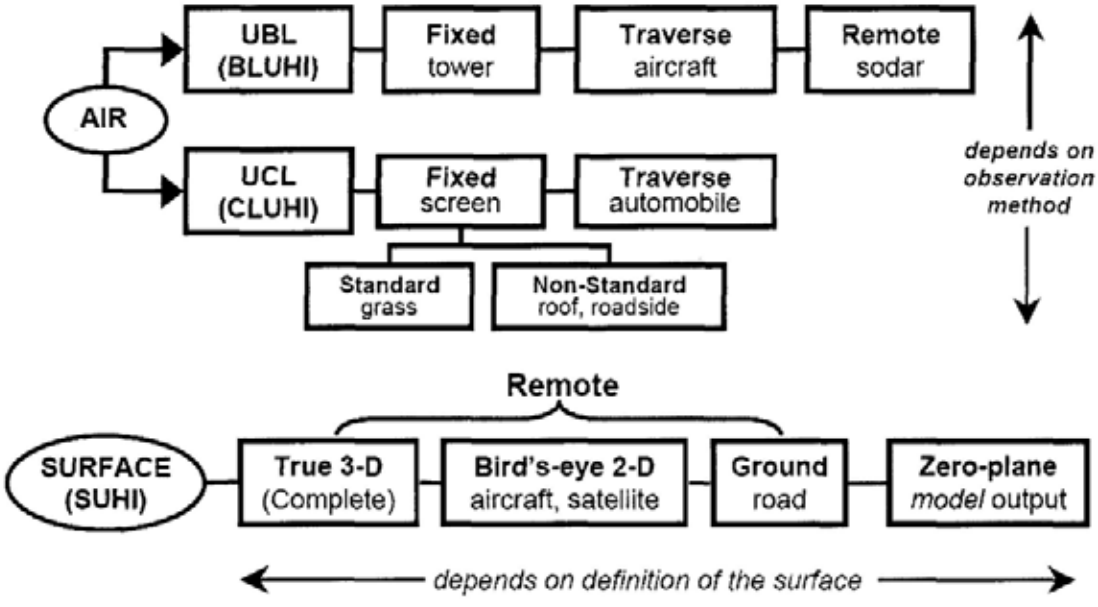

Figure 2.4 Measurement approaches of various types of UHI

Source: Voogt (EPA presentation)

Regarding the urban heating process in Vancouver, "the canopy layer thermal climate appears to be governed by the individual site character and not by the accumulation of thermally modified air from upwind areas." (Oke, 1976). The dependency of local thermal environment on local environmental setting is obvious. Referring the process at micro-scale, Voogt has a clear depiction regarding the factors that may govern and control the variation of local temperature (Figure 2.5). In this framework, urban local environmental setting plays an important role of local surface thermal environment. Apart from regional and local weather condition in particular winds speed and direction, factors including the material of land surface with various thermal

properties, urban geometry especially street canyon effect, solar variation, anthropogenic heat and pollutants etc influence local thermal environment at micro-scale.

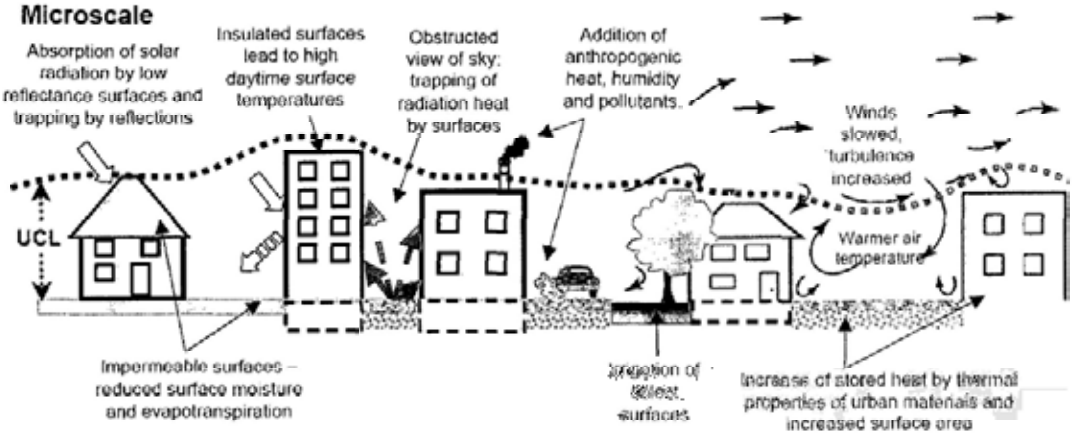

Figure 2.5 Process of UHI at micro-scale

Source: Voogt (EPA presentation)

The land surface temperature variation along with the spatial distribution of land uses, vegetative cover in Providence is identified by Brown University (2004) that "the densely populated residential districts, commercial and industrial areas represent urban heat islands, with the surface temperature as high as 43°C in summer days. On an average, the summertime land surface temperature is 20°C higher than in the surrounding suburban areas and 13°C higher than in treed neighborhoods. The highest level of mean land surface temperature of 32.5 °C is observed in mixed industrial areas, followed by industrial area and commercial with the range of 31–32°C. The maximum mean land surface temperature in high-density residential areas amounts to 28 °C." (Jusuf et al., 2007). In the diurnal change Carlson et al.'s study (1977) in the Los Angeles area revealed the temporal variation of the highest surface temperature locations, which moved from the industrial zone in the morning to the central business district and high-density residential areas in the evening. Urban impact on surface warming is very strong which is found in many previous studies. A study of urban expansion and its impact on surface temperature in the

Zhujiang Delta, China between 1989 and 1997 by Weng (2001) found that surface radiant temperature had raised 13.01K in the urbanized area related to the decrease of biomass. Weng further identified that "the spatial pattern of radiant temperature increase was correlated with the pattern of urban expansion". Lim et al.'s study (2005) in sensitivity of surface climate changes to land types and urbanization also revealed that surface warming is large for anthropogenically developed areas. Urban surface warming is obvious and widely observed in most of the cities, which the surface's radiant temperature difference between urban and rural is measured utilizing satellite derived Land Surface Temperature (LST).

Studies using satellite-derived radiant temperature have been termed as the surface temperature heat islands (Streutker, 2002). With the advent of remote sensing satellite with thermal infrared remote sensors, it is possible and widely used to study urban surface temperature distribution, in particular Surface Urban Heat Island (SUHI) with more detail when the data with high spectral, spatial and temporal resolution are available. In a review of thermal remote sensing in the study of urban climates, Voogt and Oke (2003) noted that:

> "Improvements in the spatial and spectral resolution of current and next-generation satellite-based sensors, in more detailed surface representations of urban surfaces and in the availability of low cost, high resolution portable thermal scanners are expected to allow progress in the application of urban thermal remote sensing to study the climate of urban areas." (p.370)

A variety of research based on thermal infrared remote sensing has been conducted to study SUHI. In the earlier practices with coarse resolution thermal measurements available, Rao (1972) utilized satellite thermal data at 7.4 km resolution of the Improved TIROS Operational Satellite (ITOS-1) to delineate the cities along the mid-Atlantic coast. Among the past practices, thermal infrared remote sensing data has been widely employed to measure LST and study surface temperature variations, including the Very High Resolution Radiometer (VHRR) data (Carlson et al., 1977;

Matson et al., 1978), Heat Capacity Mapping Mission (HCMM) data (Price, 1979; Byrne et al., 1984), NOAA Advance Very High Resolution Radiometer (AVHRR) data (Kidder and Wu, 1987; Brest,1987; Balling and Brazell, 1988;Roth et al., 1989; Gallo et al., 1993; Streutker, 2002; 2003), MODIS (Ochi et al.,2002; Pongracz et al.,2006 ;Takeuchi et al., 2007), Landsat TM and ETM+ (Carnahan and Larson, 1990; Kim, 1992; Nichol, 1994, 1996;Weng, 2001; Jusuf et al., 2007), and ATLAS data (Lo, et al.,1997;Quattrochi and Ridd, 1994; Quattrochi and Luvall, 1999a). In the recent practices with relative high resolution data available, Weng and Yang (2006) summarized that "more effort has been put to employ thermal infrared imagery such as from Landsat TM/ETM+, ASTER, and airborne ATLAS data, to study intra-urban temperature variations and to relate them to surface cover characteristics in current practices which remains one hot issue and needs more solid research".

The differential surface heating between urban and rural area is found to be the main cause by Scofield and Weiss (1977) for the low-level convergence of towering cumulus form (i.e. SUHI) over cities such as Washington, DC and Baltimore. The dependency of surface thermal emissions on urban surfaces and the placement of the surfaces are widely acknowledged from the previous studies. The UHI studies in several cities on the west coast of North America by Roth et al. (1989) utilizing AVHRR thermal data found that daytime thermal patterns of surface temperature were associated with land use and higher surface temperatures were observed in industrial areas than in vegetated regions. Gallo et al. (1993a) revealed that the normalized difference vegetation index (NDVI) and radiant surface temperature exhibited an inverse relationship for the Seattle, WA region. The study of a tropical city in Singapore utilizing Landsat TM data and field measurements by Nichol (1996) observed that urban morphology including vegetation biomass, surface geometry, elevation, and building density may impact local air and surface temperature. The UHI study in Vancouver, Canada by Ao and Ngo (2000) identified that the highest temperature of areas with high density, like the downtown core is related to the thermal properties of the existing structures and the street geometry, and the

relatively coolest intersection in the city was found to be closest to vegetation. Lo, Quattrochi and Luvall (1997) studied changes in the thermal signatures of urban land cover types between day and night in Alabama, Huntsville utilizing high resolution airborne thermal infrared image data at 5m spatial resolution acquired with the Advanced Thermal and Land Applications Sensor (ATLAS). A strong negative correlation between NDVI and irradiance of residential, agricultural, and vacant/transitional land cover types is identified, which indicates that "the irradiance of a land cover type is greatly influenced by the amount of vegetation present".

In summary, urban environment including urban surface and structure is conceived as dominant source for urban surface thermal anomalies, which have been identified and discussed in most of the studies. "In spite of these progresses and achievements over the past 15 years, however, thermal remote sensing of land surface temperatures and urban heat islands has largely been limited to qualitative description of thermal patterns and simple correlations with land covers" (Voogt and Oke, 2003). And "this is due partly to the tendency to use thematic land use and land cover data, not quantitative surface descriptors, to describe urban landscapes" (Voogt and Oke, 2003). Moreover quantitative evaluation regarding the influences of these local environment indicators on local surface temperature variation is scarce or partially given for a few isolated factors, such as vegetation NDVI or biomass, urban street canyon represented by Sky View Factor. This prevents the clear delineation regarding the process of local surface warming, which made a systematic investigation of urban thermal landscape valuable for a comprehensive review about the integrated effects of local environmental setting on urban surface thermal anomalies.

"The urban landscape forms a canopy acting as a transitional zone between the atmosphere and the land surface, The composition and structure of this canopy have a significant impact on the thermal behavior of the urban environment (Goward, 1981)" (Lo et al., 1997). From this point of view, the study of urban landscape impacts on local surface warming possesses practical value for exploring the

underlying process of urban warming and the urban effect on urban thermal environment as well. The urban thermal landscape study takes advantage of the continuous surface derived from thermal infrared remote sensing at the landscape scale, the detailed variation of local surface temperature can be measured and analyzed through the systematic investigation. At the same time urban environmental factors can be quantified with remote sensing and GIS techniques. This enables a systematic investigation of urban thermal landscape with a link to be established between local environmental setting and surface temperature variation. Then the mechanism which made the heterogeneity and complexity of urban surface thermal landscape can be studied in depth based on surface temperature distribution.

In this research context, the spatial heterogeneity and spatial dependency of urban thermal landscape on urban landscape observed with thermal infrared remote sensing is the main target of this thesis study. Landscape metrics provide various useful metrics to measure the structure and dynamics of the landscape pattern, which is developed based on landscape ecology with the main objective to monitor the landscape pattern and study the dynamics of underlying process through analyzing the exhibited patterns. To this end, the pattern and variation of urban surface temperature is regarded as one kind of landscape, urban thermal landscape, which is assumed as the presentation of local surface heating process upon urban landscape, and then the structure and dynamics of urban thermal landscape can be characterized with landscape metrics through introducing landscape ecology methodology into this study. The primary intention is to examine the heterogeneity pattern of surface thermal variation with descriptive metrics. The comparison based on these structure measurements in day-night and temporal dimension can be utilized to study the possible day-night and temporal change in the overall pattern of thermal landscape. Moreover the possible effect of urban development on the overall structure of urban thermal landscape in day-night and temporal dimension can be partially revealed with reference to the overall land use land cover change. The spatial dependency of urban thermal landscape on urban landscape can be further interpreted with

regressional correlation analysis, based on which to investigate the development of urban surface warming.

In the literature, quantity of methodologies for urban surface temperature measurement based on thermal infrared remote sensing has been developed with reference to various remote sensors used with diverse spatial, temporal and spectral resolution. Compared with each other in a review, both strength and weakness exist. In the following section the methodology foundation of thermal infrared remote sensing for urban surface temperature study is introduced first, at the same time various algorithms of Land Surface Temperature (LST) generation is going to be reviewed.

2.3. Basic Theory of Thermal Remote Sensing

Before the methodology was discussed, a brief introduction about the thermal infrared signal is illustrated to demonstrate the rationale of thermal infrared remote sensing used for LST derivation.

2.3.1. The Physics of Radiation

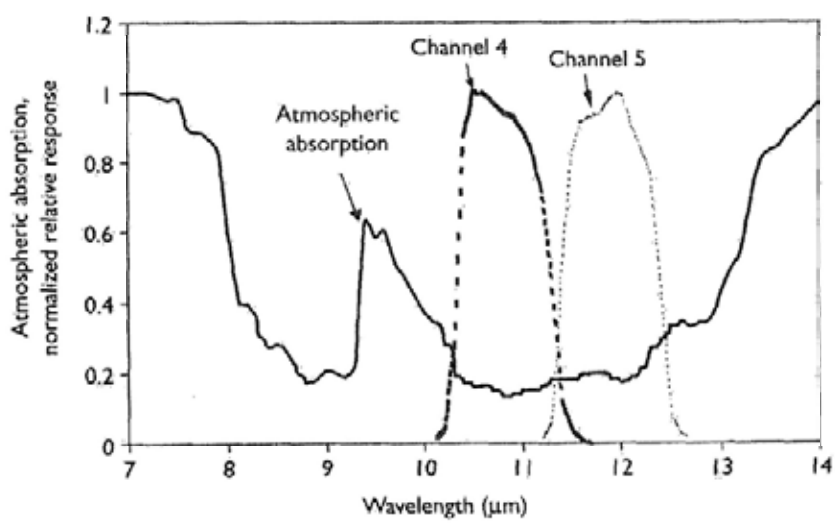

Figure 2.6 Relationship between AVHRR channels 4 and 5 (dashed lines) and the atmospheric window in the thermal infrared part of the spectrum (solid line).

Source: Quattrochi and Luvall (2004)

Thermal bands on remote sensing instruments generally observe the wavelength in the atmospheric window region of the electromagnetic spectrum, approximately between 8 and 14 μm where the signal can be transmitted through the atmosphere with relatively little interference. Figure 2.6 shows the relationship between the two thermal bands on AVHRR and the thermal window region in the atmosphere. Due to this spectrum region, the thermal information can be derived with minimized atmospheric influence from the remotely sensed signals in order to detect the radiant surface temperature of objectives on the earth.

2.3.2. Land Surface Temperature (LST) Algorithms

From physical principles and previous research, it is known that radiometric surface temperatures obtained from remote sensing measurements are a function of both the physical surface temperature and emissivity of the surface within the passband of radiometric measurements (Humes et al.). In remote sensing, LST is defined as the 'surface radiometric temperature' corresponding to the instantaneous field-of-view of the sensor (Prata et al.,1995) or, more precisely, as the 'ensemble directional radiometric surface temperature' (Norman and Backer, 1995). For a given sensor viewing direction, LST depends on the distribution of temperature and emissivity within a pixel and the spectral channel of measurement (Becker and Li, 1995). In order to obtain LST from thermal infrared radiometry, three main effects have to be considered: atmospheric, angular and emissivity effects (Franca and Cracknell, 1994).

The physical principles of thermal radiation is introduced in the book *Thermal Remote Sensing in Land Surface Processes*, according to Quattrochi and Luvall's (2004, p.12) demonstration: " The radiant energy detected by thermal sensors is a composite of energy emitted by the land surface that is transmitted through the atmosphere (not absorbed) and energy that is emitted by the atmosphere. Atmospheric water vapor content and the effective temperature of the atmospheric layer that contains the water vapor are the two primary atmospheric factors contributing to the thermal signals. This land-atmosphere coupling complicates interpretation of the remotely sensed signal."

Due to the atmosphere effects it is usually different from the surface temperature typically ranging 1 to 5k (Prata et al., 1995). In general, Land Surface Temperature (LST) generation from thermal infrared remote sensing signal follows two main steps: "The first step for retrieving surface emissivity and land surface temperature is to perform atmospheric correction. The second step is to separate emissivity and temperature from the retrieved surface leaving radiance." (Liang, 2004, p.346). For sensors that have two thermal bands, such as AVHRR and GOES, so-called split window algorithms were mostly used to estimate land surface temperature given surface emissivity. As one improvement, the TES algorithms estimate spectral emissivities and land surface temperatures simultaneously with taking advantage of the new generation of sensors with multiple thermal bands, such as ASTER and MODIS.

Split-window Algorithms for Estimating LST

Following Liang's illustration, most split-window algorithms for estimating LST is based on the assumption that LST (Ts) is linearly related to the brightness temperatures of two thermal channels. "With the assumption that surface emissivities of these two channels are known, the split-window method can largely eliminate atmospheric effects based on the differential absorption between two bands for the LST estimation" (Liang, 2004, p.346).

Price (1984) developed one of the earliest LST split-window algorithms for retrieving LST from AVHRR band 4 and band 5. Liang (2004) has pointed out that these approaches cannot completely capture the tremendous amount of variability of surface emissivity, particularly over non-vegetated regions, thus more studies have revealed that when the atmosphere is not particularly dry, the traditional split-window algorithm cannot remove the atmospheric effects completely. Thus, the emissivity correction remains a very challenging area that requires much more study. However, as Prata et al. (1995) mentioned, in fact the error due to an error in the emissivity correction is two times larger than that due to an error in atmospheric correction. With

the emergence of several space-borne sensors with multiple thermal infrared bands, MODIS and ASTER, it provides a great opportunity for accurately estimating spectral emissivity from thermal infrared imagery itself.

Temperature and Emissivity Separating (TES) Algorithm

The earlier temperature emissivity separation (TES) is review by Gillespie et al. (1999), mainly including: Reference Channel Method (Lyon, 1965), the alpha-derived emissivity ADE method (Hook et al., 1992; Kealy and Hook, 1993), Temperature-Independent Spectral Indices (TISIs) (Beck and Li, 1990; Beck and Li, 1995), The MODIS Day/Night Algorithm (Wan and Li, 1997). Gillespie et al. examined and found that these methods all require independent atmospheric correction and the inaccuracy tend to be high (+3K) due to tilts introduced into the emissivity spectral.

On the basis of previous algorithms, TES technique proposed by Gillespie et al. (1996, 1998) was for Terra-ASTER. There are three basic modules in the ASTER algorithm: NEW, ratio, and MMD. The Module structure is shown in Figure 2.7.

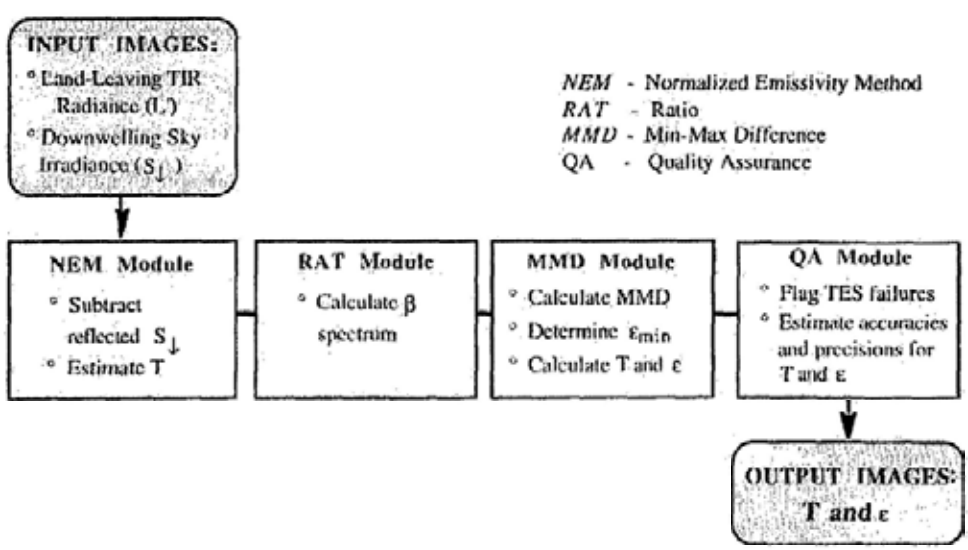

Figure 2.7 Basic design of TES algorithm

Source: Gillespie et al. (1999)

However Dash et al. (2002) pointed out, this algorithm requires an accurate atmospheric correction. The accuracy of the downwelling atmospheric irradiance is a critical issue. The ASTER atmospheric correction algorithm needs atmospheric input variables (temperature and water vapor profiles) from other sources, which may introduce large uncertainty and eventually impact the accuracy of the final products (Liang, 2004).

As above reviewed the methodologies of LST retrieving from thermal infrared data of satellites was compared with each other that weakness and strength both exist. There is no single best method for determination of LST due to the complicate thermal response between surface and atmosphere and high frequency variability of urban surface. On the other hand, the thermal infrared data received by different satellite with different spatial and temporal resolution also create different problem towards LST generation. There are no general applicable methods for use. The appropriate methodology should be chosen based on the available data and its application.

Since the TES algorithm has been utilized to produce ASTER LST and emissivity products and shows promising result. The numerical simulations show that this algorithm can recover LST to within ~1.5K and emissivity to within 0.0015 (Gillespie et al., 1998). In the thesis study, the LST data used is from ASTER, one product generalized based on TES algorithm aforementioned. Besides LST data, other data source utilized include the 3 bands in visible and near infrared (NIR), 6 bands in short wave (SWIR), to facilitate the study of urban environment. The details follow in the next chapter.

2.3.3. Advantages and Limitations of Thermal Infrared Remote Sensing

LST is the temperature at the earth's surface, however the land surface is far from being skin or homogeneous two-dimensional entity: it is composed of different materials with various geometries both of which complicate LST estimation (Qin and

Karnieli, 1999). The urban environment has complex three-dimensional structure. Regarding the complexity under urban canopy layer together with the constraints of remote sensing surface temperature measurement, the complete active surface concept was proposed by Voogt and OKe (1997), illustrated as figure 2.8. It clarified the inherent deviation generated by various remotely observation measurements from the practical complete active surface thermal performance. These incomplete observations create possible biases. "The satellite derived surface temperature mainly corresponds to the urban surface temperature observing from the viewing angle which only constitutes part of the active surface" (Voogt and OKe, 1997). It indicates one profile of urban thermal environment.

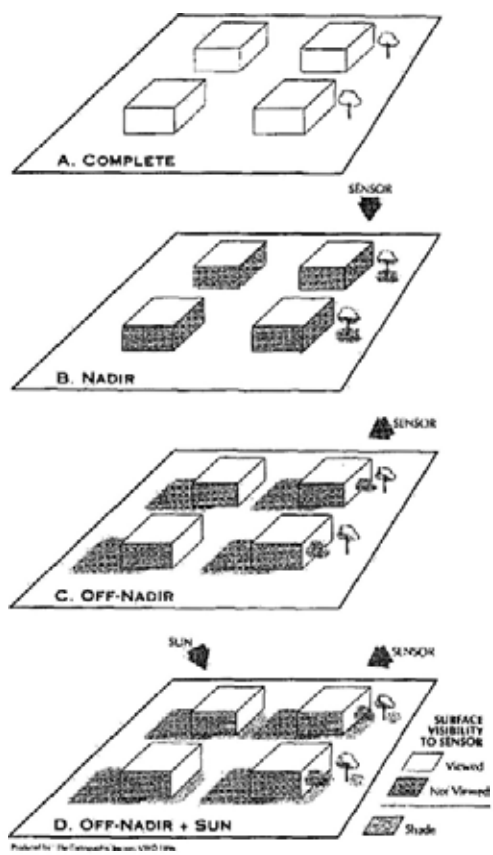

Figure 2.8 Conceptual diagram of the urban surface and biases in the surface viewed by nadir and off-nadir remote sensors. The 'complete' surface (a) is the full urban-atmosphere interface; remote sensors viewing from (b) nadir, and (C) off-nadir viewing directions see only a subset of the complete surface. With inclusion of shading effects (d) off-nadir views from different directions view different amount of sunlit and shaded surfaces.

Source: Voogt and OKe (1997)

The two types of LST derivation algorithms commonly used and discussed above mainly focused on the correction of emissivity and atmospheric effect, while the viewing angle effect is neglected. Regarding the viewing angle effects in the thermal infrared domain is not well known, most of the algorithms rarely tackle this problem. Based on the simulation result of Laurent et al, an angular variation of 6% on radiance was obtained on a heterogeneous surface between a zenith angle of 70° and on-nadir measurement (Laurent et al., 2004).This problem still remain a research area need lots of strength involved.

As a whole for UHI study, Nichol has summarized the constraints of remotely sensed measurement of surface temperature method existed for urban heat island study as following aspects (Nichol, 2003):

- Roth et al. warn against regarding remotely sensed heat islands as synonymous with those based on air temperature measurements at near ground level.
- Satellite-based sensors record mostly during day time which may constitute a heat sink.
- Surface temperature (Ts) difference (during the day-time are largest) are more pronounced than UHI based on air temperature (the greatest difference occurs at night)
- Satellites only record the temperature of horizontal surfaces, which constitutes only part of the complete active surfaces in the high-rise urban environment.
- Timing of the satellite overpass may not be optimal for detecting temperature difference.
- Satellites may provide an instantaneous view of the whole city, but cannot provide a day-night profile of temperature changes. Supplemental data from ground-based studies at intervals during the day is required.
- The satellite measured Ts can only be considered accurate in clear, dry

atmospheres.

- Low spatial resolution constitutes a further source of inaccuracy, particularly in high-spatial-frequency urban terrain. Since a low proportion of "pure" pixels are present in the image and the climate of the urban canopy layer may be discontinuous between structures especially during times of solar isolation (i.e., during the day).

Even though these limitations given, as Nichol (2003) also pointed out the main advantage of remotely sensed thermal data lies in the ability to provide a time-synchronized dense grid of temperature data over a whole city. Urban thermal landscape monitoring and analysis just takes advantage of the continued temperature surface derived from thermal remote sensing to carry out the study of local effects on surface warming.

2.4. Geographically Weighted Regression (GWR)

Linear regression is one useful technique for investigating the relationship between a set of independent or predictor variables and a dependent or response variable. When this method is applied to geographical data, which means each case corresponds to a geographical location, "but beyond this implicit agreement space plays no role in the modeling process" (Brunsdon, Fotheringham and Charlton, 1998). With the assumption of the model is globally stationary, it assumes a stationary spatial process with one global relationship estimation. The global parameters coefficients outputted from the global linear regression analysis are assumed to be the same over the whole study area, representing one globally applicable relationship between geographical variables. When applied to spatial data, typical global linear regression model may risk drawing the misleading conclusion. "If spatial heterogeneity exists, stationary coefficient models will produce parameters that are in essence an "average" value of the parameter over all locations. A failure to incorporate spatial heterogeneity will result in biased coefficients and a loss of explanatory power and may obscure important dynamics relating to local effects of geographical variables" (Bitter, 2007).

There are several techniques proposed for incorporating space to measure spatial non-stationary, including expansion method (Cassetti, 1972), spatial adaptive filtering (SAF) (Gorr and Olligschlaeger, 1994), multilevel modeling techniques (Goldstein, 1987; Jones, 1991) etc. Among the attempts of taking geographical location into its analysis of relationships between variables, Geographically Weighted Regression (GWR) is quite useful which allows complex spatial variations in parameters to be identified, mapped and modeled (Huang, 2000; Brunsdon et al., 1998). GWR is part of a growing trend in GIS towards local exploratory data analysis which intends to detect the local pattern of spatial data in spatially non-stationary relationships through local statistics technique. In the literature a number of recent publications have demonstrated the analytical utility of GWR for various urban studies (Huang and Leung, 2002; Mennis and Jordan, 2005; Mennis, 2006; Bitter, 2007), while it has been scarcely utilized in urban surface climate or urban thermal landscape analysis.

By highlighting the existence of intense spatial differentiations of variables that measure the relationships which are spatial association, i.e. non-stationary across the whole study region, GWR takes the advantage of the flexibility of local statistical technique to analyze spatially varying relationships. Local statistics technique enables an in-depth evaluation of the variation between the relationships across the whole study space. One comprehensive comparison between global and local statistics is given by Yu as following Table 2.2.

Table 2.2 Global v.s. local statistics

Global statistics	Local statistics
- Similarity across space	- Difference across space
- Single-valued statistics	- Multi-valued statistics
- Not mappable	- Mappable
- GIS "unfriendly"	- GIS "friendly"

- Search for regularities - aspatial	- Search for exceptions - spatial

Source: Yu

As one important improvement towards global model, Geographically Weighted Regression (GWR) extends global linear regression through allowing local parameters coefficients estimation through associating parameters coefficients with geographical location. Geographically Weighted Regression in essence specifies a separate regression model at every observation point, thus enabling unique coefficients to be estimated at each location (Brunsdon et al., 1996). This local statistics is realized with a weighting matrix to discriminate the relative influences of different observations with different locations on location-specific parameter coefficient estimation. The fact is in terms of Tobler's (1970, p.236) "First Law of Geography": everything is related to everything else, but near things are more related than distant things. This approach of localized statistics is based on this weighted statistics, "with each observation in the data set being weighted in terms of its proximity to any point (u,v), so that for any point (u,v) in the study area a summary for a small area around that point can be obtained" (Brunsdon et al., 2002). Therefore one commonly adopted weighting strategy is distance-decay based weighting, in particular Gaussian weighting, which made the site specific parameters coefficients estimation more emphasize on observations near around the site. Instead of studying the overall pattern of dataset within the whole study region, GWR provides a more intuitive way to examine the dataset pattern at a local scale (Fotheringham et al., 2002).

Geographically Weighted Regression (GWR) extends the utility of global linear regression methods emphasizing on the exploration of localized relationships between variables represented by the diversity of spatially varied parameter coefficients. GWR measures the spatial dependency (non-stationary) in a dataset and summarizes the relationship by local regression parameters (Su et al., 2005). In

particular, spatial variations within relationships can be detected based on regression coefficients of GWR varying across space. The inference based on the varying relationships provides more in-depth examination of local effects. In this research context, the localized exploratory data analysis of GWR enables the local patterns of surface warming to be revealed and investigated in-depth. The local statistics outputted from GWR can be used to visualize spatial variation in the correlation relationships of interest. Thus, local knowledge can be obtained easily and intuitively. The application of GWR in the studies of local effects on urban surface thermal anomalies provides a potential avenue for a comprehensive understanding of local surface warming process.

Besides urban thermal landscape study quite deviates from traditional urban heat island study based on urban rural dichotomy, the main emphasis of this research is to study the urban surface temperature pattern as whole at the landscape scale over city area. Based on thermal performance of isolated units of urban surface in different land use, location and structure etc, the relationship between urban form and thermal landscape pattern would be examined in detail. Together with the local pattern revealed by GWR analysis, the local variation in the relationship between urban environmental setting and local surface temperature variation can be examined. Finally this knowledge regarding the mechanism of local surface warming may provide a foundation for future urban landscape development in a scientific way under local opportunities and constrains.

Due to the complexity of urban thermal environment induced by the intensive variation in spatial and temporal dimension, the thesis will undertake a systematic urban thermal landscape investigation based on monitoring and analysis of urban surface temperature pattern derived from thermal infrared remote sensing images. Characterizing the spatial-temporal variations of urban thermal landscape in detail with ecology landscape metrics would help to understand the underlying process of urban surface thermal environment from surface warming aspect. And then a

systematic investigation of the relationship between urban form and urban thermal landscape in a subtropical city, Hong Kong based on statistical regression analysis can assist in a holistic understanding of local surface warming.

2.5. Summary

Through the previous depiction, it can be seen that urban thermal environment takes on its complexity in spatial and temporal dimension, expanded from which urban thermal landscape study is try to study urban surface temperature pattern based on thermal infrared remote sensing. The practices of UHI study based on thermal infrared remote sensing is reviewed, the main finding is that urban impact on surface warming is strong and the dependency of urban surface temperature on urban surface and surface geometry is obvious. The basic theory of thermal infrared remote sensing is addressed to provide the theoretical foundation for urban thermal landscape monitoring and analysis. Based the Land Surface Temperature (LST) generated from thermal infrared image, the pattern of urban thermal landscape can be studied in detail. Lastly, Geographically Weighted Regression (GWR) is introduced which enables a systematic investigation of urban impact on local surface warming in depth at local scale.

CHAPTER 3: METHODOLOGY AND DATA

3.1. Introduction

Hong Kong is a maturely developed city with a subtropical climate and an extremely high population density. It has a population of approximately 6.9 million in 2006 and an area of only 1,104 square kilometers (the population density reaching 6,350 people/sq.km). As Hui (2000) referred, "the geography of Hong Kong is hilly, with several high peaks; consequently agricultural land or indeed any flat land is scarce. Discounting such areas as country parks, conservation areas, water catchments areas, outlying islands, uplands, steep slopes and military land, the developable areas are limited. Hong Kong's urban environment has an extremely high development density pervasively filled by buildings and roads."

Lack of lands for development leads to the high rise and high density urban development, which caused lots of urban environmental issues, such as the bad urban ventilation in winter, transportation congestion, urban public heath etc. This high density and high rise development would inevitably accelerate the climate change impact on Hong Kong. According to the HKO, long term meteorological trends have been detected in Hong Kong (The HKO Technical Note No. 107). A summary of meteorological change in Hong Kong is listed in Table3.1 (Fung, 2004).

Table 3.1 Summary of climate change in HKSAR

Meteorological Characters	Changes due to Climate (in the past)
Rural temperature	Increased 0.2°C/decade
Urban temperature	Increased 0.6°C/decade
Daily diurnal range	Decreased 0.28°C/decade
Percent of time of reduced visibility	Increased 1.9%/decade
Cloud amount	Increased 1.8%/decade
Global solar radiation	Decreased 1 MJ/m^2 per decade
Evaporation	Decreased 184 mm/decade
Frequency of heavy rain	Increased 0.4 days/decade
Frequency of thunderstorms	Increased 1.7 days/decade
Number of tropical cyclones	Decreased 0.17/decade
Sea level rise	Increased 2.3 mm/year

Source: Fung (2004)

The major impact of urban warming on Hong Kong would deteriorate the stringent situation of energy consumption through increasing air-conditioning loading during summer. A study on the energy consumption of Hong Kong by Lam and Hui (2001) reported that for the year 1998, "space conditioning accounted for almost one-third of all electricity consumption and about 15% of the total end-use energy consumption". Since the oil crises in the 1970s, there is a growing need of energy conservation during the past years along with the fast urban development world wide. "Rising the ambient temperature by 1°C will increase electricity consumption by 9.02%, 3.13%, and 2.64% in the domestic, commercial and industrial sectors respectively. For 1°C rise in temperature, the total energy cost of Hong Kong will increase by HK$1.65 billion" (Fung, 2004). Due to "a significant proportion of the total energy produced in Hong Kong is consumed by the building stocks, which account for nearly half of the total energy consumption" (Chan and Yeung, 2005). There is a stringent need to solve the problems for energy sustainability with the efforts from every community, in particular urban housing since a large part of energy consumption is due to the building stocks. At the urban scale, the endeavors from scientific urban planning and design may be one of the options. Sustainable urban planning and design proved to be potential solutions to a certain degree to release the environmental pressures that urban warming induced.

With the intelligence of urban architects and planners, the sustainable urban design under high rise and high density development has been promoted and widely accepted with building energy efficiency strategies (Hui, 2003; Lee et al., 2002). Due to the complicated interactive correlation between urban building and local climate, the energy performance of buildings is dependent on the urban microclimate, which is also defined by the city (Steemers, 2003). However it is far from being certain about the urban effects on local warming, few attention has been paid to the differentiation of local effects on surface thermal disparities at a scale over whole city area during urban development, even endeavors is quite scarce to characterize and anlalyze the spatial heterogeneity and dependence of urban thermal landscape in depth aiming at

delimitating the local effects on urban surface warming via a viewpoint of local variation. There is a need for a better understanding of urban effects on local thermal environment with a systematic examination. During these efforts the study of urban surface thermal landscape provides an avenue to advance this exploration since urban thermal environment is directly controlled by the local surface temperature variation. Urban surface thermal landscape monitoring and analysis possesses practical meaning towards better understanding of urban effects on local thermal environment. Based on the thermal infrared remote sensing, the urban surface temperature can be extracted and mapped for the urban thermal landscape study which would serve as an aid in urban planning and design. Hong Kong with high rise and high density housing development would be chosen as the case study area, it hopes to contribute and advance our understanding of urban effect on local microclimate in hot-humid area.

Before any mitigation and adoption strategies formulated to guide urban development, the mechanism driving urban warming, in particular urban surface warming needs to be clarified. A systematic investigation of urban thermal landscape through monitoring and analysis the surface temperature variation derived from thermal infrared remote sensing may help to enrich the knowledge of urban surface thermal performance which may moreover contribute to understand the urban effects on local thermal environment. "The city has a myriad of microclimates that are intimately linked to the composition of its surfaces and the spatial and physical features of its structures." (Terjung and Louie, 1973). Among the factors that influence urban microclimate, urban form plays an important role in the evolution of urban warming. As Lantsberg said, "Urban form—the spatial arrangement of fixed items in an urban system—can be analyzed through multiple lenses. Measures of compactness, land use diversity, street and road connectivity, accessibility, and "excess commuting" help provide quantitative descriptions of the basic elements that constitute the outward shape and internal structure of the built environment at the town and regional levels (Horner, 2002; Song, 2003)". In the context of this thesis study urban form would be analyzed through the lens of "urban thermal landscape pattern".

In this context, this thesis tries to characterize urban thermal landscape pattern derived from thermal infrared remote sensing, and then to relate urban environmental measures with local surface temperature for a better understanding of the mechanism which formulates urban surface thermal anomalies. To this end, the methodology of urban thermal landscape monitoring and analysis would be constructed and implemented in this research practice of Hong Kong study. It hopes to provide a foundation for systematic study of urban surface thermal environment in Hong Kong based on urban thermal landscape investigation. Moreover the experience in Hong Kong would provide useful information for understanding the urban effects on local surface warming in the tropical and subtropical regions. At the same time, it may help to recognize the common issues for potential adaptive strategy design and facilitate urban thermal environmental management under similar local constrains.

3.2. Study Area and Data Source

The study area mainly covers the overlapped area of all of the remote sensing images collected for this research in Hong Kong illustrated in Figure 3.1, with all the weather stations located within the study area where the meteorological data is recorded. The related meteorological data of these stations was purchased from Hong Kong Observatory (HKO) for this study to provide simultaneous field measurements. Within the study area, the elevation ranges from 0 rising to 957 meter of Tai Mo Shan in the New Territories, where the intensive elevation variation occurs along with the mountainous region extension. Most of the extensive urban development with high density housing located sparsely in Tuen Mun, Tsuen Wan, Yuen Long, Tin Shui Wai, Sha Tin, Tai Po, Sheung Shui, Fanling, and Kowloon, mainly focusing on New Territories and part of Kowloon region, which are detached by the mountains covering the whole study area. The northwest corner of the study area contains Hong Kong wetland park and Mai Po Ramsar Sote, with fish ponds surrounded. Besides housing estates, the study area includes a few industrial development areas located in Tuen Mun, Tsuen Wan, Tai Po and Yuen Long.

Together with the mountains topography, the diverse land use in the study area provides practical meaning for the study of local effect on surface thermal anomalies under the subtropical climate.

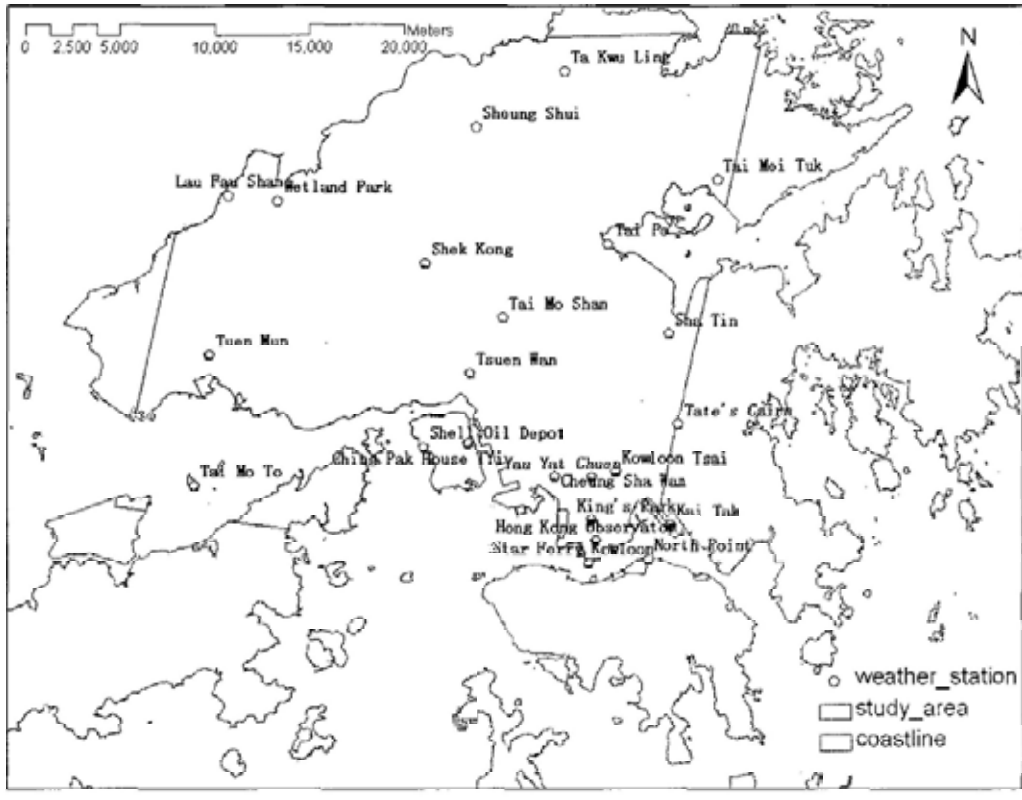

Figure 3.1 Study area with weather stations

The study period ranges from 2003 to 2006 when the ASTER data used for this site study is available. The ASTER images of these years are obtained from the achieved database in the Land Process Distributed Active Archive Center through the Earth Observing System Data Gateway (EDG), which would be demonstrated and discussed in the subsequent part of this section. Since Hong Kong is a highly developed city with mature urban infrastructure. During this study period from 2003 to 2006, Hong Kong experienced no pervasive urban development but with a few percentages of urban sprawl recognized, the reported percentages of dominant land use classification in 2003 and 2006 are listed in Table 3.2. The obvious land use change mainly resides in sectors including Urban, Grassland, Woodland, Agricultural, Mangrove and Swamp. The urban land use percentage has increased from 21.8% in

year 2003 to 23.4% in year 2006, and grassland percentage increased from 20.4% in year 2003 to 24% in year 2006, woodland decreased from 25.7% (year 2003) to 22.1% (year 2006), agricultural decreased from 5.2% to 4.6% and Mangrove and Swamp from 0.9% to 0.4% between year 2003 and 2006.

Table 3.2 The reported dominant land use classification (%) in 2003 and 2006

Year	Urban	Grassland	Shrubland	Woodland	Agricultural	Fish Ponds	Mangrove & Swamp
2003	21.8	20.4	20.8	25.7	5.2	1.2	0.9
2006	23.4	24	20.6	22.1	4.6	1.5	0.4

Source: Hong Kong Annual Report (2003; 2006)

The remote sensing data used for this research comes from ASTER (Advanced Spaceborne Thermal Emission and Reflection Radiometer) on the Terra satellite which was launched in December 1999. ASTER offers three bands in the visible and near infrared (VNIR) part of the spectrum and a near infrared backward-scanning band with a 15m resolution, six bands in the short wave (SWIR) infrared with a 30m resolution, five thermal infrared bands (TIR) with a 90m resolution (Figure 3.2, Table 3.3). For details regarding ASTER please refer to http://asterweb.jpl.nasa.gov/.

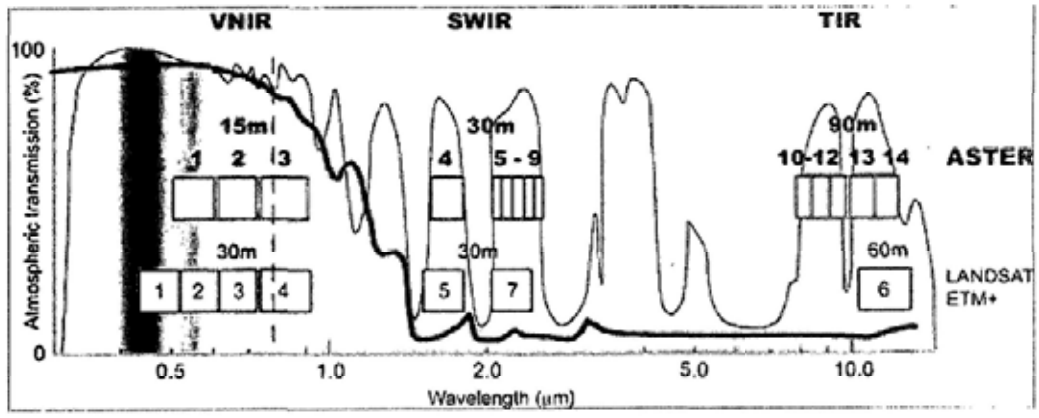

Figure 3.2 ASTER spectrum bandwidth comparison with Landsat ETM+

Source: ASTER (http://asterweb. jpl.nasa.gov/)

Table 3.3 Spectral and spatial characteristics of the ASTER bands

Band No.	Label	Wavelength(um)	Resolution(m)
1	VNIR_Band1	0.52 - 0.60	15
2	VNIR_Band2	0.63 - 0.69	15
3	VNIR_Band3N	0.76 - 0.86	15- Nadir view
4	VNIR_Band3B	0.76 - 0.86	15 - Backward scan
5	SWIR_Band4	1.60 - 1.70	30
6	SWIR_Band5	2.145 - 2.185	30
7	SWIR_Band6	2.185 - 2.225	30
8	SWIR_Band7	2.235 - 2.285	30
9	SWIR_Band8	2.295 - 2.365	30
10	SWIR_Band9	2.36 - 2.43	30
11	TIR_Band10	8.125 - 8.475	90
12	TIR_Band11	8.475 - 8.825	90
13	TIR_Band12	8.925 - 9.275	90
14	TIR_Band13	10.25 - 10.95	90
15	TIR_Band14	10.95 - 11.65	90

Source: ASTER (http://asterweb. jpl.nasa.gov/)

The temporal range of the satellite images used covers from 2003 to 2006 (Table 3.4), with 3 images in grey color rows obtained during nighttime, and 4 images obtained in daytime. The seasonal range mainly covers April, October and November, with each pair of daytime and nighttime images within the same year for potential day-night observation since the date of each image within the same year is quite close to each other. Then the vegetation NDVI of nighttime observation when VNIR observation is not acquired can be estimated based on corresponding year daytime ASTER L1B VNIR image which is simultaneously acquired for daytime observation. In this research ASTER L1B data and Land Surface Temperature (LST) product AST_08 data were both acquired for this research. ASTER L1B data is used to derive some of the ecological parameters, LST product AST_08 is employed to map urban surface temperature pattern. AST_08 data is a surface kinetic temperature product in units of degrees Kelvin which provides the surface temperature estimate based on Temperature-emissivity separation algorithm applied to atmospherically

corrected surface radiance data. The surface temperature of AST_08 can be regarded as valid for cloud-free pixels. Along with simultaneous validation and assessment of field measurements, the reported accuracy of surface temperature estimation achieved proved to be within 1.5K under ideal conditions according to the related product descriptions available on the website (http://asterweb.jpl.nasa.gov/content/03_data/01_Data_Products/release_surface_kinetic_temperatur.htm).

To facilitate further analysis, the surface temperature of AST_08 data in units of degrees Kelvin has been converted to degrees Celsius (°C) using the formula:

$$\text{Temperature Value (°C)} = \text{DN*} \text{ Scaling Factor} - 273.15 \qquad (3\text{-}1)$$

Here the scaling factor is 0.1. The primary descriptive statistics of surface temperature during these observation periods are given in the Table 3.4 to provide some background information about the surface temperature distribution within the observation periods. The overall surface temperature during the daytime of 2003-11-03 appears the highest with an average of 32.35 °C, the surface temperatures during nighttime 2004-10-05 and 2003-10-28 happen to be the coolest and the second coolest with corresponding mean values of 19.95 °C and 21.03 °C comparing with most of the observations averaging 26~28 °C. The daytime observations demonstrate a wider range of surface temperature deviation within whole study area than the nighttimes with higher Standard Deviation (STD), with the biggest residing in 2003-11-03. In comparison, the nighttime observations tend to be stable across space with the smallest STD (1.50) in 2005-10-01. In the following part, the data of remote sensing satellite images utilized in this research would be introduced first to offer one primary visual examination.

Table 3.4 Descriptive statistics of surface temperature for the images used in this research

DATE	TIMEOFDAY	MIN	MAX	MEAN	STD
2006-04-17	11:03:00.75	18.15	44.75	26.74	2.99

2005-10-23	11:02:39.38	17.15	41.85	26.60	3.18
2005-10-01	22:34:53.95	22.15	33.85	28.27	1.50
2004-11-21	11:02:10.94	14.95	42.85	25.57	3.34
2004-10-05	22:41:13.71	11.95	29.25	19.95	2.76
2003-11-03	11:03:35.52	22.25	49.45	32.35	3.46
2003-10-28	22:35:49.75	14.85	27.25	21.03	1.82

LST Images of ASTER:

It is acknowledged that the satellite LST (Land Surface Temperature) images are reliable for urban surface temperature study under clear, calm weather situation. The cloud amounts of the LST images ordered are all below 5%. In this research, the simultaneous background weather condition when the satellite images were taken is given in Table 3.5. The basic statistics description of the weather situation including wind speed in 0.1m/s, air temperature in 0.1°C, the percentage relative humidity based on the weather station records acquired from the Hong Kong Observatory is summarized. It shows that the weather situation during most of the satellite images acquisition periods is relatively stable, with most of the wind speed less than 3m/s. Except the wind speeds of the image time of daytime 11/03/2003 and nighttime 10/28/2003 are a little bit higher (5.67m/s and 4.75m/s), the relative humidity of image time in nighttime 10/01/2005 is quite high reaching 89.1%, this biggest relative humidity may cause possible bias for future analysis and should be noted before any interpretation made. During this observation period from 2003 to 2006, the highest air temperature (28.50°C) appeared in the image time of daytime 11/03/2003, which is agreed with the surface temperature observation at that time appearing to be the highest in average. Apart from this, these meteorological data also provides important ancillary information which can also be used to facilitate the interpretation of the result of statistical correlation analysis.

Table 3. 5 Meteorological background for urban thermal landscape study

	Image Time	MIN	MAX	MEAN	STD
Wind Speed (in 0.1m/s)	B04172006	2	53	28.1	14.75
	B10232005	20	44	31.9	8.74
	B10012005	0	43	15.2	15.71
	B11212004	7	45	27.8	12.41
	B10052004	0	85	11.6	26.70
	B11032003	20	126	**56.7**	30.52
	B10282003	20	115	**47.5**	27.09
Air Temperature (in 0.1 °C)	J04172006	16.3	23.80	21.79	2.05
	J10232005	15.3	24.30	22.91	2.70
	J10012005	22.7	29.10	27.35	1.83
	J11212004	14.6	22.4	21.16	2.36
	J10052004	17.2	24.8	21.53	2.84
	J11032003	21.2	30.4	**28.50**	2.66
	J10282003	16.3	25.9	23.49	2.64
Relative Humidity (in %)	M04172006	43	76	58.9	8.71
	M10232005	52	77	58.3	7.33
	M10012005	84	92	**89.1**	3.06
	M11212004	44	68	54.7	6.96
	M10052004	40	88	66.6	15.51
	M11032003	23	48	34.0	8.35
	M10282003	53	83	67.1	8.67

Source: Computed based on the weather station records of HKO

The LST images utilized in this research for urban thermal landscape study were listed below, in Figures 3.3, 3.4, 3.5, 3.6, 3.7, 3.8, 3.9. All these images have been clipped to one overlaid region of study area. Most images are of good quality, except the LST image in 10/01/2005 which contains obvious stripping noise. The useful information of LST images provided with day-night and seasonal change made urban thermal landscape study at meso-scale possible and enables the systematic study of urban effect on local surface warming based on urban thermal landscape monitoring and analysis.

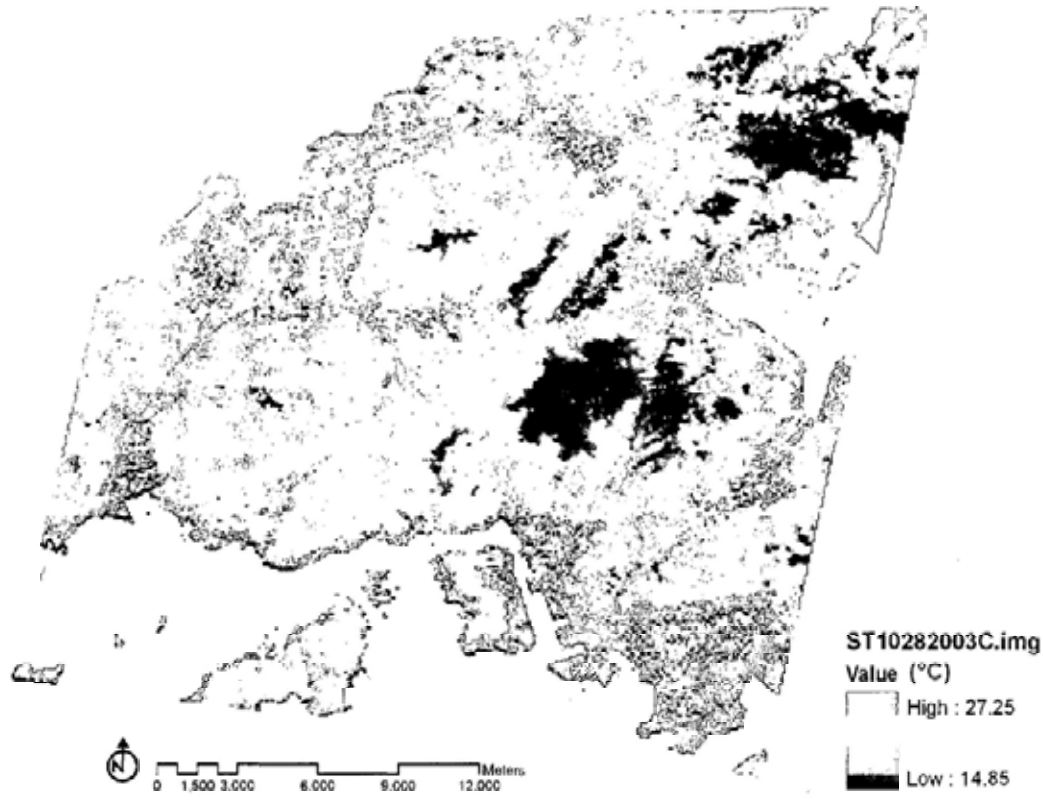

Figure 3.3 Land surface temperature image during nighttime 10.28.2003

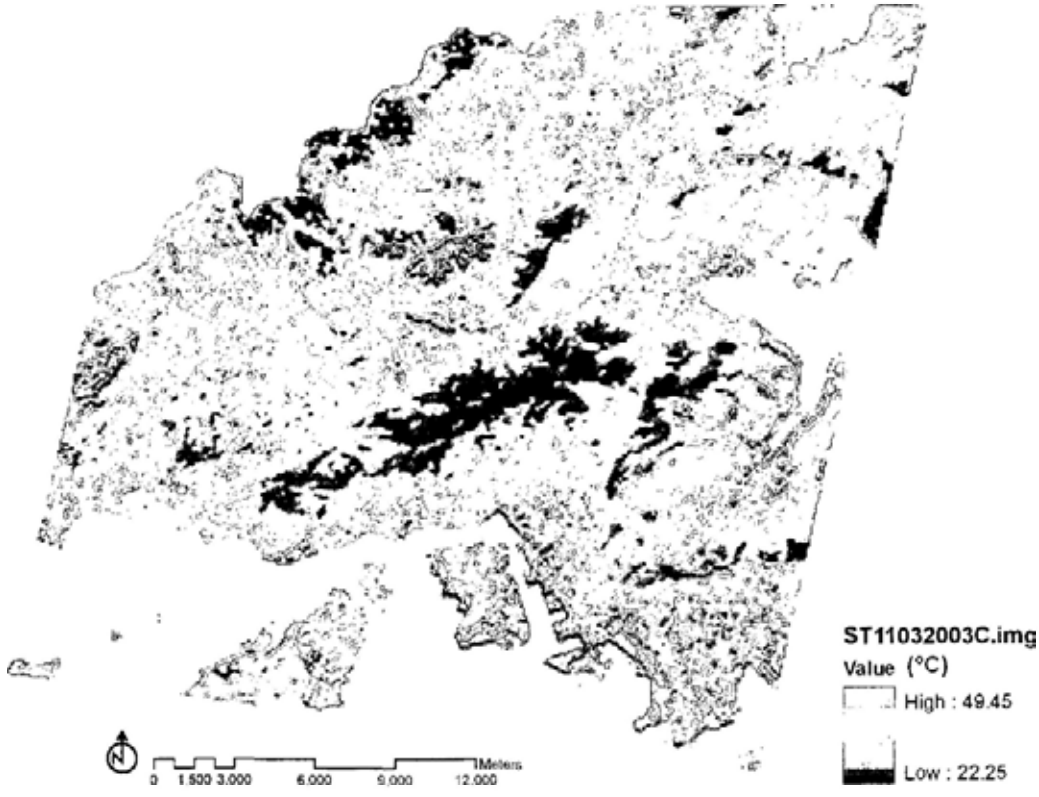

Figure 3.4 Land surface temperature image during daytime 11.03.2003

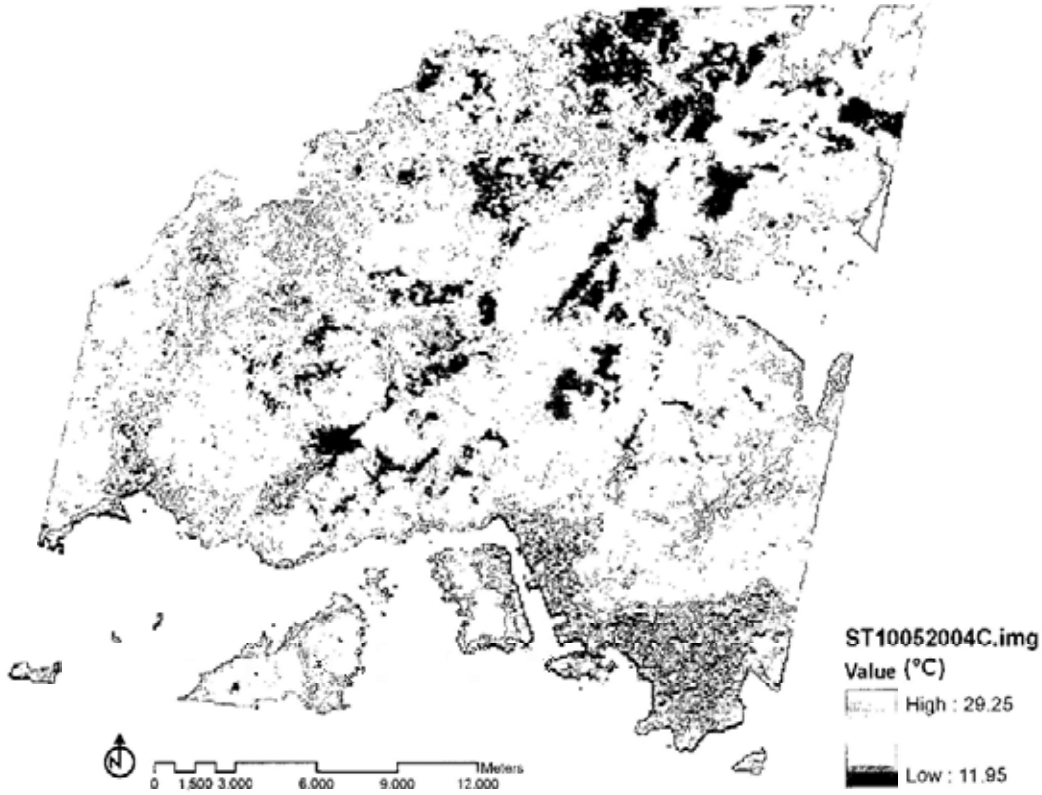

Figure 3.5 Land surface temperature image during nighttime 10.05.2004

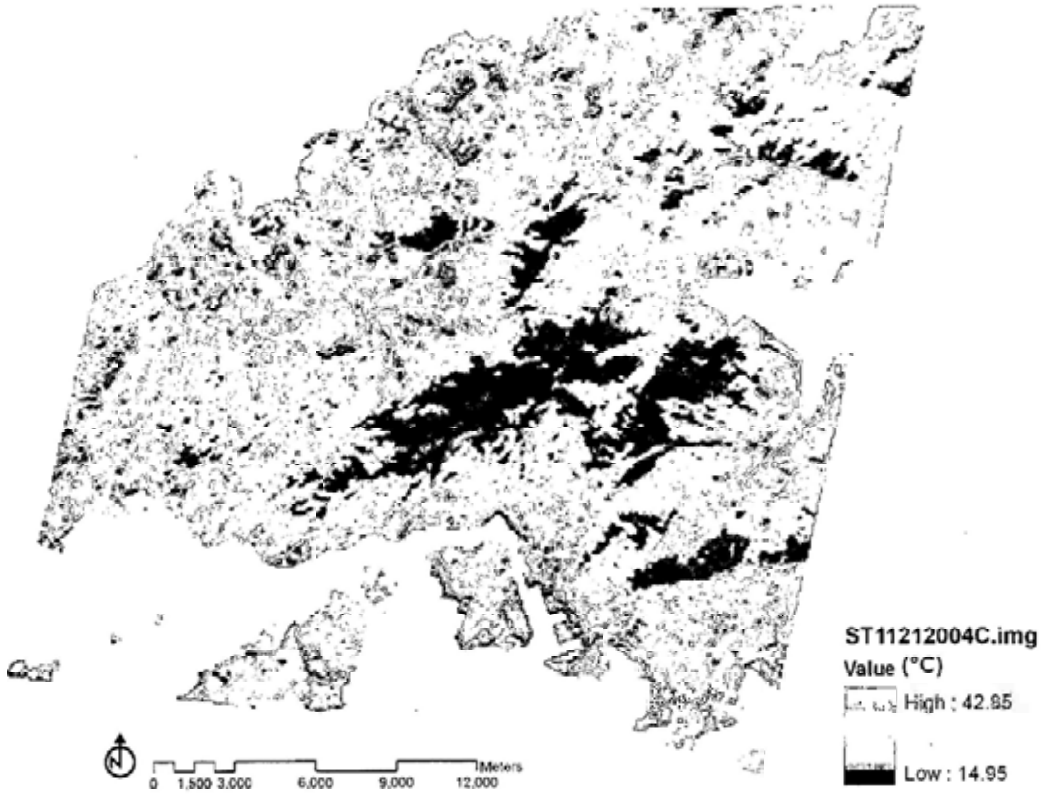

Figure 3.6 Land surface temperature image during daytime 11.21.2004

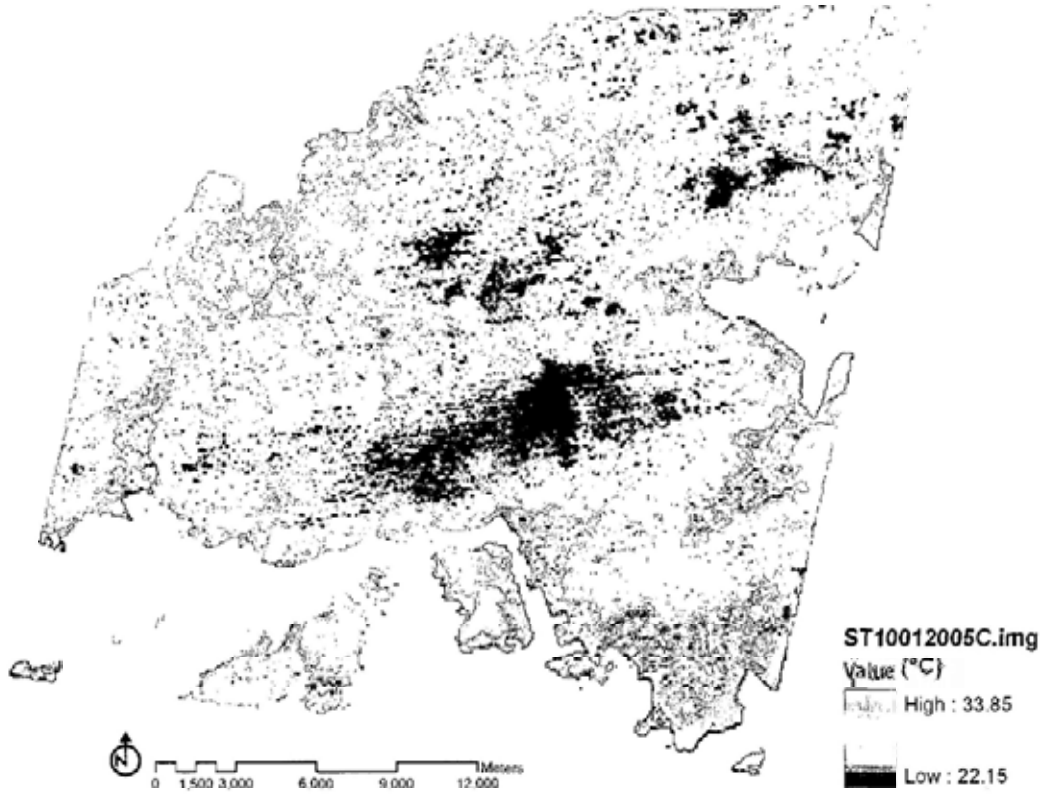

Figure 3.7 Land surface temperature image during nighttime 10.01.2005

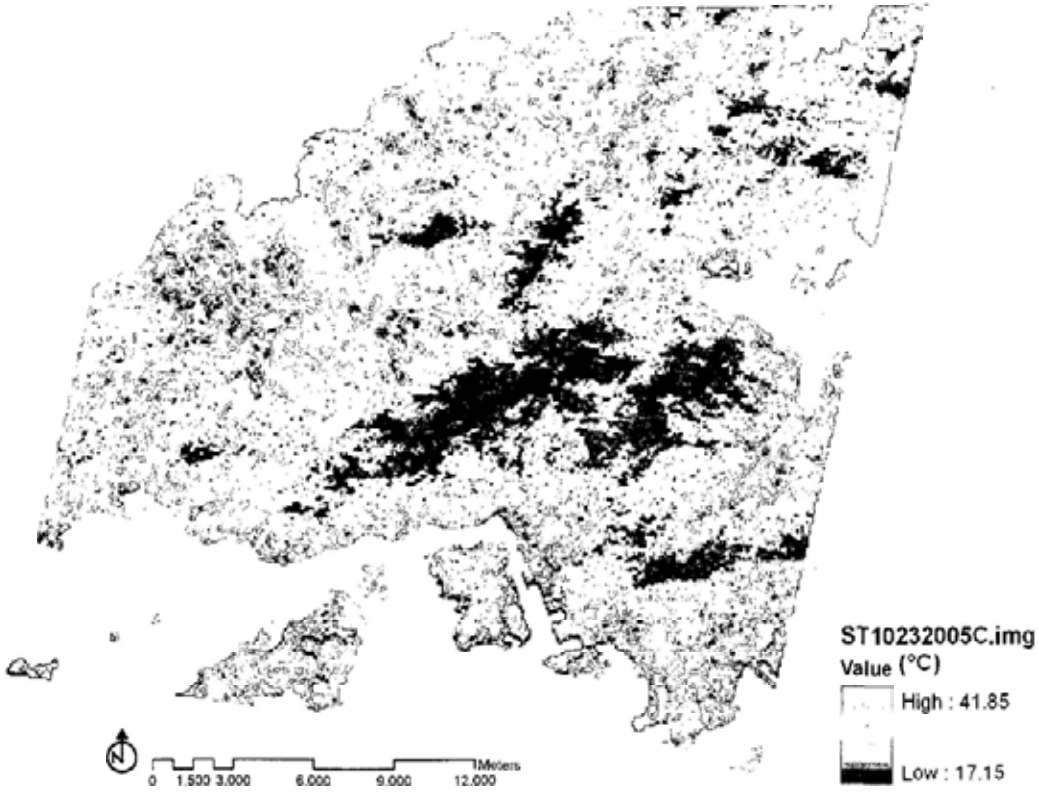

Figure 3.8 Land surface temperature image during daytime 10.23.2005

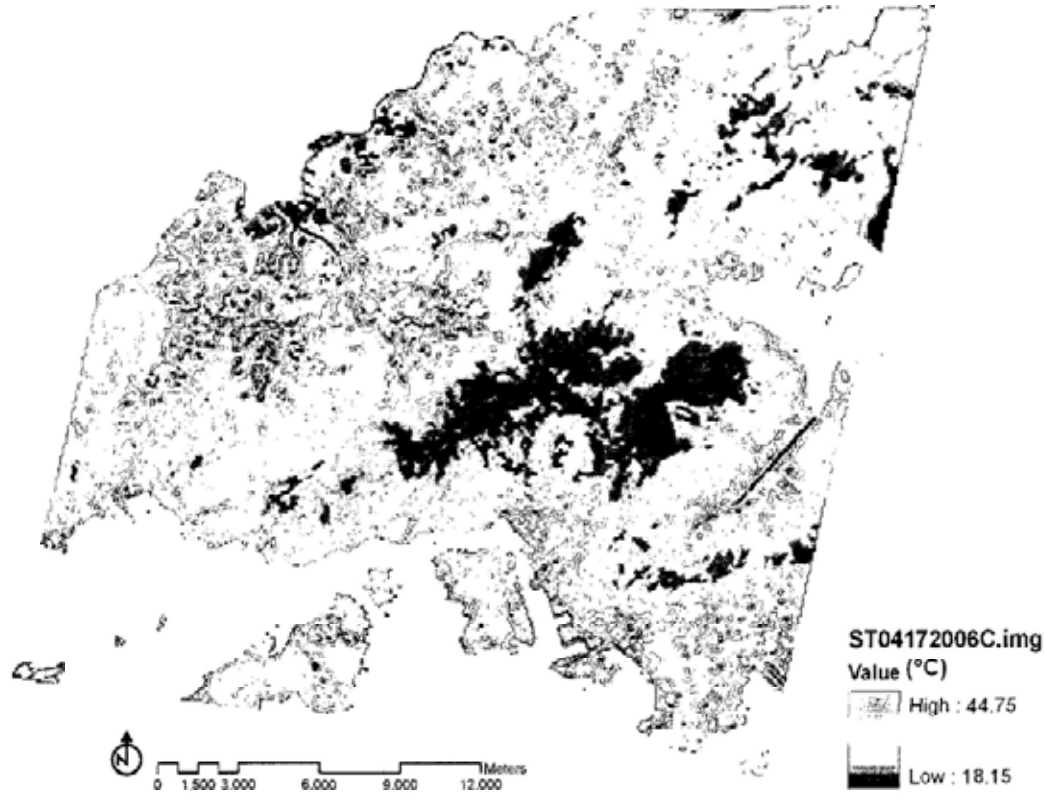

Figure 3.9 Land surface temperature image during daytime 04.17.2006

VNIR Images of ASTER:

The Visible and Near Infrared (VNIR) images are shown in Figures 3.10~3.13, to give a rough examination of urban ecological environment, mainly focusing on the vegetation situation which can be easily identified from VNIR images. During the dry season of October and December when most of the satellite images utilized in this research were acquired, hill fire happened frequently. It creates a unique phenomenon for thermal environment study during urban thermal landscape investigation and may have some special influence on local surface temperature performance. Consequently it may affect the evaluation models performance by introducing some possible bias. Compared with LST images listed before, the large fired areas can be easily identified which had an extreme high surface temperature in LST images. At the same time, these fired areas are highlighted, and then special attention is required before any interpretation made for the landscape metrics analysis and future regression analysis when these fired areas included.

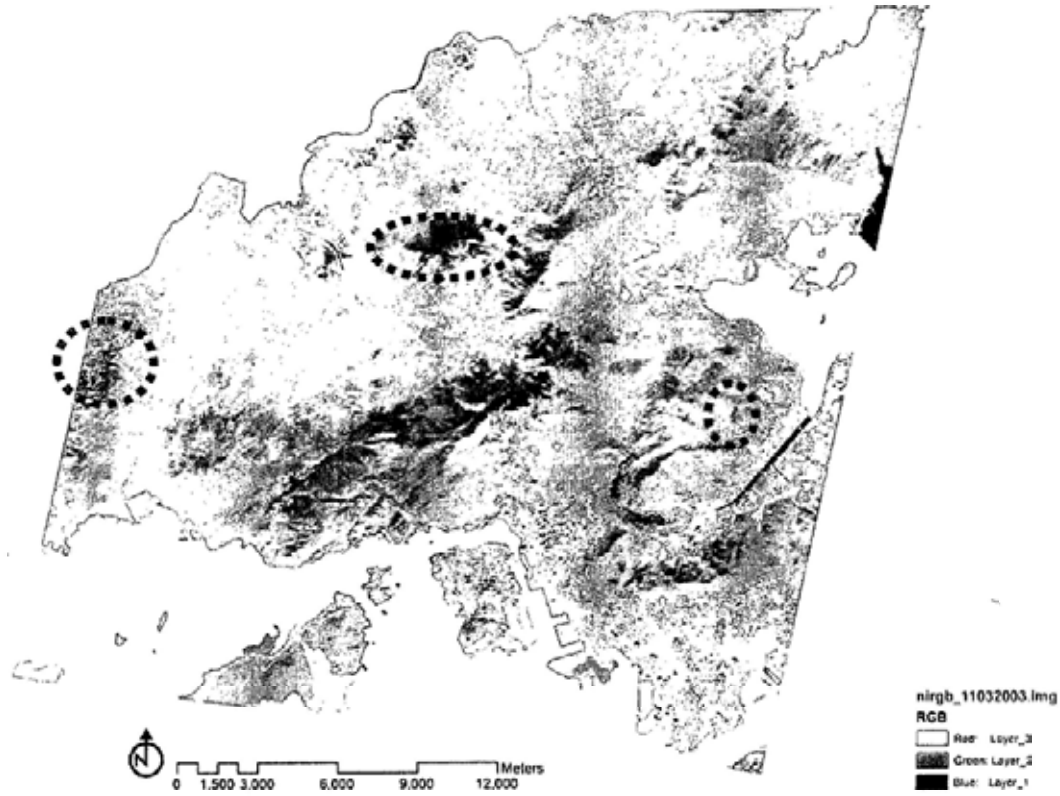

Figure 3.10 VNIR image in 11.03.2003

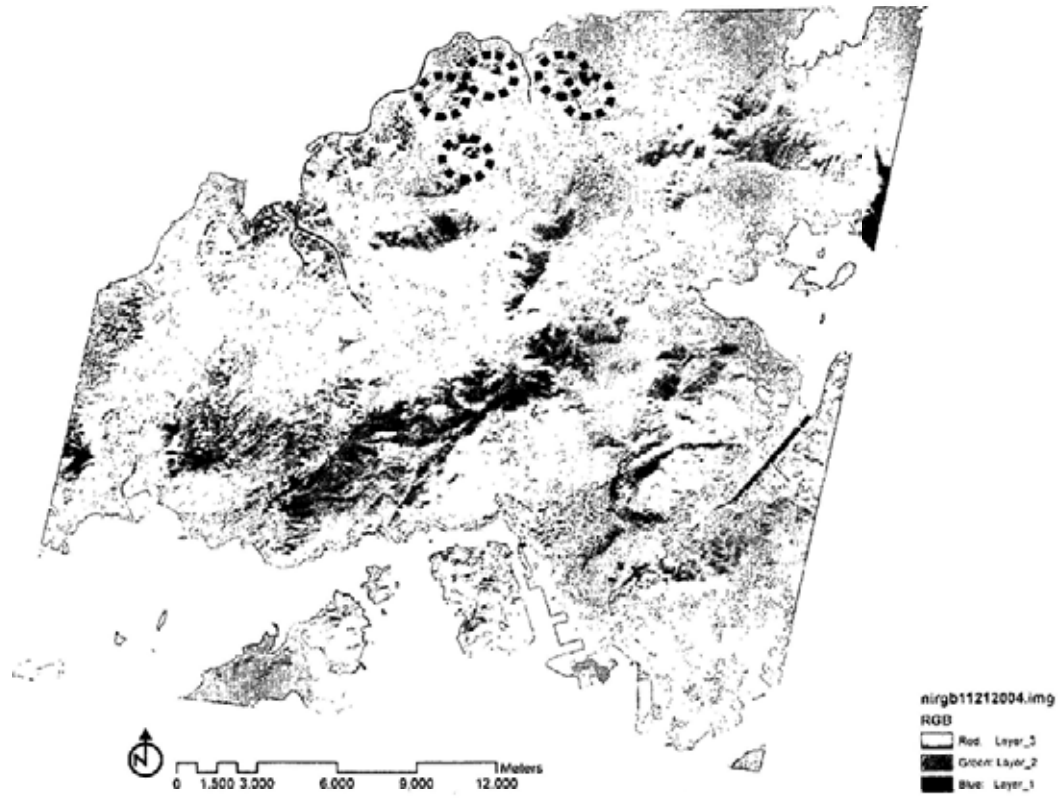

Figure 3.11 VNIR image in 11.21.2004

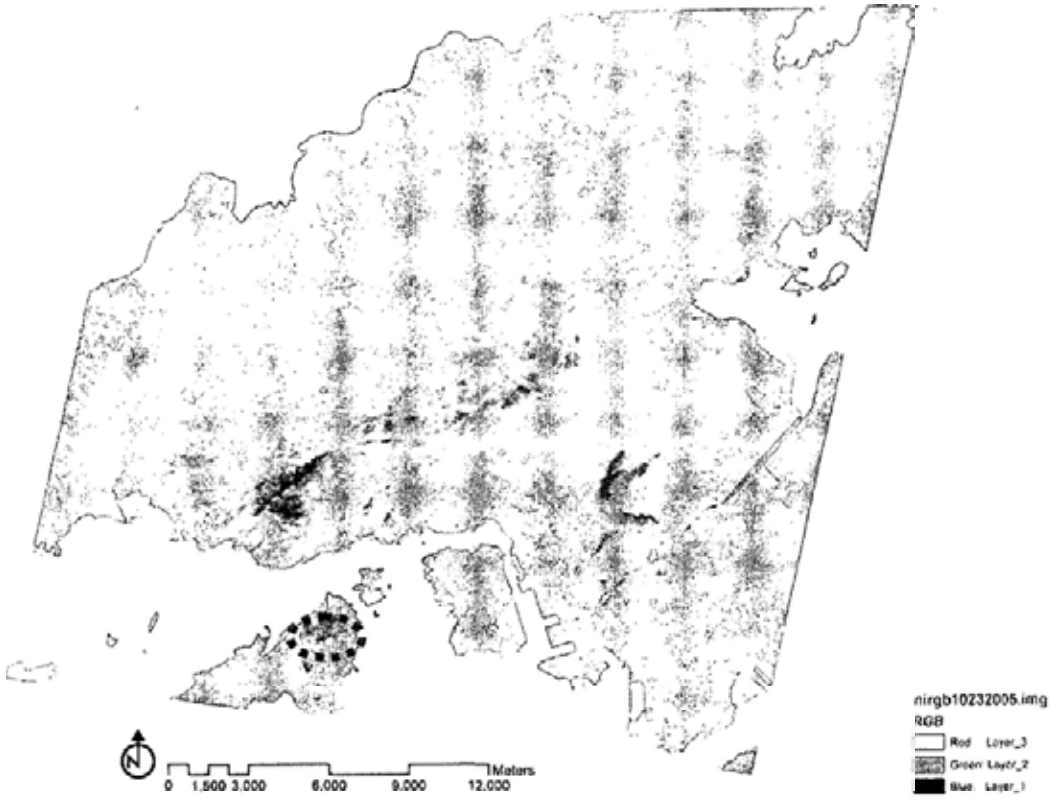

Figure 3.12 VNIR image in 10.23.2005

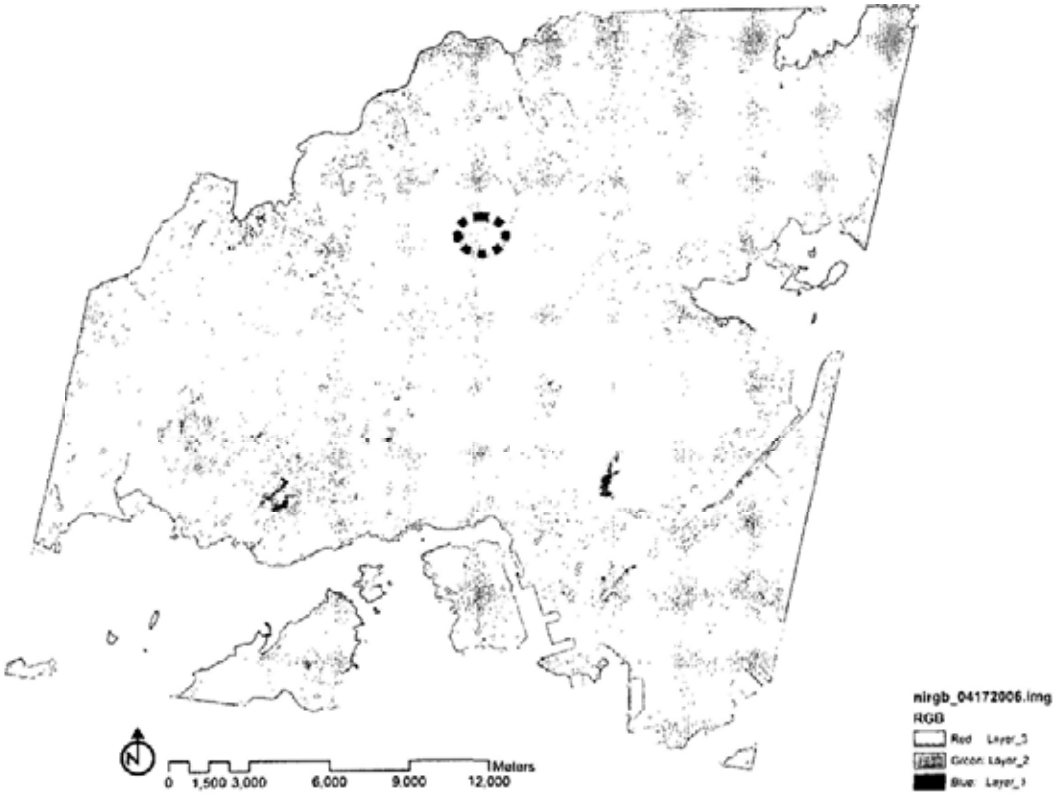

Figure 3.13 VNIR image in 04.17.2006

Besides the satellite images of ASTER LST and L1B for surface temperature and environmental parameters quantification, at the same time the map layers including building polygons, coastline, roads and railway, etc, extracted from the B5000 digital topographic map database and hydrography polygon from the B10000 vector database, DEM data in 5 meter resolution grid and the population census data of year 2001 are also acquired from the archived database of Department of Geography and Resource Management, CUHK for future geospatial analysis. The digital map data of B5000 and B10000 are originally ordered from the Survey and Mapping Office (SMO), Lands Department, the Government of HKSAR. With the meteorological data including one-minute prevailing wind direction, mean wind speed, relative humidity and air temperature, one-hour total cloud amount and visibility collected from the Hong Kong Observatory (HKO) provides simultaneous background weather conditions during the ASTER images taken in order to facilitate the interpretation of correlation analysis.

3.3. Research Assumptions

The warming of the urban environment especially in summer has many adverse impacts on local residents because of its implications for human comfort and well being (Svensson and Eliasson, 2002; Eliasson, 2000). Of course, human beings respond to air temperature rather than surface temperature (Brown and Gillespie, 1995), but the former is notoriously difficult to model and cannot be easily influenced by landscape design (Brown and Gillespie, 1995). Gill et al.'s (2007) argued that "In practice heat transfer from surfaces, and its interaction with radiative balance, is a significant factor in determining human comfort, especially on hot days with little wind (Matzarakis et al., 1999). Whitford et al. (2001) therefore considered surface temperature to be an effective indicator for energy exchange in the urban environment". Urban surface warming or urban rural surface temperature difference is notable and widely evidenced with thermal infrared remote sensing (Landsberg and Maisel, 1972; Landsberg, 1976). Despite the fact that turbulent mixing of the

atmosphere tends to obscure the influence of urban-rural daytime surface temperature differences in air temperatures, the net daytime urban impact on the atmosphere is large (Goward, 1981). To this end the urban effect on local warming can be tackled with linkage to urban surface warming in the assistance of urban surface thermal landscape study. In this thesis, the focus would be put on local surface warming based on the elevated land surface temperature derived from thermal infrared remote sensing which is regarded as important contribution and essential to the development of urban warming and can be examined through a systematic investigation of the urban surface thermal landscape in detail.

In the literature reviewed in previous chapter, urban thermal environment, in particular UHIs is the integrated output of urban geography, regional climate and ecology, with the factors affecting UHIs summarized in Figure 3.14. From the urban landscape point of view, "each component surface in urban landscapes (e.g., lawn, parking lot, road, building, cemetery, and garden) exhibits a unique radiative, thermal, moisture, and aerodynamic properties, and relates to their surrounding site environment" (Oke,1982). The surface composition and configuration of urban fabrics which is fragmented and intensively variable in the spatial distribution made the heterogeneity and complexity of urban surface thermal landscape in spatial-temporal dimension. From this perspective landscape composition and configuration are hypothesized to influence urban surface thermal landscape represented by urban surface temperature distribution. Understanding the link between spatial heterogeneity of urban environment and urban surface temperature variation is the main objective of this research. Urban surface thermal landscape pattern would be related to urban environmental setting in order to study the surface thermal performance of urban canopy. Under this assumption, this study would focus on the following urban elements which are referred to have certain impacts on urban thermal performance in the literature, based on which the correlation modeling can be constructed to study urban effect on local surface warming or local surface temperature disparities.

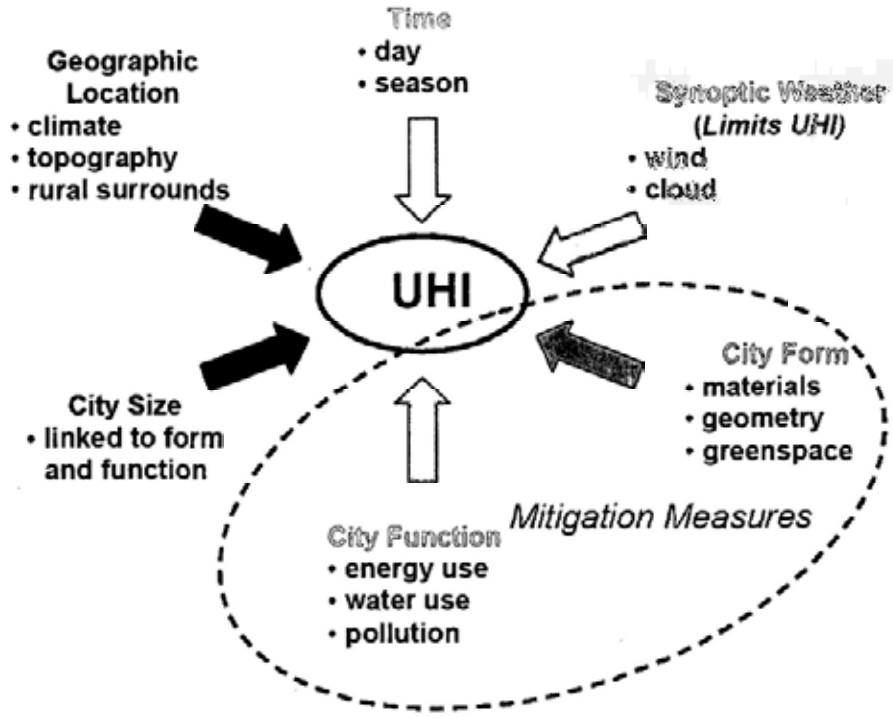

Figure 3.14 Factors affecting Urban Heat Islands (UHIs)

Source: Voogt (EPA presentation)

Solar Radiation:

Solar radiation is the dominant driving force of land surface heating and local variation of solar illumination plays an essential role on urban surface thermal dynamics during daytime (Voogt, 2004). The pattern and composition of urban surface thermal landscape is directly subject to local solar radiation situation. Knowledge of the insolation amount at specific geographic location is helpful for understanding the local heating process and the dynamics of surface thermal landscape pattern during daytime observation. There has been quantity of research undertaken to associate solar radiation with global warming with many debating received to the outputted findings and discussion (Scafetta and West, 2006; Stott et al., 2003; Foukal, et al., 2006). Here solar radiation is regarded as one dominant source of urban surface heating at daytime. Therefore in the modeling process of urban daytime surface heating, the variation in local solar illumination would be

considered as an important factor and calculated based on GIS in order to measure its influences on local surface temperature variation, which would aid interpret the local surface warming process under the confinement of urban form.

Vegetation:

Vegetation has a direct correspondence with the radiative, thermal, and moisture properties of the Earth's surface that determine land surface temperatures (Weng et al., 2004). The cooling effect of vegetation is significant in urban area through the transpiration and photosynthesis function. It is widely observed that the area covered with vegetation would be a few degrees cooler than areas without vegetation covering during daytime. At the same time, vegetation can reduce solar heat gain in buildings and can thus reduce the demand for mechanical cooling through air conditioning (Gill et al., 2007). "The difference in the NDVI between urban and rural regions appears to be an indicator of the difference in surface properties (evaporation and heat storage capacity) between the two environments that are responsible for differences in urban and rural minimum temperatures" (Gallo et al., 1995). The thermal behavior of vegetation may directly relate to the amount of vegetation and the growth situation. Increasing the amount of vegetation in urban area has been taken as one usual measure for UHI mitigation and regarded as one cost effective strategy in past urban planning and design practice.

Apart from vegetation loss, the vegetation cover is fragmented and isolated where human intrusion occurred during urbanization process, the cooling effect of vegetation may be greatly depressed. At the same time, the effectiveness of vegetation cooling presents diversely under different climate and geography situation. Increasing vegetation may lead to the moisture increase. The cooling effect may be weakened in hot humid area, which is not favorable in this region as well. In summary, the cooling effect of vegetation is subject to the growth situation, amount, coverage, etc., it is also confined by local climate. Therefore it is necessary to reexamine the effectiveness of vegetation under site specific circumstance before

formulating corresponding local knowledge for future "green" development.

Water Body:

It is normally experienced in our daily life that the temperature becomes pleasantly cool when approaching water body, especially when close to large area of water body like sea or lake. It is also widely recognized that urban parks and bodies of water can create 'cold islands' within the thermal landscape (Upmanis et al., 1998). For example, air moving along the edge of the River Thames or within urban parks is, on average, 0.6 °C cooler than air in neighboring streets (Graves et al., 2001).The thermal capacity of water body is quite high compared with other surface materials in urban area, it absorbs lots of heat during daytime, which may help keep the temperature relatively lower than other area. The cooling effect of water body is obvious when large amount exists during daytime. This may also contribute to sustain a comfortable thermal environment during hot season. Usually, the effect that a water body may have on the local climatic conditions of a site diminishes not only with distance from the water body, but with the elevation as well (Oke, 1978). In this thesis, the correlation between water body and local surface temperature would be investigated in such a hot humid city, Hong Kong, in order to discuss its local influence on urban thermal landscape.

Elevation:

Since Hong Kong is a mountainous area, the topographic complexity generates a microclimate environment with high diversity. It is widely acknowledged that the hilly topography with intensive elevation variation can directly diversify local thermal environment in general. Energy and moisture are height dependent (Piringer, et al., 2002). The influence of mixing height on local surface thermal energy is noticeable. Taken as an important element which controls the urban thermal environment, elevation is also taken into statistical model for urban surface thermal landscape analysis. This would contribute to make the analysis modeling for a

comprehensive investigation of urban surface thermal landscape integrated in a systematic way. Moreover it helps improve the statistical analysis modeling and facilitate interpretation with satisfying explanation strength.

Site openness to the Sky:

In a high rise and high density urban environment, the canyon effect of street geometry cannot be ignored. The urban canyon geometry helps to trap solar heat during daytime and make the heat transfer to open air difficult during night. It inevitably favors urban warming in a large part under high rise high density settlement. The canyon effect is important in urban energy process. Its effect on urban thermal environment can be studied with effective quantification. In the literature, Sky View Factor (SVF) has been used to quantify the site openness to the sky of street canyon. The strong correlation between SVF and UHI intensity has been recognized (Souza et al., 2004) and summarized using a formula by Oke (1987).

A quantity of research has been carried out to investigate the relationship between urban site openness to the sky and local thermal performance, most of the analysis focused on estate or local scale due to the intensive calculation required (Li et al., 2004; Souza et al., 2004), and the systematic study at urban scale is limited. How the canyon affects local surface warming in a hot humid subtropical city would be studied in this study, in which diffuse radiation would be utilized as the quantification of site openness and calculated based on GIS software package ArcGIS 9.2. With this factor taken into consideration the urban configuration can be evaluated to analyze its influences on local surface temperature variation. It will help to enrich our understanding of the effect of urban configuration on local thermal environment, at the same time it can be utilized as one potential strategy for urban cooling design with the local acknowledge acquired through site specific analysis.

Population Density:

Besides the energy directly coming from solar radiation, the anthropogenic heat

released to urban area also contributes to the urban warming due to population concentration, air pollution, transportation congestion, etc, which issues take place synchronously when huge population aggregates within urban canopy. The population distribution with various densities within city area was proved to have a close relationship with urban heat island occurrence. The strong correlation has been observed by Oke (1973) in North American and European cities, that the developed regression model successfully explained 97 percent of the variability in UHI intensity with the single predictor variable of population size. An analysis of urban temperature changes in the U.S. based on population (Karl et al., 1988) showed a local increase of approximately 1°C per 100,000 people due to urbanization. Therefore population is one factor worthy of further investigation in order to clarify its local impacts on urban surface thermal landscape. In this study population density is calculated based on census data for each region and taken into correlation analysis in order to explore the impact on urban surface warming.

Road Network Density:

The exhaust gas and heat released from transport vehicle is also a noticeable source contributing to temperature rise of urban area with a dense traffic network. The released gas significantly changes the urban thermal environment by direct heating and chemical interaction with green house gas during the heating process. The polluted air also decreases the solar radiation received on urban surface and influences local surface temperature detected by thermal infrared remote sensing. In this context, urban road network is hypothesized to have an influence on local surface temperature variation which would be taken as one measure of urban traffic in order to examine its influences on local surface warming. In this study the road network density would be calculated and serves as the surrogate quantification of urban transportation to examine the potential influence of urban traffic on local surface warming.

Building Cluster:

Regarding the influences of urban buildings on local thermal environment, Landsberg (1970) contends that even "a single block of buildings will start the process of heat island formation". Under the urban canopy, urban density is an important feature that reflects the building development of a city in urban planning and design. As Isaac referred (2001), "a given urban density can be the result of two design features: (i) the fraction of the urban land covered by buildings, and (ii) the average height of the buildings in the given urban section." The UHI studies of European and North American cities found that the density and height of buildings are significant factors affecting the steepness of the urban-rural temperature gradient (Oke, 1982). During the urbanization process with high density building development, the replacement of natural evaporative surface with concrete man-made surface significantly alters the radiative property of urban surface which directly leads to the enhanced surface temperature. Following with local surface temperature rise, UHI develops significantly in altitude and frequency along with the increase of urban density through altering the physical and geometrical character of urban canopy. Chandler (1967) found that urban-rural temperature differences were more closely related to local building density than to city size. The urban building cluster is thought to be a key factor favoring local surface warming, in this study building square footage would be calculated serving as the building cluster measurement for statistical correlation analysis. Then the influence of urban building coverage on urban surface warming in subtropical region can be evaluated.

Background Climate Condition:

Apart from urban topography, land use, urban form aforementioned which directly controls the thermal performance of urban surface would be taken into consideration for urban surface warming investigation. Moreover urban local thermal environment is under the confinement of provided regional background climate. The formation and magnitude of urban rural temperature difference and intra-urban temperature disparities also depends on weather conditions including atmospheric humidity and

wind. The urban-rural temperature difference, when it exists, is generally largest under clear sky and calm wind conditions and smallest with cloudy and windy conditions (Kidder and Essenwanger, 1995). The background regional climate which also limits the influence exertion of such factors on local surface temperature variation in a certain degree would be examined during this investigation. Thus the background climate information has been collected from the Hong Kong Observatory (HKO) and use as reference in this study, mainly including:

- Wind Speed & Direction
- Cloud Amount
- Visibility

The necessary background climate information for the study would be provided to facilitate statistical model interpretation for the study of urban effect on local surface warming.

3.4. Framework of the Research

"The city has a myriad of microclimates that are intimately linked to the composition of its surfaces and the spatial and physical features of its structures" (Terjung and Louie, 1973).The heterogeneity of urban surface composition and configuration is fragmenting urban surface thermal landscape across space and time, ultimately it directly leads to and impacts urban warming through heated urban surface. Even the urban surface in high temperature is acknowledged as the important contribution of urban warming, Quattrochi and Ridd (1998) revealed that "a number of investigators have provided evidence using thermal infrared remote sensor data that urban areas are strong daytime longwave radiators, but they have provided limited knowledge on the thermal energy responses contributed by discrete surfaces common to the urban landscape". The thermal energy responses of urban warming contributed by discrete surfaces can be tackled with an improved understanding of urban surface thermal landscape. This made a comprehensive investigation of local surface temperature variation necessary. During the previous research, effort has been made to investigate

the correlation between UHI and a few isolated parameters. Some efforts from architecture community have focused on urban street geometry, energy efficiency building design and construction, from which aspects to evaluate thermal performance in one district region or estate (Hui, 2003; Chan and Yeung, 2005). Other research activities have concentrated on the physical properties of urban surface, such as vegetation, water body, etc. influence on urban surface temperature at the urban scale (Lo et al., 1997; Hardegree, 2006). It delineates the influences of such factors on urban thermal environment. The mechanism of urban warming under the influence of these isolated factors can be explained to some extent from this isolated perspective.

However, the integrated local impact of both geometrical and physical features of urban structure on urban surface warming is scarcely examined systematically at medium scale. It is difficult to generate a comprehensive understanding regarding how the urban surface thermal environment will perform under the local environment as a whole. In this study the effort will be made to explore the mechanism of urban surface temperature heterogeneity driven by the integrated function of both geometrical and physical configuration of urban fabrics at meso-scale. All the parameters above mentioned which are assumed to be related to urban surface thermal performance will be taken into statistical analysis in order to clarify the correlation between the urban surface temperature and the integrative functionary of these factors. It would advance our understanding of urban surface warming.

"Understanding how thermal energy is portioned across a landscape, and the magnitude or variations in surface temperatures emanating from various landscape elements, is essential to defining the overall mechanisms that govern land-atmosphere interactions" (Quattrochi and Luvall, 1999b). Landscape can be viewed as an interacting mosaic of patches or ecosystems relevant to the phenomenon under consideration (McGarigal and Marks, 1995), therefore landscape change is the alteration in the structure and function of the ecological mosaic over time (Forman

and Godron, 1986). From this perspective urban surface temperature pattern could be viewed as a kind of landscape, i.e. urban surface "thermal" landscape, the variation of surface temperature across space and time can be conceived partly as the direct or indirect outcome of local environment, then the underlying process of urban surface warming could be explored by monitoring the spatial and temporal dynamics of surface thermal landscape mosaic and analyzing the interactive correlation between surface thermal landscape pattern and urban environment.

With the advancement of remote sensing technology and GIScience, it contributes great opportunity for landscape monitoring and assessment by combining remote satellite imagery of landcover, Geographic Information System (GIS) technology, and recent advances in the science of landscape ecology (Riitters et al., 1995; Forman and Godron, 1986). In this regard, for urban thermal landscape monitoring and analysis, introducing the methodology of landscape metrics to speculate on urban surface temperature pattern would assist in quantifying the structure of urban surface thermal landscape. These measurements of landscape metrics would provide quantitative descriptive statistics and prior knowledge regarding the overall structure of urban surface thermal landscape for advancing our correlation analysis. Besides, remote satellite imagery of land cover and geospatial analysis of Geographic Information System (GIS) would provide accurate quantification of local geometrical and physical structure. Based on these assumptions discussed in last section, the statistical correlation can be established between surface temperature and local environmental parameters in order to investigate the influence of local environment on urban surface warming. The systematic investigation of urban surface thermal landscape is fulfilled through urban thermal landscape monitoring and analysis. The general framework of this research is proposed as following Figure 3.15.

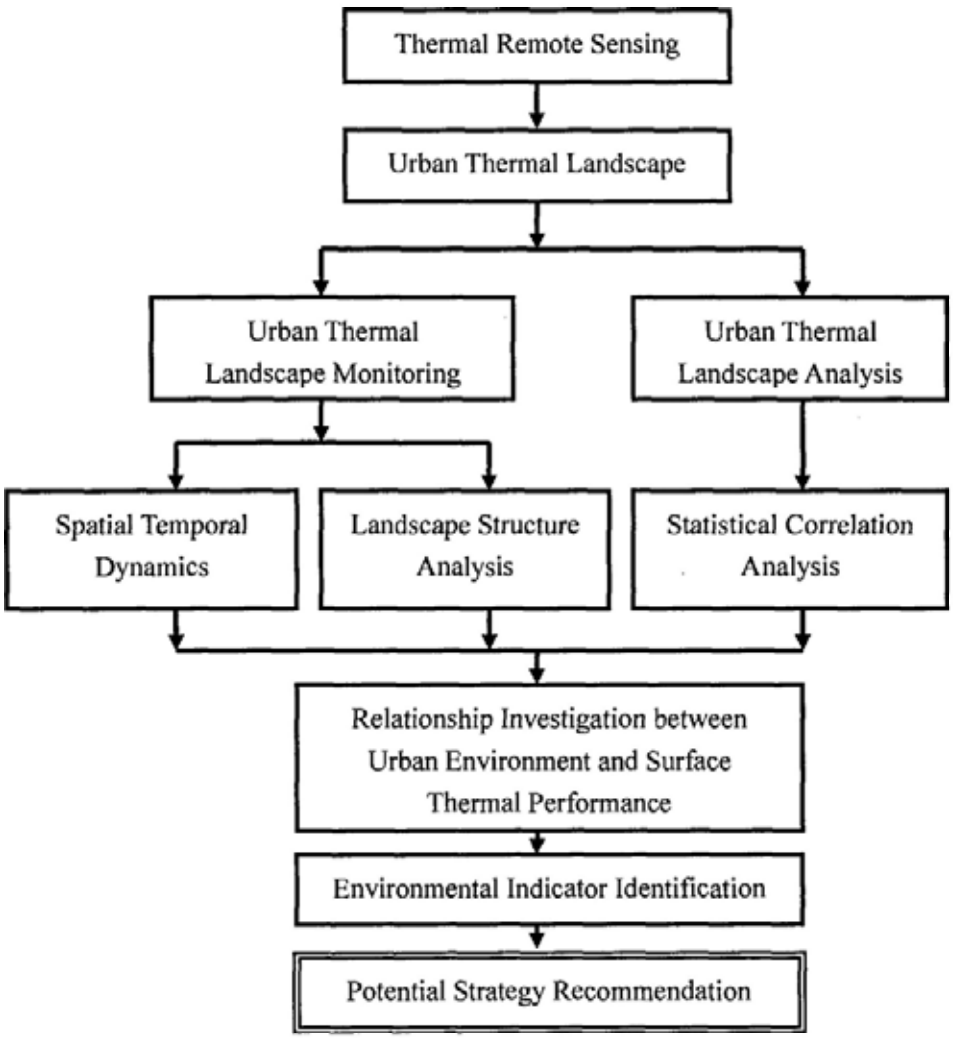

Figure 3.15 Proposed research framework

What is the surface temperature pattern observed? Has this pattern changed through time? Understanding the overall structure of surface thermal landscape pattern is necessary for a systematic investigation. A prior knowledge about the composition and configuration of spatial patterns in observed thermal landscapes would be provided first to characterize the context of research inquiry. First, the approach proposed deals with urban surface temperature map with landscape metrics methodology. The utilization of landscape metrics provides quantitative measures for characterizing the overall structure of urban surface temperature pattern, the spatial-temporal dynamics of urban surface thermal landscape first can be acknowledged by comparison across space and time in order to provide substantial context for following inference based on statistical analysis.

For urban thermal landscape analysis, the conceptual design is shown in Figure 3.16. Earth observation satellites have been frequently used in recent urban studies of local climatic variations with independent observations. "Images from satellite sensors provide a large amount of cost-effective, multi-spectral and multi-temporal data to monitor landscape processes and estimate biophysical characteristics of land surfaces" (Weng, 2002). Besides urban surface temperature map derived from remote sensing data, a host of biophysical indicators listed below can be generated from satellite images as well. In conjunction with geographic information systems (GIS) geospatial analysis, other measures of urban form, such as location and elevation, site openness to the sky, etc., which is listed in the box below, can be calculated to quantify site specific physical and spatial characteristics. All these measures would be employed in statistical models to analyze the interaction between urban form and urban surface temperature variation together with climate ancillary observation.

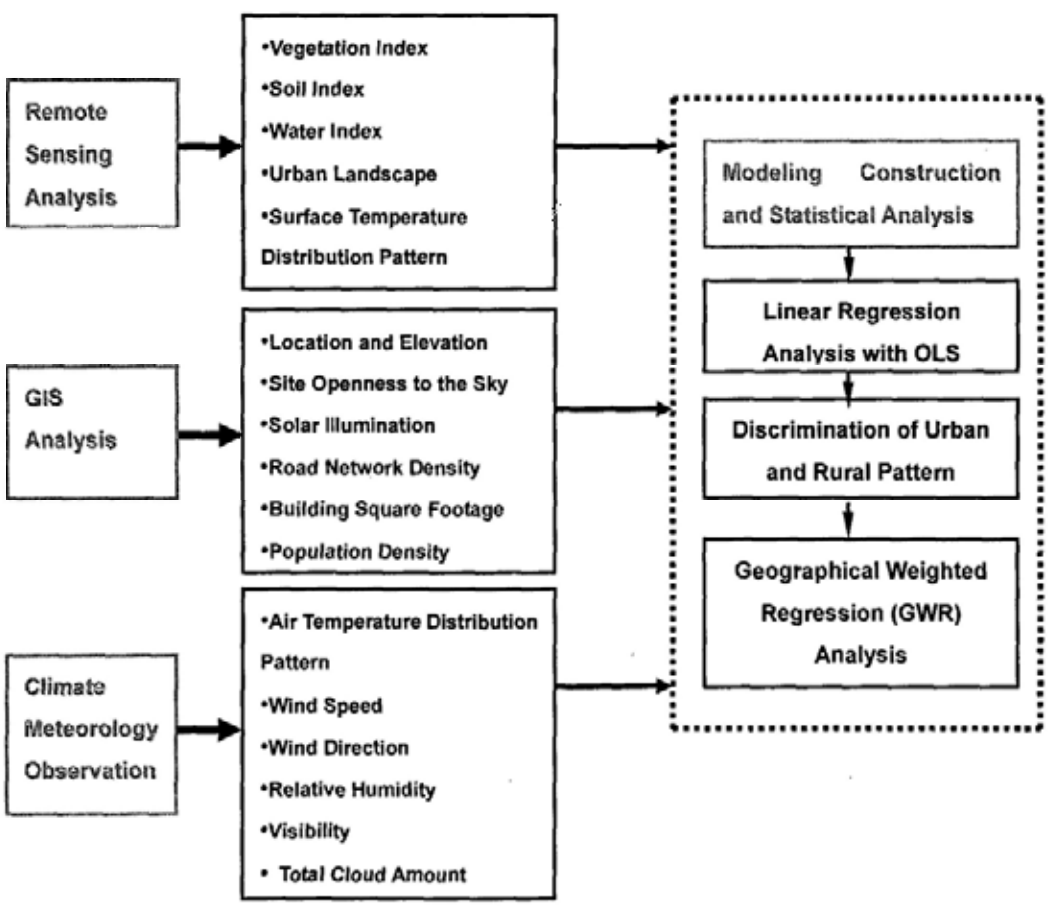

Figure 3.16 Conceptual design of thermal landscape correlation analysis

3.5. Urban Thermal Landscape Characterization and Analysis

3.5.1. Landscape Metrics

Derived from landscape ecology which the quantification of environmental heterogeneity has long been an objective (O'Neill et al., 1988), landscape metrics is often used to quantify spatial-temporal dynamics of landscape pattern. This spatial technique has been widely employed to derive quantitative measures of spatial patterns present in maps or remote sensing imagery (Carrão and Caetano, 2002). Its historical development was thoroughly reviewed by Naveh (1982). Using this technique various spatial indices have been designed to characterize the structure of spatial variability at each given time and their dynamics over different times in a variety of ways corresponding to different representations of landscape pattern. "Different from the direct comparison of two classified maps, the landscape metrics technique takes advantage of capturing inherent spatial structures of landscape pattern and biophysical characteristics of these spatial dynamics"(Tang, 2007).

There are now literally hundreds of quantitative measures of landscape pattern and various software programs to calculate them (Riiters et al., 1995; Frohn, 1998). These landscape metrics are formulated either in terms of the individual patches or in terms of the whole landscape, depending on the emphasis sought (McGarigal and Marks, 1994). Landscape metrics fall into two general categories, Landscape Composition Metrics and Landscape Configuration Metrics (Carrão and Caetano, 2002). Landscape composition metrics may measure the spatial character of the patches, configuration metrics are measures of the placement or configuration of patch types relative to other patch. There are different analysis models developed to deal with landscape heterogeneity at various levels, namely, class, patch and landscape. Condeso and Meentemeyer (2007) caveat that although a large number of landscape metrics have been developed, no single metric captures all information about landscape pattern, and strong correlations between many make choosing an appropriate suite difficult. Determining how many metrics to use and how to combine

the metrics so that the results are meaningful and interpretable remains challenging (Turner and Gardner, 1991). The choice and interpretation of metrics indices should depend on the scale and or focus of the research under investigation.

O'Neill et al. (1994) maintained that change in landscape patterns could be characterized by the three metrics of *Contagion*, *Dominance* and *Fractal Dimension*. Since the targets of current investigation is urban surface thermal landscape represented by surface temperature image taken at various time. The range of surface temperature within image (i.e., the composition of temperature categories within each image) is quite different from each other due to time variability of observation. Moreover this research concentrates on the structure of overall urban thermal landscapes within study area at each image time. Our interest is to monitor the structure change of urban thermal landscape pattern over space and across time. To this end, the structural descriptive indices may be meaningful for this purpose.

In this research, the landscape metrics evaluation would be carried out at the landscape scale for overall structure measurement in order to achieve a general overview about the heterogeneity of urban thermal landscape, the structural descriptive indices would be the main focus. The metrics are selected from each category including (Herzog and Lausch, 2001; Griffith et al., 2000; Riitters et al., 1995): patch area metrics which measure the number and size of patches; edge and shape metrics which quantify the occurrence of ecotones; diversity metrics and landscape configuration metrics. The chosen set of metrics is listed in Table 3.6, including: Number of Patches (NP); mean patch area (AREA_MN); Largest Patch Index (LPI); Landscape Shape Index (LSI); Modified Simpson's Diversity Index (MSIDI); area-weighted mean Fractal Dimension Index (FRAC_AM) and Interspersion & Juxtaposition Index (IJI). The detailed illustration of such indices formulation and the specific features of these measures are outlined, with the corresponding formulas and descriptions of indices compiled from McGarigal and Marks (1995). Our interest would focus on measuring the structure of urban surface

temperature pattern as a whole and appraisal of possible temporal evolution and dynamic change of overall structure at each image time. These metrics are essentially measures of different properties of urban thermal landscape structure from difference aspects at the landscape level. The measures resulting from these metrics may be highly correlated. Despite this redundancy, however, it is important to test them all since each one points to a slightly different aspect of the spatial structure. The computation of such indices was performed through the software FRAGSTATS (ver.3.3, www.umass.edu/landeco/research/fragstats/fragstats.html).

Table 3.6 Landscape pattern metrics used in analysis

1) Number of Patches (NP)

NP=N

N = total number of patches in the landscape.

Range NP ≥ 1, without limit.

Description

NP equals the number of patches in the landscape. Note, NP does not include any internal background patches (i.e., within the landscape boundary) or any patches at all in the landscape border, if present.

2) mean patch area (AREA_MN)

$$\text{AREA\_MN}=\frac{\sum_{i=1}^{m}\sum_{j=1}^{n}a_{ij}}{N}$$

a_{ij} = area (hectares) of patch ij.

N = total number of patches in the landscape.

3) Largest Patch Index (LPI)

$$\text{LPI}=\frac{\max(a_{ij})}{A}(100)$$

a_{ij} = area (m2) of patch ij.

A = total landscape area (m2).

Range $0 < \text{LPI} \leq 100$

Description LPI equals the area (m2) of the largest patch in the landscape divided by total landscape area (m2), multiplied by 100 (to convert to a percentage); in other words, LPI equals the percent of the landscape that the largest patch comprises. it is a simple measure of dominance. Note, total landscape area (A) includes any internal background present.

4)Landscape Shape Index (LSI)

$$LSI = \frac{E}{\min E}$$

E = total length of edge in landscape in terms of number of cell surfaces; includes all landscape boundary and background edge segments.

min E = minimum total length of edge in landscape in terms of number of cell surfaces (see below).

Range LSI ≥ 1, without limit.

Description LSI = 1 when the landscape consists of a single square (or almost square) patch; LSI increases without limit as landscape shape becomes more irregular and/or as the length of edge within the landscape increases.

5)Modified Simpson's Diversity Index (MSIDI)

$$SHDI = -\ln \sum_{i=1}^{m} P_i^2$$

P_i = proportion of the landscape occupied by patch type (class) i.

Range MSIDI ≥ 0, without limit

Description MSIDI = 0 when the landscape contains only 1 patch (i.e., no diversity). MSIDI increases as the number of different patch types (i.e., patch richness, PR) increases and the proportional distribution of area among patch types becomes more equitable.

6)area-weighted mean Fractal Dimension Index(FRAC_AM)

$$FRAC\_AM = \sum_{i=1}^{m}\sum_{j=1}^{n}\left[\frac{2.\ln(.25P_{ij})}{\ln(a_{ij})}\left(\frac{a_{ij}}{\sum_{i=1}^{m}\sum_{j=1}^{n} a_{ij}}\right)\right]$$

p_{ij} = perimeter (m) of patch ij.

a_{ij} = area (m^2) of patch ij.

Range 1 ≤ FRAC ≤ 2

Description *Fractal dimension index* is appealing because it reflects shape complexity across a range of spatial scales (patch sizes).A fractal dimension greater than 1 for a 2-dimensional patch indicates a departure from Euclidean geometry (i.e., an increase in shape complexity). FRAC_AM approaches 1 for shapes with very simple perimeters such as squares, and approaches 2 for shapes with highly convoluted, plane-filling perimeters.

7)Interspersion & Juxtaposition Index (IJI)

$$IJI = \frac{-\sum_{i=1}^{m}\sum_{k=i+1}^{m}\left[\left(\frac{e_{ik}}{E}\right)\bullet \ln\left(\frac{e_{ik}}{E}\right)\right]}{\ln(0.5[m(m-1)])}(100)$$

e_{ik} = total length (m) of edge in landscape between patch types (classes) i and k.

E = total length (m) of edge in landscape, excluding background.

m = number of patch types (classes) present in the landscape, including the landscape border, if present.

Range $0 < IJI \leq 100$

Description IJI approaches 0 when the distribution of adjacencies among unique patch types becomes increasingly uneven. IJI = 100 when all patch types are equally adjacent to all other patch types (i.e., maximum interspersion and juxtaposition).

Source: McGarigal et al. (2002) Fragstats 3.3 Documentation

3.5.2. Regression Analysis

Multiple Linear Regression:

Urban surface thermal landscape can be characterized through the landscape metrics evaluation and spatial-temporal comparison of urban surface temperature pattern. In order to further improve our understanding of urban effects on local surface warming the correlation analysis would be carried out utilizing regression analysis to examine the potential mechanism of urban surface heating. Multiple regression analysis is a widely used technique to establish relationship among a dependent variable and a set of independent variable(s), which can be used to link urban environmental factors with local surface temperature and estimate the correlation in between. Traditionally, these statistical methods of correlation analysis have been applied at a global level. In a global analysis, the regression generates one set of parameters coefficients estimation representing one stationary relationship between variables which is assumed to apply equally over the whole study area.

A typical linear regression model can be written like:

$$y_i=\beta_0 + \beta_1 x_{1i} + \beta_2 x_{2i} + \ldots\ldots + \beta_k x_{ki} + \varepsilon_i \qquad (3\text{-}2)$$

For the i-th observation, with y_i denotes the dependent or response variable, βs refers

to the regression coefficients of independent parameters, x_{ji} (j from 1 to k) representing the set of k independent explanatory variables, and ε_i the residual which assumed normally distributed with zero mean and constant variance. From this equation it can be seen that the regression coefficients corresponding to each explanatory variable have no relation with observation location, meaning that the generated estimation of these coefficients is not spatially associated and assumed uniform across space. This stationary estimation of regression coefficients is realized through taking the local bias as residual in the computation, which leads to one overall "average" estimation of coefficients within whole study area. Under this global modeling process, the modeled relationship interpreted with global regression equation is supposed to be spatially stationary and uniformly applicable within the whole study area. Under these research assumptions discussed above, the referred urban environment measures would be quantified, global linear regression analysis can be employed to relate urban surface temperature with this set of urban environment parameters in order to examine the urban environmental association with local surface temperature variation. In this study, multiple linear regression analysis would be employed for this correlation analysis first to probe the relationship between urban environment and thermal landscape diversity. The outputted model can be utilized to interpret the urban effects on surface warming and provide a general reference for further local environment thermal effects exploration.

Geographically Weighted Regression (GWR):

As reviewed, GWR is a useful local statistical technique for analyzing local spatial varying relationships within variables through allowing local site specific rather than global parameters to be estimated, which extends the traditional global regression framework with taking space into modeling process. This is achieved by estimating the location specific coefficients rather than global stationary estimation by taking the parameter coefficients as a function of geographical locations in the modeling process. To this end through rewriting the typical regression model a GWR model in

the linear formula is like:

$$y_i=\beta_0(u_i,v_i) + \beta_1(u_i,v_i)x_{1i}+ \beta_2(u_i,v_i)x_{2i}+\ldots\ldots+ \beta_k(u_i,v_i)x_{ki}+\varepsilon_i \quad (3\text{-}3)$$

In particular (u_i,v_i) denotes the location of the i-th observation in space. It can be seen from this formula, $\beta_s(s=1\ldots k)$ do not need to be the same, βs are functions of locations (u_i,v_i) and now vary along with locations (i) instead of remaining the same everywhere as the global model. In this modeling it allows the relationships to vary over space which can be interpreted by location-specific parameter coefficients estimation.

In calculation, the parameters of a GWR model are estimated as follows:

$$\beta(u_i,v_i) = (X^T W(u_i,v_i) X)^{-1} X^T W(u_i,v_i) y \quad (3\text{-}4)$$

Where $W(u_i,v_i)$ is a spatial weighting matrix, which is usually employed by the model to discriminate the various influences of the observations in different location on local parameter estimation at regression point i. The natural assumption is that near places has a greater influence than distant ones (geography matters). Therefore a distance decay weighting strategy is usually adopted. The mechanism is that "The weight assigned to each observation is based on a distance decay function centered on observation i. The distance decay function, which may take a variety of forms, is modified by a bandwidth setting at which distance the weight rapidly approaches zero" (Mennis, 2006). In order to maintain the continuity between the distance and the corresponding weighting assigned to each observation near around, a usually adopted Gaussian function distance-decay-based weighting takes the form like (Brunsdon, Fotheringham and Charlton, 1998):

$$w_{ij} = \exp\left[-(d_{ij}^2 / h^2)\right] \quad (3\text{-}5)$$

Here w_{ij} is the weight given to observation j, d_{ij} is the distance between the

locations of observation i and j and h the bandwidth. The value of the weight would decay gradually with distance, to the extent that when the observation j is quite far away from observation i, the weight given to observation j would approach zero and the influence of observation j on the parameter estimation of location i would become very small. This weighting can be adjusted with the kernel bandwidth h which controls the degree of distance-decay. The choice of the bandwidth h can be determined making use of prior theoretical knowledge about the size of influencing region. In most cases the automatic data-led determination of h is usually employed when this theoretical understanding is not available. The strategy Brunsdon et al. (1998) suggested is least square cross-validation. For a pre-specified kernel function, a modified GWR estimate of y_i is denoted (as a function of h) by $\breve{y}_i(h)$ which is obtained by omitting the ith observation (with the weight for that observation set to zero) from the model to avoid h=0 problem. The cross-validated sum of squared errors may then be written as

$$\text{CVSS(h)}= \sum_{i=1}^{n}\{y_i - \breve{y}_i(h)\}^2 \qquad (3\text{-}6)$$

Here n is the number of observations, the bandwidth h can be determined with minimizing equation (3-6).

Charlton et al. argued that the drawback of utilizing cross-validation as the bandwidth selection criterion is that adjusting the bandwidth changes the number of degrees of freedom in the model which made the comparison of their relative performances difficult within the models with different bandwidths. An alternative strategy is to find the model which minimizes the Akaike Information Criterion (AIC). The AIC takes into account the different number of degrees of freedom in different models so that their relative performances can be compared more accurately. A 'best' model can be selected with the AIC minimization. The AIC used in GWR is computed as (Fotheringham, Brunsdon, and Charlton 2002) :

$$AIC = 2n \ln(\sigma') + n \ln(2\pi) + n\left\{\frac{[n + tr(S)]}{[n - 2 - tr(S)]}\right\} \quad (3\text{-}7)$$

Where n is the number of data points,σ' is the estimated standard deviation of the residuals, and tr(S) is the trace of the hat matrix. With the appropriate h determined, the parameter coefficient for each location can be estimated through this weighting mechanism. The outputs are location specific hence mappable for the analyst to visually interpret the spatial distribution of the nature and strength of the relationships among explanatory and dependent variables (Mennis, 2006). Moreover, "The distinct spatial patterns that emerge throughout the entire area, establish an alternative approach for urban spatial phenomena interpretation and a new explanatory basis for the clarification of obscure relations" (Milaka and Photis, 2004.).

GWR is part of a growing trend in GIS towards local spatial analysis which intends to understand the spatial data in more detail through local statistics evaluation. In the literature a number of recent publications have demonstrated the analytical utility of GWR for various urban studies (Huang and Leung, 2002), while it has been scarcely utilized in urban climatic studies especially urban thermal landscape analysis. The interpretation of the local mechanism that affects and determines urban surface thermal abnormalities with the use of GWR presents significant potential for the in-depth investigation of local effects on urban surface temperature variation. The resulting outcome of GWR may help to examine the existence of potential correlation pattern in spatial inconstancy within whole study area in which way the selected environmental variables can have affected local surface temperature at different relational levels among selected variables characterizing the entire area. With this endeavor it hopes to devote to a better understanding of urban effect on local surface thermal environment by taking GWR into the analysis process.

3.6. Summary

Through this chapter, an introduction of study background is given. The progresses in GIS technology, remote sensing, and geostatistical methods represent an opportunity for developing methods for a systematic investigation of urban surface thermal landscape. In this sense an integrated framework of the research is proposed based on the assumptions discussed before. For the characterization and anlysis of local surface temperature variation based on urban thermal landscape monitoring and analysis, first the spatial pattern of urban surface temperature is treated as one kind of landscape, i.e. urban thermal landscape, and then a landscape approach is proposed to measure the structure and identify the spatial and temporal dynamics of the mosaic distribution of urban surface temperature. It will help to characterize the pattern of urban surface thermal landscape under investigation first to acknowledge the heterogeneity within the landscape. Then the statistical exploratory analysis is employed to associate local surface temperature with urban environment measures to investigate the influence of urban spatial and physical configuration on urban surface warming. The regression models, in which the remotely sensed image and GIS derived variables are related with site specific surface temperature, can be constructed to explore the urban effect on local surface thermal abnormalities. The methodology and comparison of typical linear regression and GWR is addressed in detail for statistical exploratory analysis. With these spatial statistic techniques it hopes to enhance our knowledge of urban effect on local surface thermal environment.

CHAPTER 4: DATA PREPARATION

4.1. Image Pre-processing

In this research, the L1B format and Land Surface Temperature (LST) AST_08 data of ASTER images were ordered. Primary calibration procedures have been executed. Geometric processing is a necessary procedure to rectify geometric distortions within original images during image acquisition and to match satellite images with reference to specific map projection system. This process is important to facilitate further GIS analysis. Toutin (2004) identified two major groups of geometric rectification, including empirical and physical models.

When the parameters of the acquisition system or physical geometry model are not available, geometric rectification is operated using empirical models. Empirical models for geometric rectification mostly employ multiple polynomial functions to approximate the image geometry and the relative geo-referenced location of image pixels using GCPs (Ground Control Points), all the image pixels can be transferred into an image with geographical coordinates with parts of distortion corrected in the end. Physical models mainly make use of satellite image acquisition system geometry to build mathematical equations for geometric correction. The rectification methods of physical geometrical models enable a true estimation of geographical location for all the image pixels within images through solving geometrical equations with a few GCPs. It is conceived as one rigorous deterministic model for geometric rectification (Toutin, 2004). This kind of models provide an relative robust way to coordinate satellite images with high accuracy ortho-rectification for high resolution satellite images as compared with empirical models.

In this research, 3D physical model was chosen to perform ortho-rectification for all the ASTER L1B and LST images used, which take advantages of achieving stable high accuracy while using less GCPs and image acquisition system parameters to rebuild geometrical relations (Toutin, 2004). Geometric rectification was carried out

using PCI Geomatica® v.10 OrthoEngine. In order to ensure a good rectification the locations of GCPs were evenly distributed covering the whole study area. The reported overall Root-Mean-Square (RMS) errors for all the images were less than 0.5 pixels, listed in Table 4.1. The residual error report of ortho-rectification is shown in Appendix 1.

Table 4.1 Overall RMS errors of ortho-rectification

IMAGES	TIME	GCPs	X-RMS	Y-RMS	worst 5% of points	
					RMS (x)	RMS (y)
VNIR AST_L1B	04-17-2006	37	0.35	0.28	1.11	0.15
	10-23-2005	38	0.28	0.28	0.59	0.27
	11-21-2004	32	0.37	0.33	1.01	0.39
	11-03-2003	29	0.43	0.25	1.07	0.17
LST AST_08	04-17-2006	21	0.35	0.32	0.61	0.35
	10-23-2005	36	0.30	0.25	0.57	0.67
	10-01-2005	34	0.35	0.35	0.19	0.68
	11-21-2004	23	0.36	0.34	0.67	0.23
	10-05-2004	29	0.31	0.38	0.10	0.82
	11-03-2003	22	0.29	0.32	0.05	0.69
	10-28-2003	34	0.36	0.31	0.20	0.70

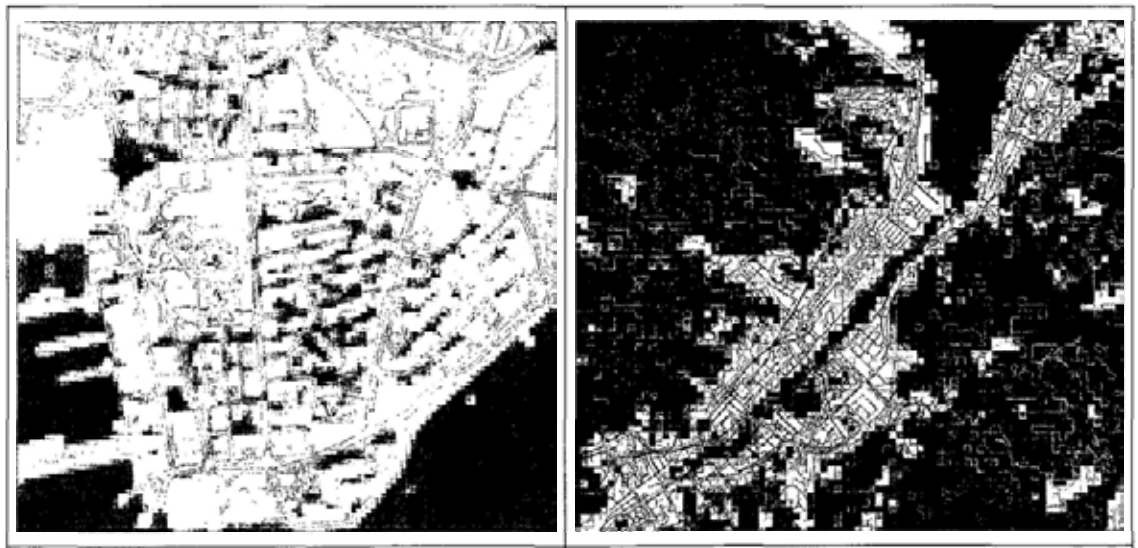

a. Rectified optical image

b. Rectified LST image

Figure 4.1 Satellite images ortho-rectification

The images were ortho-rectified with the cubic convolution resampling algorithm based on a 5-meter DEM archived in the Department of Geography and Resource Management, CUHK. The rectified images were clipped to a size of 320*381 with 90m grids and 1920*2285 with 15m grids area for further analysis. Overlaying GIS road data layers with the resultant images shows that a satisfying geometric correction is accomplished (Figure 4.1).

4.2. Explanatory Variables

The study of local effect of urban environment on surface thermal landscape process is undertaken by statistical regression analysis. The first step for the statistical analysis is the determination of variables. In this analysis urban surface temperature would be the dependent variable which can be derived from surface temperature image of ASTER Land Surface Temperature (LST) product AST_08. Table 4.2 cites all variables employed in the regression models. Under the research assumptions aforementioned, the important factors that have correlation with the urban surface temperature are listed. All the values of each correlation variables corresponding to each sample point have been calculated. In the following part the quantification of such factors would be addressed in detail with the resultant data used to derive variable values shown in Appendix 2.

Table 4.2 Variables list for regression analysis

No.	Label	Description	Note
1	ST******	surface temperature on the day/month/year******	dependent variable
1	SD****	road network density in year****	independent variables
2	TPU****	population density in year****	
3	Disttocoast	distance to water body	
4	hshad**	solar radiation at one time of day/month/year**	
5	footsqure-a	building foot square measurement with area	
6	elevationavg	elevation	
7	NDVI******	vegetation NDVI at one time of day/month/year***	
8	diffuR***	diffuse radiation at one time of day/month/year***	

Solar Radiation:

For solar radiation calculation, there are various software available to undertake this calculation, like GRASS (Hofierka and Suri, 2002), ArcGIS etc. ArcGIS 9.2 is employed to perform the viewshed calculation for an effective quantification of solar radiation. With the advancement of GIS, the instant solar radiation can be estimated for the whole study area when a surface model is available. It is noticeable that the complicated urban surface made the calculation of solar radiation highly sensitive to the local topography. The quality of urban surface model directly determines the accuracy of viewshed calculation. In order to get relatively reliable solar radiation estimation for future analysis, the influence of high rise and density buildings on the calculation of solar radiation cannot be neglected for a city like Hong Kong. Therefore the solar radiation calculation is based on an urban surface model with buildings included and executed with ArcGIS in this study. For detailed methodology and calculation of viewshed calculation, please refer to ArcGIS 9.2 user guide (ESRI, 2006).

Based on GIS, the instant solar radiation is calculated for each daytime period when the satellite image is acquired to quantify the solar radiation situation within whole study area. The solar angles information is listed below as Table 4.3. With this information as input, the instant solar radiation of overall study area at image time can be computed via ArcGIS based on surface model.

Table 4.3 List of solar angle information

DATE	TIMEOFDAY	Solar_Azimuth_Angle	Solar_Elevation_Angle
2006-04-17	11:03:00.75	119.0598	67.3314
2005-10-23	11:02:39.38	153.0688	52.5209
2004-11-21	11:02:10.94	157.2258	44.2103
2003-11-03	11:03:35.52	156.0467	49.3979

The calculated instant solar radiation has been rescaled to a grey value within 0~255 which can help stabilize the regression model calculation. The resultant images of instant solar radiation corresponding to each daytime observation period are listed in Figure A2.1~A2.4 of Appendix 2. With the visual inspection, these images have given detailed depictions of the situation of local solar radiation especially in urban area when a surface model in combining with urban building is used for calculation.

Vegetation:

Vegetation has such an intrinsic reflectance feature that the chlorophyll contained reflects distinct radiation in the red and infrared portion of the electromagnetic spectrum (EMS) incident upon it, while the reflectance of man-made and most non-vegetated surfaces in both the red and infrared part of the spectrum is similar. When the earth satellite images with visible and infrared bands available, it is easy to perform vegetation evaluation based on the difference of infrared and red reflection between vegetation and non-vegetation surfaces. There are a variety of indices in the literature developed for vegetation measurement, like Normalized Difference Vegetation Index (NDVI), Soil Adjusted Vegetation Index (SAVI), Ratio Vegetation Index (RVI), et al. Among these indices NDVI is one widely used parameter for vegetation study based on remote sensing images. The formula for NDVI calculation is as following:

$$\mathrm{NDVI}=\frac{IR-\mathrm{Re}\,d}{IR+\mathrm{Re}\,d}$$

Here IR = infrared band (usually near- infrared) and red = visible red band

NDVI ranges from − 1.0 to +1.0, which is an approximation of the vegetation amount (percentage of biomass) within a pixel of the image dataset (Lynn, 2006). With higher values associated with greater density and coverage of the plant canopy, NDVI provides a useful evaluation for vegetation monitoring taking advantage of simultaneously removing the shadow effect effectively which demonstrate

significant influences under the complex topography of urban canopy (Nichol and Lee, 2005). To this end NDVI is chosen as an easily calculated factor serving as the measurement of vegetation for regression analysis in order to ascertain how vegetation acts during the local surface thermal process.

The vegetation index of NDVI was calculated based on ASTER L1B Registered Radiance at the Sensor product data. Before NDVI calculation, the scaled DN values of the VNIR images are first converted to at-sensor radiance using the following formula:

$$\text{Radiance} = (\text{DN value} - 1) * \text{Unit Conversion Coefficient}$$

The corresponding Unit Conversion Coefficient (UCC) can be found in Table 4.4 (ASTER User Handbook, p.25-26). According to the gain information provided for each channel in the embedded HDF metadata of ASTER L1B images header file, the UCC used for Band 3N (Nir-infrered) and Band 2 (red) is 0.708 and 0.862 for the at sensor radiance calculation.

Table 4.4 ASTER unit conversion coefficients (watts/meter^2/steradian/micrometer)/DN

Band No.	High Gain	Normal Gain	Low Gain-1	Low Gain-2
VNIR				
1	0.676	1.688	2.25	N/A
2	**0.708**	1.415	1.89	N/A
3N	0.423	**0.862**	1.15	N/A
3B	0.423	0.862	1.15	N/A

Source: ASTER User Handbook, p. 25-26

In this research atmospheric correction is skipped. The resultant images are listed in Figure A2.5~A 2.8 of Appendix 2.The NDVI values of each sample points can be derived from the resultant images for different period, which would serve as the input of vegetation evaluation into the statistical regression models in order to quantify the

influence of vegetation on local surface warming.

Water Body:

In order to quantify how proximity to water body affects urban surface thermal performance, one variable that describes the distance to coast is employed in this research, the calculation can be easily implemented with GIS when the coastline data is available. When the layer of coastline is available, distance from coast is calculated via GIS and rescaled to a unit of km to avoid the possible issues introduced by large range of value for subsequent regression analysis. The resultant image is shown in Figure A2.9 of Appendix 2. The value of Distance from coast for each sample point is derived based on this image in order to examine the effect of coast on local surface temperature.

Elevation:

The variable of elevation is directly derived from DEM for each sample points based on GIS in order to explore the effects of elevation on local surface thermal performance through regression analysis. The DEM of the study area with 5m*5m grid is utilized to facilitate image preprocessing of ortho-rectificaiton and other GIS analysis in this study, there is one surface model shown in Figure A2.10 of Appendix 2 which is built based on DEM and building blocks with height from which the elevation information of each sample points can be derived and put into the calculation of regression analysis.

Site Openness to the Sky:

The quantification of site openness to the sky was fulfilled using diffuse radiation as the surrogate. It is assumed that the more diffuse radiation received the more openness of the site to the sky. Diffused radiation can efficiently reflect the situation of site openness in detail. When the DEM is available, points solar radiation module from solar radiation analysis module can be chosen which is integrated with ArcGIS

9.2 for diffuse radiation calculation of each sample points corresponding to each time when each satellite image used is acquired. This point-specific model can provide quite satisfying estimate of solar radiation for a location (Fu and Rich, 2000). The complex topography plays a major role in determining the distribution of the solar radiation on the urban surface at local scale. Therefore the resolution and quality of urban surface model is crucial to obtain a good estimation of local solar radiation.

In this research, the surface model used for calculation is a 5m*5m grid with buildings incorporated in order to achieve a reliable estimation. The data amount is huge with the whole area taken for solar radiation calculation. Under a high rise and high density urban canopy, the diffuse radiation received is highly sensitive to the intensive variation of local topography. Since the calculation is a time-consuming process, the cost of time is highly increased with the data amount of DEM used. In order to facilitate the diffuse radiation calculation of sample points, the DEM has been divided into a few portions with each portion centering on each sample point. Then the diffuse radiation calculation of each sample point can be carried out based on this portion of DEM which is centered on each sample point. It has greatly reduced the calculation cost as well as ensuring the value estimation quality. This process has been automatically executed with a VBA programming procedure working with ArcGIS 9.2. It greatly deduced the time consumption of diffuse radiation calculation process.

In this study openness to the sky of one site has been quantified based on the diffuse radiation calculation, it was assumed that the diffuse radiation can reflects one site's openness to the sky in a great extent. Due to the intensive calculation involved during this computation, only the diffuse radiation of sample points were performed based on point radiation model through a VBA programming with ArcGIS for following regression analysis. For the diffuse calculation of sample points, the parameters information is listed in Table 4.5 as the input of the point radiation model.

Table 4.5 List of parameters information for diffuse radiation calculation

DATE	TIMEOFDAY	Solar_Azimuth_Angle	Solar_Elevation_Angle	Int-Date	Decimal-Hour
2006-04-17	11:03:00.75	119.059807	67.331361	107	10.66159
2005-10-23	11:02:39.38	153.068778	52.520897	296	10.91898
2005-10-01	22:34:53.95	304.771212	-59.421340	274	22.37498
2004-11-21	11:02:10.94	157.22583	44.210273	326	10.86740
2004-10-05	22:41:13.71	305.266349	-61.880158	279	22.50573
2003-11-03	11:03:35.52	156.046685	49.397911	307	10.94019
2003-10-28	22:35:49.75	289.079542	-66.466511	301	22.47780

Population Density:

With the population census data available, the index of population density is approximated with an interpolation method. In this research only the population census data of year 2001 is available and utilized for population density calculation based on GIS. The population density is calculated based on year 2001 census data, shown in Figure A2.11 of Appendix 2. Since only year 2001 census data is available, all the regression analysis during various image time through the whole study period would be based on this data for the correlation evaluation between population density and local surface temperature.

Road Network Density:

In order to evaluate the influence of road network on local thermal performance, transportation data of road network is necessary. While the transportation data is not achieved for this study on current occasion, the utility of road network density made a sensible approximation of transportation data when road network layer is available. There are various indices developed for the measurement of road network density (Borruso, 2003). Borruso (2003; 2005) proposed that the problem of analyzing networks and their influences over space can be reduced to analyzing their point

structure. Accordingly the linear pattern of road network can be converted into a point pattern consisting of nodes of a road network. This nodes distribution dataset is used to approximate the spatial distribution of road network. Then network density is estimated over road network's nodes distribution under Borruso assumption.

A grid-based index is selected to assess the network density in an urban area (Borruso, 2003) in order to facilitate future analysis where satellite grid images would be utilized. The grid square was used to count the road junctions in order to provide an index of road network density. The grid density estimation can be realized by simply counting the number of nodes falling inside and then assigning such value to each grid. Borruso's (2003) work proved that the use of a grid square network density is efficient to quantify road network density by allowing for easy comparison. The grid cells in this study are determined to be correspondingly the same with LST image pixels, i.e. a 90m*90m grid mesh.

When the road network is available, the road network density can be approximated based on the methodology mentioned in last section. The road network density of year 2004 and 2006 has been calculated since only this two year transportation network data is available. When the instant transportation data is not available, it provides a rough estimation for urban transportation situation and enables the evaluation of transportation influence on urban local warming. The road network density for this two year is calculated and shown in Figure A2.12 and A2.13 of Appendix 2. The road density value of each sample point can be derived based on the resultant image.

Building Cluster:

In order to evaluate the influence of building coverage on urban warming, an area building square footage ratio is calculated based on the building polygons. The calculation is executed through GIS. In order to examine the influence of building mass on local surface temperature, the building square footage is quantified by the

ratio of total area of building block occupied with a sample grid and the total area of sample grid. The value of output image has a range between 0~1, shown in Figure A2.14 of Appendix 2.

4.3. Summary

In this chapter image pre-processing is introduced with image ortho-rectification result listed which locates image information in each pixel according with GIS projected coordinate system and enables the exploratory analysis with environmental indicators derived from GIS layers. The calculation of local environmental variables for correlation analysis including the quantification of urban surface and geometry is demonstrated with the resultant variable map listed in Appendix 2. The location specific environmental measures would be derived based on these maps.

CHAPTER 5: RESULTS and DISCUSSIONS

5.1. Introduction

The main objective of this study is to investigate the structure of urban thermal landscape and ascertain the effect of urban fabrics on local surface temperature variation through urban thermal landscape monitoring and analysis. In this research context, surface temperature map derived from ASTER satellite image is used to represent urban thermal landscape. Then landscape metrics analysis is introduced to examine the pattern and dynamics of urban surface temperature distribution in order to provide a quantitative overall evaluation of the urban thermal landscape. Through regression analysis the relationship between urban surface temperature and related influential factors would be constructed and analyzed for a better understanding of urban effect on local thermal landscape.

In this chapter, the systematic investigation of urban thermal landscape would be demonstrated using Hong Kong as the study site. The study of urban thermal landscape would be discussed in two sections, urban thermal landscape characterization and exploratory analysis using statistical regression models. For urban thermal landscape characterization, the qualitative descriptive analysis would be carried out first through spatial and temporal comparison of urban surface temperature pattern along with local land use categories. It aims at offering a primary description about the spatial-temporal variation of local surface thermal landscape. Second, the landscape metrics analysis is used to provide a quantitative evaluation regarding the overall composition and configuration of urban thermal landscape. Complementing the qualitative description of spatial-temporal performance, it hopes to facilitate a comprehensive characterization of urban thermal landscape across space and time. Urban thermal landscape exploratory analysis based on regression statistical analysis is delivered in order to clarify the relationship between the influential factors of urban setting and local surface temperature.

5.2. Urban Thermal Landscape Characterization

5.2.1. Spatial-Temporal Variation

In order to understand the spatial variation of urban surface temperature distribution over whole study area, a year 2000 land use map archived in Department of Geography and Resource Management, CUHK is employed to average urban surface temperature in accordance with land use and land cover (Figure 5.1). The land use pattern used in this study is at level 1 mainly including 13 land use categories shown in Table 5.1, which is computed based on the Land Utilization Plan (Planning Department HKSAR, 2001). The overall average surface temperature of each land use category within whole study area can be calculated based on land use and land cover map in order to explore the thermal characteristics of urban landscape feature. With the benchmark of urban surface material, the spatial-temporal characteristics of surface temperature variation across space are addressed on the landuse platform.

Figure 5.1 Land use map of study area in Hong Kong

Source: Planning Department of HKSAR (2001)

Table 5.1 Land use classification scheme

Code	Categories	Code	Categories
1	Residential Land	8	Other Urban or Built-up Land
2	Commercial Land	9	Agricultural Land
3	Industrial Land	10	Woodland/Shrubland/Grassland
4	Institutional Land	11	Wetland
5	Transportation	12	Barren Land
6	Open Space	13	Water
7	Vacant Land		

Source: Planning Department of HKSAR (2001)

Restricted by the hilly topography, Hong Kong has limited land suitable for potential urban development, but it is a highly developed city in Asia. No pervasive urban growth has been undergone and observed throughout the study period of 2003 to 2006. Undertaking land use and land cover mapping requires intensive working force and time for image processing and field verification. High resolution ancillary data is also needed to achieve a reliable accuracy. Due to such considerations, the land use map produced in 2000 is used as a base map which can be conceived as a reliable data source for this study. Based on this land use classification system, zonal statistics on each Land Surface Temperature (LST) image was executed within landuse zones utilizing ArcGIS. The overall average surface temperature of each category within the study area is calculated in accordance with this base map in order to examine the dependence of surface temperature on land use categories. The resultant LST image represented 13 classes of overall average LST zones corresponding to each land use classification which would categorize urban surface temperature image at each image time listed before into 13 overall average LST zones, with Figure 5.2 showing the resultant sequence of average surface temperature variation along with land use land cover at each image time.

It can be seen from Figure 5.2 that the sequence of daytime surface temperature variation along with land use land cover in solid line shows similar trend within each day time observation of the 04-17-2006, 10-23-2005, 11-21-2004 and 11-03-2003 images, except 04-17-2006 which exhibits a slight difference. Even being distinctive from the daytime trend, the nighttime sequence in doted line also demonstrates consistency within each nighttime observation including the 10-01-2005, 10-05-2004 and 10-28-2003 images. Therefore the distribution of surface temperature variation along with land use at image time of 10-28-2003, 11-03-2003 and 04-17-2006 are chosen to illustrate the seasonal and day-night variation of surface temperature pattern, shown in Figures 5.3, 5.4 and 5.5 respectively. For the day-night change between 10-28-2003 and 11-03-2003, Water (code value 13) happened to be the coolest (28.76° C) during daytime 11-03-2003, during nighttime of 10-28-2003 Vegetation (code value 10) appeared to be the coolest (20.33° C), in contrast surface temperature of Water appeared quite high (23.10° C) during nighttime. The surface temperature of Transportation (code value 5) happened to be the highest both during daytime (36.4° C for 11-03-2003) and nighttime (24.09° C for 10-28-2003). Following is vacant land (code value 7, 36.22° C) and commercial (code value 2, 36.06° C) and industrial land (code value 3, 36.07° C) with surface temperatures tending to be the second high during daytime 11-03-2003. For nighttime surface temperature of 10-28-2003, commercial land (code value 2, 23.62° C) and water body (code value 13, 23.10° C) declaimed to be the second high. It can be drawn that transportation and commercial land are dominant sources of urban surface warming both during daytime and nighttime, while the performance of water body is quite distinct between during daytime (appearing to be the coolest) and nighttime (appearing to be much warmer) due to its high thermal capacity. Vegetation area with woodland/shrubland/ grassland and agricultural land appeared simultaneously cooler during daytime in light blue color and nighttime in deep blue color which covers a large part of the study area. It is interesting to note that woodland/shrubland/grassland is relatively cooler than agricultural land during most of the daytime, while during nighttime this contrast is not as strong as during daytime.

The possible guess is that the vegetation photosynthesis plays an important role of cooling during daytime with high vegetation biomass of woodland/shrubland/grassland. The surface temperature of other urban or built-up areas, residential land, institutional land, and open space are showing a surface temperature of medium high (34.43~35.56° C in day vs. 22.39~22.81° C at night) both during daytime and nighttime. Comparatively, residential land remains relatively cool in both daytime and nighttime. The surface temperatures of wetland (code value 11) and agricultural land (code value 9) appeared much cooler both during day and night but in different order, agricultural land was warmer than wetland (31.27° C vs. 29.28° C) during day but cooler (20.72° C vs. 21.79° C) during night, this may be due to the high moisture content within wetland, which can significantly increase the heat capacity of wetland and leads to the discrepancy of day-night thermal performance.

In order to further investigate the temporal variation of surface temperature, the surface temperature pattern for 04-17-2006 image was compared with 11-03-2003 image in order to examine the possible seasonal variation of daytime surface temperature pattern. The comparison of Figure 5.4 and 5.5 shows that there is no much obvious differentiation existed in the seasonal change between 11-03-2003 and 04-17-2006, which is quite different from the obvious day-night change aforementioned. The variation of daytime surface temperature along with landuse tends to follow the similar trend in seasonal change. This may be due to the subtropical climate that the air temperature still remained quite high (all above 20 deg C) during these two periods (average 21.79 deg C for 04-17-2006 vs. average 28.5 deg C for 11-03-2003), and urban ecology environment does not show obvious seasonal variation during these warm periods. Through this visual comparison of urban surface temperature within each landuse category, it can be drawn that surface thermal behavior show obvious variation with different land use and land cover across space and time. The daytime pattern of urban thermal landscape is quite different from nighttime urban surface temperature distribution with distinct

sequence from the hottest to the coolest with the benchmark of land use. From this aspect the knowledge regarding urban thermal performance dependence on surface material and variation through day and night is roughly figured out.

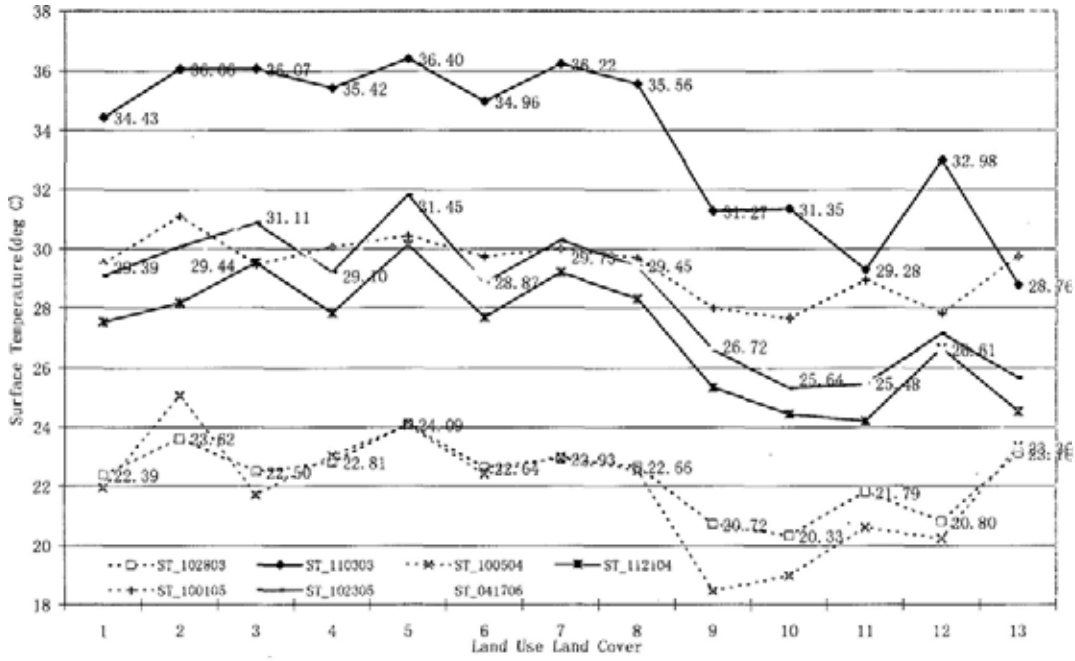

Figure 5.2 Diurnal and seasonal variations of surface temperature along with land use

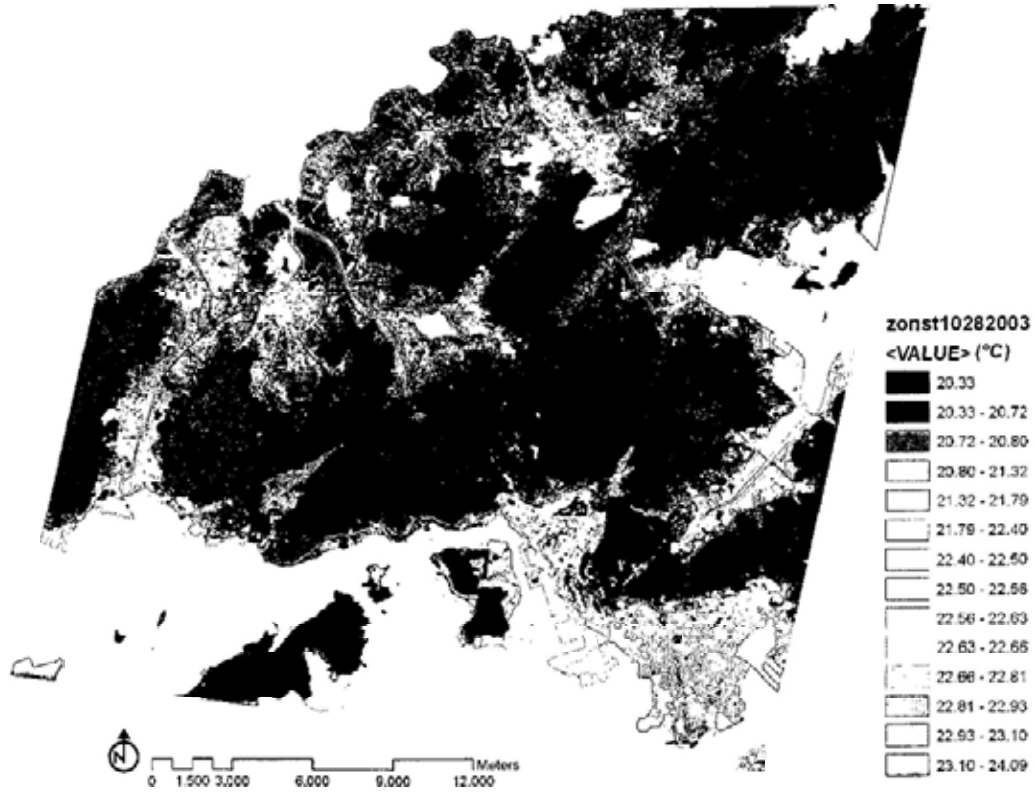

Figure 5.3 Nighttime surface temperature categorization based on land use in 10/28/2003

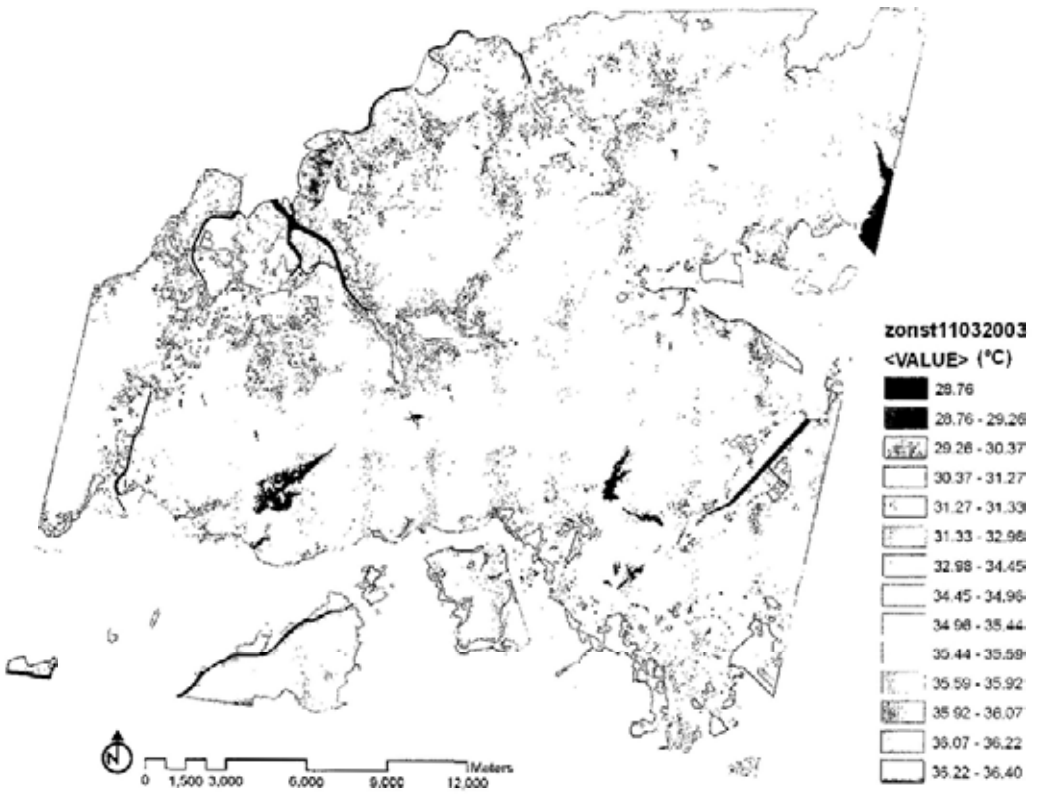

Figure 5.4 Daytime surface temperature categorization based on land use in 11/03/2003

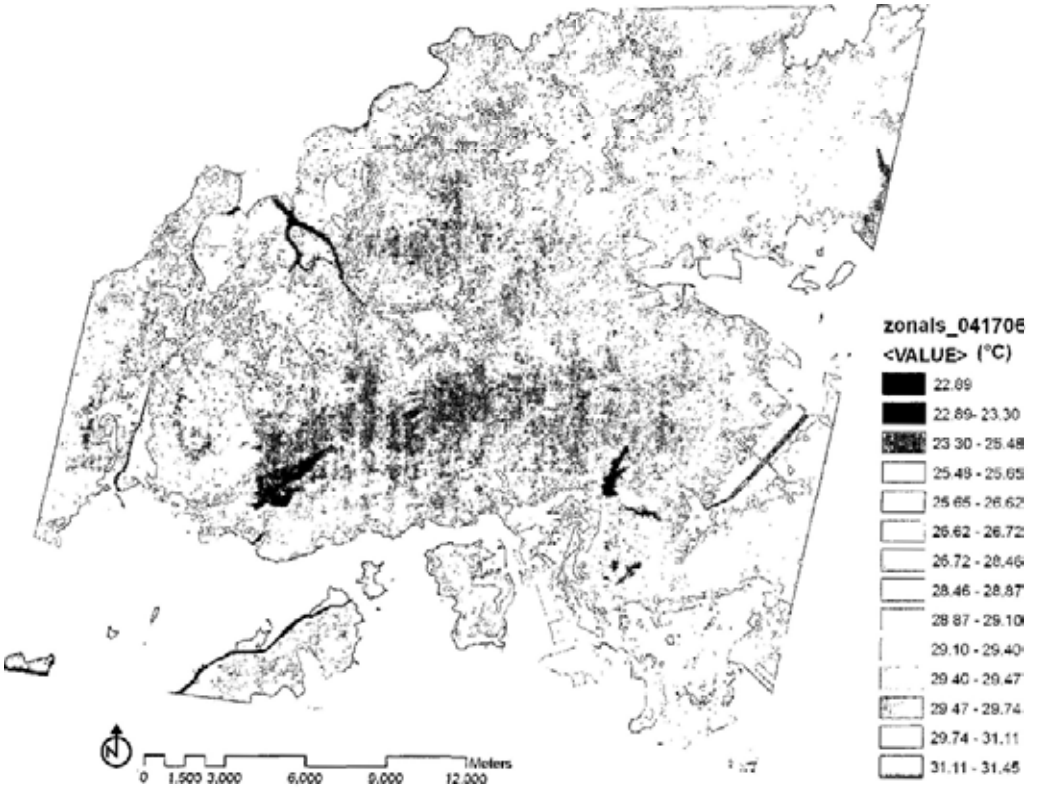

Figure 5.5 Daytime surface temperature categorization based on land use in 04/17/2006

Besides the temporal variation of urban surface temperature among different land use, a local statistic is used to study the spatial association of local surface temperature of each land use category. The local average of surface temperature is calculated for each land use category, with the resultant local averaged surface temperature image shown in Figures 5.6, 5.7 and 5.8. From these day-night and seasonal images, it can be recognized that surface temperature within each land use category shows obvious spatial variation in different locations. This confirms the importance of local environmental effect on local surface temperature variation. The summary of surface temperature variation within each land use category along with day-night and seasonal change is demonstrated in Figure 5.9 and the basic statistical descriptions are shown in Appendix 3. Surface temperature within each land use category shows a wide range of variation in different spatial locations. Comparatively there is no obvious trend that can be easily identified, which reveals the important influences of local environment on surface temperature variation besides local surface material of land use and land cover. It also underlines the complexity and diversity of the mechanism that drives local surface temperature variation. To this end, a systematic study of local effect on urban surface temperature is valuable for the study of urban warming. Urban thermal landscape study enables a comprehensive investigation regarding the mechanism that driving local warming through statistical correlation models. In this research, the related local environmental factors would be taken into the statistical regression analysis in order to scrutinize the relationship between local environmental factors and local surface temperature variation.

Besides the spatial-temporal characteristics of urban surface temperature, the geometrical character regarding overall structure of urban thermal landscape is valuable for systematic study of urban thermal landscape pattern. In the following section, landscape metrics would be employed which intend to focus on the whole pattern regarding the composition and configuration of urban thermal landscape. It aims to provide a quantitative evaluation and help us construct a whole picture about the pattern of urban surface temperature distribution within study area.

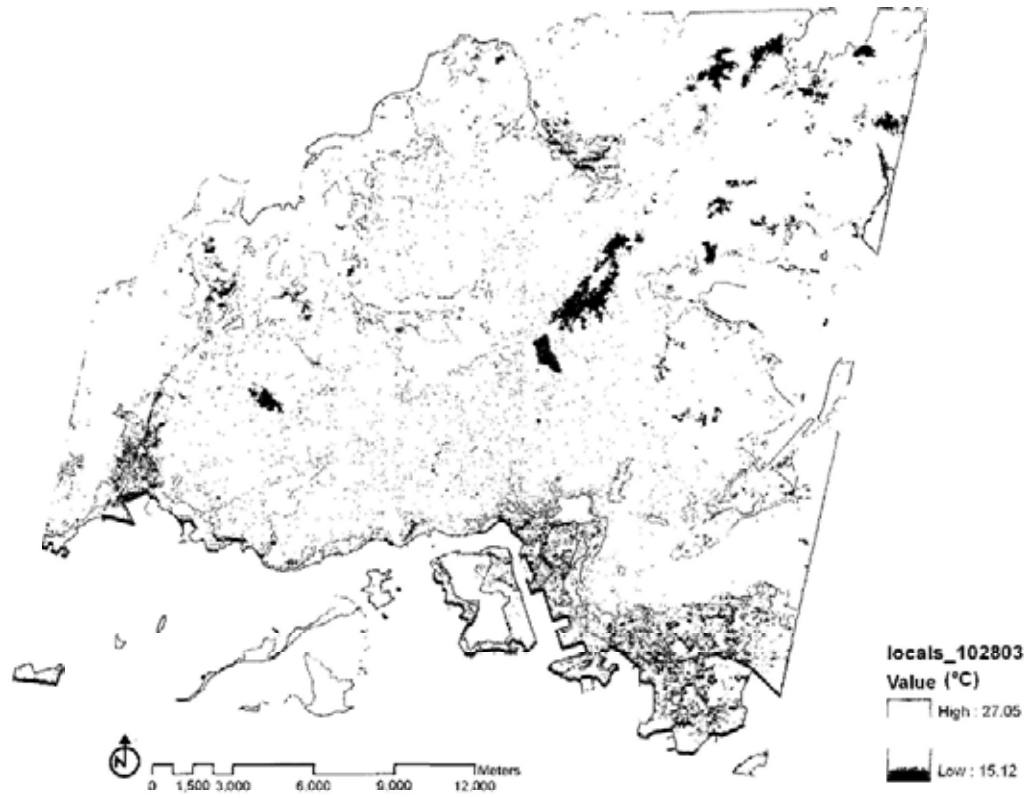

Figure 5.6 Local variations of nighttime surface temperature in 10/28/2003

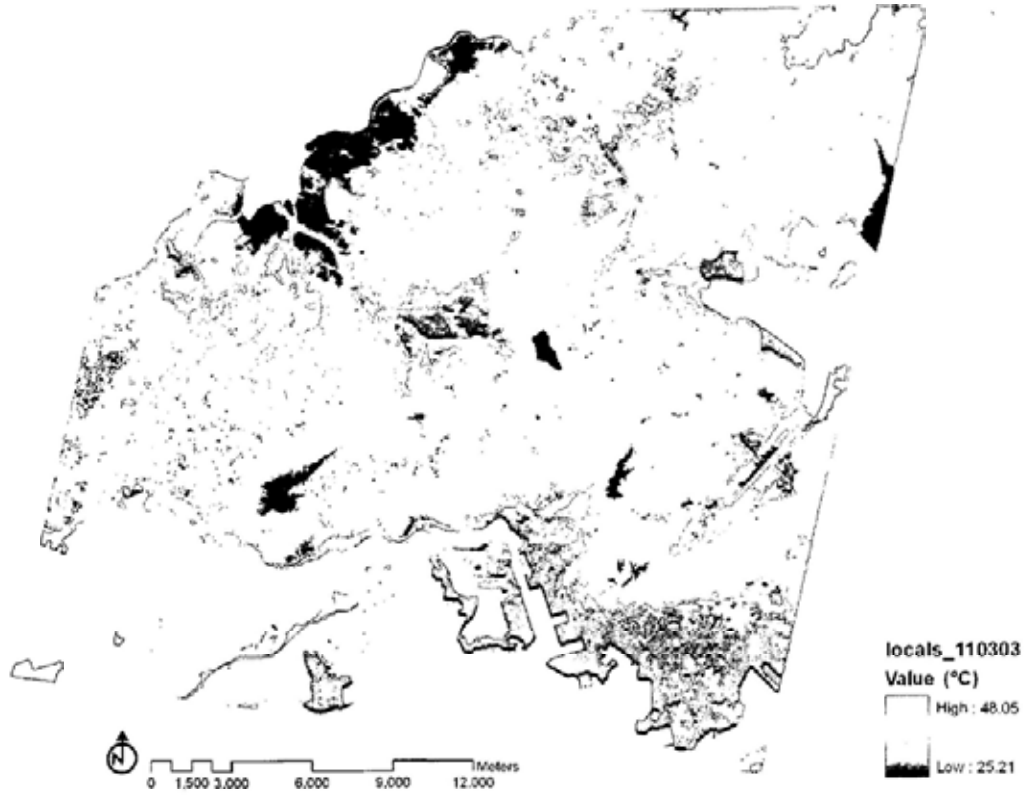

Figure 5.7 Local variations of daytime surface temperature in 11/03/2003

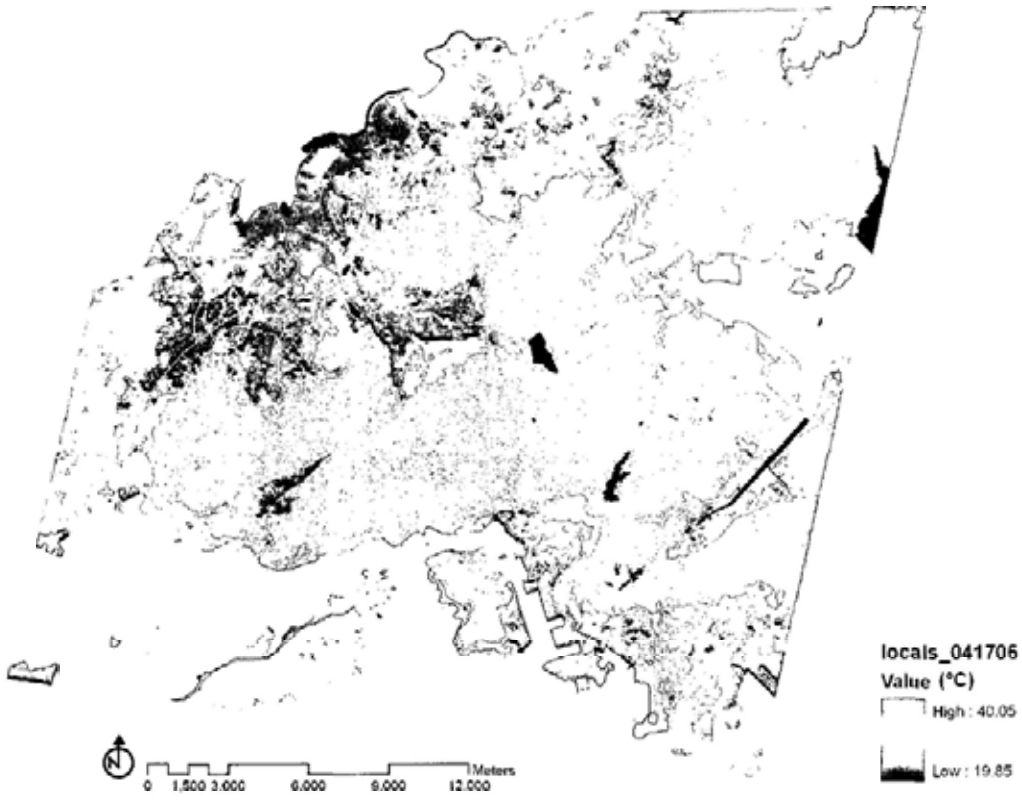

Figure 5.8 Local variations of daytime surface temperature in 04/17/2006

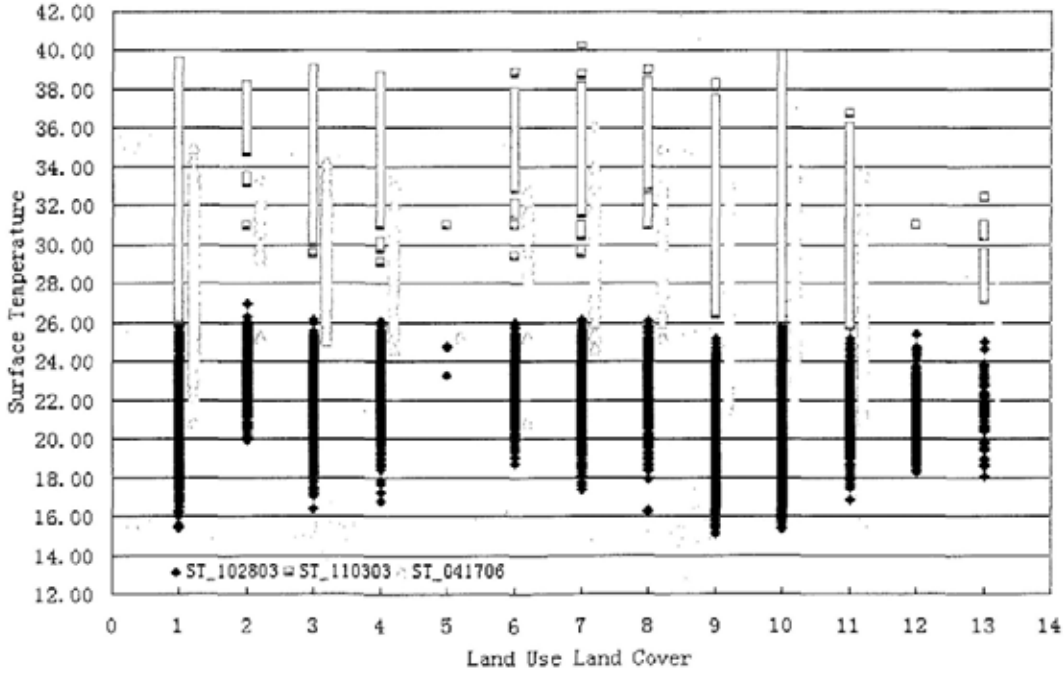

Figure 5.9 Local variations of surface temperature within each land use category

5.2.2. Landscape Metrics

The dependence of surface temperature on local environmental setting has been recognized through the spatial-temporal comparison within land use category across whole study area. Urban local environment plays an important role on local surface temperature variation which can be easily identified from aforementioned analysis. However, what is the whole picture regarding the overall structure of urban thermal landscape configuration, in which way urbanization fragmentized urban thermal landscape as a whole throughout the study period, what is the difference of urban thermal landscape existed between the daytime pattern and night time pattern as whole, and how the pattern evolved through time. In this research the urban surface temperature distribution is regarded as one representation of urban surface thermal landscape, landscape metrics was introduced to characterize the pattern and measure the dynamics of urban thermal landscape across space and time. This technique provides one quantitative evaluation about urban surface temperature distribution.

Scale is one important factor which directly determines the output of landscape metrics evaluation, in this research ASTER LST(Land Surface Temperature) images used for urban thermal landscape study have a resolution of 90m grid, all the calculations of landscape metrics indices is based on this resolution at the landscape scale. The landscape metrics calculation is imposed on the classes represented by the integer deg C of surface temperature, i.e. the classification of surface temperature image with 1 deg C spacing. The metrics evaluation is at the landscape scale which made the study focus on the overall pattern of urban surface temperature as whole within study area. At the same time it avoids the possible bias introduced by various scale of patches along with diverse classification schemes.

For the overall landscape pattern study in 90m resolution grid, the important measures describing the structure regarding the composition and configuration of overall urban thermal landscape pattern is listed in chapter 3 which possess practical meaning for urban thermal landscape characterizing were calculated using

FRAGSTATS ver.3.3 (McGarigal et al.,2002), with the result shown in Table 5.2. The rows with deeper colors are corresponding to the evaluation of nighttime surface temperature patterns, and the others are the daytime measurements. As can be seen that along with the Number of Patches (NP) value decreasing roughly from 2003 (63157) to 2006 (59890) within the daytime observations, the average grain size of surface temperature patches described by mean patch area (AREA_MN) has increased from 0.91 to 0.96 hectares. When comparing the NP and AREA_MN values within each pair of day-night observation from 2003 to 2005, as can be found that the grain size of surface temperature pattern during nighttime is generally larger than the grain size during daytime. This indicates the relative stability of nighttime pattern comparing with daytime pattern (Chen et al., 2004; Nichol et al., 2002) and demonstrates the utility of NP and AREA_MN indices for unraveling the grain size change of surface temperature pattern at the landscape scale.

Comparing the simple measure of dominance, namely Largest Patch Index (LPI), the largest LPI value (0.030) is found in the daytime surface temperature pattern during 10-23-2005, and the smallest (0.011) appeared in the daytime pattern during 11-21-2004, there is no obvious trend identified in the day-night change. Correspondingly the largest Landscape Shape Index (LSI) value (130.53) during 11-21-2004 indicates the high irregularity of the landscape shape during that time. The day-night comparison of LSI value within each pair observation of each year from 2003 to 2005 demonstrates that the overall landscape shape of daytime surface temperature pattern appeared to be more irregular, with the relatively higher LSI value, than the nighttime pattern. This may be due to more pronounced effect of local environmental setting on urban surface temperature variation, including site-specific surface material and geometry, in particular the induced effects of aspect and shadow on direct insolation (Voogt, 2004) which is highly sensitive to building spacing and orientation in urban area (Nichol, J. et al., 2002), which may increase the abrupt change of local surface temperature and cause the high irregularity of the overall pattern during daytime.

On the other hand, the area-weighted mean fractal index FRAC_AM, also shows that urban thermal landscape presents more fragmentation or shape diversity with higher values during daytime than during nighttime by comparison. During daytime observation on 04-17-2006, the daytime area-weighted mean fractal index FRAC_AM shows the highest value (1.013) compared with other daytime observations. At the same time there is an increasing trend of FRAC_AM through out of 2003 to 2006 which can be identified by comparing FRAC_AM values of daytime observations. This confirmed the temporal evolution of increasing fragmentation on urban thermal landscape pattern. This indicates that there was a slight increase in fragmentation of urban thermal landscape throughout 2003 to 2006. Moreover it can be concluded that during daytime, the urban thermal landscape tends to present more fragmentation as compared with nighttime. This may be due to solar radiation introduced more complexity to the daytime pattern of urban surface thermal landscape, while the urban surface thermal landscape tends to be stable during nighttime, which is agreed with most findings of previous study (Chen et al., 2004). During this period from 2003 to 2006, the reported area of total urban or built-up land has increased from 21.8% to 23.4%, the woodland has decreased from 25.7% to 22.1% (data from Hong Kong Annual Report 2003 and 2006). The temporal variation from 2003 to 2006 demonstrates the trend of becoming more fragmentation compared within daytime observations which may be due to this few percentages of urban development within this observation period. On the other hand, there is no obvious pattern observed regarding the fragmentation of nighttime urban thermal landscape among nighttime observations through time.

In general, the daytime urban thermal landscape has more diversity than the nighttime with comparison of diversity index, Modified Simpson's Diversity Index (MSIDI). By comparison within each year day-night observation pair, it can be easily found that daytime surface temperature patterns presents much more diversity than the nighttime with higher MSIDI, the surface temperature variation during nighttime tends to be relatively smoother than that during daytime. This may be due to the

intensive change of solar radiation situation during daytime which introduces more variation through shading by buildings or other man-made objects under a complex urban canopy with high rise high density settlements. In temporal dimension from 2003 to 2006, the daytime lowest value (4.65) of diversity index MSIDI are found in daytime observation 04-17-2006 when comparing with other daytime diversity indices MSIDI. At the same time it is interesting to find that the diversity index MSIDI are decreasing in daytime observation from 2003 to 2006. It demonstrates the trend consistency of diversity decrease in temporal evolution of urban thermal landscape pattern through out of 2003 to 2006.

The Interspersion & Juxtaposition Index (IJI) is one measure of the texture of overall landscape. Comparing the IJI values between the daytime observations, the overall landscape pattern during daytime 04-17-2006 presents more uneven distribution among the various surface temperature patches with lower IJI value than other daytime patterns. There is no obvious trend found in the day-night change within each year day-night pair observation and temporal dimension from 2003 to 2006.

Table 5.2 Landscape metrics indices during the study period

DATE	NP	AREA_MN	LPI	LSI	FRAC_AM	MSIDI	IJI
st04172006	59890	**0.96**	0.027	128.51	**1.013**	**4.65**	**75.68**
st10232005	60574	0.95	**0.030**	128.10	1.011	4.71	79.33
st10012005	54486	1.06	0.017	125.51	1.021	3.87	73.14
st11212004	63260	0.91	**0.011**	**130.53**	1.009	4.77	77.08
st10052004	60617	0.95	0.013	128.99	1.012	4.48	79.37
st11032003	63157	**0.91**	0.024	130.41	1.009	4.79	77.77
st10282003	53985	1.07	0.018	124.85	1.022	4.16	76.35

Through the landscape metrics analysis of urban thermal landscape, it can be recognized that landscape metrics had quantitatively detected the day-night and temporal dynamics regarding the structure of overall urban surface temperature

pattern at the landscape scale as whole. The diversity and fragmentation metrics had revealed the influence of urban development on overall urban landscape pattern. Along with urban development, daytime pattern of urban thermal landscape presents more fragmentation, less diversity and uneven texture distribution than before through daytime observations comparison made in temporal dimension. Moreover, higher local variation and irregularity on urban surface temperature pattern during daytime is observed and identified by the landscape metrics comparing with nighttime pattern which may be introduced by the heterogeneity of local landscape composition and configuration through affecting local solar radiation. Regression analysis would be employed to further investigate the local effect of urban environmental setting including location-specific surface and geometry on the variation of local surface temperature. Through spatial and temporal comparison and landscape metrics evaluation during the process of urban thermal landscape monitoring, a rough recognition regarding the characteristics of urban thermal landscape pattern in study area across space and time are obtained for further explanatory analysis.

5.3. Explanatory Analysis

Through the process of urban thermal landscape characterization, the variations of urban thermal landscape across space and time were identified. In this research, the formation of such variations would be investigated through statistical explanatory analysis. The statistical regression technique provides an effective avenue to relate one dependent variable (the resultant) with one set of independent variables (the causal factors). Then the relationship between urban environmental setting and local surface temperature variation can be constructed, explored and interpreted through statistical regression modeling.

For the analysis of the relationship between local surface temperature and urban environmental measures by linear regression analysis, there were 1070 sample points with systematic sampling covering the whole study area chosen as the observations

for correlation analysis which was strategically located within the whole study area illustrated in Figure 5.10. The complete set of sample points' locations provides a representative coverage of the overall study area and ensures a reliable output through reducing the possible bias introduced by the incomplete observations made. First, the sample points observations would be studied within a global regression model as a whole, second these observations would be grouped into two categories, urban and rural, to examine the possible variation in urban rural relationships.

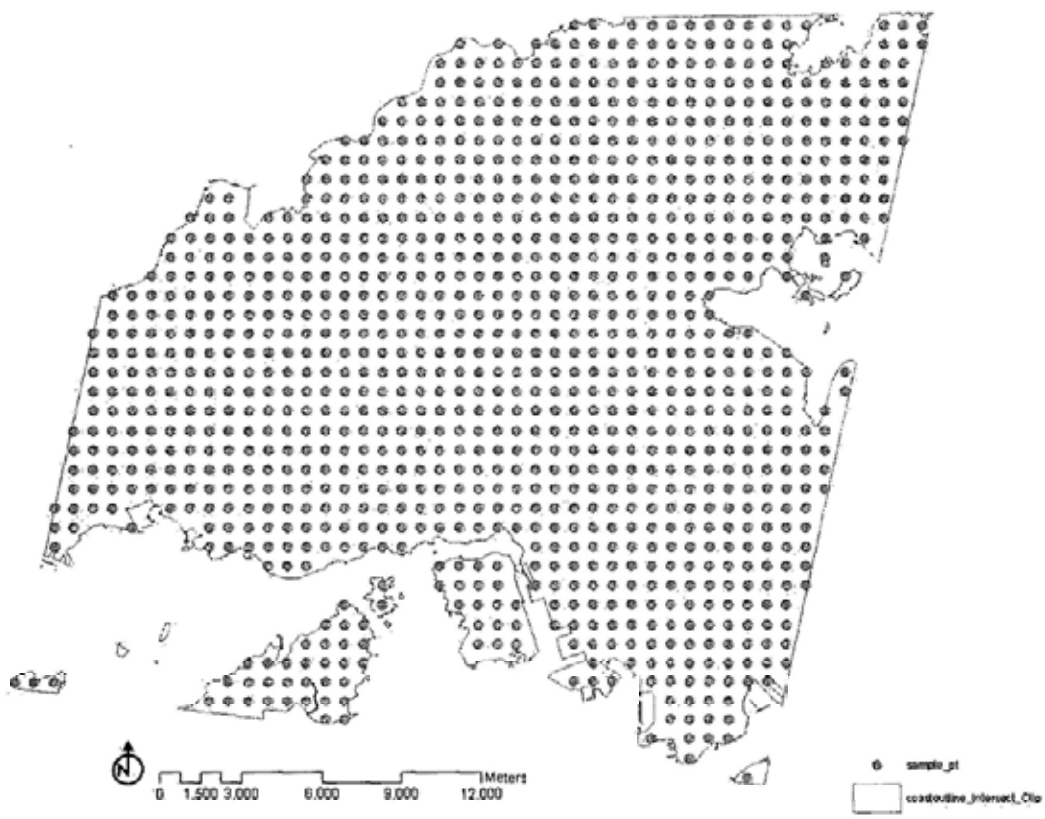

Figure 5.10 Strategically located sample points over study area

5.3.1. Global Analysis

In order to carry out global linear regression analysis, a reasonably large set of 1070 sample points using systematic sampling strategically located within study area was chosen as the observations for regression analysis. With respect to the research assumptions discussed in last chapter during which the environmental factors having correlation with surface temperature is reviewed, Table 5.3 summarized the selected

variables used for linear regression model. The influential factors should be independent from each other, which would satisfy the assumption of independency and can be used in the linear regression model. Regression diagnostics has been carried out for multicollinearity analysis to double-check the independency assumption existed in multiple variables. The Condition Indices (CI) values are shown in Appendix 4a. Belsley et al. (1980) recommended that two or more CI that are greater than or equal to 30 can be interpreted as moderate to severe collinearity existed. By inspecting the Condition Indices (CI), no strong multicollinearity was identified within this set of influential factors which can be used for multiple linear regression analysis.

Table 5.3 Variables list for regression modelling

Variables	Label	Description	Note
Y	ST	surface temperature at image time of day/month/year	dependent variable
X_1	NDVI	vegetation NDVI at image time of day/month/year	independent variables
X_2	Hshad	solar radiation at image time of day/month/year	
X_3	Footsqure	building square footage measurement with area ratio	
X_4	Elevation	elevation	
X_5	SD	road network density in year****	
X_6	Disttocoast	distance from coast	
X_7	Diffuse	diffuse radiation at image time of day/month/year	
X_8	TPU	population density in year****	

The relationship between surface temperature and local environmental parameters can be established with multiple linear regression equation for each image time. The daytime regression model can be established in the following format:

$$Y=\beta_0+\beta_1 NDVI+\beta_2 Hshad+\beta_3 Footsqure+\beta_4 Elevation+\beta_5 SD+\beta_6 Disttocoast+\beta_7 Diffuse+\beta_8 TPU \quad (5\text{-}1)$$

Since solar radiation is not available during nighttime, then the regression model can be rewritten for nighttime observations corresponding with each image time:

$$Y=\beta_0+\beta_1 NDVI+\beta_2 Footsqure+\beta_3 Elevation+\beta_4 SD+\beta_5 Disttocoast+\beta_6 Diffuse+\beta_7 TPU \quad (5\text{-}2)$$

In order to generate a relatively stable and reliable result, the variable of Disttocoast (distance from coast) is rescaled to the units of km to avoid the possible issues introduced by the large range of data values in meter unit. Vegetation NDVI is a unitless variable ranging from -1 to 1. Solar radiation variable Hshad in grey value ranges between 0~255. Square footage area has been rescaled to a value between 0~1 calculated by the building occupied area divided by the total grid area. Elevation variable is in the unit of meter. Diffuse radiation derived for each location of sample points has units of watt hours per square meter (WH/m^2). The related variable values of 1070 sample points are derived separately from corresponding parameter map in 90 meter resolution with reference to local surface temperature derived from the 90 meter resolution LST images. The basic description statistics of the environmental parameters and surface temperatures at each image time are shown in Appendix 4b Table A4b.1.

For the multiple linear regression analysis the best regression equation was determined with a stepwise strategy. The stepwise regression analysis is used to generate optimal regression models based on 1070 observations of sample points. The resultant models of global linear regression analysis for each image time are summarized in Table 5.4. As can be concluded that the models have confirmed the correlations between local surface temperature and those urban environmental factors, at the same time these correlations have been clearly quantified with acceptable correlation coefficient (R-square) about 50%~60%, which indicates that about 50%~60% variations in local surface temperature can be explained by the current regression models.

It is interesting to find that the model has the lowest value of coefficient of determination (R^2, .48.9%) and F (145.059) during the image time of 11-03-2003 when the corresponding LST image has relative high wind speed (5.67m/s) and large hilled fired area. It may be due to heat mixing effect of strong wind and the "noise" effect of fired area introduced to the model performance through weakening the

goodness-of-fit and significance of the model. At the same time the value of R^2 (63.4%) and F (307.320) for the nighttime model 10-01-2005 appears to be the highest among both daytime and nighttime models, it may be due to the even stripped noised within LST image during 10-01-2005 which leads to the misleading performance of the corresponding regression model. So besides the mathematical statistical consideration of sampling, large sample size and long time observation is necessary for statistical regression analysis in order to generate a reliable and stable output, which can avoid possible bias introduced by the potential noise.

The performance of the influential factors in daytime surface temperature pattern is distinct from that in night pattern. During daytime, most of the correlation mechanisms between urban surface temperature and influential factors represented by the regression equation are consistent with each other. Daytime urban surface temperature is closely related with vegetation, solar radiation, building square footage, elevation, road density and distance from coast. While the nighttime surface temperatures has a close relationship with these factors including vegetation, elevation, population density, road density, distance from coast and site openness to sky. This demonstrated the discrepancy of potential mechanism driving surface temperature variation between during daytime and nighttime.

The table also indicates the different influences of various environmental factors on local surface temperatures when comparing the parameter coefficients at each image time. For the constant value, as can be seen that the highest value of constant (30.621) presents in nighttime model of 10-01-2005. This may be due to the strong stripped noise appeared in the 10-01-2005 surface temperature image which leads to the biggest temperature base in the model. Besides the second highest value of constant (29.137) appeared in daytime model of 11-03-2003 which is quite higher than other models, this may be due to the most dry warm weather at image time with the lowest relative humidity of 34% and highest average air temperature of 28.5 deg C. This may favor a higher surface temperature base induced. Through comparing the

coefficients of vegetation within both daytime and nighttime models at each image time, vegetation demonstrates an important role in urban cooling both during day and night. The biggest value of vegetation coefficients (-11.508) happens in 11-21-2004 daytime model which indicates that the vegetation may play a more significant role of urban cooling during daytime than during nighttime when the photosynthesis function of chlorophyll is intensive. The smallest value of vegetation coefficients (-6.606) among daytime models shows in 11-03-2003 model which may attribute to heat mixing effect of relative strong wind (5.67m/s) and the large "noise" area of hill-fired high temperature region existed in surface temperature image of 11-03-2003. These heat mixing effect of relative strong wind and large "noise" areas of hill-fired high temperature region may help degrade the performance of vegetation on keeping local surface temperature down demonstrated in the global regression model. The smallest value of vegetation coefficients (-3.759) among nighttime models happening in 10-01-2005 model may attribute to the high relative humidity of 89.1% at that time which may limit the cooling performance of vegetation on local surface temperature.

The highest value of solar radiation coefficients (0.048) presents in model 11-03-2003 comparing with other daytime models. This indicates that the solar radiation favors the heightening of surface temperature under dry weather condition with lowest relative humidity of 34% among the observations. The 04-17-2006 daytime model possesses the highest value of building square footage coefficients (5.601). In contrast, building square footage does not show very significant correlation with nighttime surface temperature in nighttime models. This may imply that the surface with high urban building coverage plays an obvious role of surface temperature heightening during daytime than during nighttime in the quantification of urban building without consideration of building height which indicates the thermal capacity not clearly differentiated.

When comparing the overall pattern demonstrated with parameters coefficients of

regression models between during daytime and nighttime, it can be seen that solar radiation and building cluster, road density are the dominant contributions to daytime local surface heating. Moreover, vegetation NDVI plays the most important role (i.e., surface cooling) on local surface temperature variation with the highest absolute standardized parameter coefficient (STD Bata) value in negative than other factors within most models both during daytime and nighttime. In terms of standardized parameter coefficient (STD Bata), besides the dominant role of local solar radiation on surface warming evidenced through highest positive STD Bata value, building square footage demonstrates a second important influence on local surface temperature elevation during daytime through comparing the positive STD Bata within each daytime model.

On the other hand, the mechanism driving nighttime local surface temperature variation proves to be consistent during the observed series of nighttime period and quite distinct from the daytime mechanism. During nighttime population density and road density show a close relationship with nighttime surface temperature heightening, while elevation, distance from coast and openness to the sky are negatively related with nighttime surface temperature, it indicates the utility of these possible cooling measures which can be adopted for urban warming mitigation during nighttime. Comparing the standardized parameter coefficient STD Bata of each parameter within each model, apart from vegetation NDVI, elevation and distance from coast demonstrates obvious cooling effect on surface temperature with relatively high absolute STD Bata value in negative within most nighttime models. Population density plays a dominant role on nighttime surface warming comparing with other parameters which possesses the highest positive STD Bata value within nighttime models. The second important contribution of nighttime surface warming comes from road density which demonstrates the second high STD Bata value within nighttime models.

Table 5.4 Parameter coefficient estimation and the model evaluation for global linear regression analysis

Y= Surface Temperature	β_0 Constant	$+\beta_1 X_1$ Vegetation NDVI	$+\beta_2 X_2$ Solar Radiation	$+\beta_3 X_3$ Elevation	$+\beta_4 X_4$ Road Density	$+\beta_5 X_5$ Openness to Sky	$+\beta_6 X_6$ Building Square Footage	$+\beta_7 X_7$ Distance from Coast	$+\beta_8 X_8$ Population Density	R	R^2	Adjusted R^2	F (significance)
ST04172006=	22.375	-9.101	0.025	-0.005	0.100		**5.601**	0.292		0.737	0.543	0.541	210.671
(t-statistics)	(37.228)	(-16.210)	(9.371)	(-10.361)	(2.410)		(8.934)	(9.701)					0.00
(STD Bata)		(-0.436)	(0.213)	(-0.252)	(0.055)		(0.224)	(0.210)					
ST10232005=	23.949	-10.491	0.035	-0.004	0.122	-0.005	4.247			0.790	0.624	0.622	294.389
(t-statistics)	(41.523)	(-20.609)	(16.324)	(-9.020)	(2.979)	(-2.104)	(6.466)						0.00
(STD Bata)		(-0.507)	(0.358)	(-0.201)	(0.063)	(-0.053)	(0.158)						
ST11212004=	23.035	**-11.508**	0.047	-0.003		-0.013	2.972			0.787	0.619	0.617	345.864
(t-statistics)	(39.694)	(-23.304)	(23.794)	(-5.835)		(-4.593)	(4.316)						0.00
(STD Bata)		(-0.550)	(0.510)	(-0.129)		(-0.113)	(0.105)						
ST11032003=	**29.137**	**-6.606**	**0.048**	-0.002	0.137	-0.016	3.903		2.47E-005	0.699	**0.489**	**0.485**	**145.059**
(t-statistics)	(36.473)	(-13.053)	(19.205)	(-2.683)	(3.388)	(-5.180)	(4.782)		(4.333)				0.00
(STD Bata)		(-0.363)	(0.486)	(-0.069)	(0.082)	(-0.163)	(0.135)		(0.119)				
ST10012005=	**30.621**	**-3.759**	N/A	-0.003	0.084	-0.001		-0.152	1.13E-005	0.796	**0.634**	**0.632**	**307.320**
(t-statistics)	(120.768)	(-16.342)		(-12.174)	(4.468)	(-3.753)		(-11.377)	(5.394)				0.00
(STD Bata)		(-0.394)		(-0.264)	(0.094)	(-0.084)		(-0.221)	(0.127)				
ST10052004=	24.289	-9.105	N/A	0.001	0.097	-0.003		-0.340	3.29E-005	0.760	0.578	0.576	242.582
(t-statistics)	(46.694)	(-20.959)		(3.103)	(3.187)	(-4.438)		(-12.580)	(7.676)				0.00
(STD Bata)		(-0.519)		(0.071)	(0.070)	(-0.107)		(-0.257)	(0.193)				
ST10282003=	22.556	-3.933	N/A	-0.004	0.052			-0.076	1.76E-005	0.742	0.551	0.548	260.634
(t-statistics)	(250.884)	(-15.920)		(-13.812)	(2.565)			(-4.147)	(6.950)				0.00
(STD Bata)		(-0.400)		(-0.327)	(0.057)			(-0.088)	(0.157)				

In summary, the global statistical regression analysis confirmed the correlation relationship between urban surface temperature and local environmental factors. This finding agreed with previous research while providing a quantitative evaluation regarding this discrepancy of surface warming between daytime and nighttime. The most importance of vegetation on daytime and nighttime surface temperature variation and local surface cooling is recognized within most of daytime and nighttime models comparing with other parameters for this site study. At the same time it also reveals the difference of the mechanism driving surface temperature variation between daytime and nighttime with distinct regression model coefficients. During daytime apart from local solar radiation, building square footage plays the second important role on surface temperature elevation. In contrast population density is reported to be the most important contribution to nighttime surface warming within these nighttime models, the second following that is road density. While the building square footage shows no obvious role statistically on nighttime surface warming for this study site. Besides the daytime and nighttime mechanism difference, there is the possibility of urban and rural discrepancy existing in local warming mechanism since surface temperature is greatly dependent on the local environmental setting. At the same time the high rise high density urban canopy in study area made the local environment intensively varying across space, which would favor local effect on surface temperature variation. In the subsequent section urban and rural discrepancy in local surface heating mechanism would be examined and discussed.

5.3.2. Urban and Rural Pattern

From the characterization of thermal landscape pattern based on spatial-temporal comparison and landscape metrics evaluation during monitoring process, it indicates the heterogeneity of local urban surface temperature is greatly laid on the diversity of local environmental setting. This also suggests the possible presence of the potential variation regarding local surface warming mechanism within whole study area.

Within the study area, urban and rural area coexists upon a hilly topography. The high rise high density development in urban area made the urban environmental setting distinctive from rural area. In order to probe the possibility of local surface warming mechanism discrepancy between urban and rural area, the sample points are grouped into urban and rural categories in according with the land use map. There are 276 sample points selected correspondingly for urban and rural area and taken into a linear regression model separately to examine the possible difference in local warming mechanism. The location of each 276 urban and rural sample points are shown in Appendix 5, with the basic description statistics of dependent and independent variables shown in Appendix 4b Table A4b.2 and A4b.3.

The statistical result of the regression analysis is summarized in Table 5.5. Within each set of rows of the table, the upper row shows the urban regression model, and the lower row shows the rural regression model. The rows in deep color are related to nighttime models, others are daytime evaluations. In general most of the rural models have a better fit than urban models during daytime when comparing the R-square of the models, except the 11-03-2003 and 11-21-2004 models when large hill fired area occurs in rural area. This may be due to the relatively simple local environment affecting local warming in rural area than in urban areas, where the air pollution, anthropogenic heat, etc, have not cause obvious problems. However the influences of such factors are obvious in urban area and not taken into consideration within current statistical model. While during the urban warming process these factors may play a noticeable role which should not be overlooked. On the other hand there is no obvious trend which can be identified for nighttime models between urban and rural.

All the models demonstrate consistency regarding the negative effect of vegetation on local surface temperature variation both during day and night, in urban and rural area. By comparing the value of vegetation coefficients between urban and rural, it can be seen that the coefficient value of vegetation is bigger in urban models than

rural models within most of the image time. This indicates that vegetation plays a more obvious role on urban surface cooling than rural area. It confirmed the discrepancy of parameter coefficients between urban and rural area and may indirectly indicate the potential existence of local pattern regarding surface heating represented by spatially varying parameter coefficients. At the same time solar radiation shows significant correlation with daytime surface temperature. The positive values of solar radiation coefficients indicate that more sensitivity is induced by solar radiation regarding surface temperature enhancement in both urban and rural area. Comparatively, the parameter coefficient of solar radiation in rural model is mostly bigger than the corresponding urban model within each daytime observation. This indicates that solar radiation plays an obvious role of surface heating in rural area and confirmed the variation of local pattern within the relationships between surface temperature and solar radiation across the whole study area. Moreover, distance from coast plays a distinct role on local surface warming during daytime and nighttime by comparing corresponding regression model coefficients varying from positive to negative. Distance from water body has a positive correlation with daytime surface temperature and indicates possible warming effect during daytime, which means increasing the distance from water may lead to the location-specific surface temperature heightening and implies a cooling effect when approaching large water body like coast (decreasing the distance from coast) during daytime when the surface temperature of coast is relatively lower than land surface temperature which is identified in most daytime observations. While it is negatively related with the nighttime surface temperature which indicates that the increase in distance from coast may have an effect causing local surface temperature decrease (i.e., surface cooling) and implies warming effect when being closer to coast during nighttime when the coast surface temperature is relatively higher than land surface temperature observed in nighttime LST images.

By comparing these overall regression models between urban and rural, urban local surface warming has a close relationship with vegetation, solar radiation, building

square footage, and distance from coast. Besides these factors, while the surface temperature in rural area shows more sensitivity with the geographical situation of local environment including elevation. At the same time population density plays an important role on local surface warming during nighttime in both urban and rural area. Besides the variation in daytime and nighttime surface heating mechanism, the regression models between urban and rural area also shows obvious discrepancy when comparing the parameter coefficients of constant, vegetation NDVI, distance from coast, openness to sky and population density. This revealed the existence of local coefficients variation between urban and rural. Moreover the influence of geographical situation has been recognized in rural surface warming models but not identified in urban models. It indirectly implied the possibility of significant local variation in relationships between surface temperature and environmental factors within whole study area.

In summary, due to the distinction of urban and rural environmental setting which is represented and quantified with the referred location-specific environmental factors in this study, the relationship of surface temperature variation and the referred environmental setting exhibits deviation between urban and rural in terms of the mechanism and coefficient inconsistency. The illustrated discrepancy of urban rural pattern within each daytime and nighttime regression models revealed the spatial association of the relationship between surface temperature variation and local environment setting. This indicates the possibility of significant variation of spatially varying relationships between local surface temperature and location-specific environmental setting including site specific surface composition and configuration, which would be testified and investigated with local spatial statistic technique of Geographically Weighted Regression (GWR) in the next section. Based on the location-specific quantification of surface temperature and environmental setting, the location specific correlation can be explored with GWR for further investigation of the local relationship between environment setting and surface warming.

Table 5.5 Discrepancy of global linear regression model between urban and rural

Y= Surface Temperature	β_0 Constant	$+\beta_1 X_1$ Vegetation NDVI	$+\beta_2 X_2$ Solar Radiation	$+\beta_3 X_3$ Building Square Footage	$+\beta_4 X_4$ Elevation	$+\beta_5 X_5$ Road Density	$+\beta_6 X_6$ Distance from Coast	$+\beta_7 X_7$ Openness to Sky	$+\beta_8 X_8$ Population Density	R	R^2	Adjusted R^2	F
ST04172006=	24.064	-13.137	.023	2.219			.318		-1.28E-005	.567	.322	.309	25.590
(t-statistics)	(18.870)	(-9.662)	(4.303)	(2.654)			(5.240)		(-2.166)				***
ST04172006=	21.649		.015	17.580	-.005		.419			.602	.363	.353	38.569
(t-statistics)	(13.994)		(2.213)	(5.732)	(-5.323)		(6.864)						***
ST10232005=	24.804	-13.598	.030	1.638						.659	.435	.429	69.731
(t-statistics)	(32.274)	(-13.133)	(7.517)	(2.173)									.000
ST10232005=	20.626	-2.881	.030	15.197	-.005		.175			.697	.486	.477	51.131
(t-statistics)	(25.547)	(-3.467)	(7.830)	(5.925)	(-5.988)		(3.333)						***
ST11212004=	24.654	-13.890	.041					-.011	-1.25E-005	.681	.463	.455	58.468
(t-statistics)	(34.740)	(-13.384)	(7.739)					(-2.819)	(-2.215)				***
ST11212004=	23.560	-4.767	.045	10.201	-.003		.251	-.026		.679	.462	.450	38.430
(t-statistics)	(10.060)	(-5.079)	(10.745)	(3.319)	(-3.092)		(4.093)	(-2.413)					***
ST11032003=	**32.157**	-9.962	.037			.096	-.179	-.010		.623	.388	.377	34.271
(t-statistics)	(45.646)	(-9.531)	(5.969)			(2.252)	(-2.839)	(-2.588)					***
ST11032003=	33.605		.051	12.224			.294	-.049		.591	.349	.339	36.284
(t-statistics)	(13.218)		(10.313)	(3.634)			(4.282)	(-4.853)					***
ST10012005=	**30.130**	-4.165	N/A			.089	-.204		7.74E-006	.708	.501	.493	67.933
(t-statistics)	(262.540)	(-7.347)				(3.586)	(-7.182)		(3.086)				***
ST10012005=	29.671	-4.148	N/A		-.002		-.185		2.60E-005	.764	.583	.577	94.699
(t-statistics)	(260.972)	(-10.839)			(-5.628)		(-7.810)		(3.585)				***
ST10052004=	24.922	-12.402	N/A	-1.439			-.456	-.002	2.32E-005	.811	.658	.653	130.358
(t-statistics)	(41.988)	(-12.425)		(-2.099)			(-9.058)	(-2.933)	(4.516)				***
ST10052004=	21.809	-9.559	N/A		.003		-.397		3.44E-005	.674	.455	.447	56.516
(t-statistics)	(88.277)	(-12.193)			(3.107)		(-7.652)		(2.129)				***
ST10282003=	23.082	-5.270	N/A				-.135		1.16E-005	.598	.358	.351	50.543
(t-statistics)	(154.649)	(-8.342)					(-3.527)		(3.511)				***
ST10282003=	22.166	-4.510	N/A		-.004					.670	.448	.444	110.899
(t-statistics)	(163.283)	(-9.708)			(-6.670)								***

*** = significant at .1% level

5.4. Geographically Weighted Regression

Geographical Weighted Regression (GWR) analysis is chosen to further conduct statistical analysis and measure the possible spatial varying relationship between the referred local environmental factors and surface temperature with the use of a software package GWR 3.0 (Fotheringham et al., 2002). In this calculation, the significance of potential spatial variation in relationship is measured and verified with a Monte Carlo statistical test. P-value for each variable is given and compared to offer a formal evaluation about the significance of spatial variation within each influential factor coefficient. This statistic provides an efficient evaluation to detect the existence of local variation within the relationships pattern. The outputted estimation of parameter coefficients for each variable from the GWR analysis can be conveniently mapped with ArcGIS to facilitate visual inspection and comparison. This visualization provides one intuitive presentation regarding the pattern of local variations within the correlation between each parameter and surface temperature. GWR provides the utility to scrutinize the potential discrepancy of local relationship patterns within each parameter through spatially located parameter coefficient estimation of each parameter across the whole study area, which was impossible using the Ordinary Least Squares (OLS) approach conducted before.

Bandwidth is one important factor which directly determines the outputted model of GWR. If it is too large, the local variation cannot be captured in enough detail due to the 'smoothing' effect of the bandwidth. On the other hand, small bandwidth may mislead interpretation through introducing intensive local variation. An appropriate bandwidth can be determined based on prior knowledge about the spatial variation of the relationships or through spatial statistical estimation. Because the adaptive kernel is more capable to reflect the scale of local variation resulting from the equal amount of sample data at each regression point as compared to the fixed kernel (Su et al., 2005), the adaptive kernel with AIC (Akaike Information Criterion) minimization bandwidth selection is adopted for GWR analysis in this study. On the other hand it would provide one valued reference indicating the grain size of local varying patterns existed and the further inference of local fragmentation in the relationship pattern within whole study area can be made.

The Monte Carlo significance test of spatial variation corresponding to each variable is summarized in Table 5.6, with the grey color rows showing the nighttime models, others corresponding with the daytime models. The goodness-of-fit of GWR models within each image time period can be evaluated with the adjusted R-square in this table. In general, the R-square has greatly improved from about 50%~60% generated from the OLS global linear regression model to over 70% correspondingly as generated as GWR. The highest value of adjusted R-square (0.772) appears in daytime model of 11-21-2004. On the other hand, the R-square value of daytime models is consistently higher than the values of nighttime models, which implies that the daytime surface temperature can be better modeled with current environmental variables than nighttime surface temperature. In summary the F values of GWR models at each time show that the relationships between urban environmental factors and local surface temperature are significant. When comparing the calculated bandwidth of each GWR model between daytime and nighttime, it can be found that the bandwidths of nighttime models is larger than the ones of daytime models, this also confirmed the relative stable surface heating pattern during nighttime than during daytime, the surface heating pattern in daytime possess much more intensive variations within local area which lead to a smaller bandwidth generated. It is noted that the bandwidth of GWR model during 10/01/2005 is the biggest (184) among the daytime and nighttime models. This may be due to the strong "smoothing" effect of even 'noise' introduced by the stripped LST image and the highest relative humidity (89.1%) at this image time.

From the P-value of The Monte Carlo significance test of spatial variation corresponding to each variable in Table 5.6, the vegetation NDVI and Elevation show significant spatial variations within the parameter coefficients estimation both during daytime and nighttime. Furthermore the spatial variations in parameter coefficients of Distance to water body, Openness to the sky and Population Density are captured in these models. This indicates the varying influences of these factors on local surface temperature variation under local circumstance both during daytime and nighttime.

Table 5.6 Geographically weighted regression diagnosis

P-value (Monte Carlo)	Constant	Vegetation NDVI	Solar Radiation	Building Square Footage	Elevation	Road Density	Distance from Coast	Openness to Sky	Population Density	Kernel Bandwidth	R^2	Adjusted R^2	Effective number of parameters	F
ST04172006= (significance)	0.00 ***	0.00 ***	0.12	0.00 ***	0.00 ***	0.13	0.00 ***	0.00 ***	0.00 ***	114	0.778	0.737	165.6	6.11
ST10232005= (significance)	0.00 ***	0.01 **	0.07	0.00 ***	0.00 ***	0.75	0.00 ***	0.00 ***	0.00 ***	162	0.778	0.750	120.4	5.89
ST11212004= (significance)	0.00 ***	0.00 ***	0.00 ***	0.00 ***	0.00 ***	0.42	0.00 ***	0.00 ***	0.00 ***	99	**0.812**	**0.772**	186.5	5.10
ST11032003= (significance)	0.00 ***	0.00 ***	0.00 ***	0.03 *	0.00 ***	0.01 **	0.00 ***	0.00 ***	0.00 ***	114	0.785	0.746	163.7	8.05
ST10012005= (significance)	0.12	0.00 ***	N/A	0.21	0.00 ***	0.24	0.00 ***	0.03 *	0.00 ***	**184**	0.76	0.738	93.1	6.06
ST10052004= (significance)	0.06	0.00 ***	N/A	0.18	0.00 ***	0.89	0.00 ***	0.00 ***	0.00 ***	162	0.735	0.707	104.0	5.97
ST10282003= (significance)	0.00 ***	0.00 ***	N/A	0.28	0.00 ***	0.58	0.00 ***	0.00 ***	0.00 ***	173	0.731	0.704	97.6	7.21

*** = significant at .1% level

** = significant at 1% level

* = significant at 5% level

During daytime the Intercept and Building square footage demonstrate spatial association correlation with local surface temperature. While during nighttime these spatial variations of parameter coefficients tend to be less obvious. Except these factors referred above, no significant spatial association was found and detected for Constant in night models, Solar Radiation and Road Density parameters within most of the models of this study during the GWR analysis. The spatial variations of the refereed parameters proved the mixed correlation between such evaluation variables and local surface temperature across the whole study area, which is not uniformly stationary within the whole study area and may change from negative correlation to positive correlation under local circumstance.

Since each environmental measurement has various range of value, moreover the NDVI values range from negative to positive, this made the direct comparison of parameter coefficient difficult in order to measure the importance of each parameter impact on local surface temperature variation, including the direction (the possible cooling or warming effect) and extent (the altitude of local surface temperature change induced). For easy comparison between the influences of environmental factors on local surface temperature variation across space and time, the indicating impacts of each environmental parameter can be quantified with the statistical variation of surface temperature induced by each factor, i.e. here called component contribution using the following formula:

Component Contribution (CC) =factor value * parameter coefficient

Then all the component contribution to surface temperature variation corresponding to each factor have been calculated in order to measure the influence of each environmental factor on local surface temperature change within each image time, with positive CC value indicating the possible warming effect by increasing local surface temperature with corresponding statistical CC value ° C, and negative CC value indicating the possible cooling effect by decreasing local surface temperature with CC value ° C. The basic statistic description is shown in Table 5.7, with the grey color rows showing the nighttime models, others corresponding with the daytime models.

Table 5.7 Statistical descriptions of CC value of 1070 sample points

Components	MODEL		Statistical Description			
	Image Time/Significance		MIN	MAX	MEAN	STD
Constant	04-17-2006	***	12.82	36.83	23.08	3.88
	10-23-2005	***	16.46	35.83	24.17	3.42
	11-21-2004	***	1.24	53.17	**22.17**	5.88
	11-03-2003	***	13.80	62.98	**29.82**	5.83
	10-01-2005		28.56	35.29	**30.89**	1.30
	10-05-2004		15.18	32.40	24.00	2.74
	10-28-2003	***	16.85	28.78	22.78	2.05
Solar Radiation	04-17-2006		0.92	15.53	**5.81**	2.40
	10-23-2005		1.23	12.12	6.51	1.84
	11-21-2004	***	-4.23	15.66	7.70	2.65
	11-03-2003	***	1.25	18.26	**8.96**	2.80
Vegetation NDVI	04-17-2006	***	-7.14	2.27	-1.61	1.95
	10-23-2005	**	-7.56	2.49	**-2.41**	2.08
	11-21-2004	***	-9.40	3.22	-2.13	2.22
	11-03-2003	***	-8.27	2.17	-1.92	2.09
	10-01-2005	***	-2.75	1.10	-0.79	0.71
	10-05-2004	***	-4.73	2.99	-1.06	1.34
	10-28-2003	***	-3.81	1.37	**-0.55**	0.79
Openness to Sky	04-17-2006	***	-20.61	8.48	-0.90	4.13
	10-23-2005	***	-17.92	5.22	-1.73	3.58
	11-21-2004	***	-39.19	19.83	-2.20	6.40
	11-03-2003	***	-49.35	8.26	**-5.07**	7.60
	10-01-2005	*	-5.58	0.76	-1.28	1.42
	10-05-2004	***	-12.08	6.76	-2.64	3.25
	10-28-2003	***	-5.26	5.00	**-0.69**	1.82
Elevation	04-17-2006	***	-2.77	2.25	-0.39	0.63
	10-23-2005	***	-2.76	1.84	-0.37	0.55
	11-21-2004	***	-3.56	5.96	**-0.09**	0.80
	11-03-2003	***	-4.68	2.78	-0.11	0.88
	10-01-2005	***	-2.80	0.09	-0.39	0.48
	10-05-2004	***	-2.07	2.73	0.06	0.48

	10-28-2003	***	-5.92	0.00	**-0.56**	0.79
Distance from Coast	**04-17-2006**	***	-2.39	4.66	**0.52**	1.06
	10-23-2005	***	-1.81	4.47	0.29	0.94
	11-21-2004	***	-4.63	5.08	0.03	1.31
	11-03-2003	***	-3.08	7.50	0.40	1.54
	10-01-2005	***	-1.30	0.92	-0.24	0.29
	10-05-2004	***	-2.90	2.52	**-0.51**	0.80
	10-28-2003	***	-2.01	2.58	0.01	0.70
Building Square Footage	**04-17-2006**	***	-.43	8.40	**0.17**	0.57
	10-23-2005	***	-.78	3.48	0.13	0.41
	11-21-2004	***	-1.57	3.18	0.08	0.30
	11-03-2003	*	-.92	6.38	0.10	0.39
	10-01-2005		-.88	1.04	-0.00	0.12
	10-05-2004		-1.94	1.54	**-0.03**	0.22
	10-28-2003		-.95	1.28	0.01	0.13
Road Density	**04-17-2006**		-1.79	2.51	0.016	0.22
	10-23-2005		-0.95	1.92	0.026	0.18
	11-21-2004		-2.30	2.09	-0.011	0.23
	11-03-2003	**	-1.46	2.81	0.017	0.21
	10-01-2005		-1.09	2.00	0.043	0.16
	10-05-2004		-0.49	2.04	**0.046**	0.19
	10-28-2003		-0.48	2.22	0.021	0.13
Population Density	**04-17-2006**	***	-1.66	0.93	-0.004	0.210
	10-23-2005	***	-1.74	0.73	-0.021	0.201
	11-21-2004	***	-2.89	2.22	-0.027	0.366
	11-03-2003	***	-0.89	2.47	0.067	0.275
	10-01-2005	***	-0.20	1.15	0.050	0.147
	10-05-2004	***	-0.14	3.07	**0.153**	0.367
	10-28-2003	***	-0.59	2.02	0.062	0.218

***** = significant at .1% level** **** = significant at 1% level** *** = significant at 5% level**

By comparing the average CC values between the listed parameters, as can be seen that among these seven models, in general during daytime Solar radiation play a dominant role of increasing local surface temperature variation which contributes

heightening surface temperature statistically by average 5.81° C (CC value in 04-17-2006, with average relative humidity 58.9%) to 8.96° C (CC value in 11-03-2003, with average relative humidity 34%). Secondly, the parameters which have relative strong impact on local surface temperature variation have possible cooling effect both during day and night with the statistical altitude induced in the rough order of average -0.69° C~-5.07° C(Openness to the sky), -0.55° C ~-2.41° C (Vegetation NDVI) and -0.09° C ~-0.56° C (Elevation). Besides the above referred factors, Distance from Coast and Building Square Footage also have obvious influence on local surface temperature variation at each image time with corresponding altitude -0.51° C (at night of 10-05-2004) ~ 0.52° C (during daytime of 04-17-2006) and -0.03° C (at night of 10-05-2004) ~ 0.17° C (during daytime of 04-17-2006), but with distinctive direction from positive in daytime models (indicating possible warming effect during day) to negative in most nighttime models (indicating possible cooling effect during night). Road density and Population density show relative weak impact on local surface temperature variation with comparative low CC values both during day and night within the models of this study based on current data used. Within the day-night comparison of CC values related to each factor, as can be drawn that Vegetation NDVI has a stronger impact on surface temperature cooling during daytime as evidenced by the comparative lower negative CC values in the daytime models than the nighttime models. This may be due to the more obvious photosynthesis and evaporation of vegetation during daytime (Miller et al., 1976). Even the relative weak influence on local surface temperature change implied with the comparative lower statistical average CC values, Population density shows distinctive effect from warming (indicating by positive CC values in nighttime models) to cooling (indicating by negative CC values in most daytime models) in day-night change. This may be due to the more congested human activities in outdoor space during night and the thermal inertia would be higher in the settlement with high population density, the longwave radiation is obvious during night and weak during daytime.

In order to demonstrate the local variation pattern of such factors which present significant spatial association, the illustration would emphasize on parameters whose coefficients distribution show significant spatial variation along with the seasonal and day-night change. To this end, the parameters coefficients outputted from GWR

analysis in daytime models during 04/17/2006 and 11/03/2003 together with nighttime model during 10/28/2003 were chosen as examples and mapped against the corresponding VNIR image to facilitate further interpretation (Appendix 6). This would also be used to depict the coefficients variation pattern within the whole study area along with the day-night and seasonal changes. Due to the intensive spatial variation of high density and high rise urban environment together with hilly topography, local surface thermal landscape varied intensively under the intensive varying local environment. It is not appropriate to derive coefficients surfaces based on the sample points with 720m spacing for each significant spatial varying parameter with interpolation methods, which may be under-representative for the pattern of local varying relationship across the whole study area. Therefore in this presentation only the parameter coefficients of evenly located sample points are mapped to address the spatial variation of the correlations between each parameter and local surface temperature corresponding to each sample point. At the same time, the CC values related to each parameter are mapped in order to depict the impact of each factor on surface temperature variation which is shown in Figures 5.11~5.32.

Within these three models in possible seasonal and day-night change, the primary comparison regarding the implied relative influence of each factor on surface temperature variation at each image time can be made by comparing the CC values related to each factor in Table 5.7. As can be seen that daytime models, especially model 11-03-2003, demonstrates the strongest influences of most of the environmental factors on local surface temperature variation as evidenced by the highest average CC values, including Intercept (29.82), Vegetation NDVI (-1.92), Population Density (0.067) and Openness to the sky (-5.07). This may indicate that such referred factors have stronger impact on local surface temperature variation during daytime of 11-03-2003 than other two image time. This may be due to the fact that vegetation is in relative good situation (with NDVI average 0.235) in 11-03-2003 compared with in 04-17-2006 (with NDVI average 0.165) and the relative humidity is lower (34%) in this time compared with (67.1% during nighttime of 10-28-2003 and 58.9% during daytime of 04-17-2006). The environmental situation at this image time with vegetation remained in good situation and the relative dry weather condition may favor the impact of such parameters on local surface temperature variation including the highest average surface temperature base

(indicating by the highest average constant CC value), the strongest cooling effect of vegetation during daytime (evidenced by the lowest negative average Vegetation NDVI CC value), and the more obvious impact developed at this image time on local surface temperature variation related to Population Density and Openness to the sky. While Building Square Footage shows more obvious correlation (average CC value 0.17) in model 04-17-2006 than in model 11-03-2003 (average CC value 0.10). This may be due to the relative low wind speed (average 2.81 m/s) at daytime of 04-17-2006 compared with the image time of 11-03-2003 (average 4.75 m/s). Elevation shows a stronger role during nighttime 10/28/2003 indicating by the highest CC value of -0.56 than the other two daytime models. The highest CC value of Distance from coast (0.52) appears in model 04-17-2006 comparing with other two daytime and nighttime models, indicating a stronger average warming effect than other two image time. This may be due to the lowest wind speed at image time 04-17-2006 (2.81m/s) than image time 10-28-2003 (4.75 m/s) and 11-03-2003 (5.67m/s), which weakened the cooling effect of coast on local surface.

When comparing the intercept coefficients of nighttime and daytime models during 10/28/2003 and 11/03/2003 with Figures 5.11 and Figure 5.12, the day-night pattern is distinct from each other. As can be seen that in the green circle area where the vegetation is maintained in good situation, the intercepts of these area kept lower both during day and night. While in the yellow circle area where most low grass is covered the intercept appears relatively higher during night but lower during daytime. This demonstrated the day-night difference of surface temperature base corresponding with different land surface. When comparing the intercept coefficients of daytime models during 11/03/2003 and 04/17/2006 with Figure 5.12 and Figure 5.13, the pattern tends to be consistent with each other except that the intercept of 11/03/2003 model has a comparatively larger range than the one of 04/17/2006 model, since 11/03/2003 remained in relative dry condition (relative humidity 34%) while 04/17/2006 was in wet situation (relative humidity 58.9%), this may lead to the difference of the base value of surface temperature.

The CC distribution related to Solar Radiation in daytime model 11/03/2003 shows significant spatial variation (Figure 5.14). As can be seen that in most of urban area especially in green circles with high rise high density development like Kowloon, the

CC values appeared relatively less positive within the site indicating that solar radiation contributes less (referred as a weak "warming" effect) to local surface temperature heightening than other areas. This may be due to the fact the solar radiation received within these urban area is relatively lower due to the shading effect of tall buildings nearby. The mountain area with high altitude like Tai Mo Shan especially the solar illuminated side shows relative higher positive CC than the shaded side. The badland area located in the west part of the study area in yellow circle also demonstrates relative high CC values of Solar Radiation on local surface temperature variation, indicating the larger surface temperature increase due to solar radiation (referred as the implied strong "warming" effect of solar radiation on local surface). As can be drawn that GWR model clearly differentiated the spatial variation of solar radiation impact on local surface temperature variation which is much related to the land cover and the amount of received solar radiation during daytime

Figures 5.15, 5.16, 5.17 demonstrate Vegetation NDVI component contribution to surface temperature variation for nighttime model 10/28/2003, and daytime model 11/03/2003 and 04/17/2006. Figure 5.15 shows that within water body area in some area of yellow circle, the CC values to local surface temperature variation related to NDVI are positive, indicating the component contribution of heightening local surface temperature related to water body (here referred as local "warming" effect of water body) during night 10/28/2003.While during daytime, model 11/03/2003 and 04/17/2006 demonstrates that within water body area, the surface temperature CC value related to NDVI is negative, indicating the local cooling effect of water body on surface during daytime. The distinct warming and cooling impact of water body on local surface temperature variation during nighttime and daytime has been detected by GWR models exactly. However the high negative CC values in dense vegetation area shows consistent cooling effect of vegetation both during daytime especially in the green circle area. It is interesting to find that the CC values appeared positive in the green circle area during 10/28/2003 indicating the contribution of heightening local surface temperature (here referred as possible warming impact) of vegetation during night. It may be due to the relative low hill valley region where the green circle area located that favored the warming effect under the weather condition of 4.75 m/s wind speed and 67% relative humidity at image time. The spatial variation of the Vegetation NDVI CC to surface temperature variations with various

color within vegetated area revealed the varied influences of vegetation with different species on local surface temperature under various local environment. At the same time, the 11/03/2003 daytime model appeared to be more significantly varied across the whole study area with a wider range of component contribution values than the 04/17/2006 model. It indicates that vegetation has more diverse correlation with local surface temperature during 11/03/2003 than 04/17/2006. This may be due to the fact that vegetation is in relative good situation (with NDVI average 0.235) in 11-03-2003 compared with in 04-17-2006 (with NDVI average 0.165) and the relative humidity is lower (34%) in this image time compared with (58.9%) during daytime of 04-17-2006. This may be also due to the relatively high surface temperature (mean 32.35) and air temperature (mean 28.5) of 11/03/2003 than that (mean surface temperature 26.74, mean air temperature 21.79) of 04/17/2006, and the relatively hazy image of 04/17/2006. The Kowloon urban area in red circle demonstrates the complicated CC from negative to positive which indicates warming and cooling impact of Vegetation NDVI subject to the various local environmental setting. It can be drawn from this comparison that GWR analysis is more capable to reveal the spatial variation in correlation relationship between Vegetation NDVI and local surface temperature existed within whole study area.

Only model 11/03/2003 shows significant spatial variation of road network density coefficients, accordingly the CC distribution is shown in Figure 5.18. As can be seen that some of the urban areas within site in yellow circles show positive CC values, indicating that the CC of Road Density to local surface temperature heightening (referred as implied 'warming' effect on local surface) has been detected partly by GWR model. It is quite interesting to found that the CC values in the green circle area where the high density building developed together with high road network density happened to be negative which indicates a cooling effect on local surface temperature variation in this daytime observation (evidenced by the CC to the decrease of local surface temperature). This may be due to the nearby buildings shading effect introduced by the high rise high density development within these areas during daytime. However most of the sample points within study area demonstrate negative CC values. No obvious pattern can be identified regarding the local influence of road network on local surface temperature change. The speculation may be that a 90m resolution of LST image may not be detailed enough to study the

effect of urban road network on local surface temperature variation. Or this may be due to the inaccuracy of road network density estimation based on road network line graph used in this research leading to this misleading result.

The population density coefficients also show significant spatial variation both in daytime and nighttime models, the corresponding CC distribution of population density for nighttime model 10/28/2003, and daytime model 11/03/2003 and 04/17/2006 is shown in Figures 5.19, 5.20 and 5.21. Figure 5.19 shows that most of CC values of population density in 10/28/2003 nighttime pattern appeared to be positive indicating positive correlation with local surface temperature except the dark blue sample points' area. Especially in the yellow areas where most of the urban area located, the CC values appear higher indicating a stronger warming effect attribute to population density in urban area during night of 10/28/2003. While the correlation in daytime patterns shows much more diversity within whole study area. In Figures 5.20 and 5.21, the CC values of some area with high rise and high density in region within green circle appear to be negative which means in this area the population density is negatively correlated with surface temperature. On the contrary, the area in yellow circle the CC values happened to be positive indicating positive correlation with local surface temperature. This may be partly due to the high rise high density development within west part areas along Nathan road which has an urban cooling effect during daytime with nearby buildings shading effect, while within the east part area the solar shading effect is not obvious with relatively mixed use of land. The solar radiation situation of local areas at this two image time can be seen in Appendix 2 Figures A2.1 and A2.4. By comparison, model 11/03/2003 demonstrates higher CC values in wider range than model 04/17/2006, this may be due to the fact that the relative dry weather at image time 11/03/2003 than 04/17/2006 may favor the impact of population density on local surface temperature variation. In general, GWR cannot differentiate the variation of the population density influence on local surface temperature within urban area with various population densities. This may be due to the population density estimation based on district census not be able to reflect the population variation exactly across the whole study area.

With the comparison of the CC values distribution of distance from coast for nighttime 10/28/2003, and daytime 11/03/2003 and 04/17/2006 shown in Figures

5.22, 5.23 and 5.24, it is easy to find that the CC values ranges from negative to positive when being far away from coast. Within a certain distance to the coast which may vary with local wind speed and direction and relative humidity, proximity to coast shows a significant negative correlation with the local surface temperature which indicates the obvious cooling effect on local surface within this extent. This confirmed that GWR model revealed the cooling effect of proximity with coast, when being further far away from coast the cooling effect vanished, instead of warming effect emerging. Comparing the pattern of CC variation in Figures 5.23 and 5.24 in daytime model 11/03/2003 and 04/17/2006, when approaching coast (the blue sample points area), the daytime model 11/03/2003 tends to show a more obvious negative correlation by a lower negative CC value with wider covering than the model 04/17/2006. This may be due to the relatively higher wind speed (5.67 m/s) at image time 11/03/2003 than at image time 04/17/2006 (2.81m/s) which favored the cooling effect of coast. Moreover with the wind direction change from blowing from coast to land (at image time of 11/03/2003) to blowing from land to coast (at image time of 04/17/2006) in yellow circle area, the CC values appeared from negative to positive indicating that the component contribution (CC) of proximity with coast to local surface temperature variation from temperature decrease to increase (referred as from cooling effect to warming effect) within this area. This may be due to the fact that when the wind blows from land to coast, the coast in low surface temperature during daytime may have no obvious cooling effect on local surface, even slightly contributes to the heightening of the local surface temperature with low positive CC values.

The CC of building square footage shows significant spatial variation in daytime models during 11/03/2003 and 04/17/2006 in Figures 5.25 and 5.26. As can be seen that CC values of the most built area within whole study area during 11/03/2003 and 04/17/2006 appear positive which demonstrate a positive correlation with local surface temperature. There is still some area in yellow circle CC values appear to be negative which indicates a cooling effect on local warming, it may be caused by the cooling effect induced by the high rise building shading effect on local surface. At the same time it is interesting to find that the lowest negative CC values of building square footage during 11/03/2003 tend to be lower (-0.92~0) than those (-0.43~0) during 04/17/2006. This may be due to the fact that the solar elevation angle during

04/17/2006 is larger (67.33 deg) compared with during11/03/2003 (49.39 deg), which may help to reduce the building shading effect with a higher solar elevation angle. The location discrepancy of sample points with negative CC values maybe owe to the solar azimuth angle difference within these two observation periods.

Both the nighttime and daytime models during 10/28/2003 and 11/03/2003, 04/17/2006 demonstrate significant spatially varying relationships between Elevation and local surface temperature with diverse parameter coefficients of Elevation within whole study area, CCs of Elevation at each image time are mapped in Figures 5.27, 5.28 and 5.29. Figure 5.27 shows that the nighttime model in 10/28/2003 demonstrates consistent negative correlation between Elevation and local surface temperature which implies a stable cooling effect of Elevation on local warming during nighttime period. The cooling effect is becoming stronger with lower negative CC values along with the altitude rising, with the lowest located in the peak of the hill indicating the strongest cooling effect in high altitude area. On the other hand the daytime models with seasonal change during 11/03/2003 and 04/17/2006 demonstrate a more diverse correlation ranging from positive to negative within whole study area in Figures 5.28 and 5.29, this may be induced by the various heating situation created with solar radiation during daytime under intensive elevation variation of urban canopy. Most of the areas with positive CC values indicating a heating effect on local surface temperature located in relatively low elevation area, under these low elevations area increasing the elevation may increase the opportunity to receive more solar radiation and then heighten the local surface temperature. At the same time it is interesting to find that the area coverage and value of positive CC is larger (with the biggest value 2.78) during dry season 11/03/2003 than during the growing season 04/17/2006(with the biggest value 2.25). This may be due to the fact that the solar elevation angle during 04/17/2006 is larger (67.33 deg) compared with 11/03/2003 (49.39 deg), which helps decrease the area coverage and influence of solar shading.

The coefficients of site openness to sky demonstrate significantly spatial variation ranging from negative (indicating cooling effect) to positive (indicating warming effect) in both nighttime and daytime models of during 10/28/2003 and 11/03/2003, 04/17/2006, CC values are mapped for each image time in Figures 5.30, 5.31 and

5.32. Figure 5.30 shows that most of the urban areas in green circles have negative site openness CC values except the areas in yellow circles, it indicates that increasing the site openness may help cool the local area surface during night. The CC values of yellow circle area in Kowloon appeared positive indicating possible warming effect of increasing site openness in this area. This may be due to the intensive night activities happened during night in this CBD area. On the other hand, during daytime some of the areas with positive CC values (the red sample points area in Figure 5.31 and the yellow and red sample points area in Figure 5.32) mainly located in hill canyon area, indicating warming effect of site openness on local surface, it may be due to hilly topography in this area that increasing the site openness will increase the opportunity to receive more solar radiation and then an heightened surface temperature.

The standard residual distribution of the models in 10/28/2003,11/03/2003 and 04/17/2006 confirmed that spatial association has been successfully removed with GWR model, shown as Appendix 6 Figures A6.23, A6.24 and A6.25. This also proves that the GWR models provide a satisfying capture of the spatial variation of the relationships between local environmental factors and local surface temperature represented by the diverse parameters coefficients outputted from the GWR models. One more detailed illustration of the nonstationary relationships within study area can be provided which provides more local information regarding local effect on surface temperature variation. This made the thorough examination of local correlation is possible by offering local models with better goodness-of-fit.

The local comparisons of the relative magnitudes of CC among environmental variables are carried out to investigate the relative contributions of the independent variables to local surface temperature variation. The local dominant factors which contribute most to location specific surface temperature variation represented with the factor possessing the site specific biggest CC can be mapped and compared to differentiate the relative contribution of environmental factors. Since solar radiation play a dominant role on daytime surface heating, for example during 11/03/2003, which can be seen with the local dominant factors shown in Appendix 6 Figure A6.26. For easy comparison with nighttime models when the solar radiation is not available, the local comparisons among environmental variables in daytime models

are made without including solar radiation to avoid the possible obscuring effect on other factors when solar radiation is taken into consideration, which made the focus on other factors with more practical meaning for local urban design. The referred local dominant factors contributing most to the site specific surface temperature variation in 10/28/2003, 11/03/2003, and 04/17/2006 are mapped shown in Figures 5.33, 5.34 and 5.35.

As can be seen that the local dominant factors to surface temperature variation are varying in space and time. By comparison of Figures 5.33 and 5.34, during daytime 11/03/2003 the surface temperature of hill region is contributed most from vegetation NDVI when the photosynthesis and evaporation is more active during daytime, while during nighttime elevation and openness to the sky play a dominant role. This uncovered the local disparities of surface heating mechanism, which also indicates the dynamics of local effect of environmental factors on local surface heating in space and time, at one specific location, the order in relative magnitudes of environmental indicators contributing to local surface temperature variation is varied with geographical location and time. Especially in urban area it is difficult to generate a local pattern regarding the relative importance of environmental factor on site specific surface temperature due to the highly variation of the local dominant factors, which may in part due to the relative low resolution in sampling and measurement of some factors like population density and road density comparing with the intensive variation of urban landscape. The varying relationships between urban surface temperature and local environmental setting in space and time represented with the referred environmental factors made the emerged pattern of local dominant factors in terms of component contribution (CC) challenging to be interpreted and explained which may be due to limitations in the definition and measure of environmental indicators (Holt and Lo, 2008). It also made the clear delineation in the relative importance of environmental indicators on surface temperature variation, in particular surface warming difficult due to the complexity induced by the local varying effect in space and time.

5.5. Summary

In this chapter the urban thermal landscape study was divided into two sections in order to achieve a comprehensive understanding of urban effect on local surface

warming. In the urban thermal landscape characterization section, the spatial and temporal characteristics of urban surface temperature distribution was figured out by the visual comparison of urban surface temperature categories in relative to urban land use land cover. The day-night change of urban surface temperature was recognized, at the same time spatial dependency of urban surface temperature variation on local environment was identified through local statistical analysis. This provided necessary context for further correlation analysis based on multiple linear regression. In order to study the urban effect on local warming, a global linear regression analysis was performed first to study the relationship between urban environmental factors and surface temperature through time. The association of urban surface temperature with local environmental factors was confirmed. The global regression model had also revealed the discrepancy between daytime and night surface warming with regression coefficients inconsistency in extent and direction. While the consistency in the relationship between surface temperature and local environmental factors proved to be held in both daytime and nighttime pattern correspondingly. The urban rural comparison of local warming mechanism through time also revealed the spatial influence on local warming by grouping sample points into urban and rural categories and undertaking regression analysis separately. The urban rural discrepancy in surface warming mechanism suggests the possible variation of relationships across space which made the global regression model questionable. And then geographically weighted regression analysis was conducted to study the local patterns in relationships between urban environmental factors and local surface temperature. GWR facilitated the local investigation based on local statistical technique and confirmed the existence of spatial variation in relationships, it offered an in-depth investigation of urban effect on local surface warming through the mapped distribution of parameter coefficients.

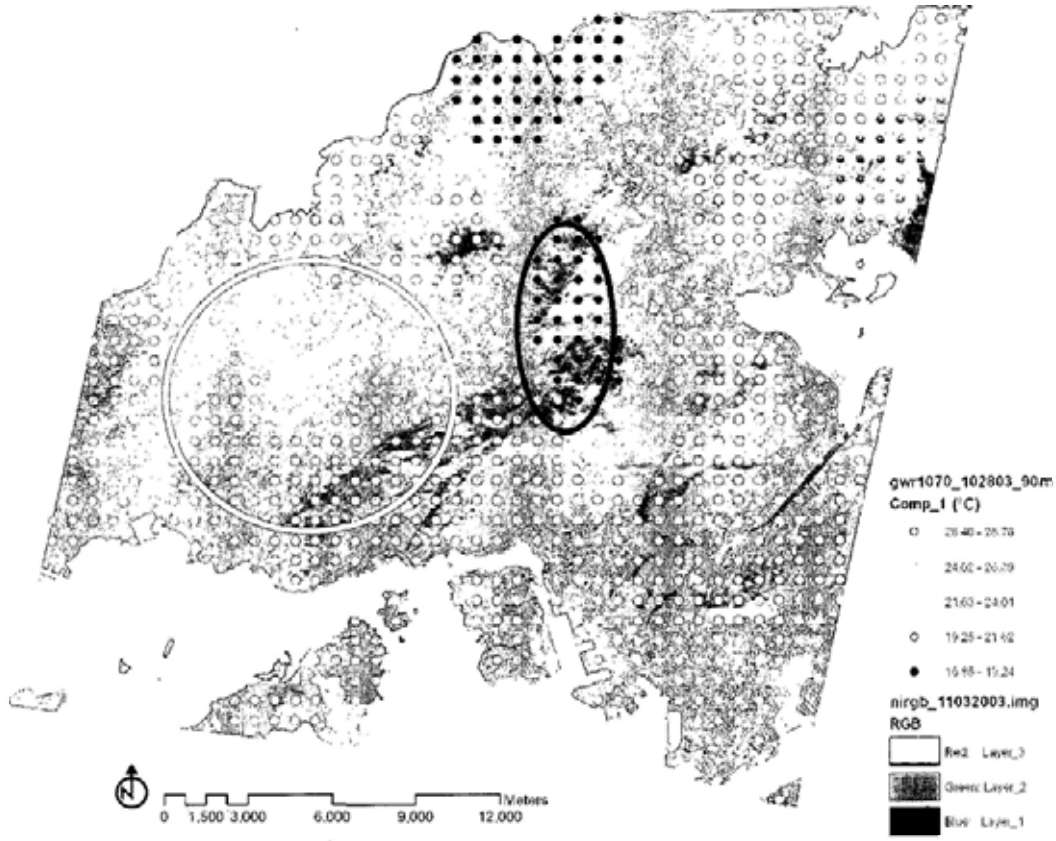

Figure 5.11 Coefficients contribution of Intercept in nighttime model 10/28/03

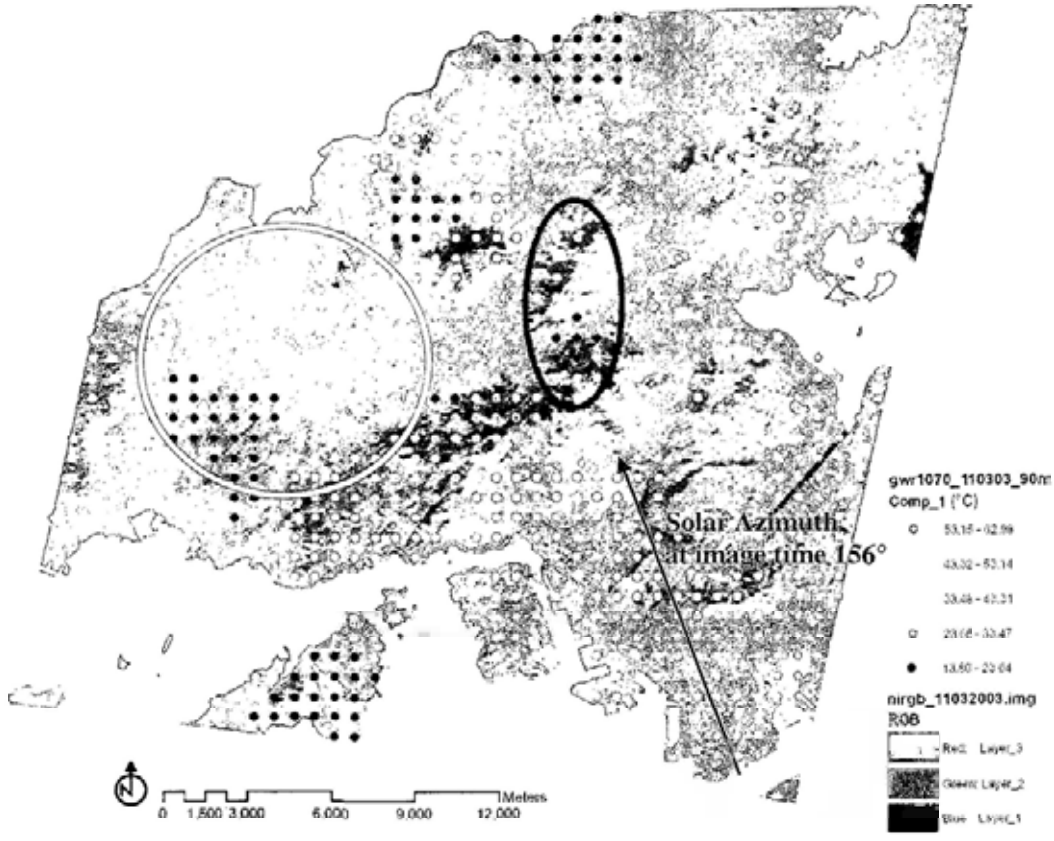

Figure 5.12 Coefficients contribution of Intercept in daytime model 11/03/03

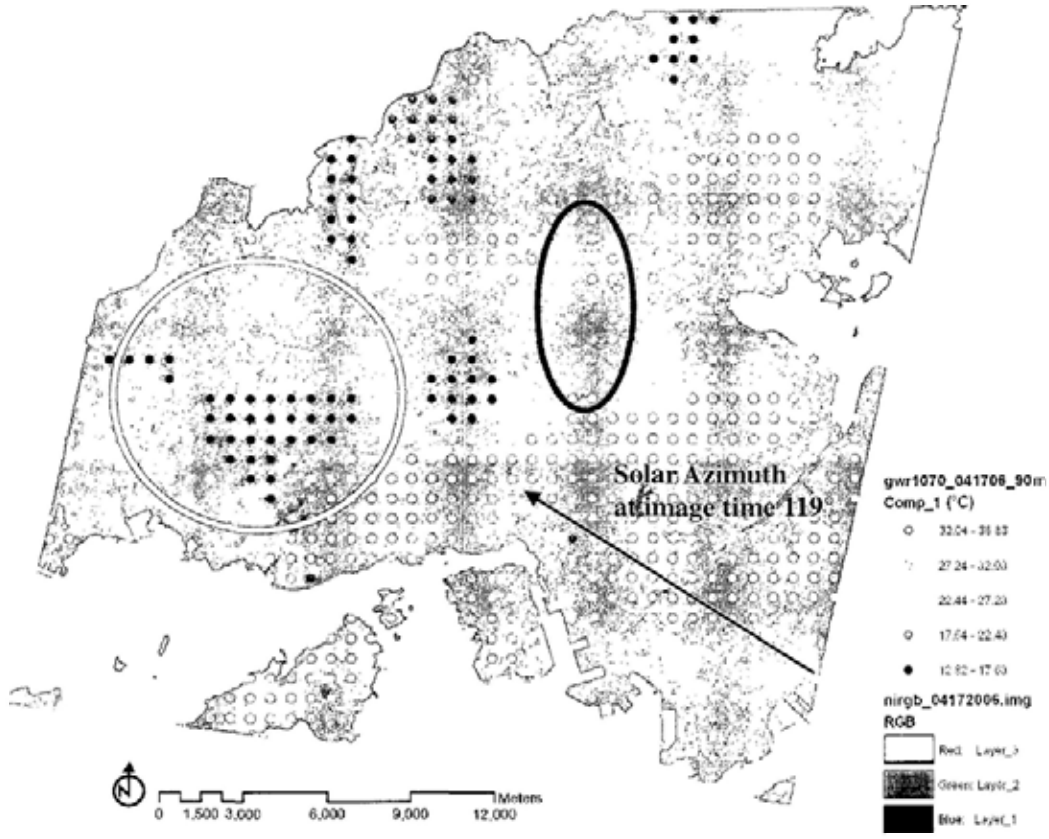

Figure 5.13 Coefficients contribution of Intercept in daytime model 04/17/06

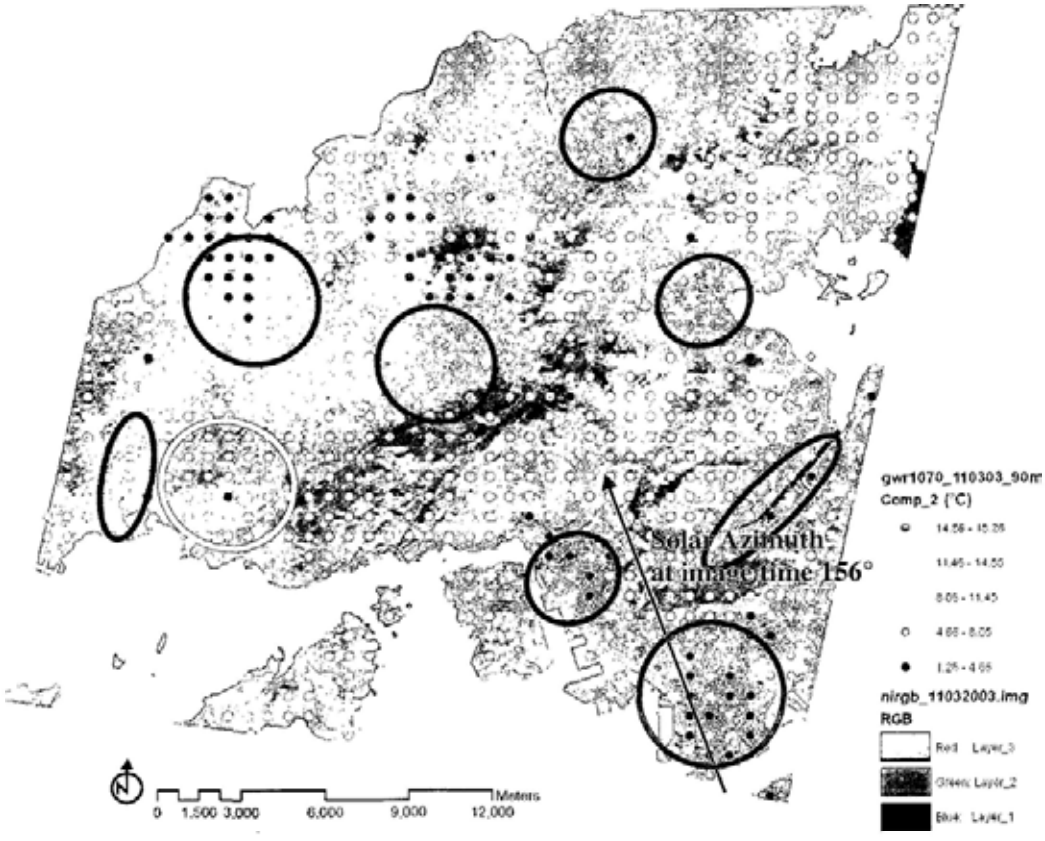

Figure 5.14 Coefficients contribution for Solar Radiation in daytime model 11/03/03

Figure 5.15 Coefficients contribution of Vegetation NDVI in nighttime model 10/28/03

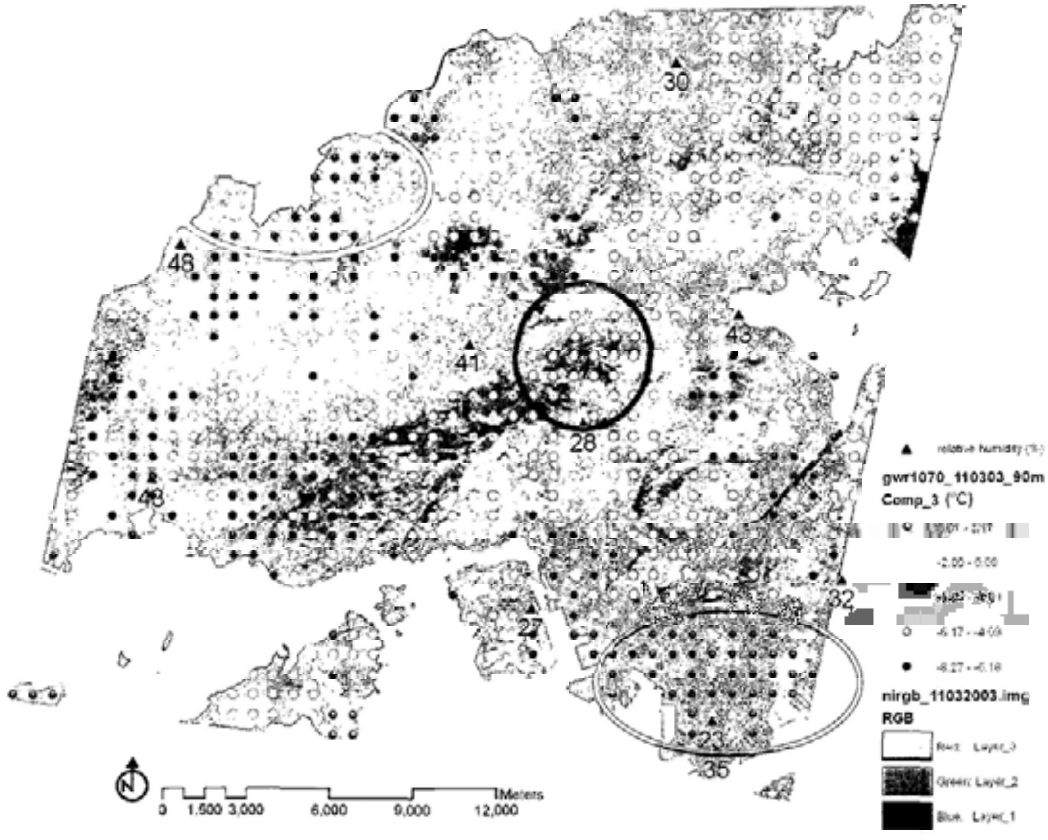

Figure 5.16 Coefficients contribution of Vegetation NDVI in daytime model 11/03/03

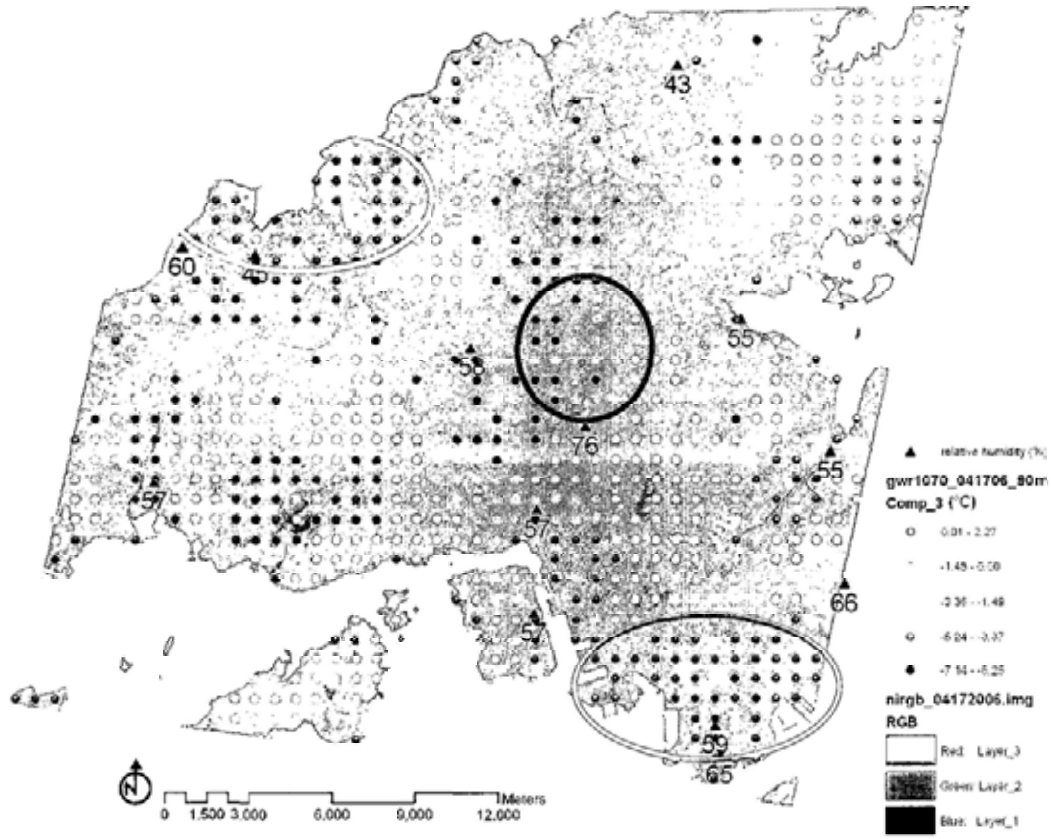

Figure 5.17 Coefficients contribution of Vegetation NDVI in daytime model 04/17/06

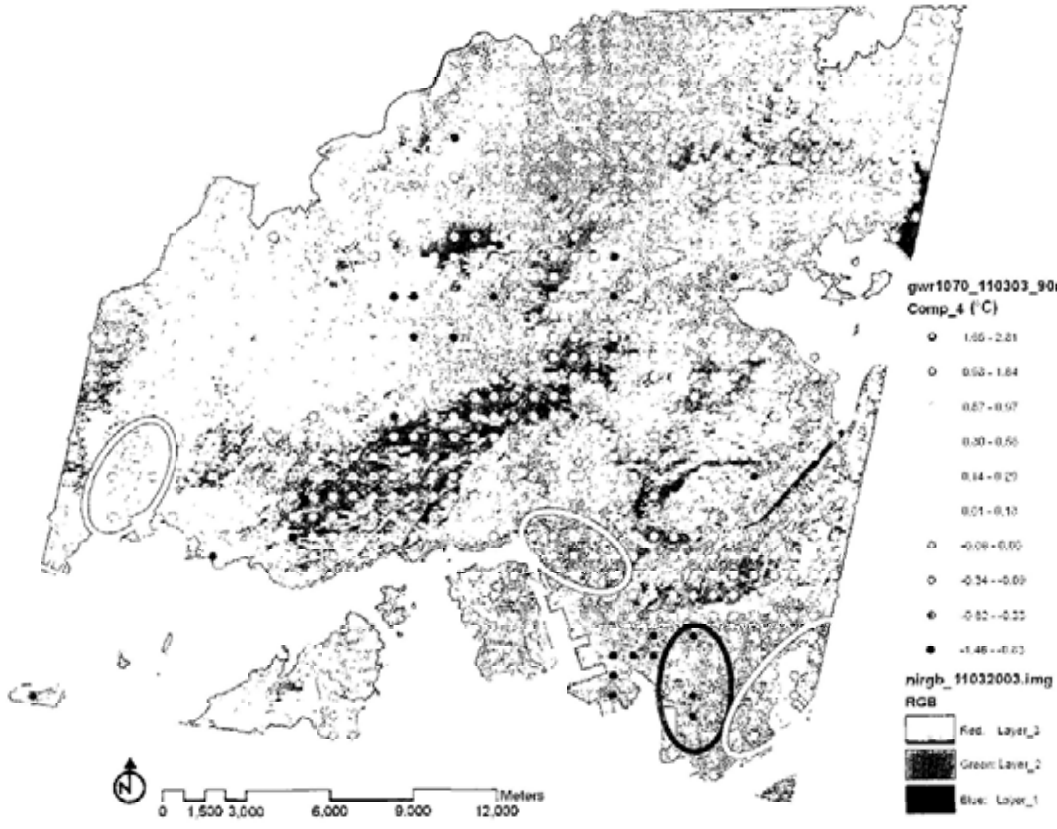

Figure 5.18 Coefficients contribution of Road Density in daytime model 11/03/03

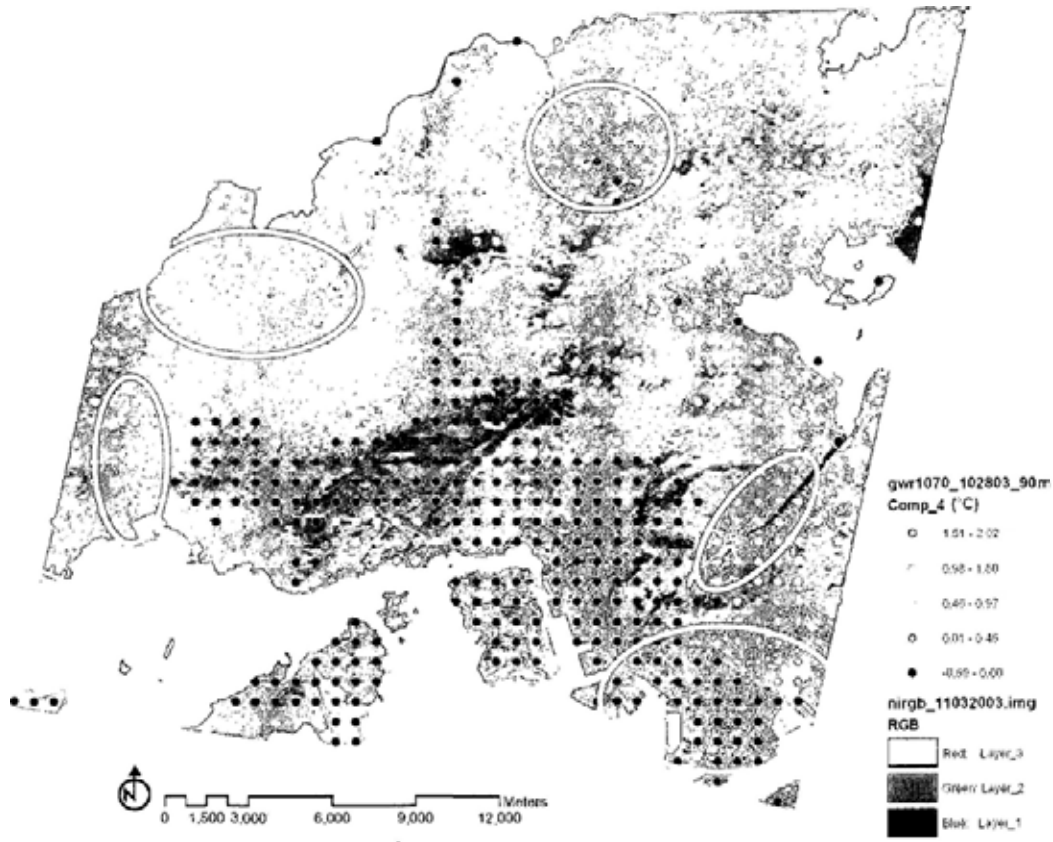

Figure 5.19 Coefficients contribution of Population Density in nighttime model 10/28/03

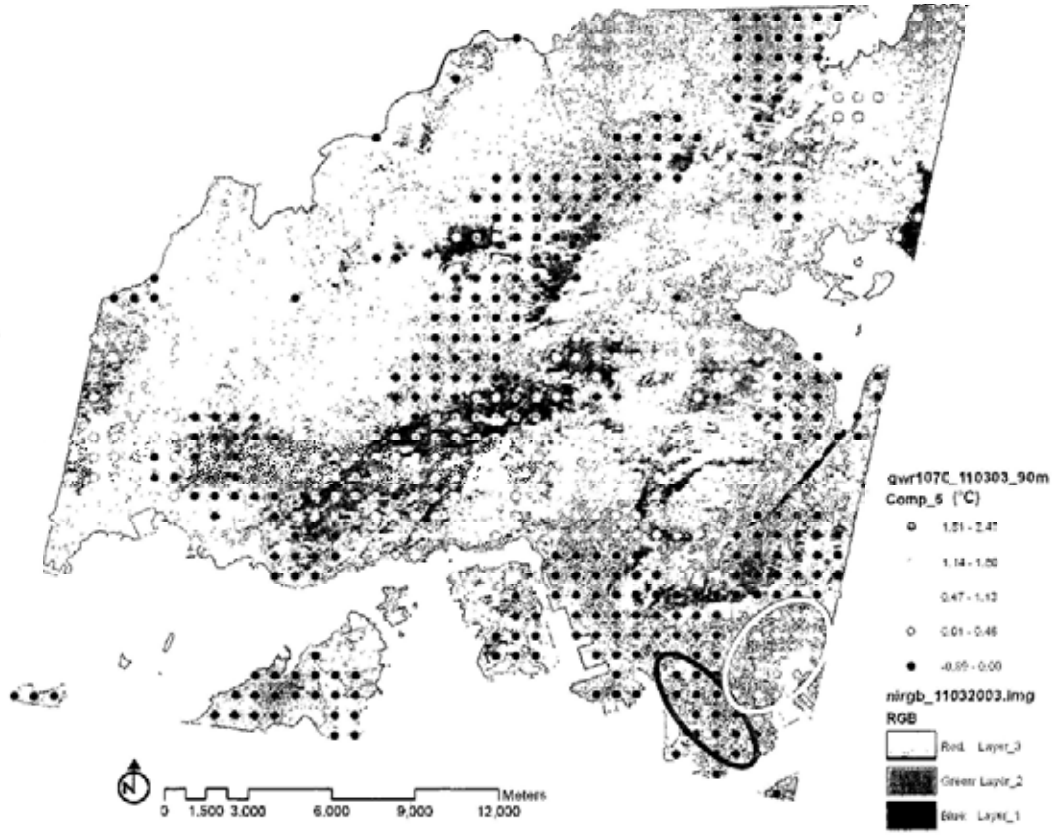

Figure 5.20 Coefficients contribution of Population Density in daytime model 11/03/03

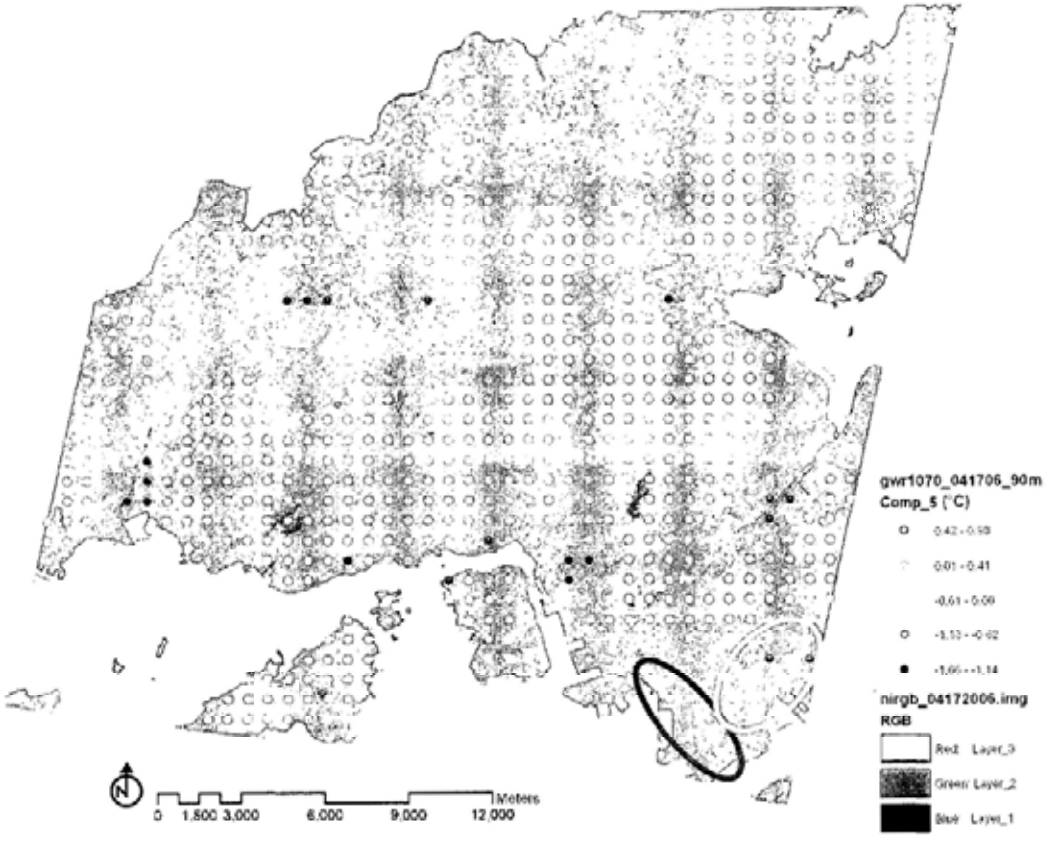

Figure 5.21 Coefficients contribution of Population Density in daytime model 04/17/06

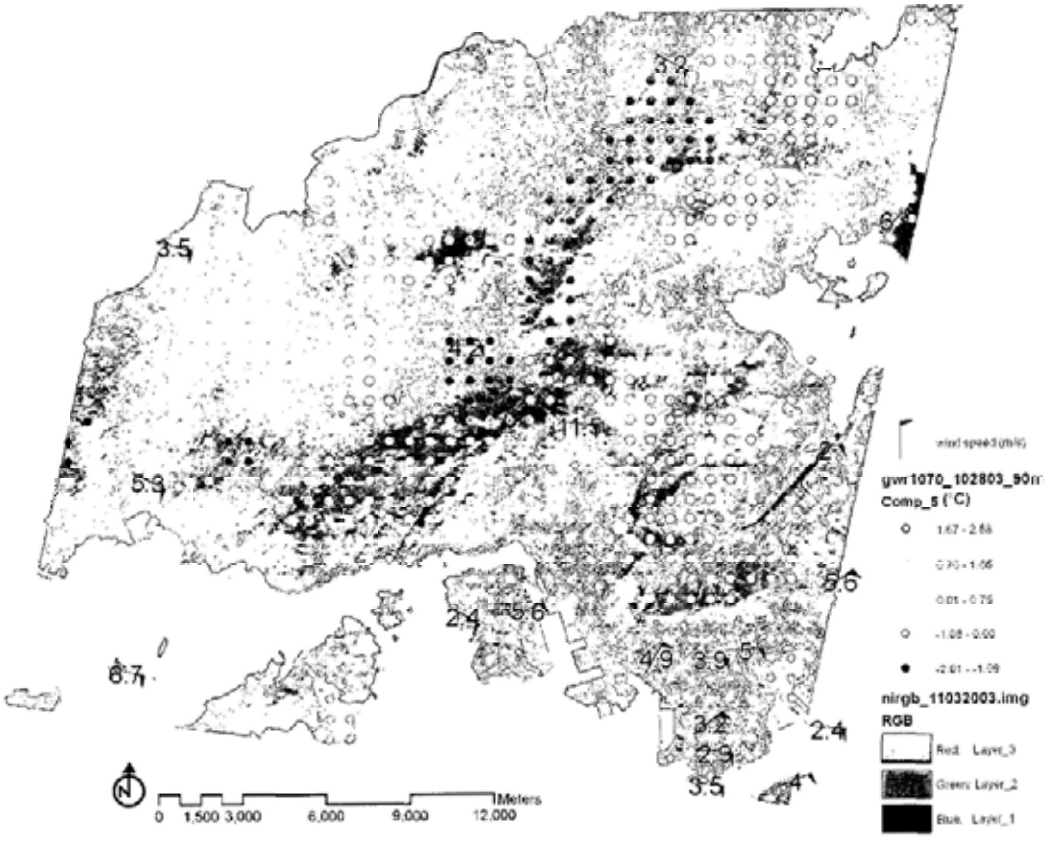

Figure 5.22 Coefficients contribution of Distance from coast in nighttime model 10/28/03

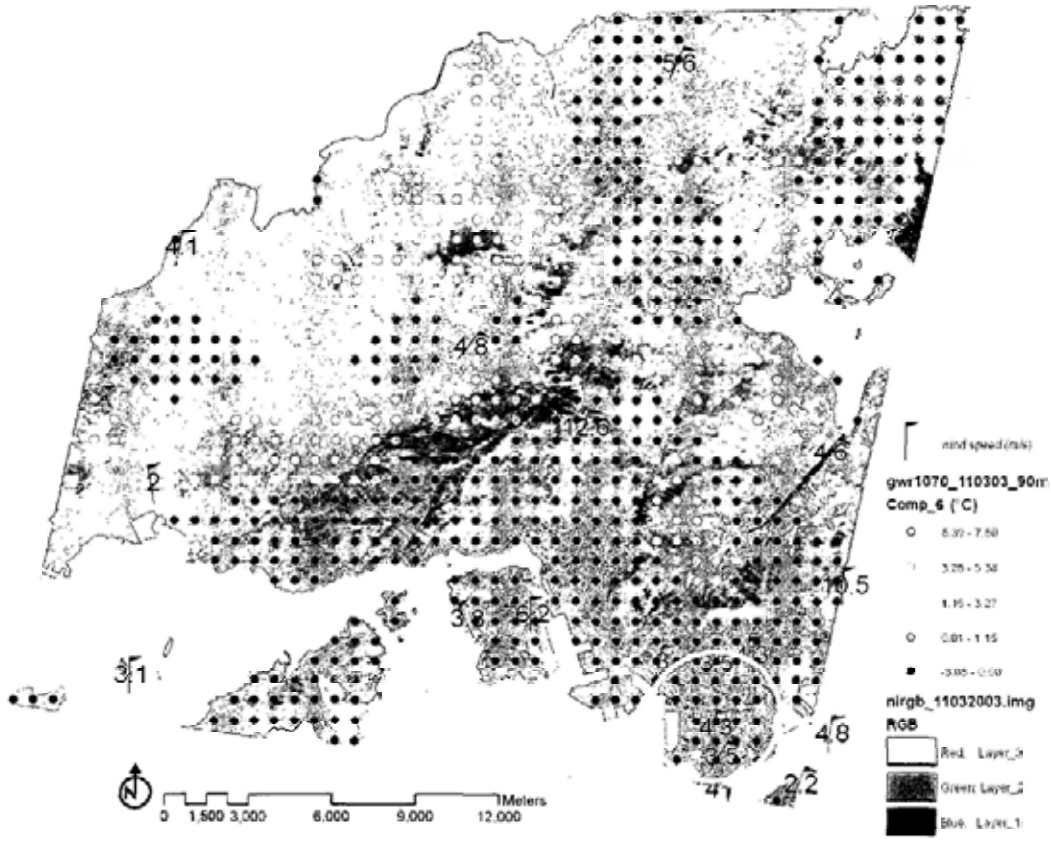

Figure 5.23 Coefficients contribution of Distance from coast in daytime model 11/03/03

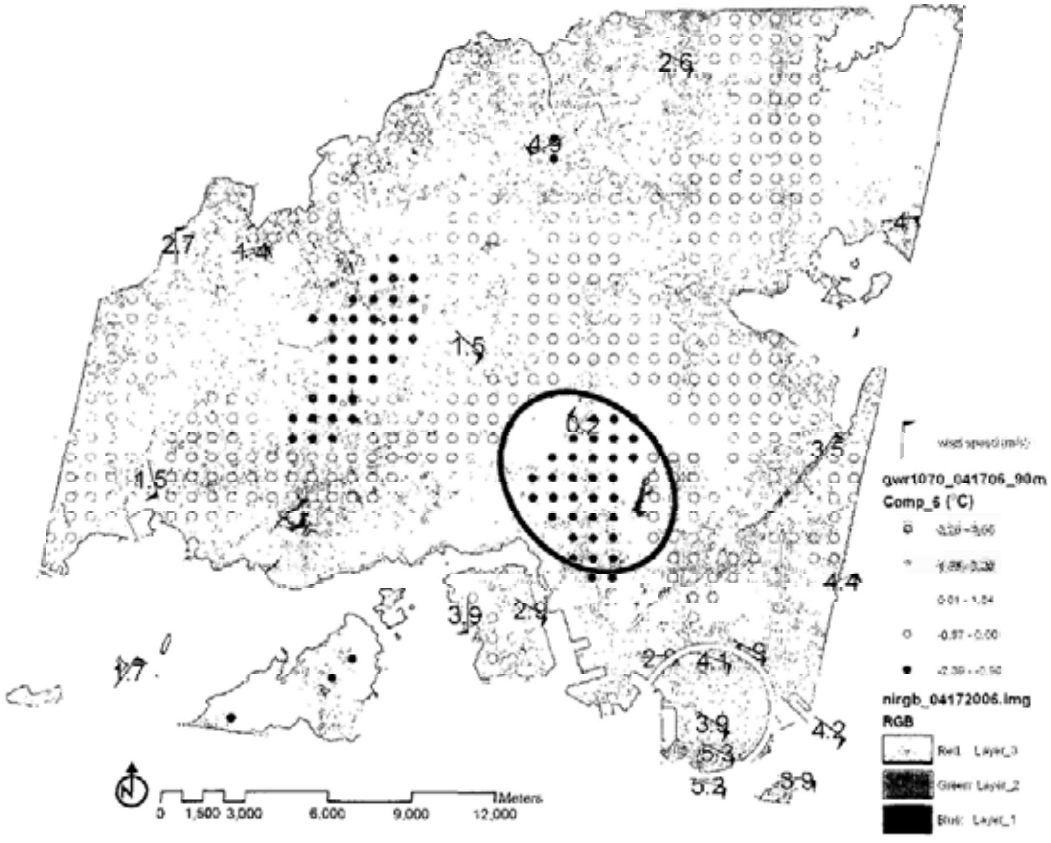

Figure 5.24 Coefficients contribution of Distance from coast in daytime model 04/17/06

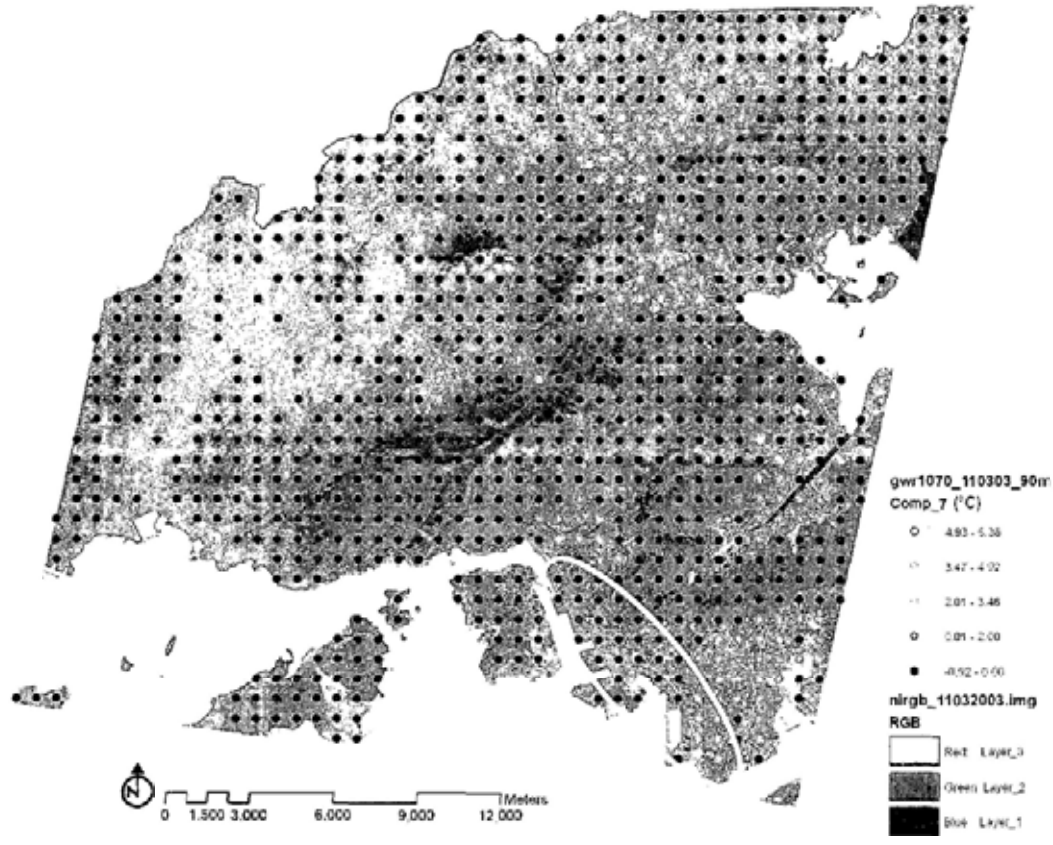

Figure 5.25 Coefficients contribution of Building footsq_a in daytime model 11/03/03

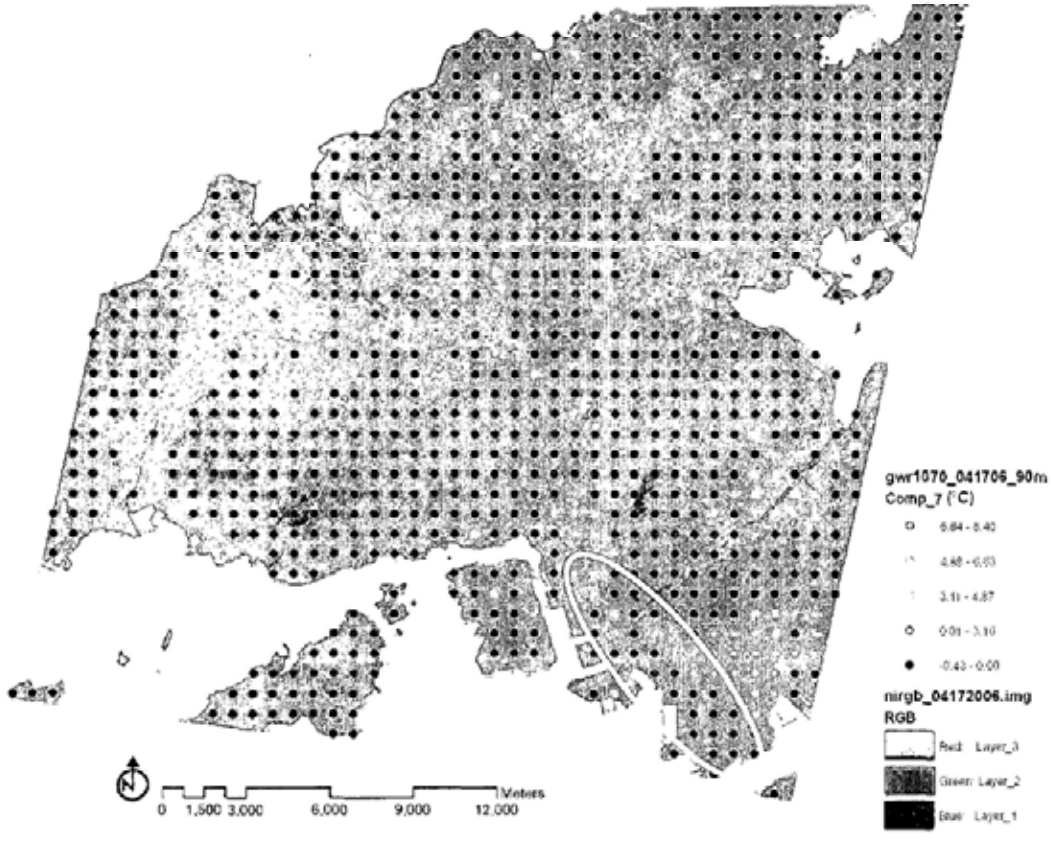

Figure 5.26 Coefficients contribution of Building footsq_a of daytime in model 04/17/06

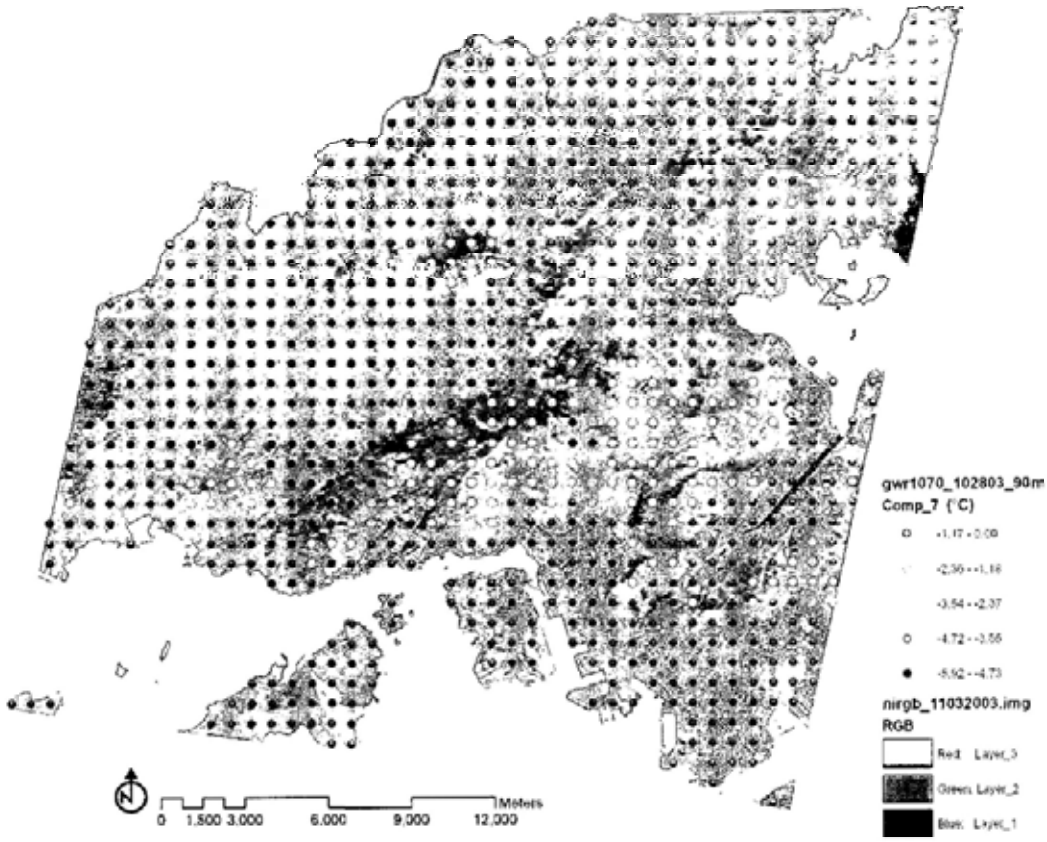

Figure 5.27 Coefficients contribution of Elevation in nighttime model 10/28/03

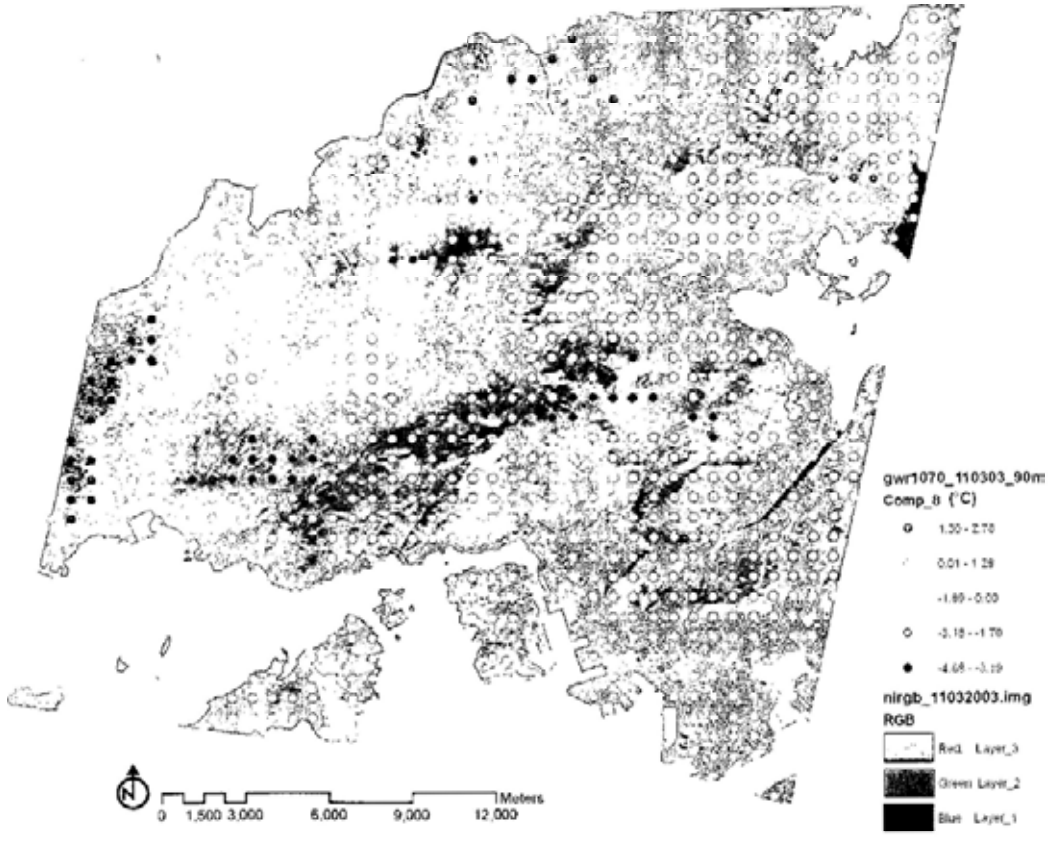

Figure 5.28 Coefficients contribution of Elevation in daytime model 11/03/03

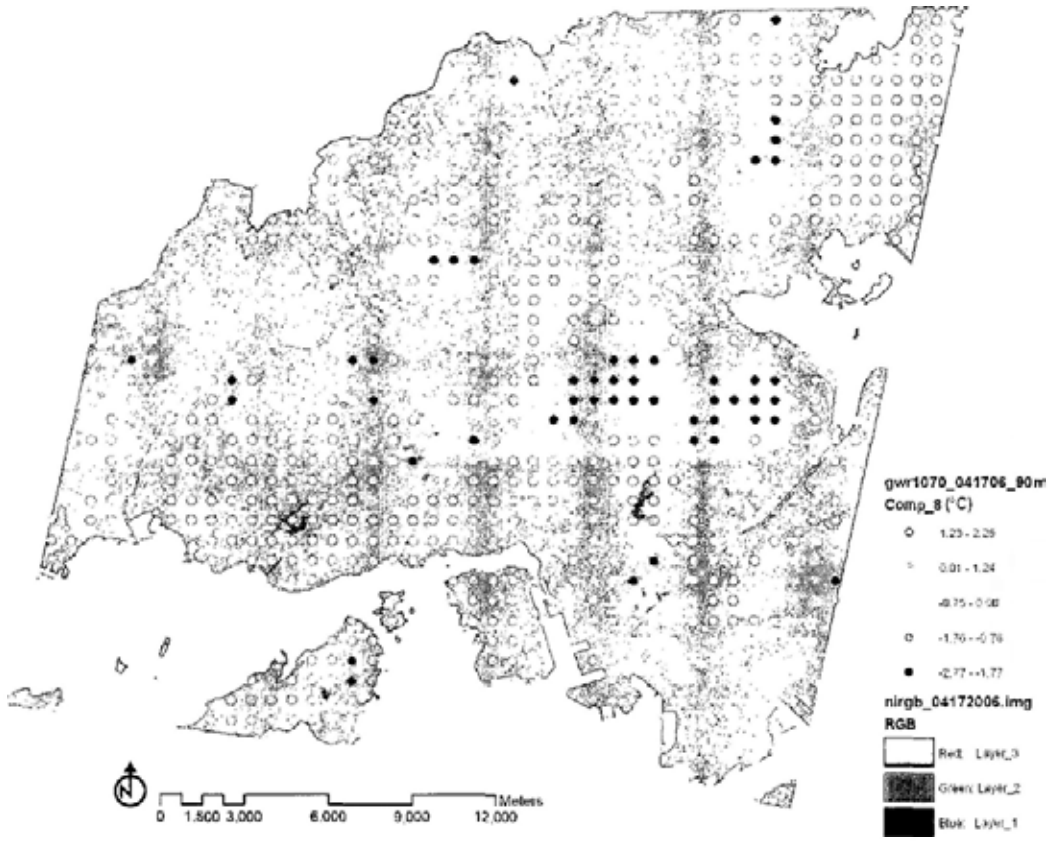

Figure 5.29 Coefficients contribution of Elevation in daytime model 04/17/06

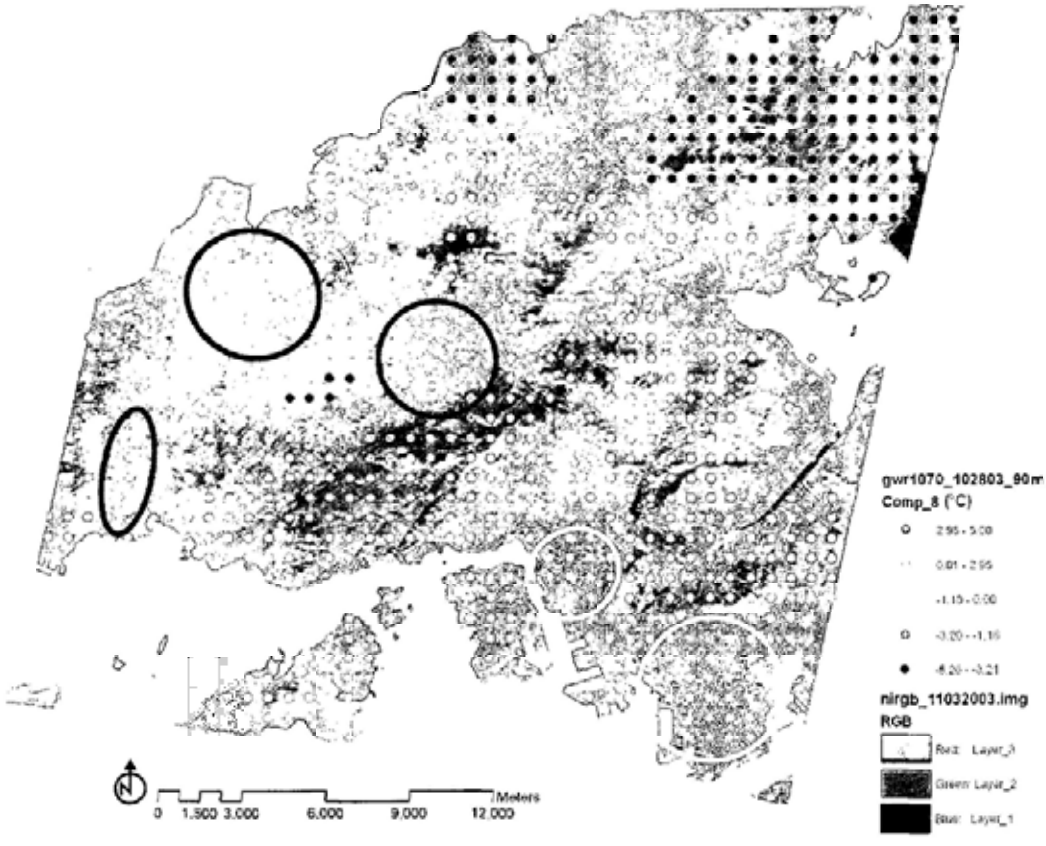

Figure 5.30 Coefficients contribution of Site Openness in nighttime model 10/28/03

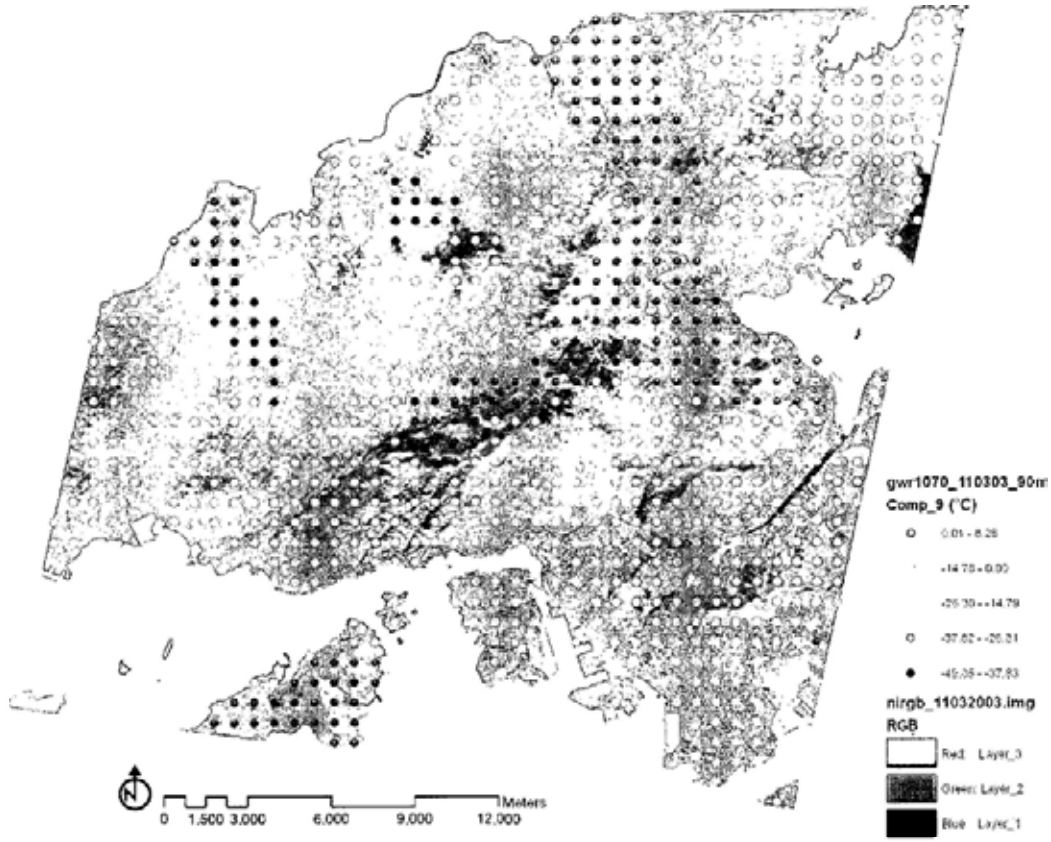

Figure 5.31 Coefficients contribution of Site Openness in daytime model 11/03/03

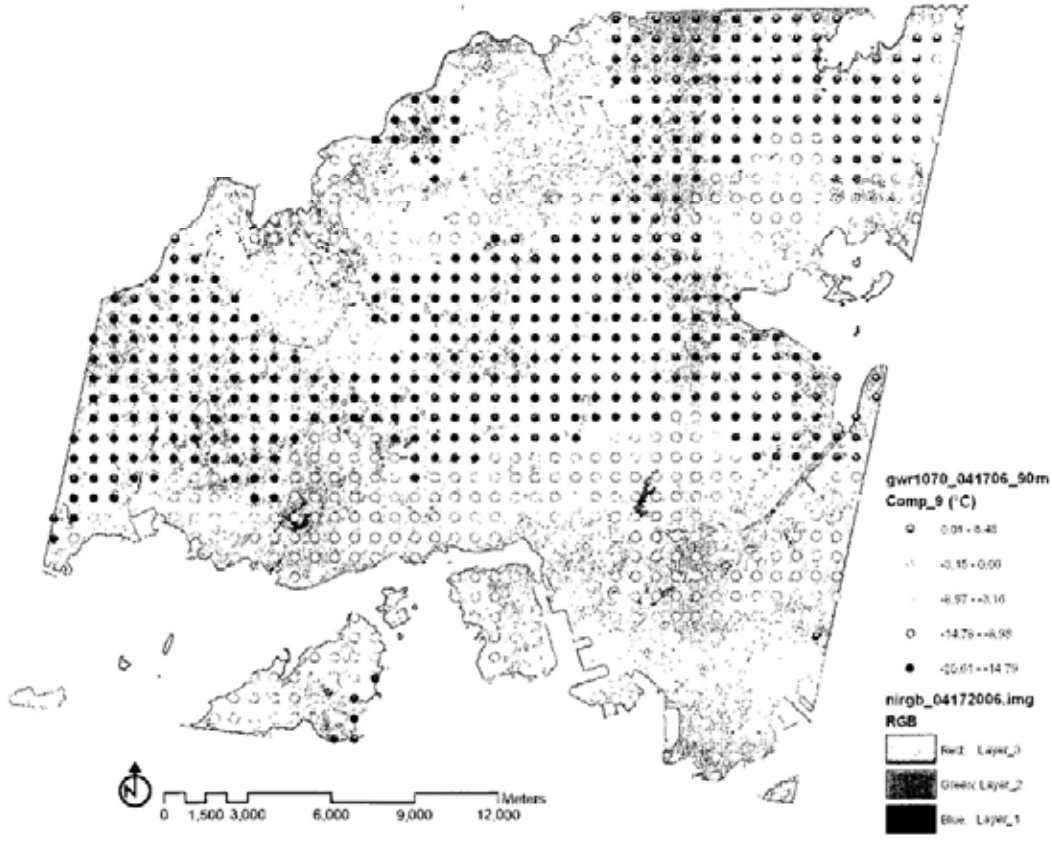

Figure 5.32 Coefficients contribution of Site Openness in daytime model 04/17/06

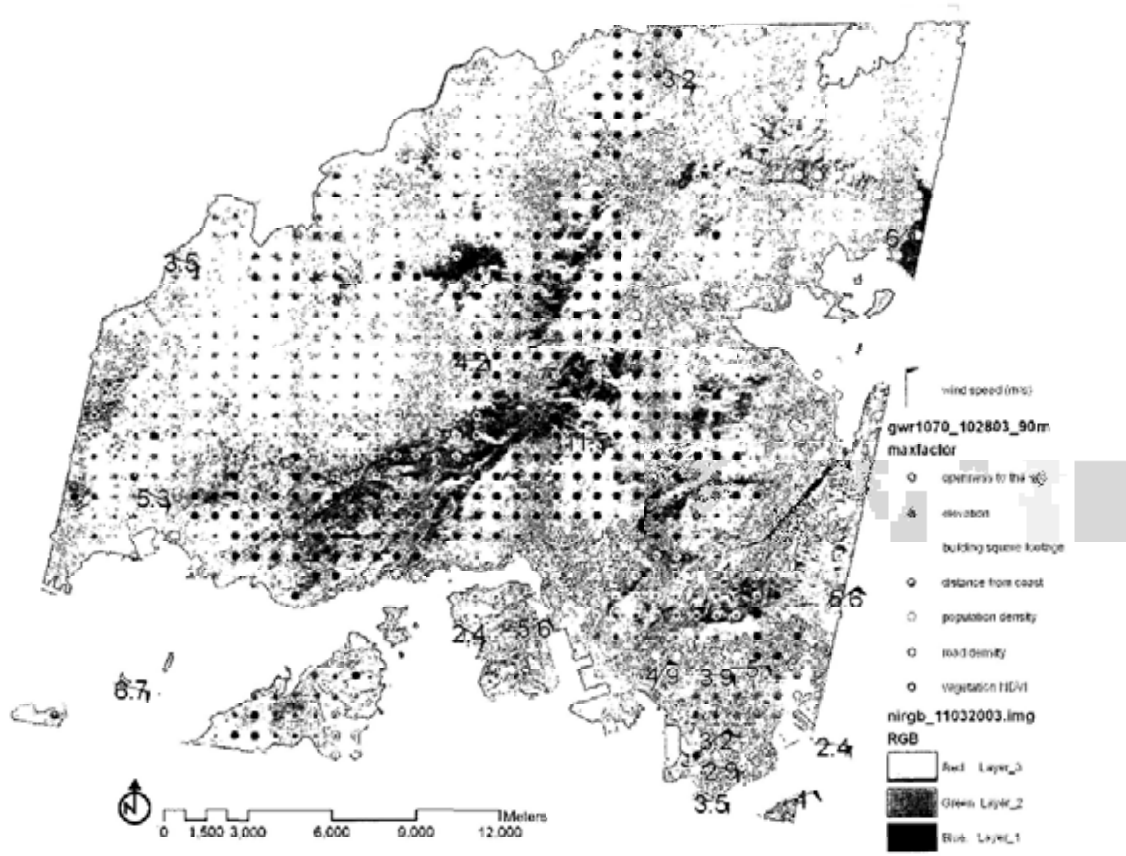

Figure 5.33 Local dominant factor to LST variation in nighttime model 10/28/03

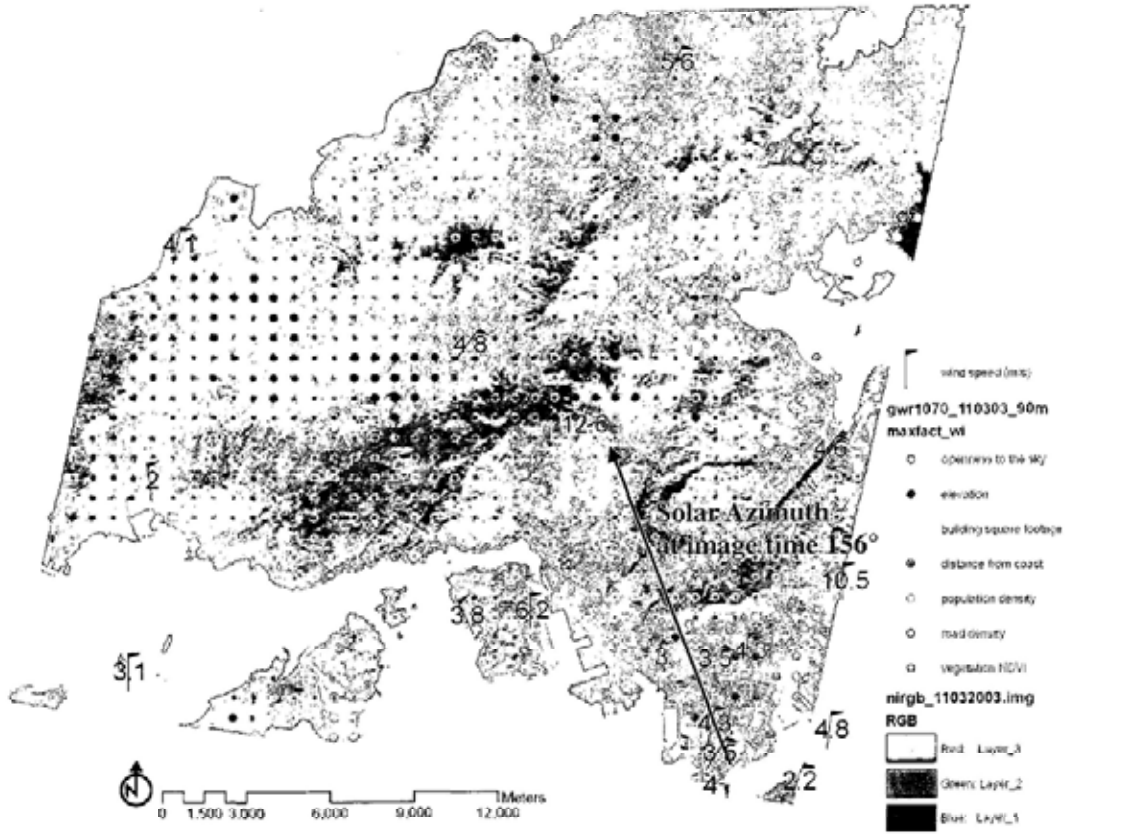

Figure 5.34 Local dominant factor to LST variation in daytime model 11/03/03

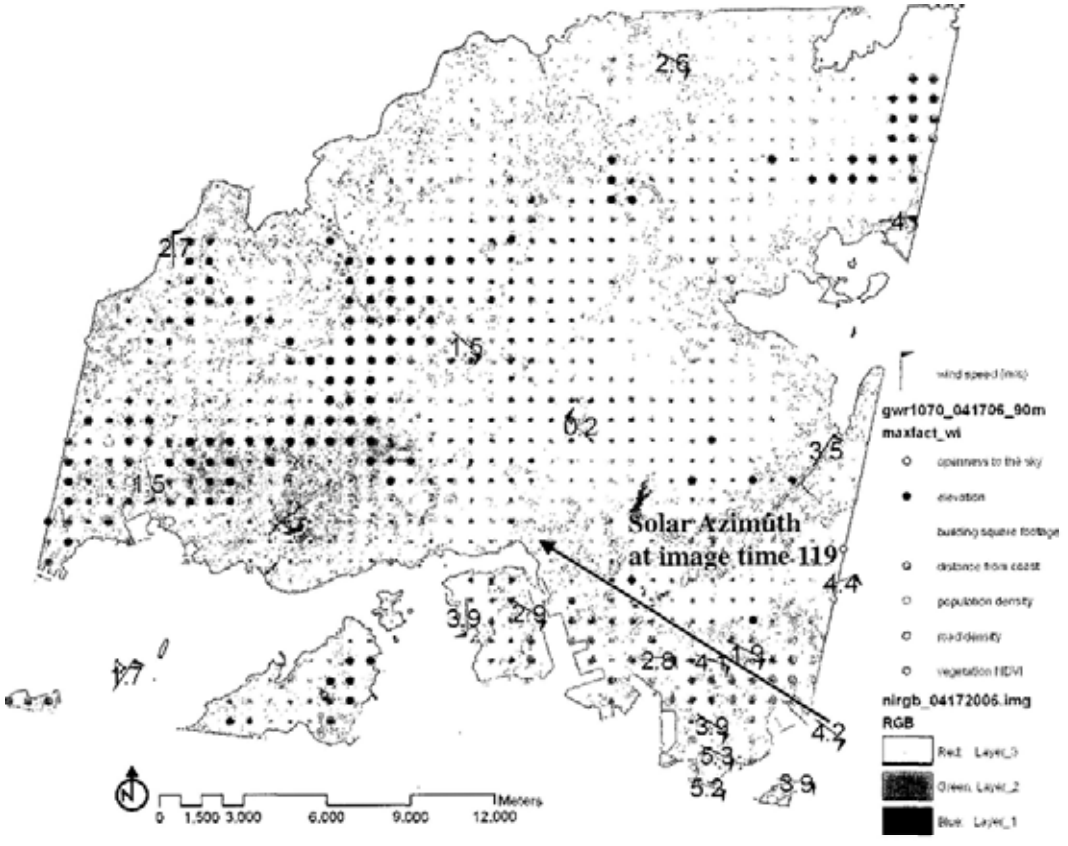

Figure 5.35 Local dominant factor to LST variation in daytime model 04/17/06

CHAPTER 6: CONCLUSIONS

6.1. Summary

During the process of worldwide urbanization along with high rise and high density housing development in large cities, urban warming has received growing concern among the environmental issues corresponding with urban landscape change. This irreversible process along with the urban transition from natural vegetated surfaces to impervious concrete heat absorbing materials deteriorates the urban thermal environment. A lot of issues including public heath, urban pollution, etc are becoming threats to human life as a result of urban warming. The endeavor to mitigate the negative effect of urbanization on urban climate has been set up with most of the communities from urban climate, geography, urban planning and design. Sustainable urban planning and design is one of the strategies promoted by urban architects and planners towards the adaptation and mitigation of global warming. The efficiency of these strategies in sustainable urban planning and design is also confined by the local climate which obscured these efforts with the interactive relationship between urban building and climate. Due to the complicated interplay between urban environment and local climate, it is far from certain about the urban effects on local warming, few attention has been paid to the variations of local effects on urban thermal performance at a scale over whole city area during urban development, even endeavors is quite scarce to characterize and analyze the spatial heterogeneity and dependency of urban thermal landscape aiming at delimitation of local effects on surface warming at city scale combining the measurement of urban surface and geometry via a viewpoint of local variation in space and time.

There is a need for a better understanding of urban effects on local climate with systematic evaluation. The progress in GIS technology, remote sensing, and geostatistical technique present an opportunity to develop systematic methodology for comprehensive studying urban surface microclimate. Based on the thermal

infrared remote sensing, the urban surface temperature can be extracted and mapped, and a detailed investigation of urban thermal landscape can be possible with a meso-resolution satellite image, which provides a platform to study urban effect on local climate for urban planning and design. Located in a subtropical region, Hong Kong's development with high rise and high density housing made it a suitable site for studying urban effect on local warming. This research chose Hong Kong as the case study and hopes to enrich our knowledge regarding urban local thermal performance and advance our understanding of urban microclimate in hot-humid weather area. The integrative utility of thermal remote sensing, landscape metrics methodology, geospatial statistical analysis for a comprehensive study of urban effect on local surface warming made this research unique since relatively scarce work has been reported in the literature.

During this attempt, a systematic analysis of urban surface temperature pattern across space and time was enabled based on urban thermal remote sensing. The dynamics in spatial heterogeneity and dependency of urban thermal landscape on urban landscape was characterized through spatial-temporal comparison and landscape metrics. The descriptive measures of landscape metrics captured the changes in overall structure of urban thermal landscape across space and time with the comparison made in the spatial and temporal dimension. In day-night change, higher local variation and irregularity on urban surface temperature pattern during daytime was observed and identified by the landscape metrics comparing with nighttime pattern. The diversity and fragmentation metrics had revealed the influence of urban development on overall urban landscape pattern. Along with urban development, daytime pattern of urban thermal landscape presented more fragmentation, less diversity and uneven texture distribution through the comparison of daytime observations in temporal dimension.

Then statistical regression analysis was employed to address the correlations between urban environmental factors and surface temperature. To this end the urban effect on

local surface temperature was interpreted based on statistical regression model. In summary, global regression analysis confirmed the relationship between environmental factors and surface temperature and gave a general overview of environmental effect on local surface warming, which can be taken as a general overview for urban effect study. The distinctive mechanism of dominating day-night surface warming was uncovered by regression analysis. For this study site within the observation periods, in terms of standardized parameter coefficient, vegetation was recognized playing the most important role referred as surface cooling in average to local surface temperature variation comparing with other measures of local environment setting both during daytime and nighttime. Besides the dominant role of local solar radiation on surface warming, building square footage demonstrated a second important influence on local surface temperature elevation during daytime. During nighttime population density played a dominant role on nighttime surface warming compared with other parameters, with the second important contribution of nighttime surface warming coming from road density. While elevation and distance from coast demonstrated obvious cooling effect on local surface within most nighttime models. According to this relative association of environmental parameter with local surface temperature variation the local strategies for surface cooling should be adopted in according with site specific day-night needs.

GWR analysis offered an in-depth investigation of local effect on surface temperature variation which was proved to be spatially varying and influenced by local weather condition with local environmental setting quantified with the referred site specific environmental factors. The spatial variation in relationships between environmental setting and surface temperature was significant with Monte Carlo significance test and distinctive in day-night change. The local dominant factor accounted for most to the site specific surface temperature variation was highly varied in space and time which prevented a general delineation of the relative association among environment factors to surface temperature disparities. This implied that the effect of environmental parameters which can be used as adaptive

measures for surface warming is confined in spatial-temporal dimension and the local findings in the relative association between environmental setting and surface temperature variation can not be easily transferable world wide without careful discrimination. The effective adaptive measures should be devised locally with reference to day-night needs in the identification of this feature. Comparatively, GWR facilitated the site specific investigation based on local statistical technique. The inference based on GWR model provided enriched information regarding the spatial variation of local environment effect on surface temperature variation which global model cannot approach. Complemented with each other, the global regression analysis and GWR demonstrated the utility of a thorough examination of the correlation between urban environment and local surface warming.

6.2. Implications

Based on thermal infrared remote sensing, urban thermal landscape monitoring and analysis provided much more detailed information about local warming that conventional meteorological study of urban climate cannot reach by loosely located weather station records. In the urban thermal landscape monitoring section, the spatial and temporal characteristics of urban surface temperature distribution was figured out by the visual comparison of urban surface temperature categories in relative to urban land use and land cover. The day-night change of urban surface temperature was recognized, at the same time spatial dependency of urban surface temperature variation on local environment was identified through local statistical analysis. The recognition of day-night difference of local surface thermal performance informed the urban thermal environment management process that strategies should be formulated according to functionality and local environment configuration to efficiently mitigate the possible negative effect of local warming in the practices of sustainable urban planning and design. Therefore in order to maintain a sustainable urban thermal environment, the strategies of urban thermal management must be formulated in acknowledgment with the spatial-temporal

difference in local heating mechanism.

Since the findings of this study is based on the observation period of October, November and April, so it is worth of note before any applicable exercise that the related strategies formulated based on this findings should be feasible only for this observation period regarding the local warming mitigation and adaptation in a strict logical sense. In this regard the following strategies may be underlined with a time period referring to this observation period. For example the open space within the residential community may emphasize on daytime warming adaptation and mitigation since the usage of the facility happens most on daytime. Besides vegetation, feasible shading facility with thermal friendly material can be adopted to avoid solar radiation in order to provide a thermal comfort entertainment place. At the same time replacement of impervious concrete heat absorbing materials with emissive roofing and paving materials can significantly mitigate local warming by reducing the influence of building square footage. While increasing the openness of the site cannot provide significant aid to maintain a pleasant thermal environment in according with the speculation based on the findings of this study. For those areas which need to focus on nighttime local warming mitigation, like residential building, the strategies may be different from those areas where daytime mitigation is necessary. At the same time the findings of local warming mechanism during nighttime in this study suggest that reducing population density may be used to sustain nighttime local thermal environment.

The output of urban thermal landscape monitoring provided enriched knowledge with respect to the characteristics of local thermal performance, at the same time the correlation analysis based on multiple linear regression confirmed the association of urban surface temperature with local environmental factors. The regression analysis also had revealed that local warming discrepancy existed between day and night with regression coefficients discrimination. Besides this, one of the most important findings of this research was the realization that relationships between urban

environmental factors and local surface temperature was varying spatially within the study area. The GWR analysis of local warming mechanism through time confirmed the spatial influence on local warming. The variation of relationships across space indicates the strategies should be formulated locally corresponding with local environmental setting. Since the existence of localized mechanism in regarding with local warming, the general guidelines of sustainable urban planning and design may be inappropriate for world wide application. At least to improve the efficiency of such strategies the local warming problems should be examined first under local circumstance to find the site specific influential factors which dominate local warming mechanism. This implied the necessity and importance of local warming issues to be studied locally before any procedure gone through for negative effects mitigation.

6.3. Limitations and Future Work

This study provided a framework for comprehensive study of urban effect on local surface warming. The utility of such a proposed framework was demonstrated within this research. Under this framework, some new understanding had been added for the study of urban effect on local climate with this research. However there are lots of factors which cannot be approached or quantified at current time while have noticeable effect on local warming, like ozone gas of air pollution, etc., they had not been taken into consideration under the current evaluation framework of this study. It leaded to parts of surface temperature variations being explained to certain extent with the model based on the correlation between the referred urban environmental factors and local surface temperature. Moreover the interpretation and explanation for the pattern in CC and local dominant factor outputted from GWR analysis remained challenging which may be in part due to limitations in the definition and measurement of environment factors (Holt and Lo, 2008). Further refinement is needed for a more accurate and clear delineation of the local effect on surface warming. Within an expanded framework of this study, more factors influencing

local warming should be incorporated into the evaluation model in order to improve the model and consolidate the output which would significantly benefit our practice of sustainable urban planning and design in the end.

This study mainly emphasized on urban surface thermal landscape study represented by urban surface temperature derived from thermal infrared remote sensing, the meteorological information was used as a reference for data quality examination and statistical regression relationships interpretation. With a much denser strategically located observation grid, the meteorological data can be related with urban surface temperature for an in-depth study of urban surface-air temperature studies. It poses significant meaning for the improvement of urban local warming studies in bridging the gaps of urban climates studies and remote sensing. The significant contribution can be made to take the application of urban climate on environmental concerned urban planning and design step forward beyond current cumbersome situation.

The primary findings of this research was based on the images during corresponding observation period when the satellite image was available, mainly in April, October and December of the relatively dry season. Since not all the seasons were included in the analysis, possible bias may be induced when the observations were made on two seasons only. The road density and population census data used in this study may not be representable for urban transportation situation with current resolution. Therefore the influence of these factors cannot be exactly detected in this research. On the other hand vegetation was quantified with NDVI in this research, which measurement of vegetation is said corresponding more to the vegetation cover. Moreover during the dry season when most of the observations were made for this study, together with against a light urban surface background in Hong Kong, due to the sub-optimal timing of the images the NDVI cannot effectively differentiate various vegetation biomasses from diverse density and structure (Nichol and Lee, 2005). However it is necessary to quantify the vegetation biomass including vegetation cover and density in order to exactly examine the vegetation effect on local surface temperature. The

vegetation biomass evaluation remains an area needs to be refined based on current satellite images in order to improve the regression model. Even though the study showed the usefulness of thermal infrared remote sensing application on urban climate and the utility of this research framework for the study of urban effect on local surface warming.

In this research, summer and winter observations were not included in the analysis when surface temperature distribution may be different from the two seasonal observations in this research. Whilst the observations during summer and winter are crucial and typical for urban thermal environment study and may be more beneficial for urban surface warming study as well. The investigation based on two seasonal observations in temporal resolution prevents more comprehensive knowledge generation regarding the development of local surface warming. At the same time 90 meter resolution ASTER LST images used in this study prevents a clear delimitation of surface thermal performance with reference to various urban landscape composition and configuration under an intensive varied urban environment which is induced with the mixed pixel problem. Therefore the knowledge of urban effect on local warming obtained from this research with current resolution data remained insufficient for a holistic capture of local thermal performance in relative to the intensive variation of local warming in spatial and temporal dimension.

For the GWR analysis, it was difficult to provide a clear delimitation for the spatial variation of correlation relationship between each parameter and local surface temperature across whole study area based on current sampling resolution due to the intensive spatial variation of high density and high rise urban environment together with hilly topography. Even the diversity had been ensured by this strategically sampling method for regression analysis to generate a reliable inference and to reduce the computation cost as well. At the same time, the utility of GWR analysis based on this sampling method for a thorough investigation of urban effect on local climate at meso-scale was also demonstrated. It provided comprehensive knowledge

background for future application. However for the practical application of urban planning and design, the inference based on the sample points mapping becomes cumbersome without a visual impressive representation of the clearly delimitated coefficients surface corresponding to local environment. In order to illustrate the heterogeneous correlation between urban environment and surface temperature at local scale for the practical exercise in urban planning and design, a pixel based sampling for GWR analysis may be more suitable when the correlation spatial variations can be exactly mapped with the coefficients surface, which may be possible with the high performance of grid enabled GWR analysis (Harris, et. al., 2006) to facilitate the subsequent extremely intensive computation needed.

The spatial and temporal resolution of satellite image data used in this research demonstrated limited utility for urban study especially for urban planning and design with local warming concerned. High spatial and temporal resolution thermal infrared images are necessary for a comprehensive study of local warming. With the advancement of image acquisition system, high spatial and temporal resolution image can be available with the airborne sensor platform for the urban study of local warming. On the other hand, besides high resolution image acquisition system, the usage of image fusion techniques for thermal images resolution enhancement represents the potential alternative for urban thermal environment study at micro-scale based on current LST images of low resolution (Nichol and Wong, 2005). With more high spatial and temporal resolution data incorporated into this research model, more clear delimitation of local surface thermal performance in spatial and temporal dimension would be possible which may help advance current study of urban effect on local warming.

APPENDIX 1: Residual Error Report of Ortho-Rectification of ASTER Images

Table A1.1: Residual info for AST_L1B 04-17-2006 image
Residual Units: Image Pixels
GCPs: 37 X-RMS: 0.35 Y-RMS: 0.28

Point ID	Elev (m)	Res	Res X	Res Y	Type	Photo X	Photo Y	Comp X	Comp Y
G0001	542.855	1.12	1.11	-0.15	GCP	1287.4	3417.6	1288.5	3417.4
G0002	6.690	0.8	-0.72	-0.35	GCP	2138.1	3224	2137.3	3223.7
G0003	2.000	0.76	-0.67	0.36	GCP	1997.9	3463.1	1997.3	3463.4
G0004	83.211	0.57	0.07	-0.57	GCP	1039.9	3409	1040	3408.4
G0005	6.305	0.56	0.55	-0.12	GCP	2524.5	3861.5	2525	3861.4
G0006	1.843	0.54	-0.37	0.4	GCP	1456.9	3700.1	1456.5	3700.5
G0007	14.540	0.54	-0.34	0.42	GCP	2297	2847	2296.7	2847.4
G0008	6.765	0.51	-0.49	-0.16	GCP	1818	2967.1	1817.5	2966.9
G0009	0.739	0.49	0.04	0.49	GCP	2477	3544	2477	3544.5
G0010	4.494	0.49	-0.49	0	GCP	1516.1	3919.7	1515.6	3919.7
G0011	4.315	0.46	-0.16	0.43	GCP	880	2826	879.8	2826.4
G0012	8.839	0.46	0.13	0.44	GCP	614.1	3246	614.2	3246.4
G0013	65.815	0.46	0.4	-0.22	GCP	3029.9	3367	3030.3	3366.8
G0014	3.524	0.45	-0.37	-0.25	GCP	973.1	3113.9	972.7	3113.7
G0015	1.00	0.44	0.2	-0.39	GCP	1025	4118	1025.2	4117.6
G0016	465.039	0.42	0.11	0.41	GCP	1136	2975.9	1136.1	2976.3
G0017	5.77	0.41	-0.35	-0.21	GCP	509.6	3474.6	509.2	3474.4
G0018	90.235	0.4	0.4	-0.04	GCP	2140.4	2462.6	2140.8	2462.6
G0019	159.295	0.39	0.33	-0.2	GCP	746.5	3434.5	746.8	3434.3
G0020	3.064	0.38	0.37	0.08	GCP	566.9	3019	567.3	3019.1
G0021	8.968	0.37	-0.02	-0.37	GCP	1525.9	2328	1525.9	2327.6
G0022	1.246	0.34	-0.07	-0.33	GCP	1022.6	2579.6	1022.5	2579.2
G0023	5.339	0.33	0	-0.33	GCP	1319	2527.9	1319	2527.5
G0024	2.416	0.33	0.16	0.29	GCP	463.9	3663.6	464.1	3663.9
G0025	18.850	0.31	0.02	-0.31	GCP	2873	3114.9	2873	3114.6
G0026	4.600	0.31	0.27	0.16	GCP	2870.4	3172.5	2870.7	3172.7
G0027	3.522	0.25	-0.25	0.02	GCP	2170.6	3902.6	2170.3	3902.6
G0028	2.958	0.24	-0.22	0.1	GCP	2008	2215.9	2007.8	2216

G0029	22.301	0.22	0.2	0.09	GCP	2864.4	2925.9	2864.6	2926
G0030	2.2750	0.2	0.17	0.1	GCP	723.6	2975.6	723.8	2975.7
G0031	84.752	0.19	-0.12	-0.14	GCP	1385.5	3803.9	1385.4	3803.7
G0032	17.472	0.18	0.05	0.17	GCP	1567	2714.9	1567	2715.1
G0033	20.388	0.17	0.13	0.1	GCP	1751.9	2434	1752	2434.1
G0034	11.708	0.15	-0.15	-0.02	GCP	800.5	3224.5	800.3	3224.5
G0035	1.931	0.13	0.02	0.13	GCP	655.1	3760	655.1	3760.1
G0036	5.856	0.06	0	-0.06	GCP	1876.5	3995.4	1876.5	3995.4
G0037	7.956	0.05	0.04	0.02	GCP	304.9	4134.0	305.0	4134.0

RMS (x, y) for worst 5% of points in list: 1.11, 0.15

Table A1.2: Residual info for AST_L1B 10-23-2005 image
Residual Units: Image Pixels
GCPs: 38 X-RMS: 0.28 Y-RMS: 0.28

Point ID	Elev (m)	Res	Res X	Res Y	Type	Photo X	Photo Y	Comp X	Comp Y
G0001	0.739	0.65	0.59	-0.27	GCP	2843	3544.9	2843.6	3544.7
G0002	3.064	0.64	0.16	-0.62	GCP	934.4	3019.5	934.5	3018.9
G0003	20.388	0.57	-0.56	0.13	GCP	2119.7	2433.9	2119.2	2434
G0004	5.856	0.55	-0.15	0.53	GCP	2243.9	3995	2243.8	3995.6
G0005	2.416	0.54	-0.14	-0.53	GCP	831.5	3664.5	831.4	3663.9
G0006	83.211	0.53	-0.22	-0.48	GCP	1408	3408.9	1407.7	3408.4
G0007	3.522	0.51	-0.5	0.1	GCP	2537.7	3902.7	2537.2	3902.8
G0008	7.956	0.5	-0.46	0.19	GCP	671.9	4134	671.5	4134.2
G0009	8.968	0.5	-0.07	0.49	GCP	1892.9	2327	1892.8	2327.4
G0010	2.275	0.47	0.25	-0.39	GCP	1091	2976	1091.2	2975.6
G0011	89.904	0.44	-0.1	0.43	GCP	2507.9	2463	2507.8	2463.5
G0012	2.159	0.43	0.21	0.38	GCP	1823.8	3700	1824	3700.4
G0013	22.301	0.42	0.15	-0.39	GCP	3230	2926.6	3230.2	2926.2
G0014	6.575	0.41	0.29	0.28	GCP	875.8	3474	876.1	3474.2
G0015	6.353	0.4	-0.36	-0.18	GCP	2185	2967	2184.6	2966.8
G0016	5.339	0.39	0.23	0.31	GCP	1686.1	2527.1	1686.3	2527.4
G0017	6.445	0.37	0.37	0.04	GCP	2890.7	3861.9	2891.1	3861.9
G0018	4.315	0.37	0.27	0.25	GCP	1247	2826	1247.3	2826.2
G0019	65.815	0.37	-0.35	0.09	GCP	3395.9	3366.9	3395.6	3367

G0020	1.000	0.33	0.02	0.33	GCP	1392.6	4117.5	1392.6	4117.8
G0021	159.295	0.33	-0.27	0.19	GCP	1114	3434	1113.7	3434.2
G0022	542.855	0.33	0.27	-0.19	GCP	1655.5	3417.4	1655.7	3417.2
G0023	19.663	0.32	-0.22	-0.24	GCP	3239	3114	3238.7	3113.8
G0024	11.516	0.32	0.21	0.23	GCP	1167.3	3224	1167.5	3224.3
G0025	1.246	0.31	-0.31	0.01	GCP	1390	2579	1389.7	2579
G0026	465.039	0.28	-0.25	0.14	GCP	1503	2976	1502.8	2976.1
G0027	4.494	0.28	0.27	-0.1	GCP	1883	3919.9	1883.3	3919.8
G0028	3.631	0.28	0.27	-0.05	GCP	1339.7	3113.8	1340	3113.8
G0029	85.480	0.26	0.07	-0.25	GCP	1752.6	3804	1752.7	3803.8
G0030	2.958	0.26	0.22	-0.13	GCP	2374	2216	2374.2	2215.9
G0031	1.931	0.25	-0.22	0.13	GCP	1022.9	3760.1	1022.6	3760.2
G0032	14.540	0.25	0.23	-0.09	GCP	2663.5	2847.6	2663.7	2847.5
G0033	1.831	0.24	-0.18	-0.15	GCP	2364.5	3463.5	2364.3	3463.4
G0034	1.845	0.23	0.22	-0.06	GCP	2505	3224	2505.2	3223.9
G0035	8.839	0.2	0.05	-0.2	GCP	981.6	3246.5	981.6	3246.3
G0036	17.472	0.19	-0.19	-0.02	GCP	1934.9	2715	1934.7	2715
G0037	1.000	0.14	0.14	0	GCP	432.6	3576.5	432.8	3576.5
G0038	5.485	0.09	0.06	0.07	GCP	3237	3172	3237	3172.1

RMS (x, y) for worst 5% of points in list: 0.59, 0.27

Table A1.3: Residual info for AST_L1B 11-21-2004 image
Residual Units: Image Pixels
GCPs: 32 X-RMS: 0.37 Y-RMS: 0.33

Point ID	Elev (m)	Res	Res X	Res Y	Type	Photo X	Photo Y	Comp X	Comp Y
G0001	6.353	1.09	-1.01	-0.39	GCP	3819.1	2967	3818	2966.6
G0002	3.064	0.85	0.39	-0.75	GCP	2569.6	3019.6	2570	3018.9
G0003	0.739	0.8	0.75	0.28	GCP	4478	3544	4478.7	3544.3
G0004	1.831	0.77	-0.64	-0.43	GCP	3998.5	3463.5	3997.9	3463.1
G0005	542.855	0.69	0.69	-0.09	GCP	3289.6	3416.9	3290.2	3416.8
G0006	4.494	0.57	-0.1	-0.56	GCP	3517	3920	3516.9	3919.4
G0007	8.968	0.56	-0.13	0.55	GCP	3528	2326.9	3527.9	2327.5
G0008	1.000	0.52	-0.31	0.41	GCP	3027	4116.9	3026.7	4117.3
G0009	159.295	0.5	0.33	0.37	GCP	2748.5	3433.6	2748.8	3433.9

G0010	89.904	0.49	0.15	0.46	GCP	4142	2462.9	4142.1	2463.3
G0011	2.958	0.48	0.46	-0.15	GCP	4009	2216	4009.5	2215.9
G0012	17.472	0.47	-0.45	-0.14	GCP	3569.1	2715.1	3568.6	2714.9
G0013	85.480	0.46	0.22	0.4	GCP	3386	3802.9	3386.2	3803.3
G0014	1.000	0.46	0.32	0.33	GCP	2068.9	3576	2069.3	3576.3
G0015	14.540	0.43	0.39	-0.19	GCP	4297.6	2847.4	4298	2847.2
G0016	7.956	0.41	0.16	-0.37	GCP	2306.9	4134.1	2307.1	4133.7
G0017	20.388	0.41	-0.39	-0.12	GCP	3754.1	2434.1	3753.7	2433.9
G0018	3.522	0.4	0.03	0.4	GCP	4172	3901.9	4172	3902.3
G0019	2.416	0.4	-0.33	0.22	GCP	2466.6	3663.4	2466.2	3663.6
G0020	83.211	0.4	-0.38	0.13	GCP	3042	3408	3041.6	3408.1
G0021	465.039	0.38	0.33	-0.18	GCP	3137.9	2976.1	3138.3	2975.9
G0022	1.845	0.38	0.05	-0.38	GCP	4138.9	3224	4139	3223.7
G0023	4.315	0.37	0.22	0.3	GCP	2881.9	2825.9	2882.2	2826.2
G0024	3.631	0.33	0.05	-0.33	GCP	2973.9	3114	2974	3113.7
G0025	8.839	0.3	-0.03	-0.3	GCP	2616.5	3246.5	2616.5	3246.2
G0026	2.159	0.29	-0.29	-0.01	GCP	3457.6	3700	3457.3	3700
G0027	11.516	0.27	-0.2	0.18	GCP	2802	3223.9	2801.8	3224.1
G0028	5.339	0.26	-0.04	0.26	GCP	3321.1	2527.1	3321	2527.4
G0029	6.575	0.18	-0.12	0.14	GCP	2511.1	3473.9	2511	3474
G0030	1.931	0.1	-0.04	-0.1	GCP	2657	3759.9	2657	3759.8
G0031	1.246	0.1	-0.1	0.01	GCP	3025	2579.1	3024.9	2579.1
G0032	5.856	0.07	0.05	0.04	GCP	3878	3995.1	3878.1	3995.1

RMS (x, y) for worst 5% of points in list: 1.01, 0.39

Table A1.4: Residual info for AST_L1B 11-03-2003 image
Residual Units: Image Pixels
GCPs: 29 X-RMS: 0.43 Y-RMS: 0.25

Point ID	Elev (m)	Res	Res X	Res Y	Type	Photo X	Photo Y	Comp X	Comp Y
G0001	3.522	1.08	1.07	0.17	GCP	4463.1	3902.9	4464.1	3903.1
G0002	1.000	0.79	0.74	-0.27	GCP	2359.9	3575.9	2360.6	3575.6
G0003	8.039	0.76	-0.73	0.22	GCP	4110.4	2966.9	4109.7	2967.2
G0004	1.843	0.73	-0.72	-0.09	GCP	3750	3701	3749.3	3700.9
G0005	543.374	0.72	0.65	0.3	GCP	3581	3417.9	3581.7	3418.2

G0006	1.000	0.66	-0.65	0.12	GCP	3318.5	4117.9	3317.8	4118
G0007	6.575	0.59	-0.39	0.44	GCP	2802.5	3474	2802.1	3474.4
G0008	89.904	0.55	0.45	0.32	GCP	4433	2463.1	4433.4	2463.4
G0009	84.752	0.5	0.3	-0.4	GCP	3677.9	3804.6	3678.2	3804.2
G0010	1.931	0.47	-0.46	-0.09	GCP	2948.6	3760.4	2948.1	3760.3
G0011	2.958	0.47	0.4	-0.24	GCP	4300	2216	4300.4	2215.8
G0012	1.831	0.42	-0.29	-0.3	GCP	4290.1	3464	4289.8	3463.7
G0013	1.246	0.42	-0.28	0.31	GCP	3316	2579	3315.7	2579.3
G0014	465.039	0.41	0.37	-0.19	GCP	3429	2977	3429.3	2976.8
G0015	8.968	0.38	-0.28	-0.25	GCP	3818.9	2327.8	3818.7	2327.6
G0016	5.339	0.36	-0.02	-0.36	GCP	3611.9	2527.9	3611.9	2527.6
G0017	83.211	0.36	-0.1	-0.35	GCP	3333	3409.1	3332.9	3408.7
G0018	2.416	0.34	0.34	0.01	GCP	2757	3664.1	2757.3	3664.1
G0019	159.295	0.31	0.11	-0.29	GCP	3039.9	3434.9	3040	3434.6
G0020	8.839	0.3	0.01	0.3	GCP	2907.6	3246.3	2907.6	3246.6
G0021	3.064	0.3	-0.06	0.29	GCP	2861	3018.9	2860.9	3019.2
G0022	17.472	0.27	-0.12	0.25	GCP	3859.9	2714.9	3859.8	2715.2
G0023	20.388	0.23	-0.23	0.04	GCP	4044.9	2434	4044.7	2434
G0024	4.315	0.2	0.19	-0.06	GCP	3172.9	2826.6	3173.1	2826.6
G0025	5.856	0.2	-0.19	0.02	GCP	4170	3996	4169.8	3996
G0026	3.524	0.18	-0.14	-0.11	GCP	3265.9	3114.1	3265.7	3114
G0027	1.845	0.18	-0.09	0.15	GCP	4431	3224	4430.9	3224.1
G0028	7.956	0.15	0.07	0.14	GCP	2597.9	4134	2598	4134.1
G0029	11.516	0.11	0.07	-0.09	GCP	3092.9	3224.6	3092.9	3224.5

RMS (x, y) for worst 5% of points in list: 1.07, 0.17

Table A1.5: Residual info for 04-17-06 AST_08 LST image
Residual Units: Image Pixels
GCPs: 21 X-RMS: 0.35 Y-RMS: 0.32

Point ID	Elev (m)	Res	Res X	Res Y	Type	Photo X	Photo Y	Comp X	Comp Y
G0001	4.542	0.71	0.61	0.35	GCP	376.9	592	377.6	592.4
G0002	2.473	0.67	0.44	0.5	GCP	368	709	368.4	709.5
G0003	32.869	0.65	-0.22	0.61	GCP	202.6	577	202.3	577.6
G0004	3.119	0.63	-0.3	-0.55	GCP	267	696.9	266.7	696.4

G0005	1.213	0.61	0.41	-0.45	GCP	212.4	454.5	212.9	454.1
G0006	4.476	0.6	-0.45	-0.39	GCP	413.9	534.9	413.4	534.5
G0007	0.476	0.57	-0.53	0.18	GCP	68.9	645.9	68.4	646.1
G0008	461.996	0.49	-0.44	0.22	GCP	221.1	522.9	220.6	523.2
G0009	329.26	0.44	0.44	0.06	GCP	114.1	608.9	114.5	609
G0010	103.268	0.43	-0.33	-0.28	GCP	301.9	543.9	301.5	543.7
G0011	74.257	0.43	0.32	-0.29	GCP	125	582.8	125.3	582.5
G0012	4.251	0.42	-0.09	-0.41	GCP	123.5	698.5	123.4	698.1
G0013	599.833	0.39	-0.38	-0.1	GCP	394	636	393.6	635.9
G0014	8.650	0.37	0.36	-0.06	GCP	145	529	145.4	528.9
G0015	629.033	0.34	0.32	-0.13	GCP	318	587.1	318.3	586.9
G0016	1.000	0.31	0.09	0.29	GCP	218	640	218.1	640.3
G0017	4.01	0.28	0.06	0.28	GCP	131.9	504	131.9	504.3
G0018	8.309	0.25	-0.21	0.15	GCP	182.9	490.9	182.7	491.1
G0019	0.295	0.19	-0.18	-0.04	GCP	171.5	465.4	171.3	465.4
G0020	350.817	0.17	0.07	0.16	GCP	314.9	488	315	488.2
G0021	2.517	0.08	0.02	-0.08	GCP	105.9	678.9	106	678.9

RMS (x, y) for worst 5% of points in list: 0.61, 0.35

Table A1.6: Residual info for 10-23-2005 AST_08 LST image
Residual Units: Image Pixels
GCPs: 36 X-RMS: 0.30 Y-RMS: 0.25

Point ID	Elev (m)	Res	Res X	Res Y	Type	Photo X	Photo Y	Comp X	Comp Y
G0001	3.069	0.88	-0.57	-0.67	GCP	184	709	183.4	708.3
G0002	630.449	0.66	0.66	-0.07	GCP	378	598	378.7	597.9
G0003	0.295	0.58	-0.28	-0.5	GCP	232	475.9	231.7	475.4
G0004	1.213	0.56	-0.27	-0.49	GCP	273.6	464.6	273.3	464.1
G0005	143.279	0.54	-0.28	0.46	GCP	389	455	388.7	455.5
G0006	349.034	0.52	0.5	-0.13	GCP	375	499	375.5	498.9
G0007	1.000	0.49	-0.48	0.04	GCP	497	691	496.5	691
G0008	1.195	0.45	0.44	0.07	GCP	202	654.6	202.4	654.6
G0009	7.105	0.44	0.4	0.18	GCP	649	572	649.4	572.2
G0010	4.010	0.41	0.29	0.3	GCP	192	514	192.3	514.3
G0011	76.057	0.41	-0.38	-0.14	GCP	185.9	592.9	185.6	592.8

G0012	1.000	0.41	0.09	-0.4	GCP	278.3	651	278.4	650.6
G0013	1.052	0.4	0.4	-0.04	GCP	88	602	88.4	601.9
G0014	3.115	0.4	0.24	0.31	GCP	124.5	700.6	124.7	700.9
G0015	0.476	0.39	-0.22	0.32	GCP	128.7	655.9	128.5	656.2
G0016	374.405	0.37	-0.35	0.14	GCP	160.5	566.5	160.2	566.6
G0017	147.372	0.36	-0.03	0.36	GCP	111	592	111	592.4
G0018	6.800	0.36	-0.34	-0.13	GCP	556	429	555.7	428.9
G0019	4.451	0.34	0.32	-0.12	GCP	492	748	492.3	747.9
G0020	602.522	0.33	-0.33	0.05	GCP	454.5	647	454.2	647.1
G0021	329.260	0.33	-0.33	-0.01	GCP	175	619.5	174.6	619.5
G0022	4.542	0.27	0.21	-0.16	GCP	437.9	603	438.2	602.8
G0023	114.698	0.24	0.24	0.01	GCP	168	539	168.2	539
G0024	3.728	0.22	-0.22	-0.02	GCP	572	651.4	571.8	651.4
G0025	35.481	0.22	0.1	0.19	GCP	262.5	588	262.6	588.2
G0026	8.309	0.21	0.12	0.18	GCP	243	501	243.1	501.2
G0027	88.783	0.21	0.13	-0.17	GCP	145.9	607.9	146.1	607.8
G0028	9.041	0.21	-0.15	0.15	GCP	206	539	205.8	539.1
G0029	2.473	0.21	-0.11	0.17	GCP	429	719.9	428.9	720.1
G0030	1.350	0.18	0.12	0.13	GCP	166	689	166.1	689.1
G0031	4.476	0.17	0.17	0.01	GCP	474	545	474.2	545
G0032	3.119	0.17	-0.04	-0.16	GCP	327	707	327	706.8
G0033	461.996	0.16	-0.01	-0.16	GCP	281	534	281	533.8
G0034	1.244	0.13	-0.08	0.1	GCP	586	724	585.9	724.1
G0035	103.268	0.1	0.04	0.09	GCP	362	554	362	554.1
G0036	1.000	0.09	0.01	0.09	GCP	601	496.9	601	497

RMS (x, y) for worst 5% of points in list: 0.57, 0.67

Table A1.7: Residual info for 10-01-2005 AST_08 LST image
Residual Units: Image Pixels
GCPs: 34 X-RMS: 0.35 Y-RMS: 0.35

Point ID	Elev (m)	Res	Res X	Res Y	Type	Photo X	Photo Y	Comp X	Comp Y
G0001	58.500	0.7	0.19	0.68	GCP	784.5	202.3	784.7	203
G0002	13.425	0.7	0.7	-0.02	GCP	186.6	422.4	187.3	422.4
G0003	23.694	0.68	0.18	-0.65	GCP	664.5	243.5	664.7	242.8

G0004	91.393	0.66	-0.31	-0.58	GCP	639	302.4	638.7	301.9
G0005	14.173	0.65	0.6	-0.25	GCP	767.5	59.9	768.1	59.7
G0006	103.268	0.64	0.17	0.62	GCP	531.9	122.3	532.1	122.9
G0007	19.967	0.6	-0.6	0.08	GCP	625.5	16	624.9	16.1
G0008	59.643	0.57	-0.55	0.15	GCP	410.3	184.4	409.7	184.5
G0009	33.617	0.57	-0.54	-0.18	GCP	727.5	30.5	727	30.3
G0010	8.650	0.56	0.52	-0.2	GCP	375	107.9	375.5	107.7
G0011	16.793	0.55	-0.09	-0.54	GCP	448	318.7	447.9	318.1
G0012	29.050	0.54	0	-0.54	GCP	678.4	128.4	678.4	127.8
G0013	53.276	0.52	-0.23	0.46	GCP	240.5	371.9	240.3	372.4
G0014	18.722	0.52	0.11	0.5	GCP	728.9	83.8	729	84.3
G0015	20.560	0.51	-0.08	0.51	GCP	765.9	121	765.8	121.5
G0016	10.740	0.5	-0.22	0.45	GCP	410.9	241.8	410.7	242.3
G0017	27.492	0.49	-0.39	-0.29	GCP	275.6	408.9	275.2	408.6
G0018	8.309	0.48	0.05	-0.48	GCP	412.9	70.4	413	70
G0019	3.119	0.47	-0.34	0.33	GCP	497.4	274.5	497.1	274.8
G0020	11.866	0.47	-0.46	0.09	GCP	188.4	353.6	187.9	353.7
G0021	20.100	0.43	-0.43	-0.05	GCP	775.6	297.4	775.2	297.4
G0022	44.155	0.43	0.42	-0.06	GCP	534.9	420.9	535.4	420.8
G0023	36.599	0.42	0.06	0.42	GCP	330.4	386.9	330.5	387.3
G0024	1.875	0.4	0.36	-0.19	GCP	478.8	212.8	479.1	212.6
G0025	16.022	0.4	0.39	0.03	GCP	627.9	96.5	628.3	96.5
G0026	5.629	0.37	0.37	-0.01	GCP	294.9	269.5	295.3	269.5
G0027	43.250	0.34	0.22	-0.26	GCP	405.4	372.9	405.6	372.6
G0028	0.476	0.33	-0.32	-0.08	GCP	298.6	224.5	298.3	224.4
G0029	32.869	0.31	-0.29	-0.09	GCP	432.9	156.5	432.6	156.4
G0030	0.295	0.3	0.11	-0.28	GCP	401.4	44.6	401.5	44.3
G0031	4.542	0.23	0.21	0.09	GCP	607.9	171	608.2	171.1
G0032	1.000	0.17	0.04	0.17	GCP	327	211	327	211.2
G0033	2.517	0.16	0.02	0.15	GCP	335.9	257	336	257.2
G0034	1.213	0.13	0.13	0.01	GCP	443.1	33	443.2	33

RMS (x, y) for worst 5% of points in list: 0.19, 0.68

Table A1.8: Residual info for 11-21-2004 AST_08 LST image
Residual Units: Image Pixels
GCPs: 23 X-RMS: 0.36 Y-RMS: 0.34

Point ID	Elev (m)	Res	Res X	Res Y	Type	Photo X	Photo Y	Comp X	Comp Y
G0001	148.994	0.71	-0.67	0.23	GCP	380.1	638.9	379.5	639.1
G0002	329.260	0.69	0.45	-0.52	GCP	442.5	665.8	442.9	665.2
G0003	4.542	0.68	0.38	-0.57	GCP	705.5	649.6	705.9	649.1
G0004	461.996	0.67	-0.67	-0.03	GCP	549.6	579.5	548.9	579.5
G0005	1.052	0.64	0.62	-0.14	GCP	356.4	648.5	357.1	648.4
G0006	0.476	0.55	0.09	0.54	GCP	396.9	701.9	397	702.5
G0007	8.650	0.54	-0.16	0.52	GCP	474	584.9	473.8	585.5
G0008	629.033	0.54	0.47	0.26	GCP	646	642.9	646.5	643.2
G0009	350.817	0.54	0.4	-0.35	GCP	642.9	545	643.3	544.6
G0010	4.251	0.49	-0.18	-0.46	GCP	452	754.9	451.8	754.5
G0011	32.869	0.48	0.3	-0.38	GCP	530.4	634.5	530.7	634.1
G0012	4.476	0.46	-0.15	0.44	GCP	742	590.9	741.8	591.3
G0013	8.309	0.44	-0.35	-0.27	GCP	511.5	547.9	511.2	547.7
G0014	103.268	0.41	-0.17	0.37	GCP	630	599.9	629.8	600.2
G0015	1.213	0.4	0.25	-0.31	GCP	541	511	541.2	510.7
G0016	2.4730	0.4	-0.35	0.2	GCP	697	765.9	696.7	766.1
G0017	1.000	0.4	0.37	-0.14	GCP	546	696.9	546.4	696.8
G0018	2.517	0.29	-0.07	0.28	GCP	434.5	734.9	434.4	735.2
G0019	4.010	0.26	0.08	0.25	GCP	460.4	560.6	460.5	560.8
G0020	0.295	0.26	-0.23	0.12	GCP	500	521.9	499.8	522
G0021	599.833	0.26	-0.19	0.18	GCP	722	692.1	721.8	692.2
G0022	3.119	0.2	-0.11	-0.16	GCP	595	753.1	594.9	752.9
G0023	74.257	0.14	-0.13	-0.06	GCP	453.9	638.9	453.8	638.9

RMS (x, y) for worst 5% of points in list: 0.67, 0.23

Table A1.9: Residual info for 10-05-2004 AST_08 LST image
Residual Units: Image Pixels
GCPs: 29 X-RMS: 0.31 Y-RMS: 0.38

Point ID	Elev (m)	Res	Res X	Res Y	Type	Photo X	Photo Y	Comp X	Comp Y
G0001	18.722	0.83	-0.1	-0.82	GCP	635.4	382.4	635.3	381.6
G0002	10.740	0.72	-0.67	-0.27	GCP	317	539.8	316.3	539.5
G0003	16.793	0.69	0.36	-0.59	GCP	353	616	353.4	615.4
G0004	1.000	0.66	0.08	0.65	GCP	233	507.9	233.1	508.5
G0005	5.629	0.63	0.03	-0.63	GCP	201.5	567.5	201.5	566.9
G0006	20.560	0.62	0.6	0.16	GCP	671.8	418.8	672.3	418.9
G0007	8.650	0.6	0.53	0.27	GCP	280.8	404.7	281.3	405
G0008	59.643	0.58	0.27	-0.52	GCP	315	482.1	315.3	481.6
G0009	0.295	0.53	0.38	-0.37	GCP	306.9	341.9	307.3	341.6
G0010	9.640	0.52	-0.48	-0.21	GCP	213.9	680	213.4	679.8
G0011	2.517	0.48	-0.05	0.48	GCP	242	554	241.9	554.5
G0012	23.694	0.47	0.47	0.02	GCP	570	540.1	570.5	540.1
G0013	12.787	0.46	0.25	0.39	GCP	292.5	651.5	292.7	651.9
G0014	4.542	0.44	-0.15	0.41	GCP	513.9	468	513.8	468.4
G0015	16.022	0.44	-0.31	0.31	GCP	534.4	393.5	534.1	393.8
G0016	20.100	0.43	-0.26	0.34	GCP	682	594.5	681.7	594.8
G0017	91.393	0.39	0.1	0.38	GCP	544.1	598.5	544.2	598.9
G0018	19.967	0.38	-0.28	0.26	GCP	530.9	313.1	530.7	313.3
G0019	23.384	0.38	0.05	-0.38	GCP	426	580.9	426	580.5
G0020	32.869	0.36	-0.3	0.2	GCP	338.5	453.4	338.2	453.6
G0021	1.213	0.36	-0.23	-0.28	GCP	349.1	330.6	348.8	330.3
G0022	29.050	0.33	-0.2	-0.27	GCP	584.5	425.4	584.3	425.1
G0023	0.476	0.31	0.03	0.31	GCP	204.5	521.5	204.5	521.8
G0024	14.173	0.29	0.29	-0.01	GCP	674.4	357.1	674.7	357.1
G0025	58.500	0.28	-0.19	-0.21	GCP	691.5	500.5	691.3	500.3
G0026	33.617	0.28	-0.26	0.11	GCP	633.5	327.5	633.2	327.6
G0027	8.309	0.28	-0.18	0.21	GCP	318.9	367	318.7	367.2
G0028	103.268	0.21	0.1	0.19	GCP	437.4	419.6	437.5	419.8
G0029	1.875	0.21	0.15	-0.14	GCP	384.4	510	384.6	509.9

RMS (x, y) for worst 5% of points in list: 0.10, 0.82

Table A1.10: Residual info for 11-03-2003 AST_08 LST image
Residual Units: Image Pixels
GCPs: 22 X-RMS: 0.29 Y-RMS: 0.32

Point ID	Elev (m)	Res	Res X	Res Y	Type	Photo X	Photo Y	Comp X	Comp Y
G0001	148.994	0.7	-0.05	0.69	GCP	425	633.6	425	634.3
G0002	2.473	0.69	0.11	0.68	GCP	747.6	747.4	747.7	748.1
G0003	1.213	0.63	0.63	-0.07	GCP	580.9	499.4	581.6	499.4
G0004	74.257	0.57	-0.21	-0.53	GCP	499.5	631.5	499.3	631
G0005	350.817	0.54	-0.5	-0.2	GCP	685.5	529.6	685	529.4
G0006	4.251	0.5	0.06	-0.5	GCP	502	746.9	502.1	746.4
G0007	8.309	0.48	-0.48	0.02	GCP	553.4	537.5	553	537.5
G0008	0.476	0.47	-0.41	0.23	GCP	445.6	696.5	445.2	696.7
G0009	3.119	0.45	-0.31	-0.33	GCP	645.5	739.4	645.2	739
G0010	4.010	0.44	0.03	0.44	GCP	502.8	552.3	502.8	552.7
G0011	1.052	0.43	0.38	-0.2	GCP	402.6	644.5	403	644.3
G0012	103.268	0.41	0.2	0.36	GCP	673.7	584.9	673.9	585.3
G0013	329.260	0.37	0.36	-0.09	GCP	489.1	658	489.4	657.9
G0014	8.650	0.32	-0.27	-0.18	GCP	517.4	576.9	517.2	576.8
G0015	1.000	0.31	0.3	0.06	GCP	594	684.9	594.3	685
G0016	4.542	0.29	0.21	-0.2	GCP	751.9	631.1	752.1	630.9
G0017	4.476	0.24	-0.16	-0.17	GCP	786	571.9	785.8	571.8
G0018	629.033	0.16	0.15	-0.05	GCP	692	627.9	692.1	627.9
G0019	2.517	0.12	-0.12	-0.03	GCP	484	727.9	483.9	727.9
G0020	32.869	0.11	0.07	0.08	GCP	575.9	623	576	623.1
G0021	0.295	0.1	0.03	-0.1	GCP	540.5	512.4	540.5	512.3
G0022	461.996	0.09	-0.01	0.09	GCP	591.9	568	591.9	568.1

RMS (x, y) for worst 5% of points in list: 0.05, 0.69

Table A1.11: Residual info for 10-28-2003 AST_08 LST image
Residual Units: Image Pixels
GCPs: 34 X-RMS: 0.36 Y-RMS: 0.31

Point ID	Elev (m)	Res	Res X	Res Y	Type	Photo X	Photo Y	Comp X	Comp Y
G0001	0.476	0.72	-0.2	0.7	GCP	290.5	226.3	290.3	226.9
G0002	18.722	0.69	-0.69	0.02	GCP	721.5	86.3	720.8	86.3

G0003	14.173	0.67	0.05	0.67	GCP	759.9	60.9	760	61.6
G0004	8.650	0.67	0.23	-0.62	GCP	367.5	110.5	367.7	109.9
G0005	29.050	0.65	0.65	-0.05	GCP	669.4	130.1	670.1	130
G0006	20.100	0.64	-0.64	0.03	GCP	766.9	299.9	766.3	300
G0007	58.500	0.61	0.59	-0.16	GCP	775.5	205.5	776.1	205.3
G0008	0.295	0.58	-0.58	-0.08	GCP	394.5	46.4	393.9	46.3
G0009	44.155	0.54	-0.25	-0.48	GCP	526.5	424.4	526.3	423.9
G0010	16.793	0.53	-0.31	0.43	GCP	439.6	320.5	439.3	320.9
G0011	13.425	0.51	0.27	-0.43	GCP	178.6	425.9	178.9	425.5
G0012	1.213	0.5	-0.48	-0.14	GCP	436	35.1	435.5	35
G0013	19.967	0.48	0.1	-0.47	GCP	616.9	18.4	617	18
G0014	4.542	0.48	-0.08	-0.47	GCP	599.9	173.9	599.8	173.4
G0015	53.276	0.47	-0.46	-0.1	GCP	232.4	375.5	231.9	375.4
G0016	32.869	0.47	0.46	-0.11	GCP	424.1	158.9	424.6	158.8
G0017	23.694	0.47	-0.42	-0.21	GCP	656.4	245.6	656	245.4
G0018	91.393	0.45	0.41	0.17	GCP	629.4	304.4	629.8	304.6
G0019	10.740	0.43	0.42	-0.1	GCP	402	244.9	402.4	244.8
G0020	33.617	0.43	0.33	0.27	GCP	718.6	31.9	719	32.2
G0021	2.517	0.41	-0.11	0.4	GCP	327.9	259.4	327.8	259.8
G0022	16.022	0.4	0.26	-0.3	GCP	619.9	98.9	620.2	98.6
G0023	36.599	0.38	-0.06	0.37	GCP	321.9	389.9	321.9	390.3
G0024	43.250	0.38	0.37	0.09	GCP	396.5	375.5	396.9	375.6
G0025	5.629	0.35	0.23	0.27	GCP	286.9	271.9	287.2	272.1
G0026	103.268	0.32	0.11	0.3	GCP	523.9	124.9	524	125.2
G0027	27.492	0.31	-0.26	-0.16	GCP	266.9	411.9	266.6	411.7
G0028	1.875	0.28	-0.28	0.03	GCP	471.1	215	470.8	215
G0029	11.866	0.28	0.27	-0.01	GCP	179.5	356.6	179.8	356.6
G0030	59.643	0.21	0.2	0.06	GCP	401.4	186.9	401.6	187
G0031	20.560	0.18	-0.15	0.11	GCP	757.6	123.5	757.5	123.6
G0032	8.309	0.18	-0.18	-0.02	GCP	405.4	72.1	405.3	72
G0033	3.119	0.14	0.1	-0.09	GCP	488.4	277.6	488.5	277.5
G0034	1.000	0.12	0.08	0.09	GCP	318.9	213.6	319	213.7

RMS (x, y) for worst 5% of points in list: 0.20, 0.70

APPENDIX 2: Maps of Urban Environmental Variables

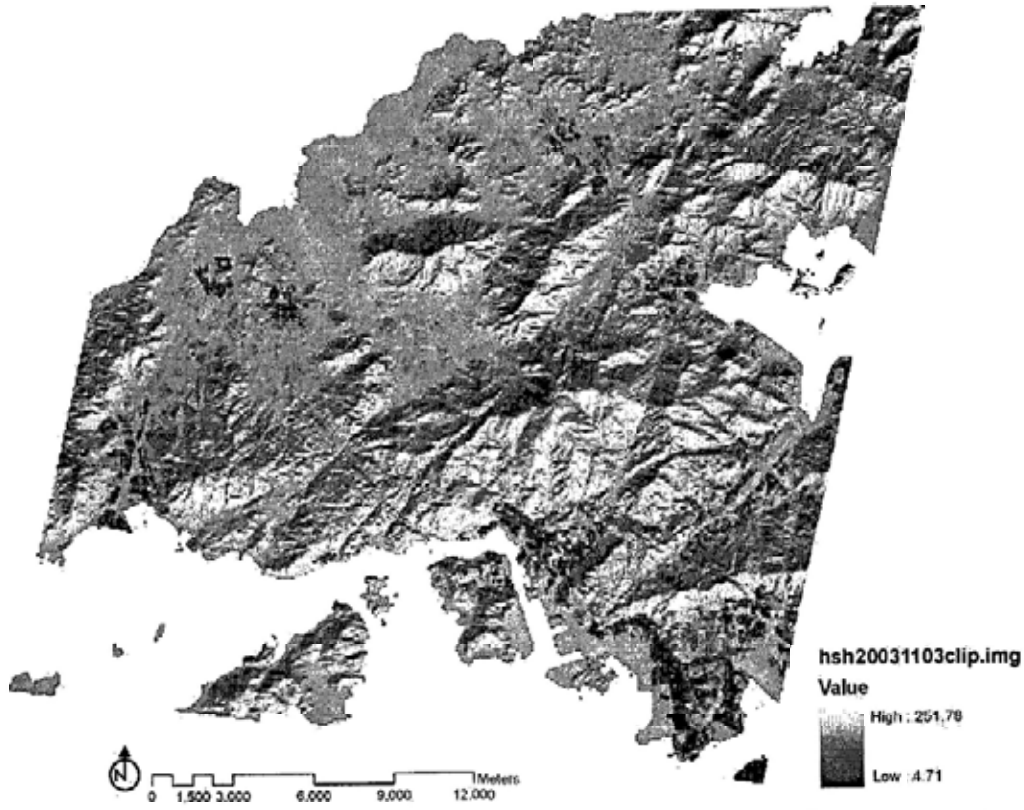

Figure A2.1 Solar radiations distribution during daytime 11.03.2003 (hshad03)

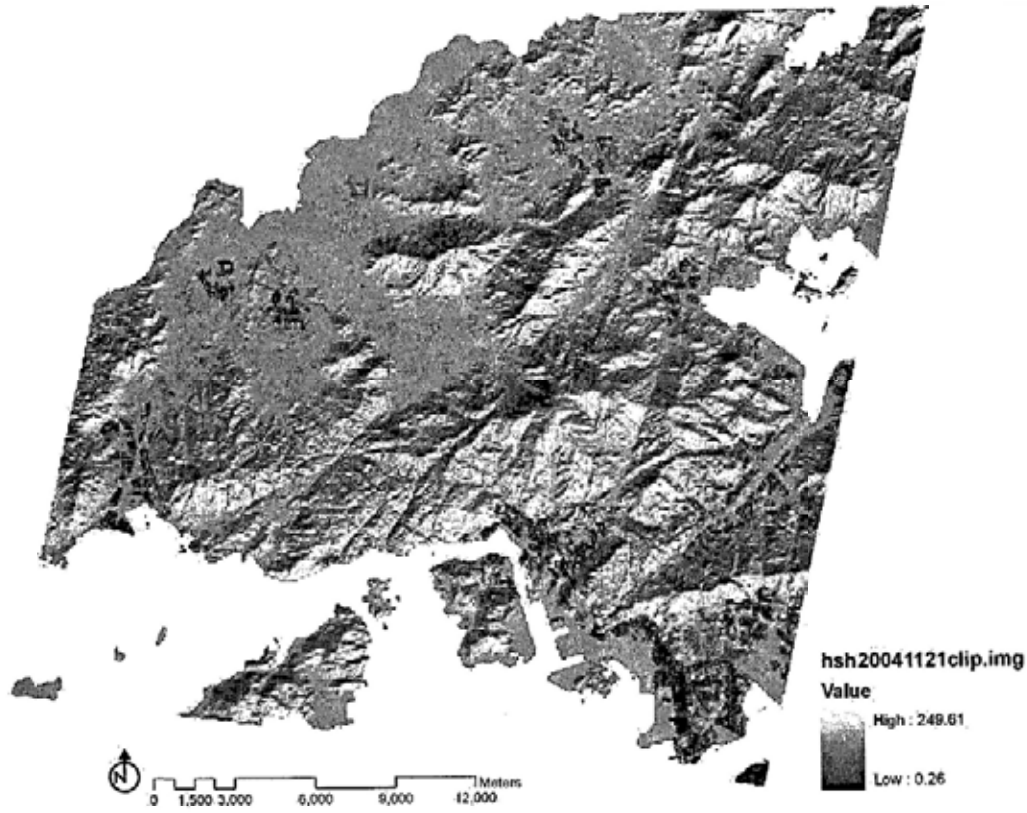

Figure A2.2 Solar radiations distribution during daytime 11.21.2004 (hshad04)

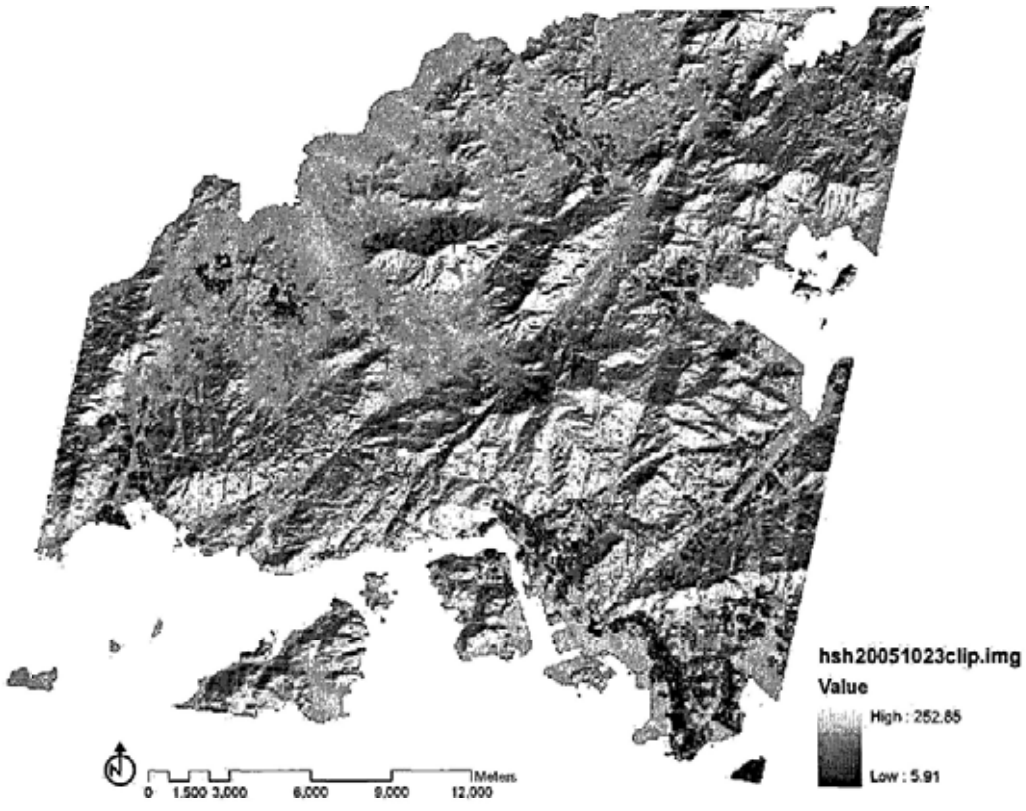

Figure A2.3 Solar radiations distribution during daytime 10.23.2005 (hshad05)

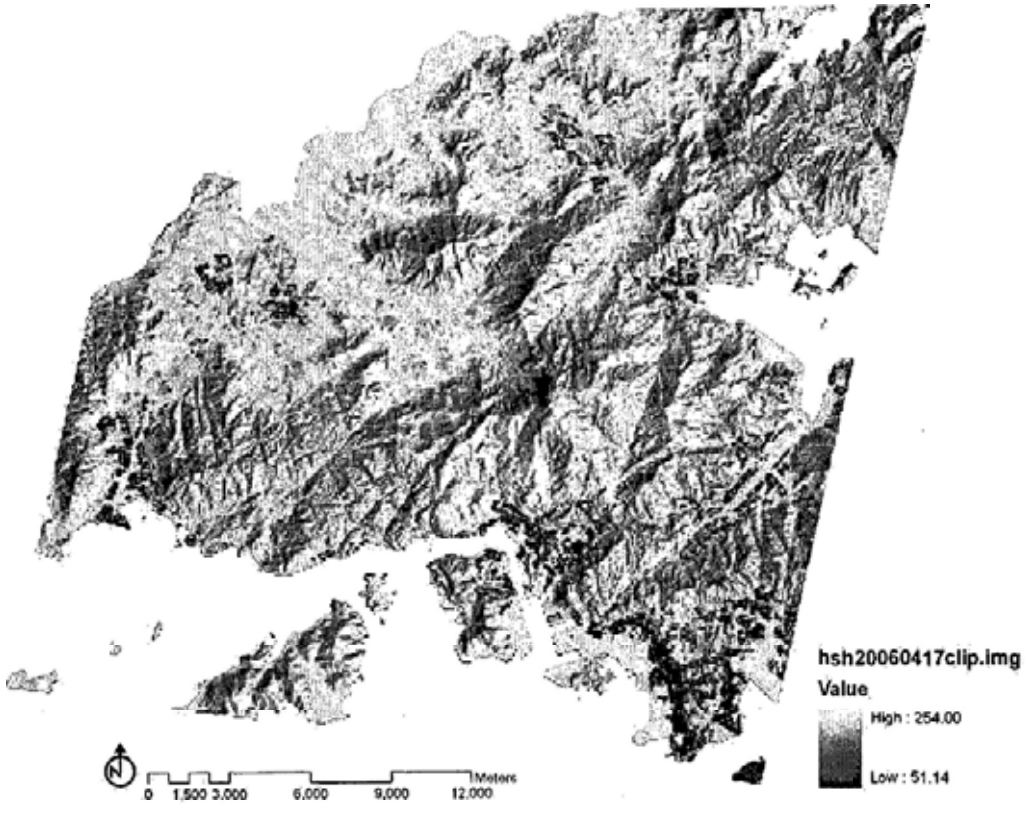

Figure A2.4 Solar radiations distribution during daytime 04.17.2006 (hshad06)

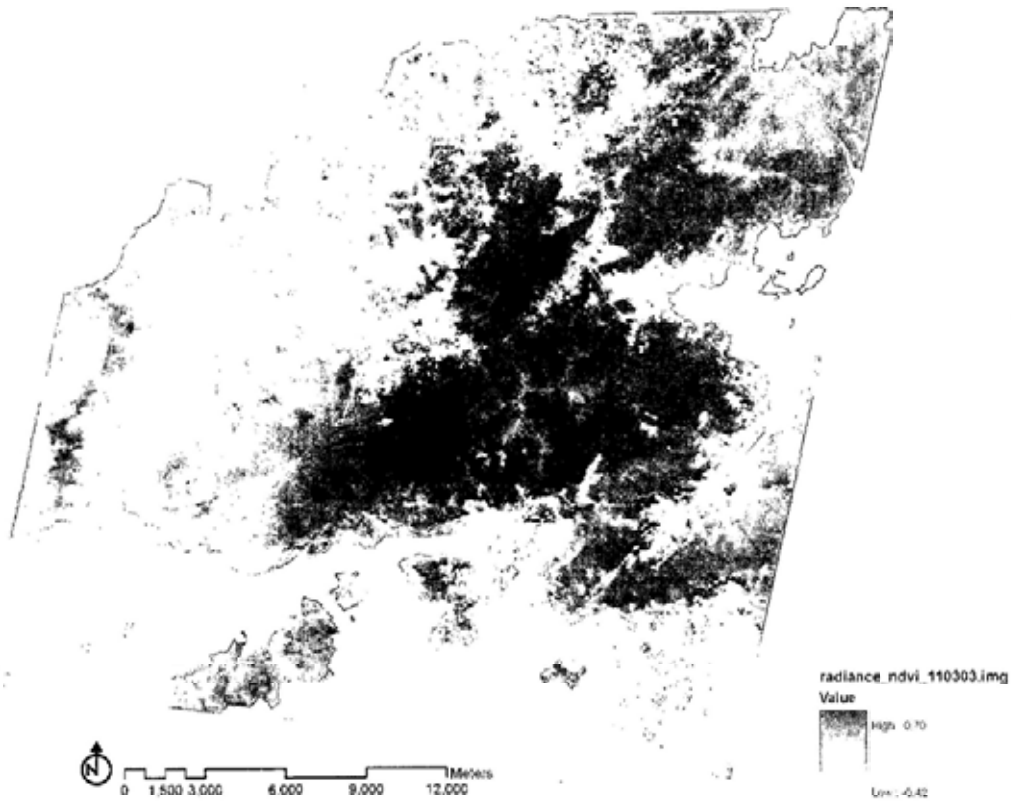

Figure A2.5 Vegetation NDVI image during daytime 11.03.2003 (NDVI110303)

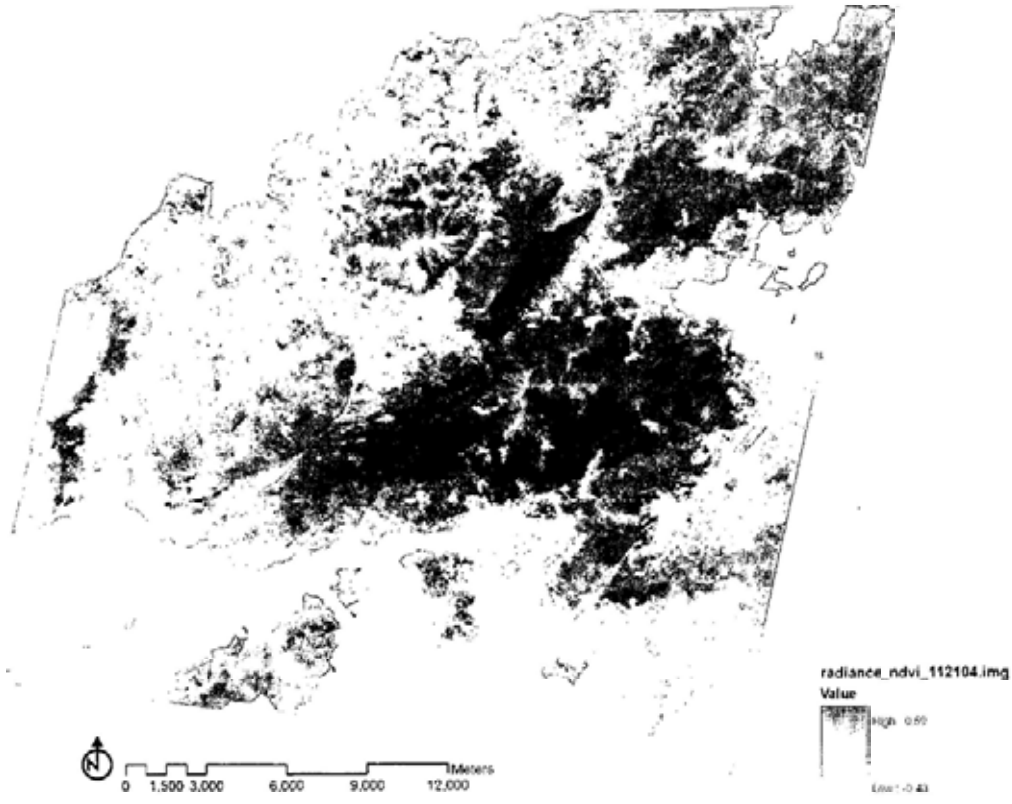

Figure A2.6 Vegetation NDVI image during daytime 11.21.2004 (NDVI112104)

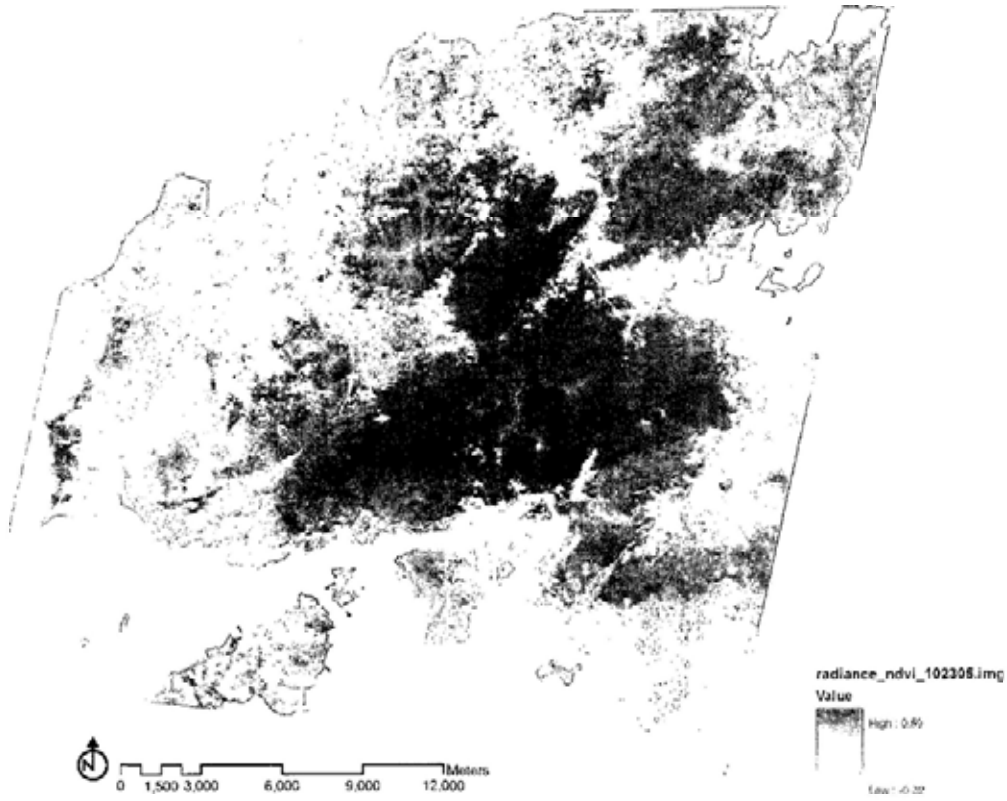

Figure A2.7 Vegetation NDVI image during daytime 10.23.2005 (NDVI102305)

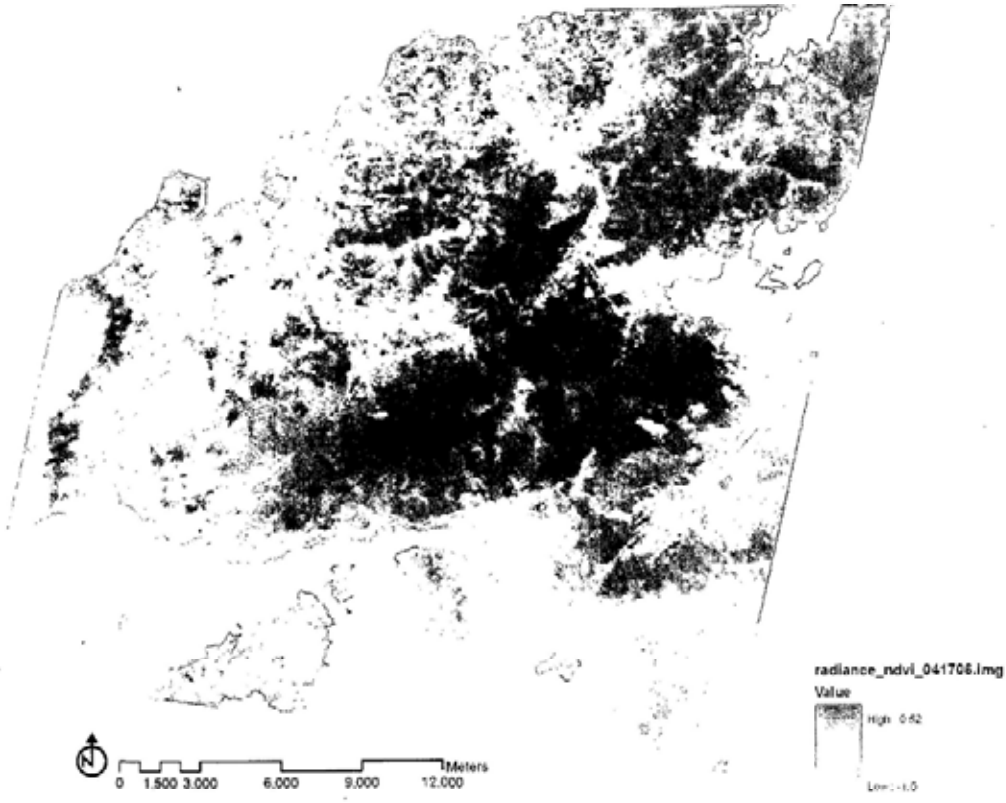

Figure A2.8 Vegetation NDVI image during daytime 04.17.2006 (NDVI041706)

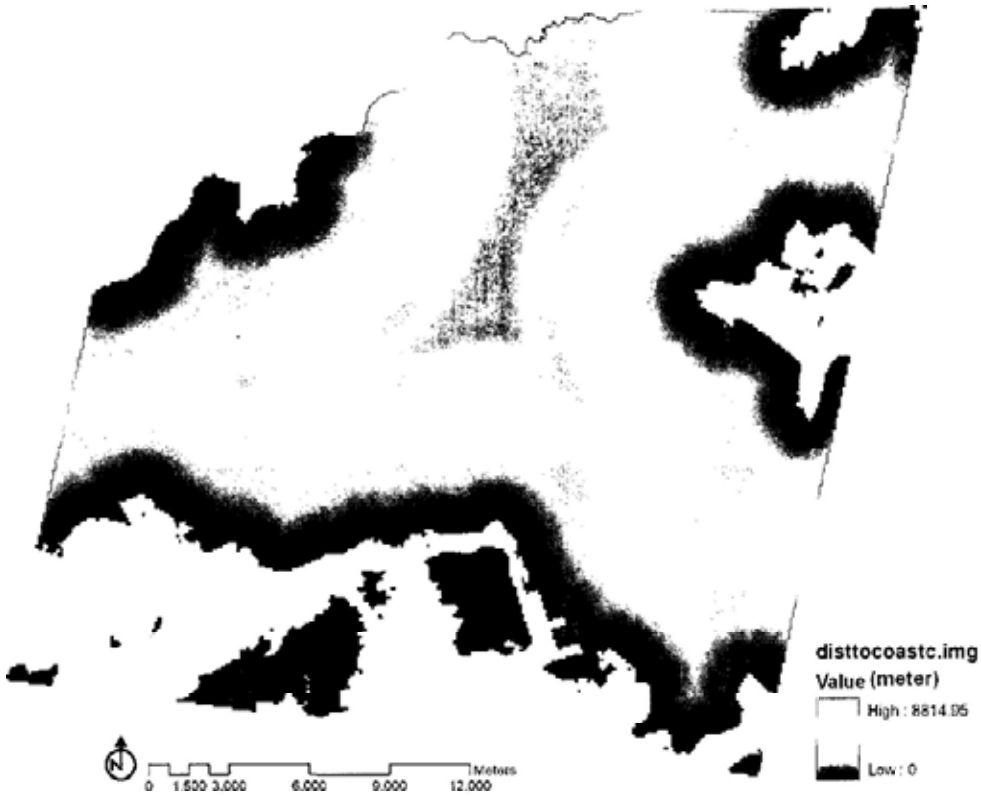

Figure A2.9 Distance from coast (Disttocoast)

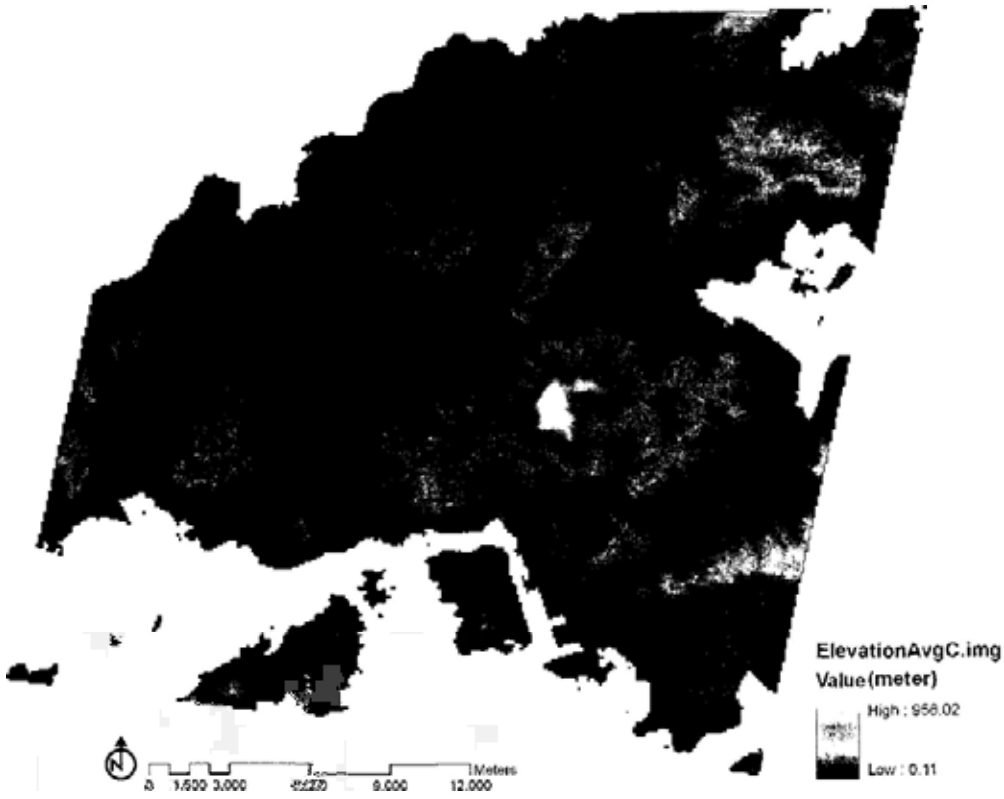

Figure A2.10 DEM of study area utilized in this research (elevationavg)

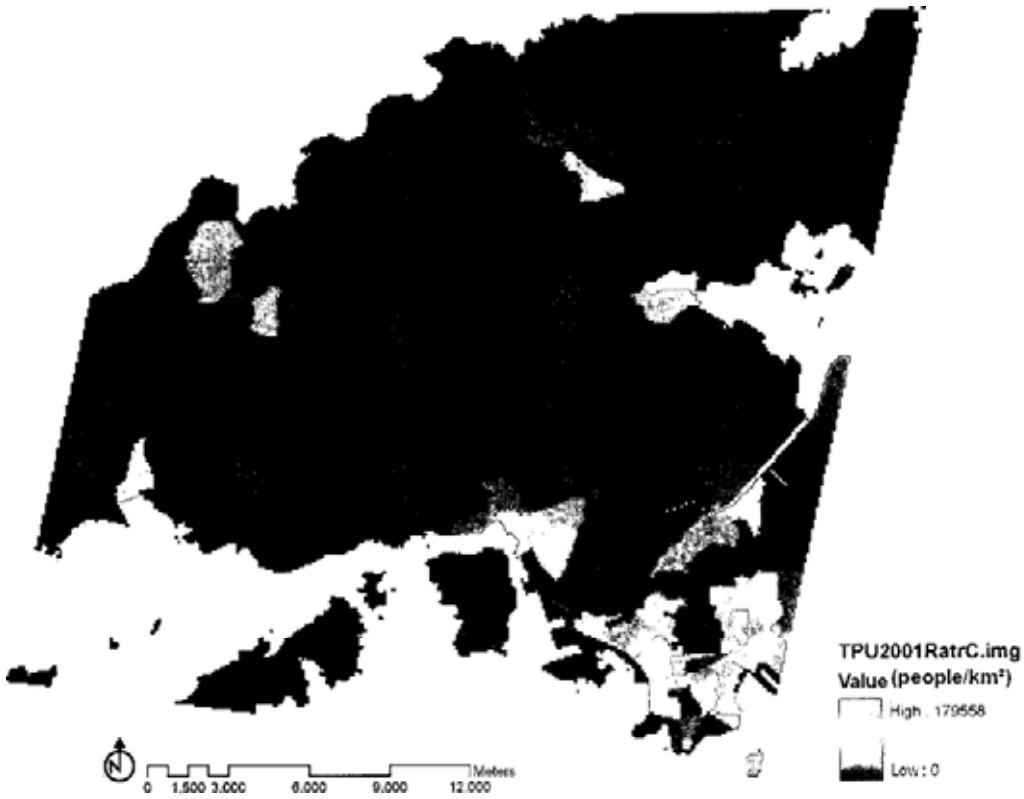

Figure A2.11 Population density of study area (TPU2001)

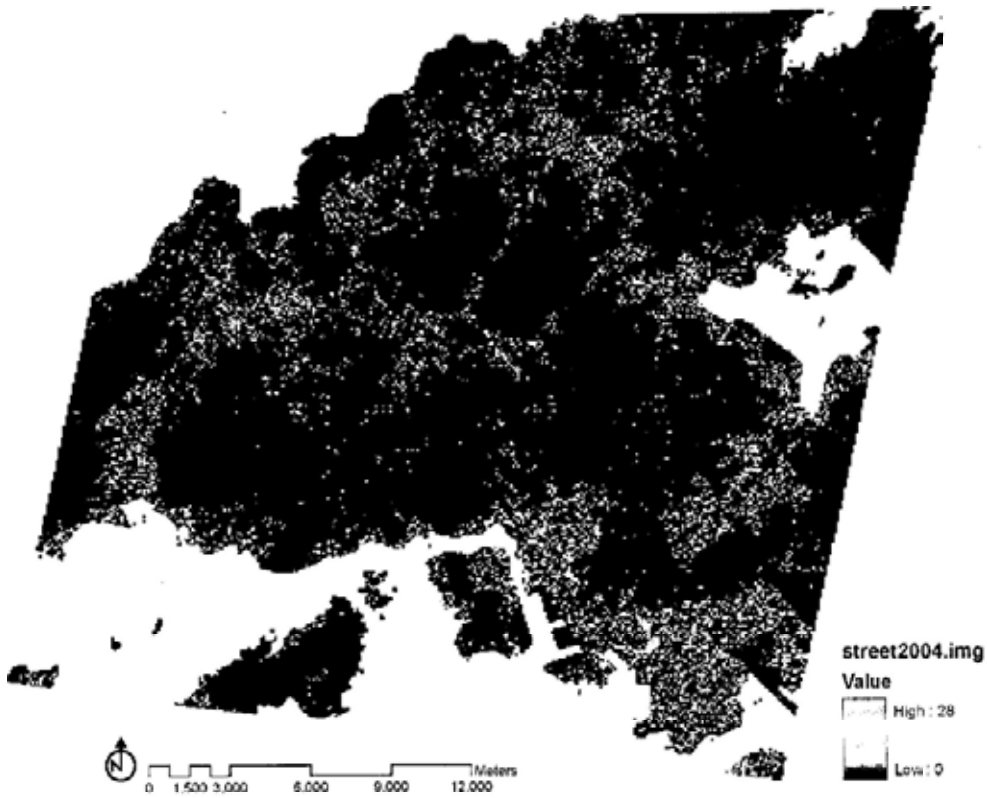

Figure A2.12 Road network density in year 2004 (SD2004)

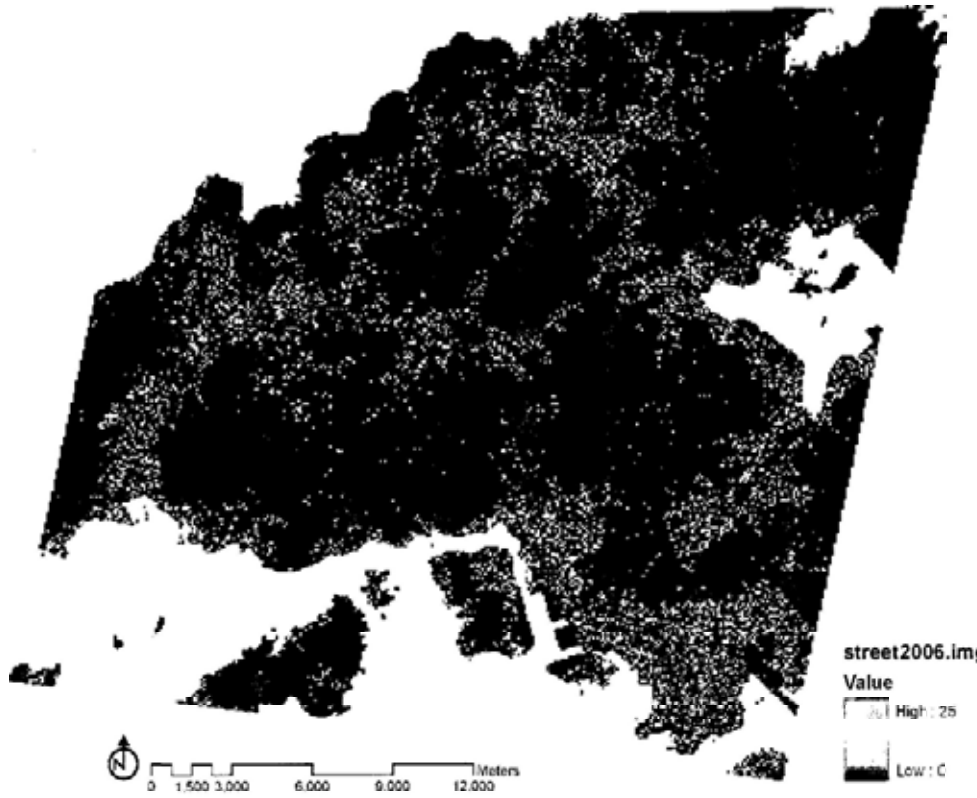

Figure A2.13 Road network density in year 2006 (SD2006)

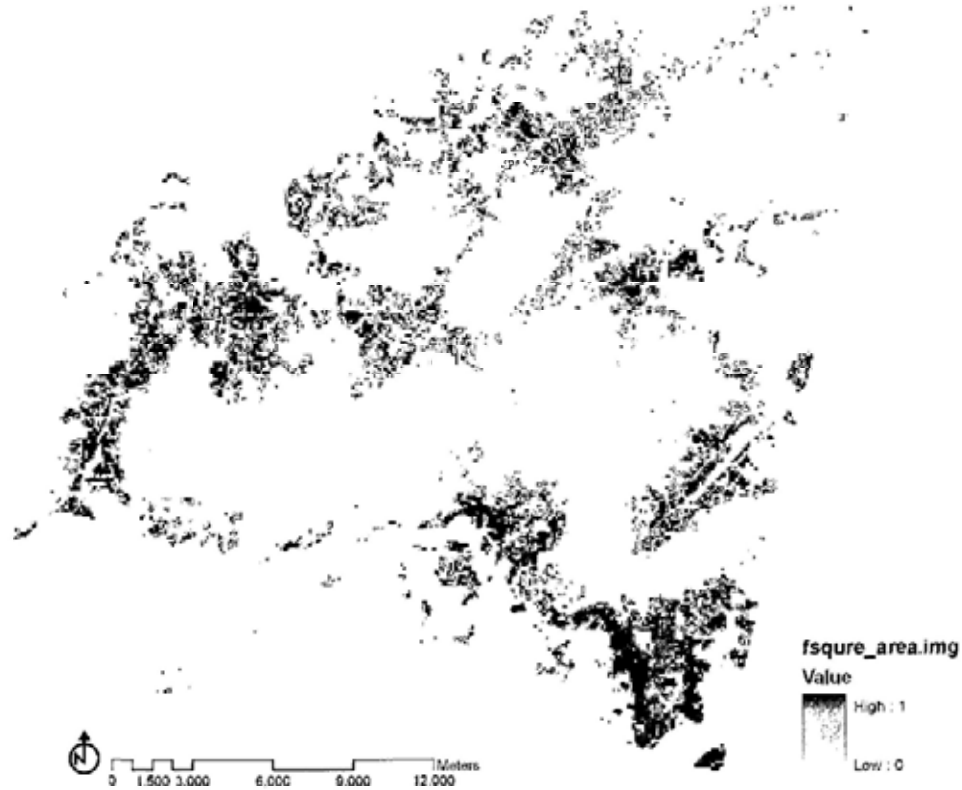

Figure A2.14 Building square footage of study area (footsqure_a)

APPENDIX 3: Statistical Descriptions of Local Surface Temperature Variation Along with Land Use Land Cover

Table A3.1 Statistical descriptions of surface temperature with reference to each land use category

Land Use (code)	Number	Image Time	STATISTICAL DESCRIPTION			
			MIN	MAX	MEAN	STD
Residential Land (1)	7112	ST_102803	15.41	27.05	21.27	1.46
		ST_110303	26.15	39.45	31.57	1.49
		ST_041706	20.85	34.95	26.08	1.79
Commercial Land (2)	629	ST_102803	19.95	26.95	23.51	1.14
		ST_110303	30.95	38.20	31.27	1.29
		ST_041706	25.19	33.35	25.55	1.46
Industrial Land (3)	1693	ST_102803	16.38	26.15	21.75	1.46
		ST_110303	29.52	39.09	31.79	1.74
		ST_041706	25.05	34.22	26.27	2.08
Institutional Land (4)	1330	ST_102803	16.75	26.05	22.71	1.48
		ST_110303	29.11	38.65	31.26	1.16
		ST_041706	24.61	33.55	25.55	1.27
Transportation (5)	3	ST_102803	23.23	24.75	24.23	0.87
		ST_110303	30.95	30.95	30.95	0
		ST_041706	25.19	25.19	25.19	0
Open Space (6)	938	ST_102803	18.75	26.00	23.03	1.32
		ST_110303	29.35	38.84	31.16	1.02
		ST_041706	20.85	32.80	25.42	1.12
Vacant Land (7)	1307	ST_102803	17.35	26.15	22.49	1.55
		ST_110303	29.56	40.21	31.41	1.42

		ST_041706	24.65	36.12	25.72	1.57
Other Urban or Built-up Land (8)	1076	ST_102803	16.25	26.05	22.59	1.60
		ST_110303	30.95	38.95	31.30	1.30
		ST_041706	25.19	34.95	25.56	1.36
Agricultural Land (9)	4928	ST_102803	15.12	25.15	20.50	1.48
		ST_110303	26.35	38.27	31.24	1.22
		ST_041706	21.05	33.25	25.61	1.44
Woodland/Shrub land/Grassland (10)	7787	ST_102803	15.35	27.05	21.57	1.64
		ST_110303	26.05	39.75	31.33	1.47
		ST_041706	21.54	38.75	25.76	1.62
Wetland (11)	839	ST_102803	16.85	26.25	21.73	1.30
		ST_110303	25.75	36.71	30.26	1.80
		ST_041706	20.55	33.75	25.26	1.78
Barren Land (12)	1196	ST_102803	18.25	25.35	20.95	0.97
		ST_110303	30.95	30.95	30.95	0
		ST_041706	25.19	25.19	25.19	0
Water (13)	83	ST_102803	18.07	24.99	21.35	1.40
		ST_110303	27.11	32.43	30.48	1.12
		ST_041706	21.22	27.85	24.91	1.04

APPENDIX 4a: Collinearity Diagnostics of the Variables

Table A4a.1 Collinearity diagnostics of model 04-17-2006

Model	Dimension	Eigenvalue	Condition Index	Variance Proportions						
				(Constant)	Rndvi_06	elevationavg	distowater	footsqure_a	hsh2006	SD2006
ST04172006	1	4.171	1.000	.00	.01	.01	.01	.00	.00	.00
	2	1.419	1.714	.00	.02	.02	.00	.17	.00	.21
	3	.581	2.678	.00	.00	.02	.01	.40	.00	.68
	4	.412	3.182	.00	.00	.65	.10	.17	.00	.00
	5	.223	4.321	.01	.00	.03	.83	.00	.01	.03
	6	.188	4.714	.00	.97	.20	.05	.11	.00	.07
	7	.006	27.429	.99	.00	.07	.00	.14	.98	.01

Table A4a.2 Collinearity diagnostics of model 10-23-2005

Model	Dimension	Eigenvalue	Condition Index	Variance Proportions						
				(Constant)	Rndvi_05	hsh2005	elevationavg	footsqure_a	SD2006	diffuR296
ST10232005	1	4.432	1.000	.00	.01	.00	.01	.00	.00	.00
	2	1.395	1.782	.00	.01	.00	.02	.15	.21	.00
	3	.577	2.773	.00	.00	.00	.01	.37	.67	.00
	4	.418	3.257	.00	.00	.01	.65	.13	.01	.00
	5	.157	5.319	.00	.96	.01	.26	.07	.06	.00
	6	.015	17.131	.16	.00	.96	.03	.02	.00	.09
	7	.006	27.292	.84	.02	.02	.01	.25	.04	.91

Table A4a.3 Collinearity diagnostics of model 10-01-2005

Model	Dimension	Eigenvalue	Condition Index	Variance Proportions						
				(Constant)	Rndvi_05	elevationavg	distowater	TPU2001	SD2006	diffuR274
ST10012005	1	4.266	1.000	.00	.01	.01	.01	.00	.00	.00
	2	1.377	1.760	.00	.01	.02	.00	.15	.23	.00
	3	.551	2.782	.00	.00	.01	.00	.46	.63	.00
	4	.432	3.144	.00	.00	.64	.14	.05	.02	.00
	5	.214	4.469	.01	.03	.09	.84	.03	.00	.01
	6	.155	5.248	.01	.94	.23	.00	.04	.08	.01
	7	.006	26.443	.99	.00	.00	.00	.26	.03	.98

Table A4a.4 Collinearity diagnostics of model 11-21-2004

Model	Dimension	Eigenvalue	Condition Index	Variance Proportions					
				(Constant)	Rndvi_04	hsh2004	diffuR326	elevationavg	footsqure_a
ST11212004	1	4.246	1.000	.00	.01	.00	.00	.01	.00
	2	1.081	1.982	.00	.03	.00	.00	.04	.37
	3	.422	3.171	.00	.01	.01	.00	.58	.19
	4	.219	4.407	.00	.94	.00	.00	.33	.12
	5	.026	12.838	.10	.00	.96	.06	.04	.02
	6	.006	26.198	.90	.01	.03	.94	.01	.29

Table A4a.5 Collinearity diagnostics of model 10-05-2004

Model	Dimension	Eigenvalue	Condition Index	Variance Proportions						
				(Constant)	Rndvi_04	distowater	TPU2001	diffuR279	SD2004	elevationavg
ST10052004	1	4.148	1.000	.00	.01	.01	.00	.00	.00	.02
	2	1.375	1.737	.00	.02	.00	.15	.00	.24	.02
	3	.596	2.638	.00	.00	.00	.42	.00	.64	.01
	4	.443	3.060	.00	.03	.17	.08	.00	.02	.52
	5	.242	4.137	.00	.53	.38	.00	.00	.01	.39
	6	.189	4.682	.01	.41	.43	.07	.02	.07	.05
	7	.006	25.976	.99	.00	.00	.27	.98	.02	.00

Table A4a.6 Collinearity diagnostics of model 11-03-2003

Model	Dimension	Eigenvalue	Condition Index	Variance Proportions							
				(Constant)	Rndvi_03	hsh2003	diffuR307	footsqure_a	TPU2001	SD2004	elevationavg
ST11032003	1	4.539	1.000	.00	.01	.00	.00	.00	.01	.00	.01
	2	1.677	1.645	.00	.01	.00	.00	.09	.08	.11	.02
	3	.654	2.635	.00	.00	.00	.00	.17	.06	.81	.00
	4	.499	3.016	.00	.00	.00	.00	.35	.66	.01	.01
	5	.417	3.299	.00	.00	.01	.00	.12	.00	.02	.65
	6	.191	4.873	.00	.93	.01	.00	.06	.00	.04	.26
	7	.018	15.834	.10	.00	.97	.08	.01	.01	.00	.03
	8	.005	30.531	.90	.04	.01	.91	.20	.18	.01	.00

Table A4a.7 Collinearity diagnostics of model 10-28-2003

Model	Dimension	Eigenvalue	Condition Index	Variance Proportions					
				(Constant)	Rndvi_03	elevationavg	TPU2001	distowater	SD2004
ST10282003	1	3.311	1.000	.01	.02	.03	.01	.02	.01
	2	1.339	1.572	.00	.01	.02	.21	.00	.26
	3	.596	2.358	.00	.00	.01	.56	.00	.64
	4	.413	2.831	.02	.00	.55	.07	.27	.01
	5	.218	3.897	.01	.64	.39	.00	.33	.01
	6	.123	5.194	.95	.32	.00	.15	.37	.07

APPENDIX 4b: Statistical Descriptions of the Variables

Table A4b.1 Statistical descriptions of the variables for 1070 sample points

VARIABLES	UNITS	INDICES	STATISTICAL DESCRIPTION			
			MIN	MAX	MEAN	STD
Surface Temperature	Degrees Celsius (°C)	ST04172006	20.25	37.45	26.726	2.952
		ST10232005	18.95	40.45	26.604	3.173
		ST10012005	23.45	32.75	28.269	1.463
		ST11212004	17.05	40.45	25.562	3.350
		ST10052004	13.25	27.95	19.947	2.810
		ST11032003	23.95	46.25	32.277	3.407
		ST10282003	15.85	26.75	21.039	1.839
Vegetation NDVI	Unitless	NDVI041706	-0.211	0.422	0.165	0.142
		NDVI102305	-0.161	0.484	0.209	0.153
		NDVI112104	-0.323	0.511	0.175	0.160
		NDVI110303	-0.183	0.579	0.235	0.187
Road Density	Number	SD2006	0	12	0.56	1.635
		SD2004	0	21	0.64	2.031
Population Density	People/ km^2	TPU2001	0	140658.9	7267.2	16435.6
Distance from Coast	Kilometer	DisttoCoast	0	8.67	3.073	2.126
Solar Radiation	Gray value	hshad06	106.76	251.80	215.16	25.592
		hshad05	38.89	249.30	183.26	32.773

		hshad04	23.67	242.88	159.74	36.263
		hshad03	33.78	247.48	174.85	34.1526
Square Footage	Percentage	**footsqure_a**	0	0.798	0.048	0.118
Elevation	Meter	**elevationavg**	0	943.82	124.26	143.871
Diffuse Radiation	WH/ m^2	**diffuR107**	31.10	409.58	340.335	46.828
		diffuR296	24.56	328.39	269.348	37.131
		diffuR326	19.52	264.81	214.411	29.623
		diffuR307	22.87	307.34	250.965	34.622
		diffuR274	81.46	1066.81	890.789	122.492
		diffuR279	79.29	1040.08	867.272	119.279
		diffuR301	69.56	920.35	761.726	104.868

Table A4b.2 Statistical descriptions of the variables for 276 urban sample points

VARIABLES	UNITS	INDICES	STATISTICAL DESCRIPTION			
			MIN	MAX	MEAN	STD
Surface Temperature	Degrees Celsius (°C)	**ST04172006**	21.45	37.45	29.601	2.517
		ST10232005	23.35	35.45	29.65	2.636
		ST10012005	26.05	32.75	29.676	1.400
		ST11212004	21.85	36.95	28.287	2.667
		ST10052004	14.15	27.95	22.497	3.065
		ST11032003	27.45	42.85	35.216	2.846
		ST10282003	17.15	26.05	22.663	1.697

Vegetation NDVI	Unitless	**NDVI041706**	-0.211	0.318	0.026	0.109
		NDVI102305	-0.161	0.371	0.051	0.122
		NDVI112104	-0.222	0.401	0.013	0.119
		NDVI110303	-0.182	0.489	0.055	0.141
Road Density	Number	**SD2006**	0	12	1.65	2.584
		SD2004	0	21	1.91	3.347
Population Density	people/ km^2	**TPU2001**	0	140659	19379.1	25628.22
Distance from Coast	Kilometer	**DisttoCoast**	0	8.67	2.634	2.322
Potential Solar Radiation	Gray value	**hshad06**	106.76	245.77	210.49	31.827
		hshad05	38.89	229.49	176.03	34.710
		hshad04	23.67	212.72	151.21	35.136
		hshad03	33.78	223.94	167.06	35.081
Square Footage	Percentage	**footsqure_a**	0	0.798	0.157	0.185
Elevation	Meter	**elevationavg**	0	202.71	23.434	29.39
Diffuse Radiation	WH/ m^2	**diffuR107**	31.10	375.84	312.167	78.576
		diffuR296	24.56	297.34	246.63	62.063
		diffuR326	19.52	236.61	195.989	49.307
		diffuR307	22.87	277.01	229.661	57.788
		diffuR274	81.46	983.86	817.582	205.815
		diffuR279	79.29	957.85	795.851	200.339
		diffuR301	69.56	841.10	698.306	175.757

Table A4b.3 Statistical Descriptions of the Variables for 276 Rural Sample Points

VARIABLES	UNITS	INDICES	STATISTICAL DESCRIPTION			
			MIN	MAX	MEAN	STD
Surface Temperature	Degrees Celsius (°C)	ST04172006	20.25	35.25	25.853	2.613
		ST10232005	19.85	32.65	25.831	2.42
		ST10012005	23.65	31.45	27.912	1.247
		ST11212004	17.05	38.45	24.771	2.783
		ST10052004	13.25	27.05	19.001	2.428
		ST11032003	23.95	43.45	31.098	2.867
		ST10282003	15.85	25.15	20.542	1.669
Vegetation NDVI	Unitless	NDVI041706	-0.185	0.417	0.190	0.138
		NDVI102305	-0.147	0.458	0.234	0.143
		NDVI112104	-0.323	0.511	0.201	0.150
		NDVI110303	-0.183	0.566	0.259	0.175
Road Density	Number	SD2006	0	6	0.14	0.709
		SD2004	0	7	0.16	0.741
Population Density	People/ km^2	TPU2001	0	57339.6	2346.1	6809.02
Distance from Coast	Kilometer	DisttoCoast	0	8.57	3.218	2.107
Potential Solar Radiation	Gray value	hshad06	141.77	251.75	221.09	20.787
		hshad05	80.15	243.27	188.33	28.609
		hshad04	47.16	230.99	164.48	32.435
		hshad03	67.55	238.46	179.79	30.057

Square Footage	Percentage	**footsqure_a**	0	0.327	0.014	0.043
Elevation	Meter	**elevationavg**	0.54	728.36	117.18	139.856
Diffuse Radiation	WH/ m^2	**diffuR107**	265.16	385.66	352.433	19.887
		diffuR296	209.75	307.20	278.873	15.712
		diffuR326	166.88	246.12	221.954	12.509
		diffuR307	195.40	286.87	259.823	14.638
		diffuR274	694.16	1007.00	922.514	52.107
		diffuR279	675.80	981.10	898.142	50.715
		diffuR301	593.38	864.91	788.759	44.478

APPENDIX 5: Location of 276 Urban and Rural Sample Points

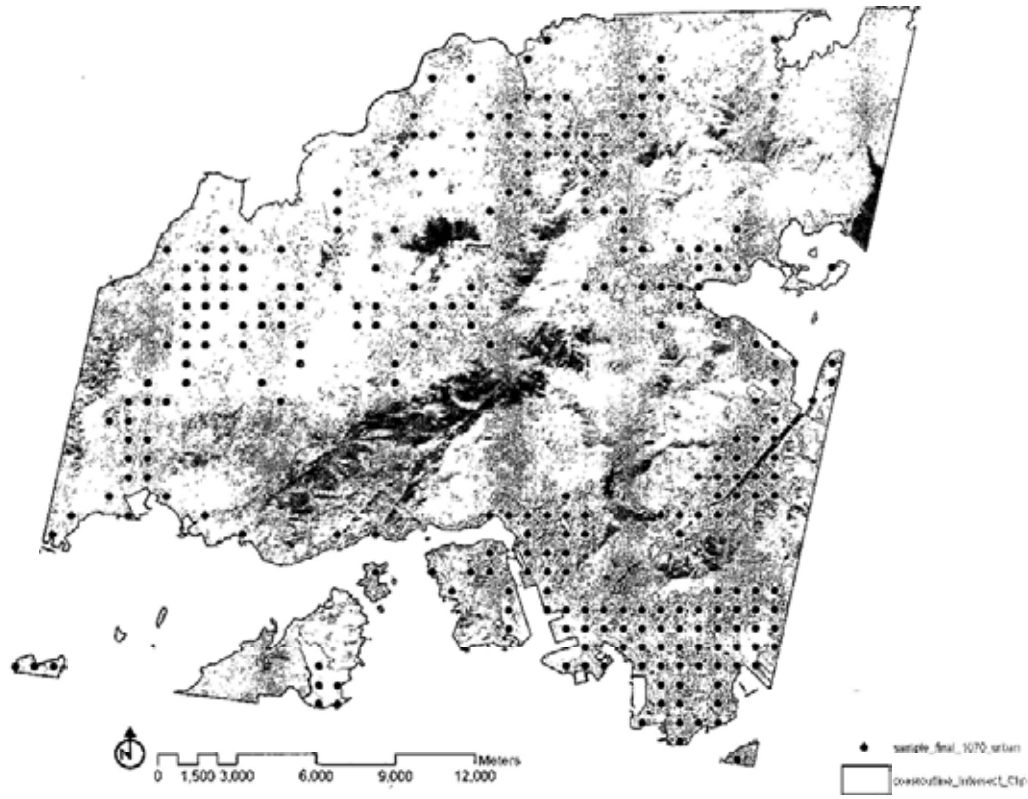

Figure A5.1 Location of 276 urban sample points

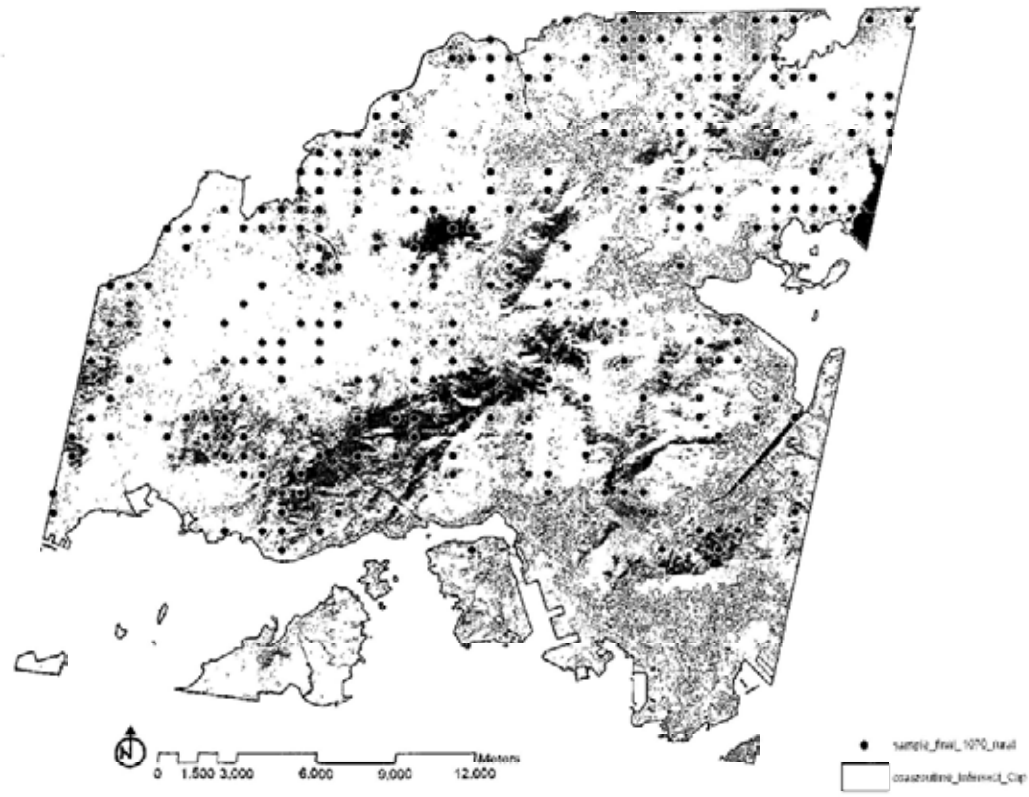

Figure A5.2 Location of 276 rural sample points

APPENDIX 6: Coefficients Distribution of Environmental Variables

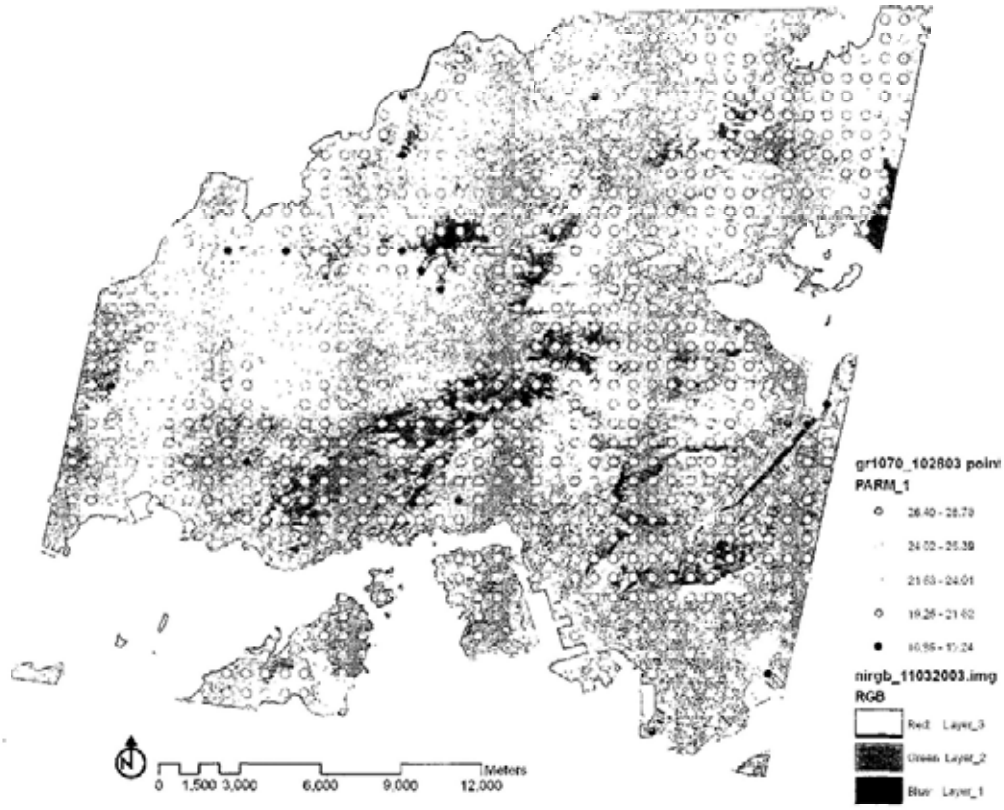

Figure A6.1 Coefficients distribution of Intercept in nighttime model 10/28/03

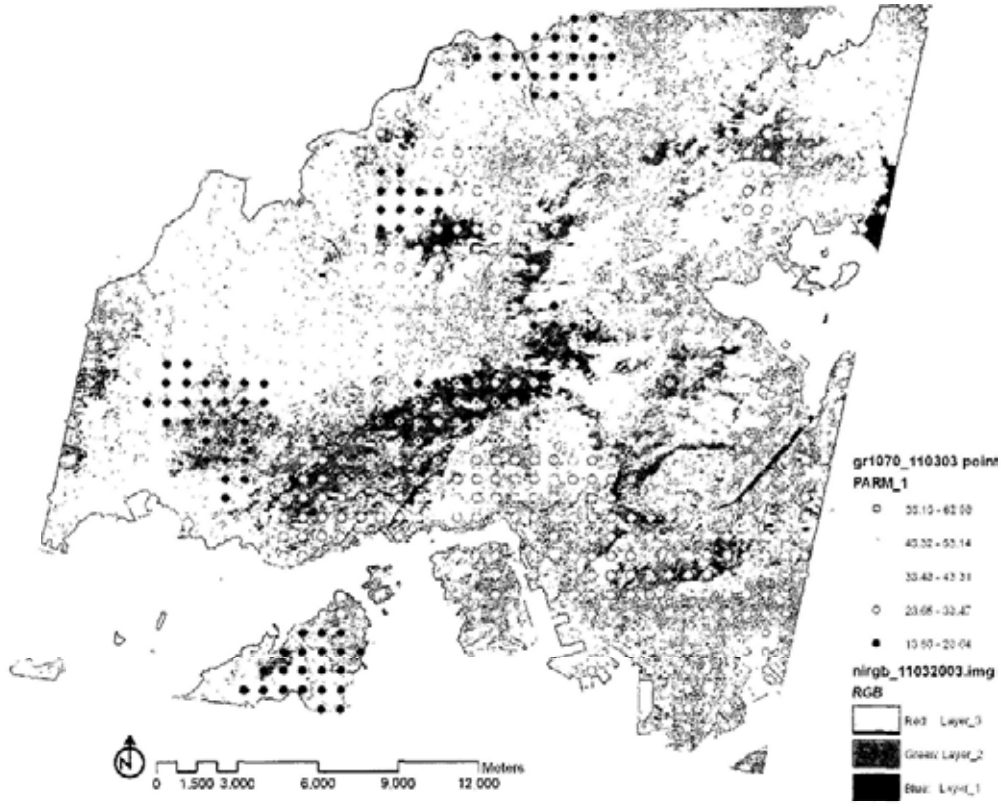

Figure A6.2 Coefficients distribution of Intercept in daytime model 11/03/03

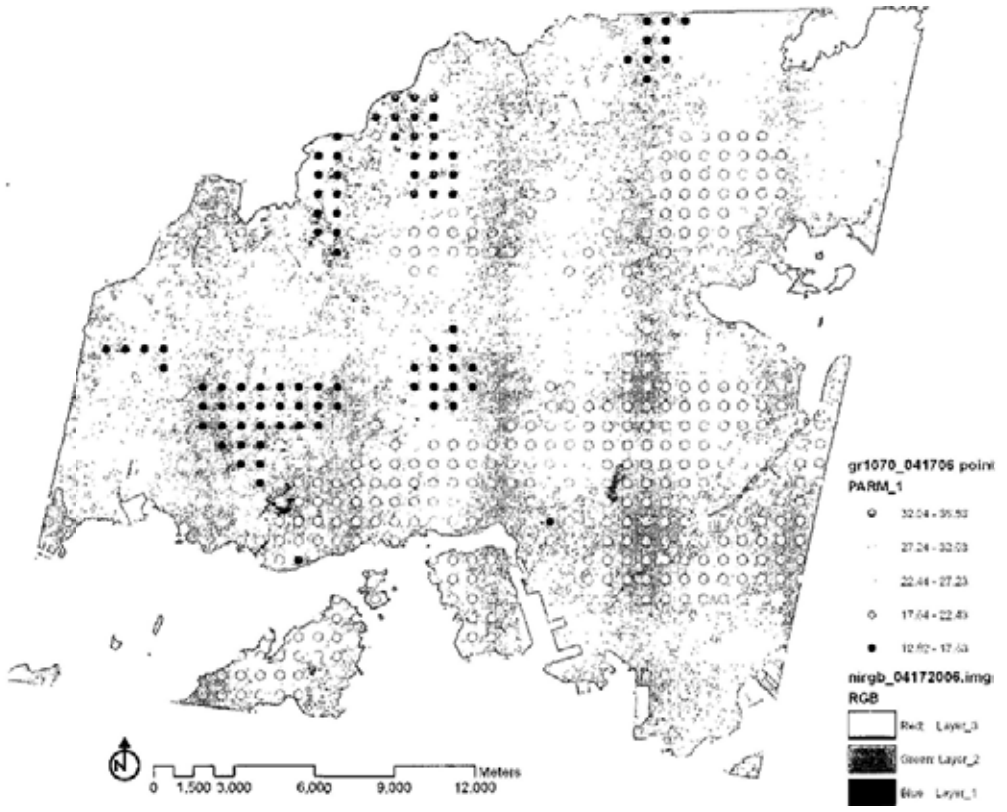

Figure A6.3 Coefficients distribution of Intercept in daytime model 04/17/06

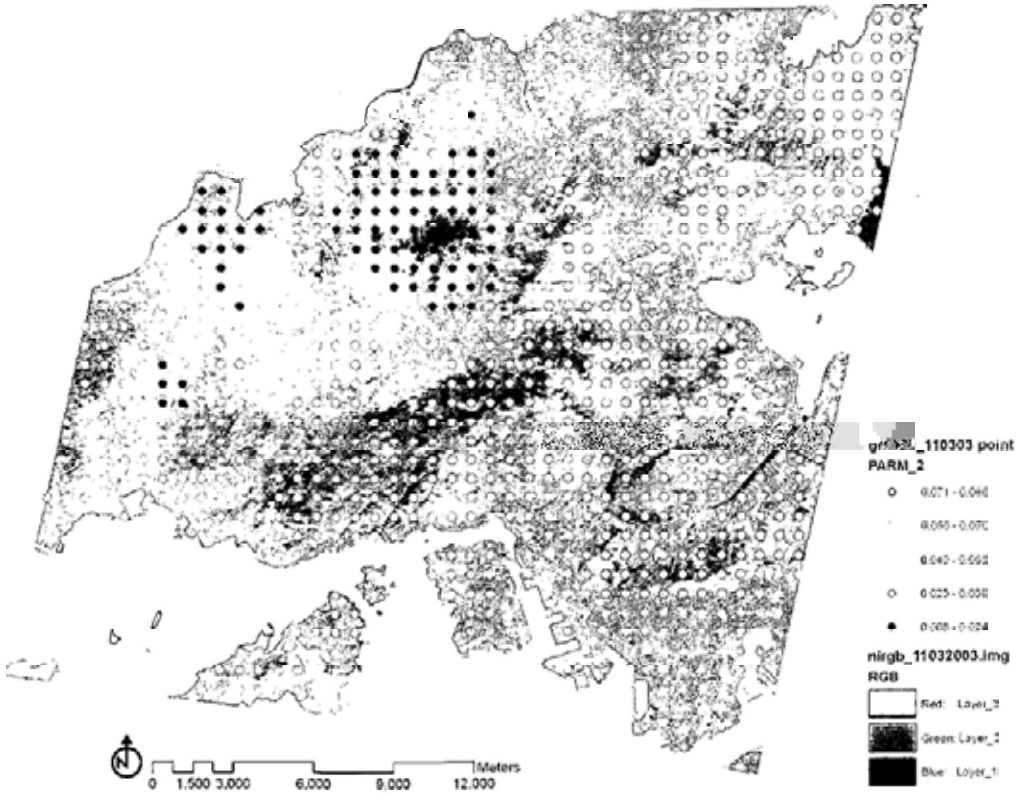

Figure A6.4 Coefficients distribution of Solar Radiation in daytime model 11/03/03

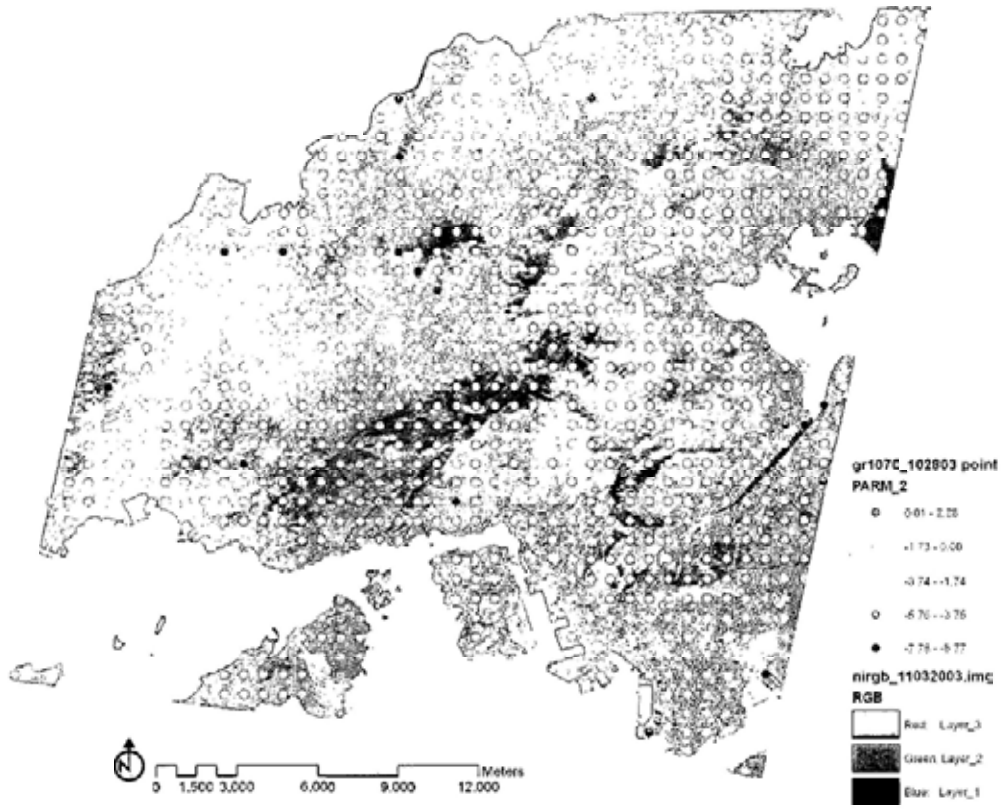

Figure A6.5 Coefficients distribution of Vegetation NDVI in nighttime model 10/28/03

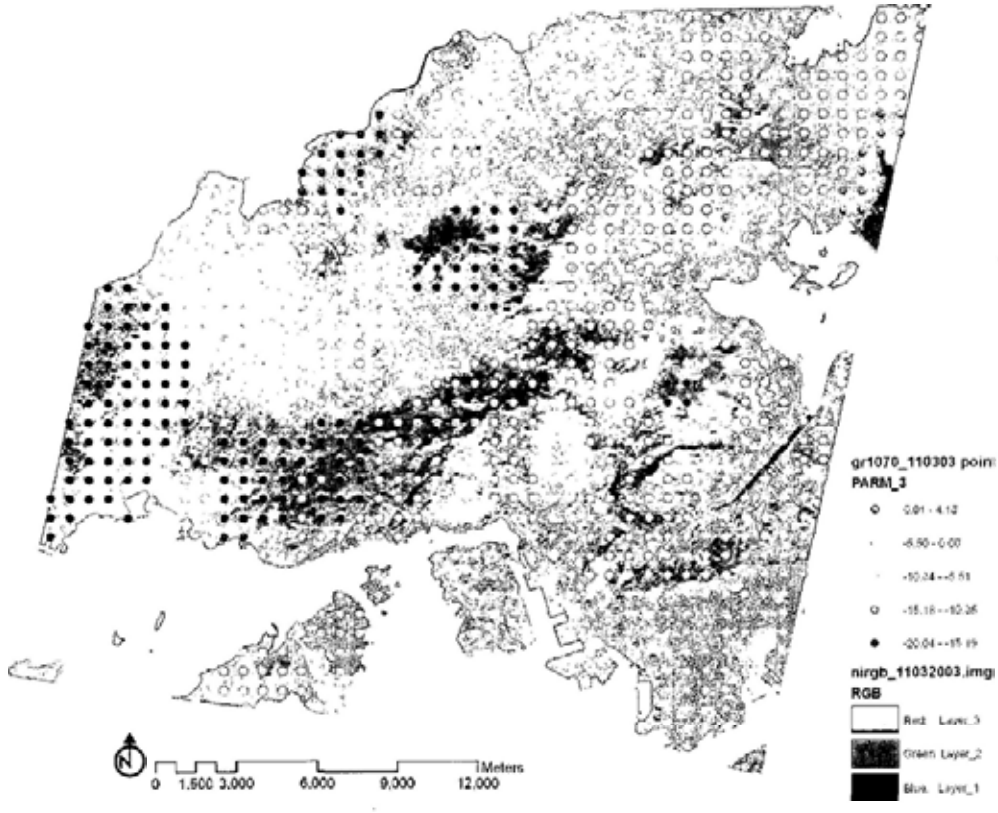

Figure A6.6 Coefficients distribution of Vegetation NDVI in daytime model 11/03/03

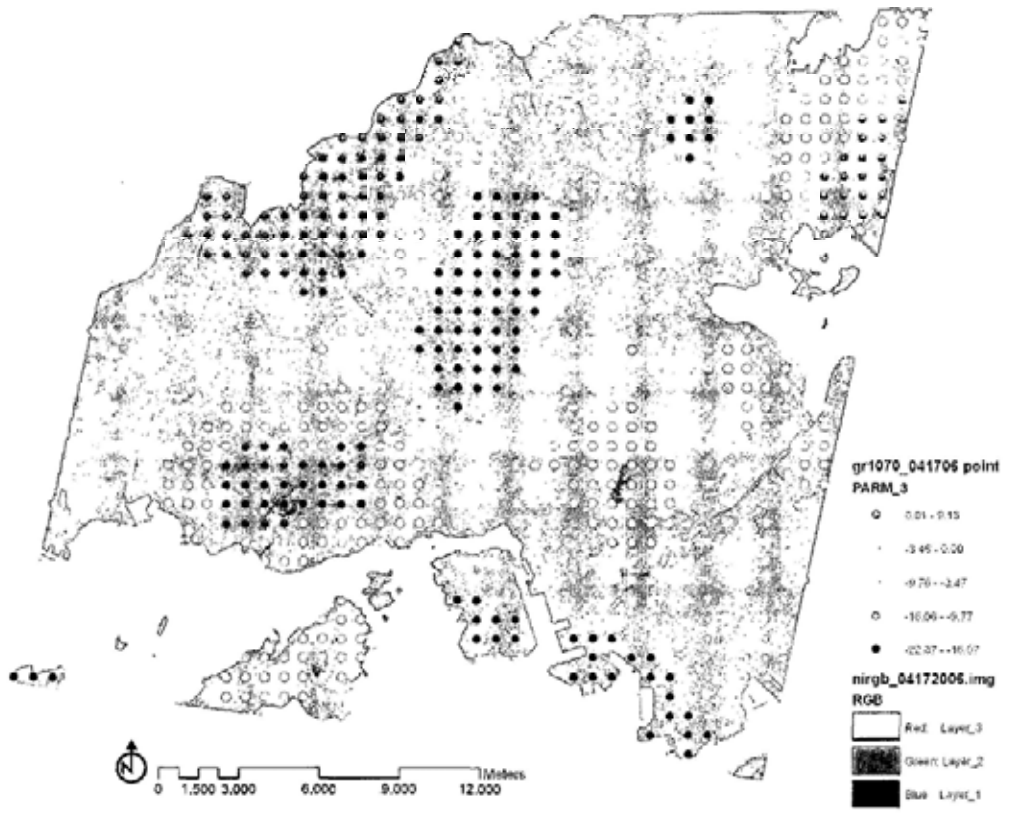

Figure A6.7 Coefficients distribution of Vegetation NDVI in daytime model 04/17/06

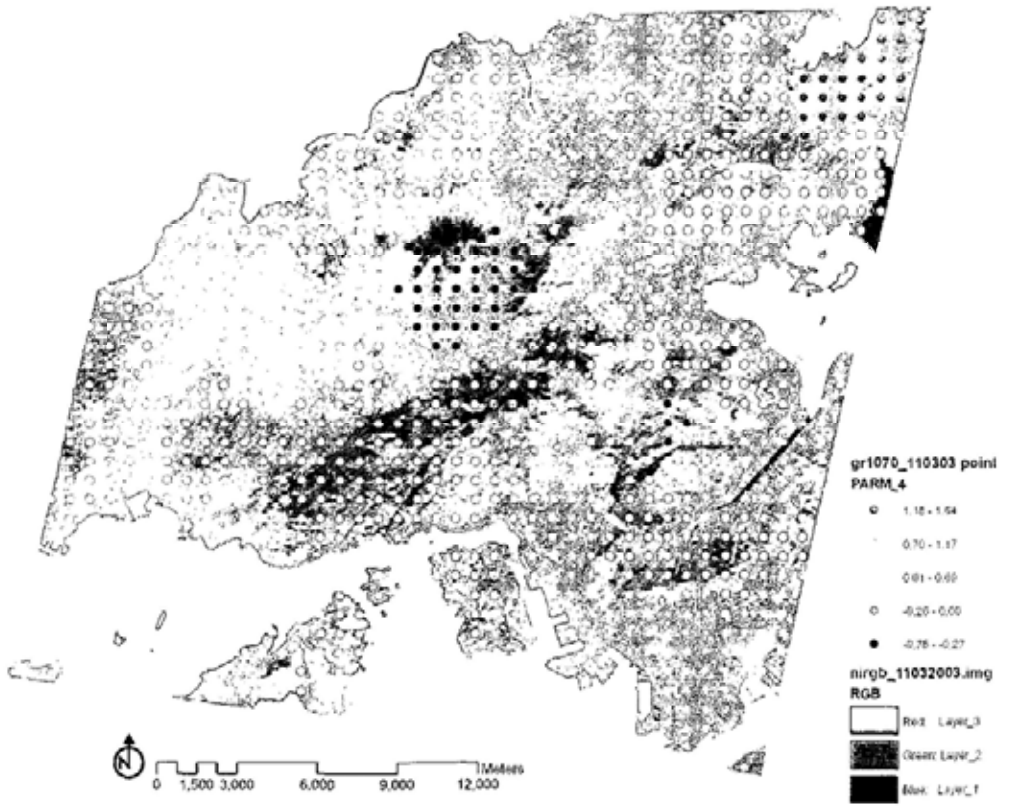

Figure A6.8 Coefficients distribution of Roadnetwork Density in daytime model 11/03/03

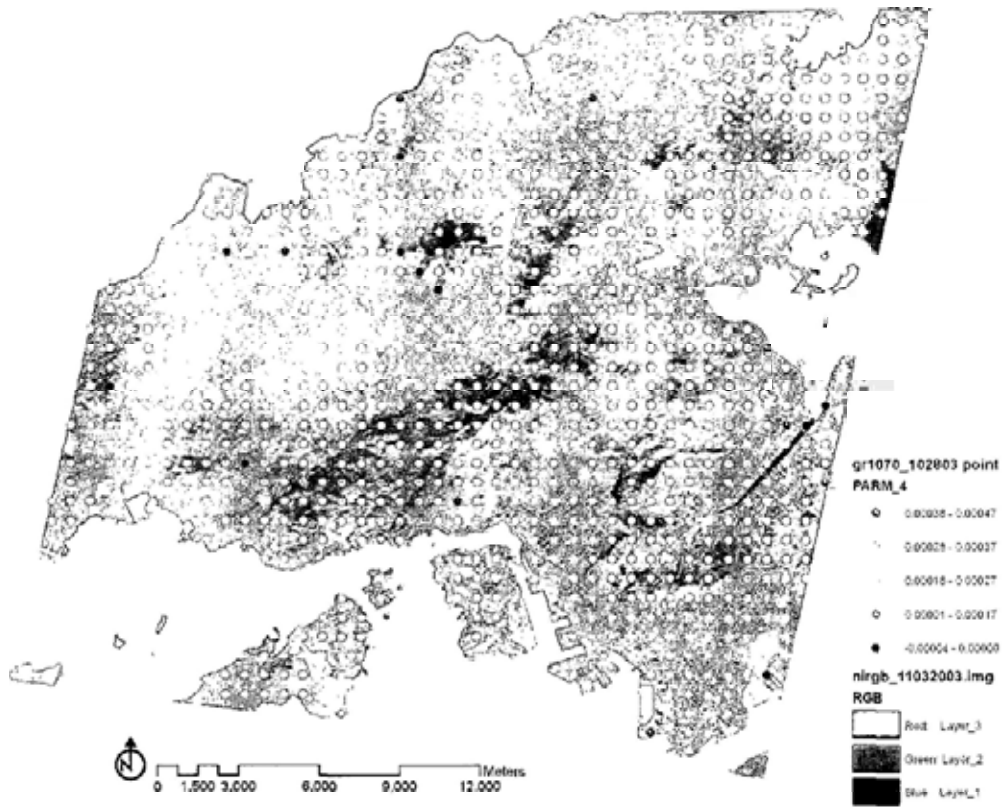

Figure A6.9 Coefficients distribution of Population Density in nighttime model 10/28/03

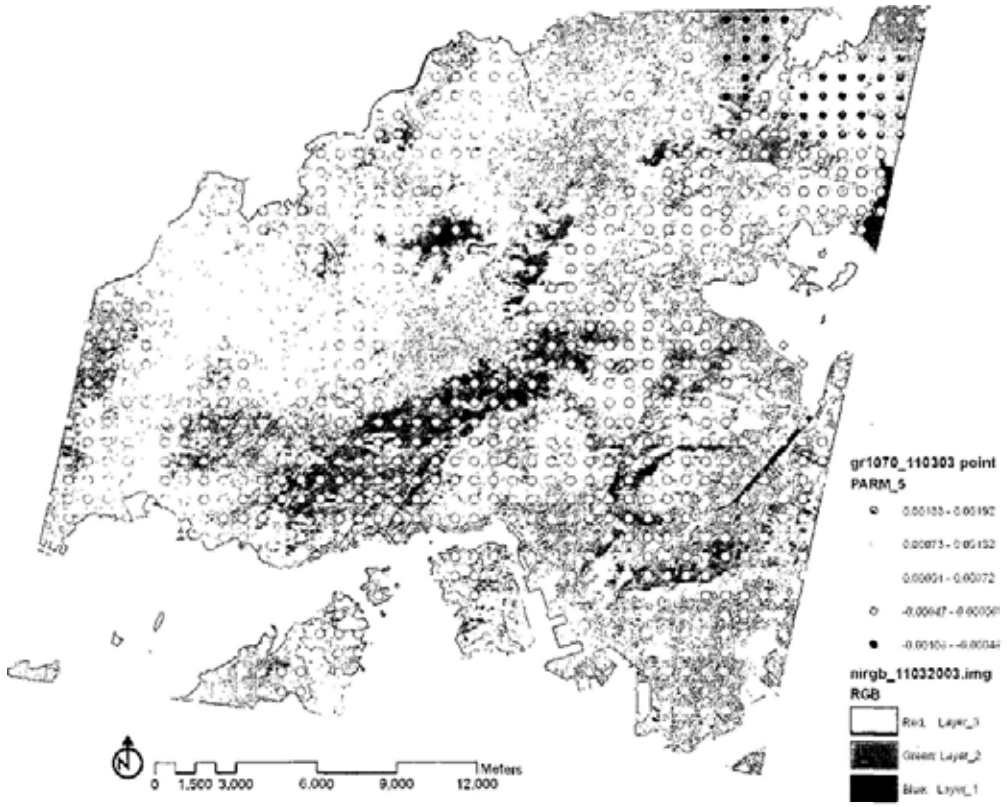

Figure A6.10 Coefficients distribution of Population Density in daytime model 11/03/03

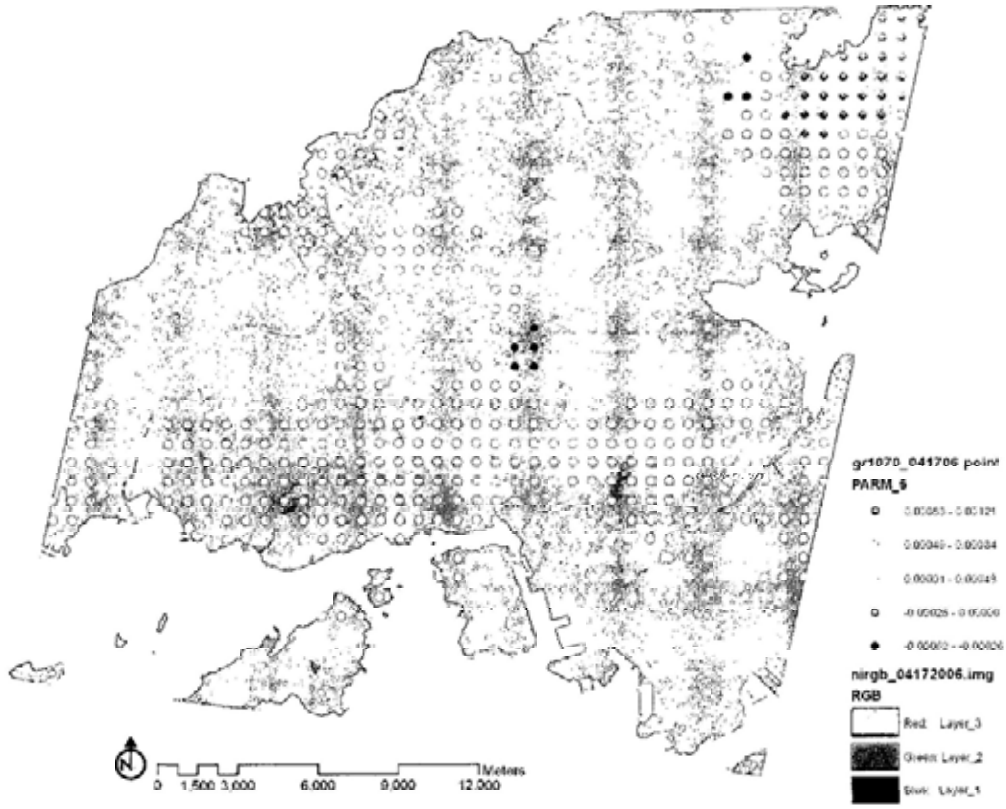

Figure A6.11 Coefficients distribution of Population Density in daytime model 04/17/06

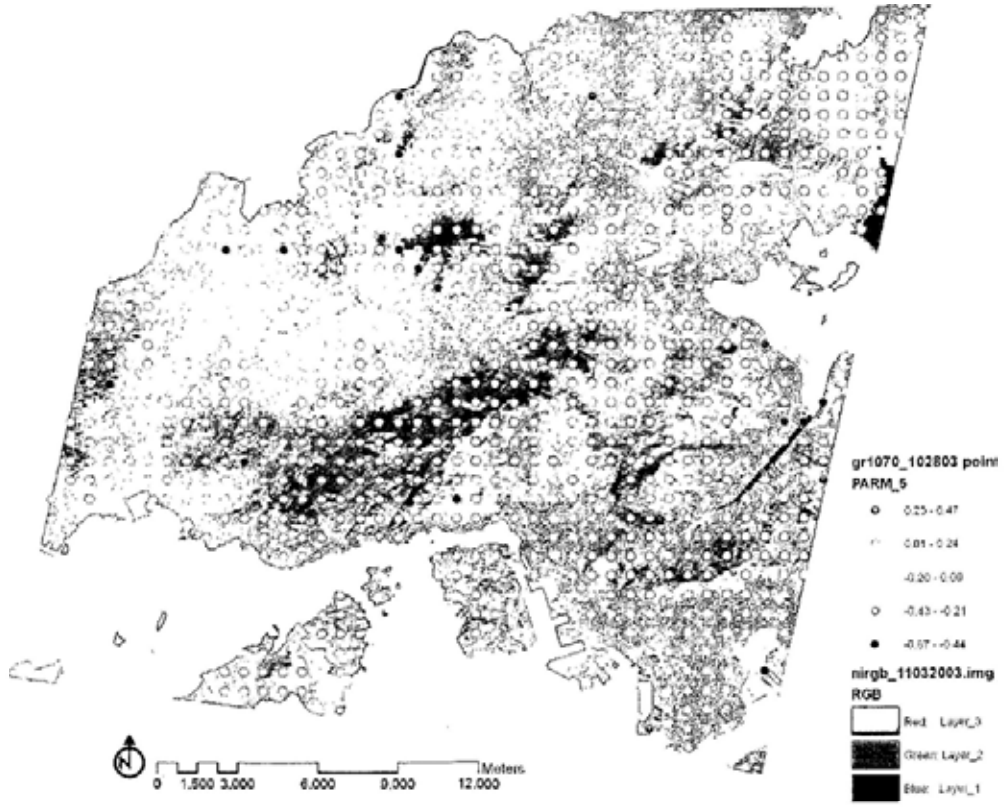

Figure A6.12 Coefficients distribution of Distance from Coast in nighttime model 10/28/03

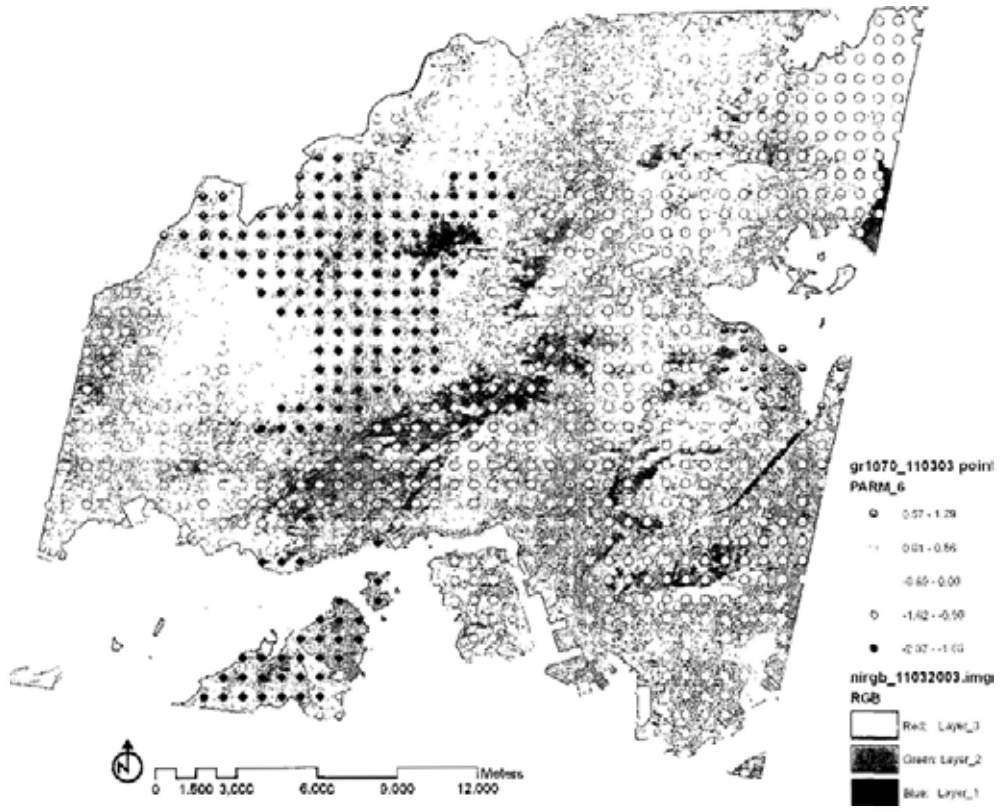

Figure A6.13 Coefficients distribution of Distance from Coast in daytime model 11/03/03

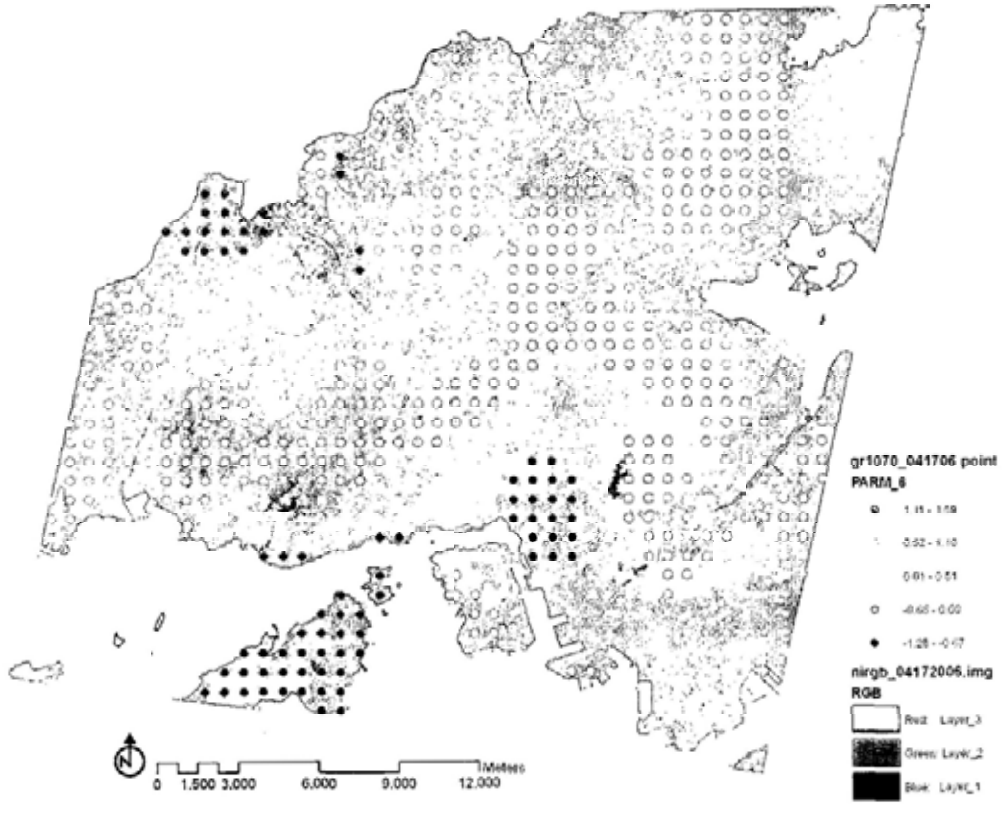

Figure A6.14 Coefficients distribution of Distance from Coast in daytime model 04/17/06

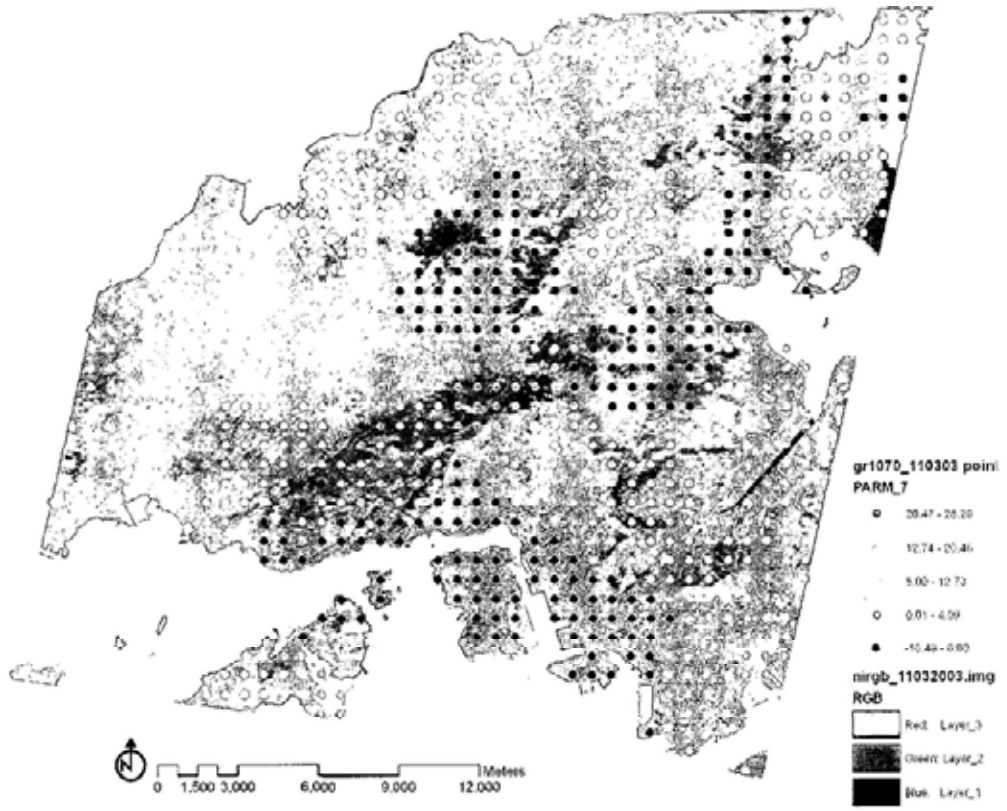

Figure A6.15 Coefficients distribution of Building footsq_a in daytime model 11/03/03

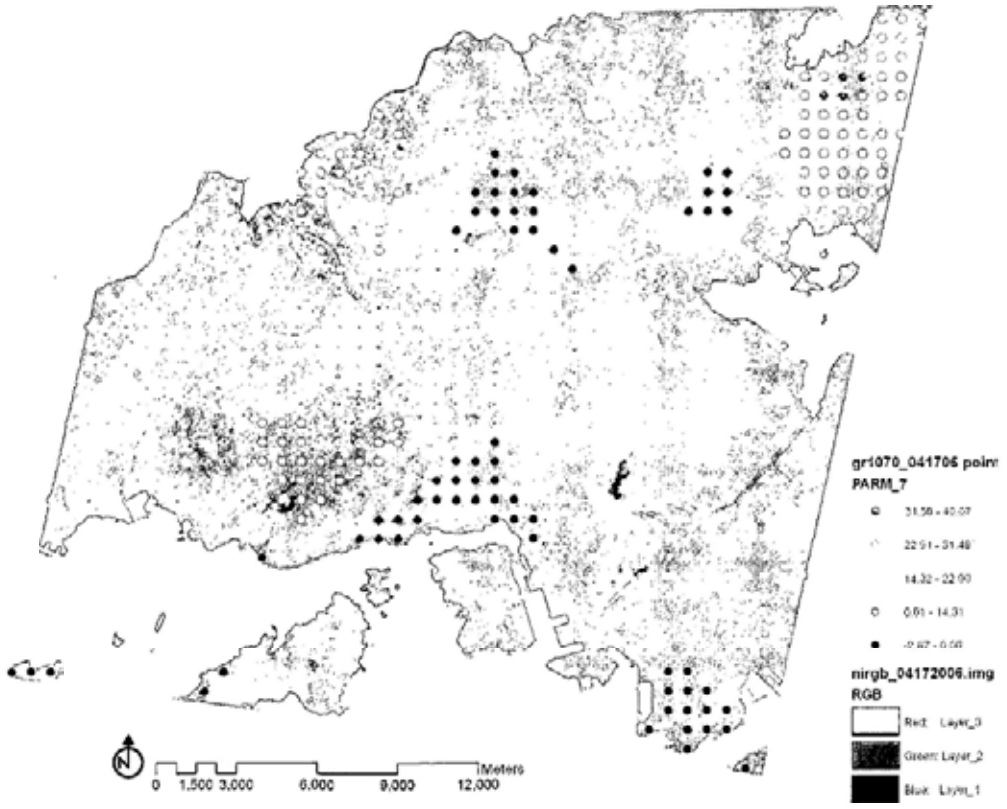

Figure A6.16 Coefficients distribution of Building footsq_a in daytime model 04/17/06

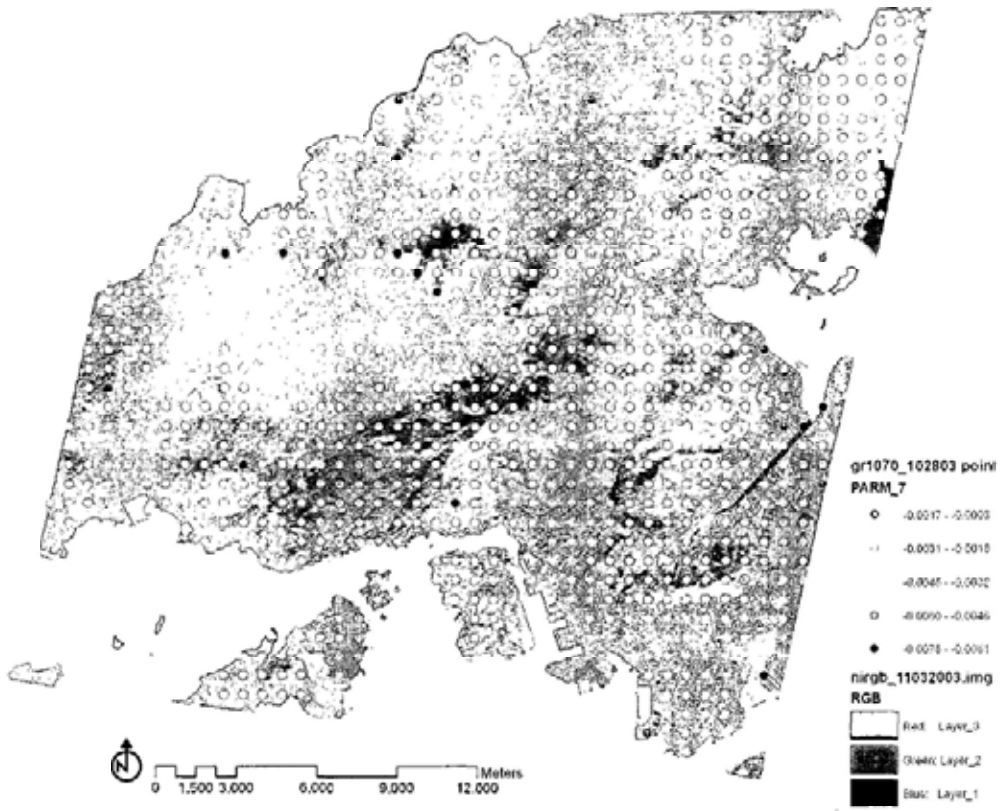

Figure A6.17 Coefficients distribution of Elevation in nighttime model 10/28/03

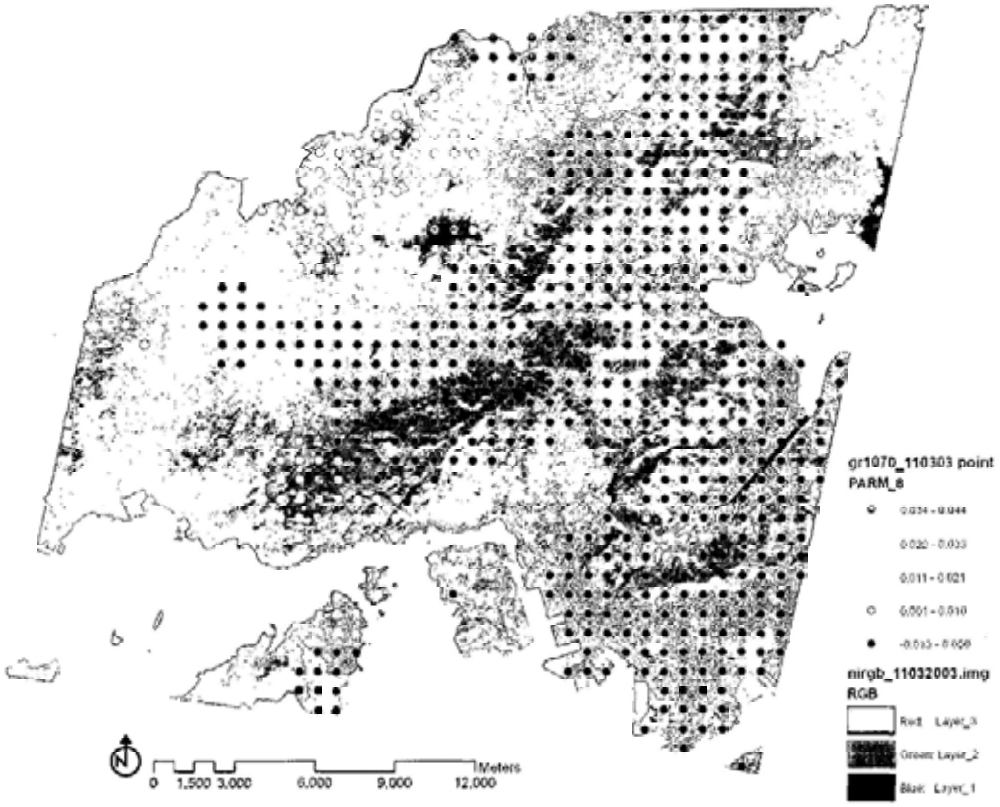

Figure A6.18 Coefficients distribution of Elevation in daytime model 11/03/03

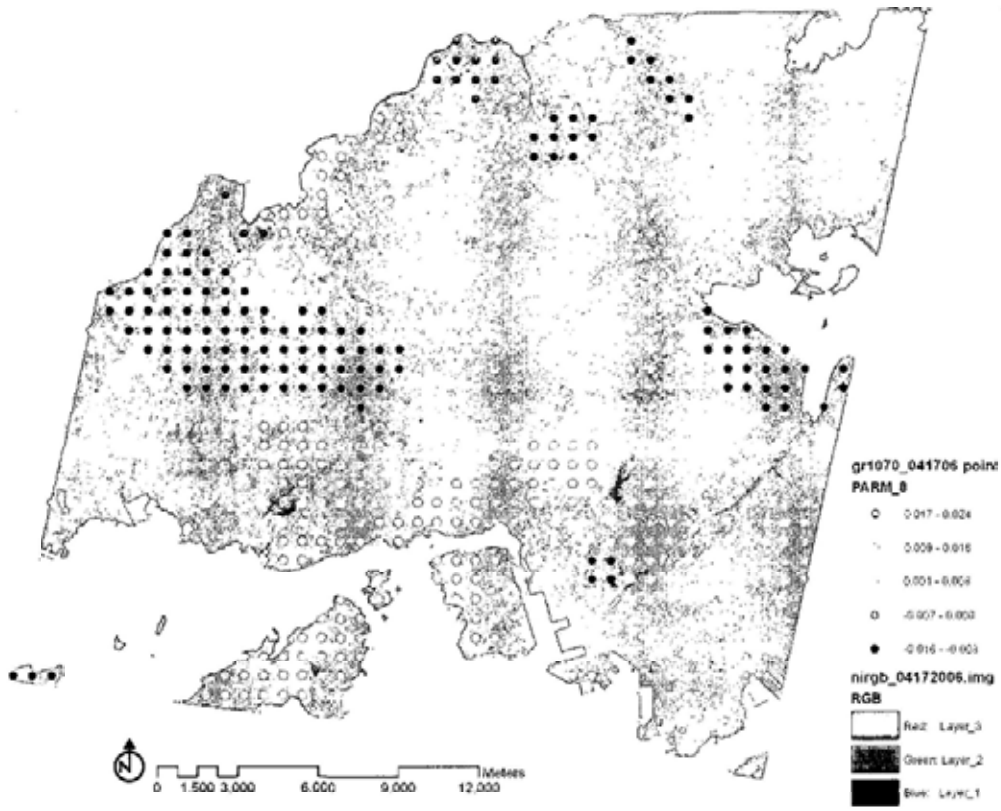

Figure A6.19 Coefficients distribution of Elevation in daytime model 04/17/06

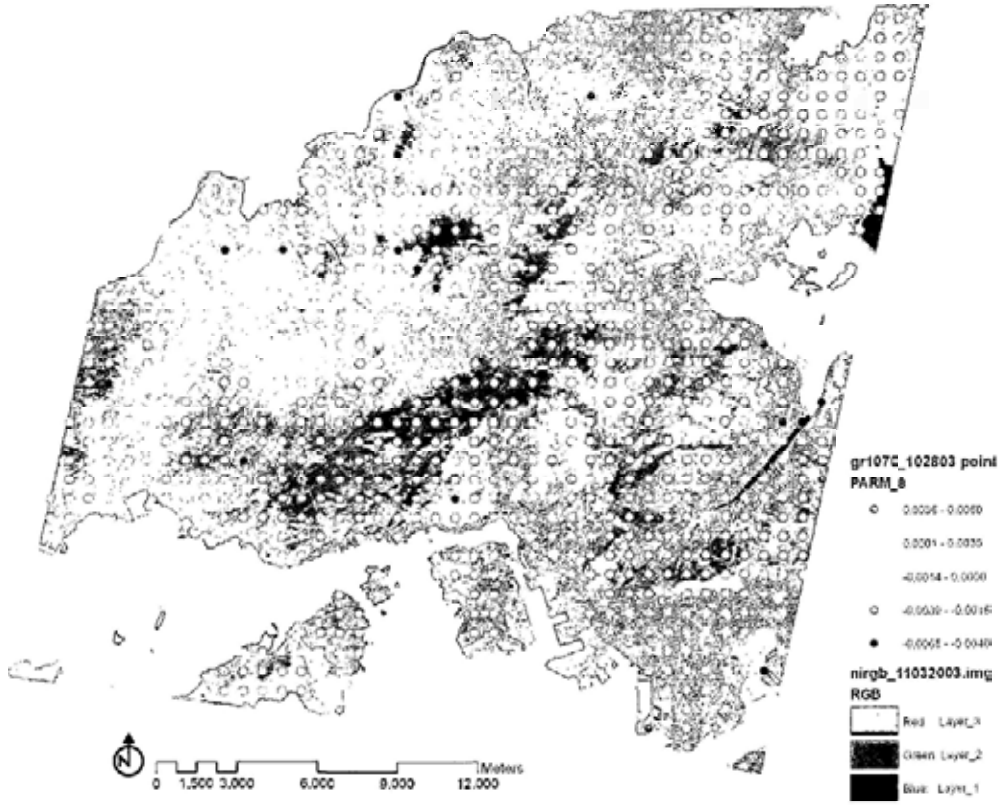

Figure A6.20 Coefficients distribution of Site Openness in nighttime model 10/28/03

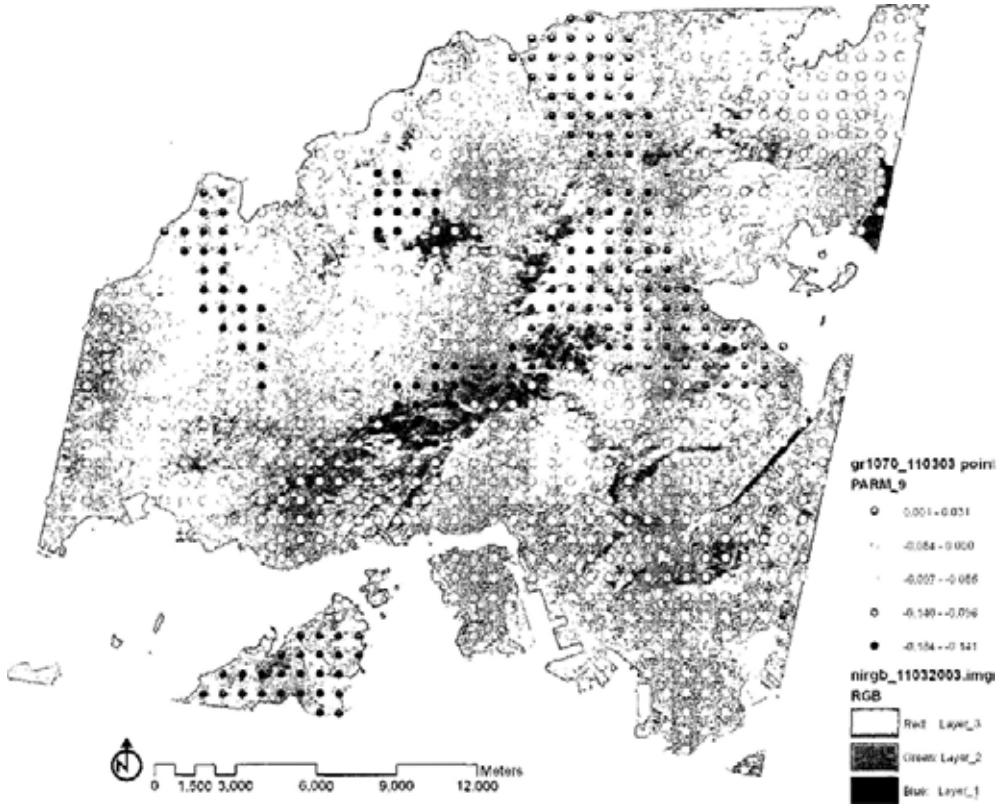

Figure A6.21 Coefficients distribution of Site Openness in daytime model 11/03/03

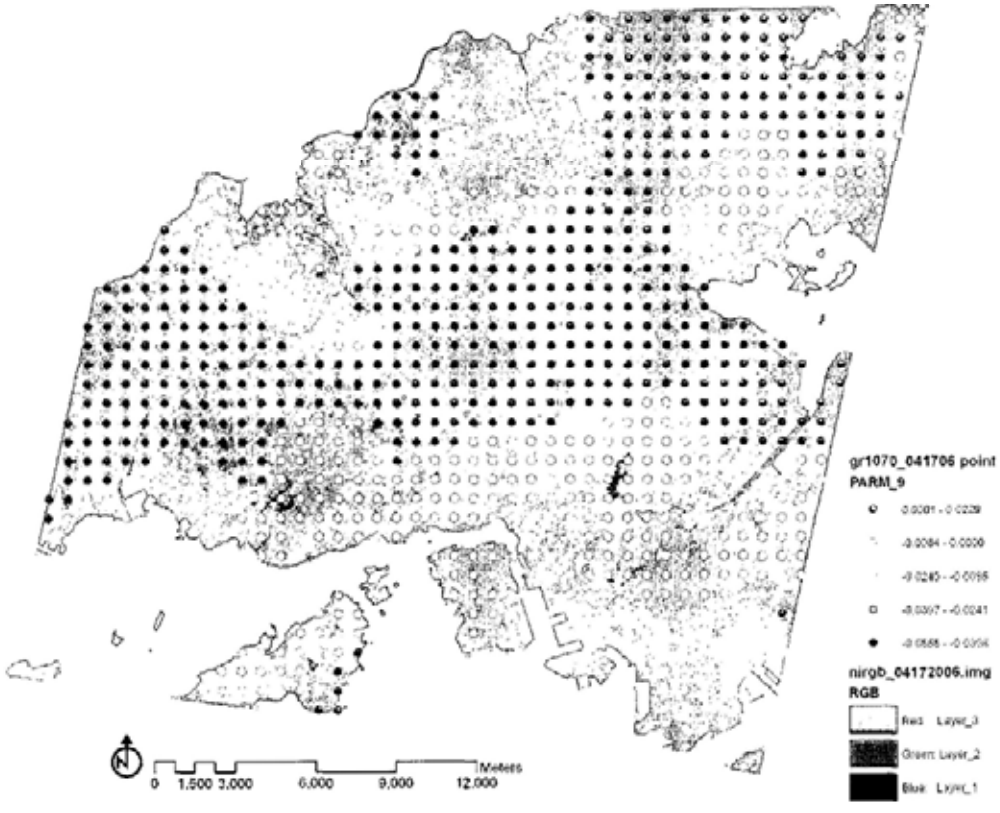

Figure A6.22 Coefficients distribution of Site Openness in daytime model 04/17/06

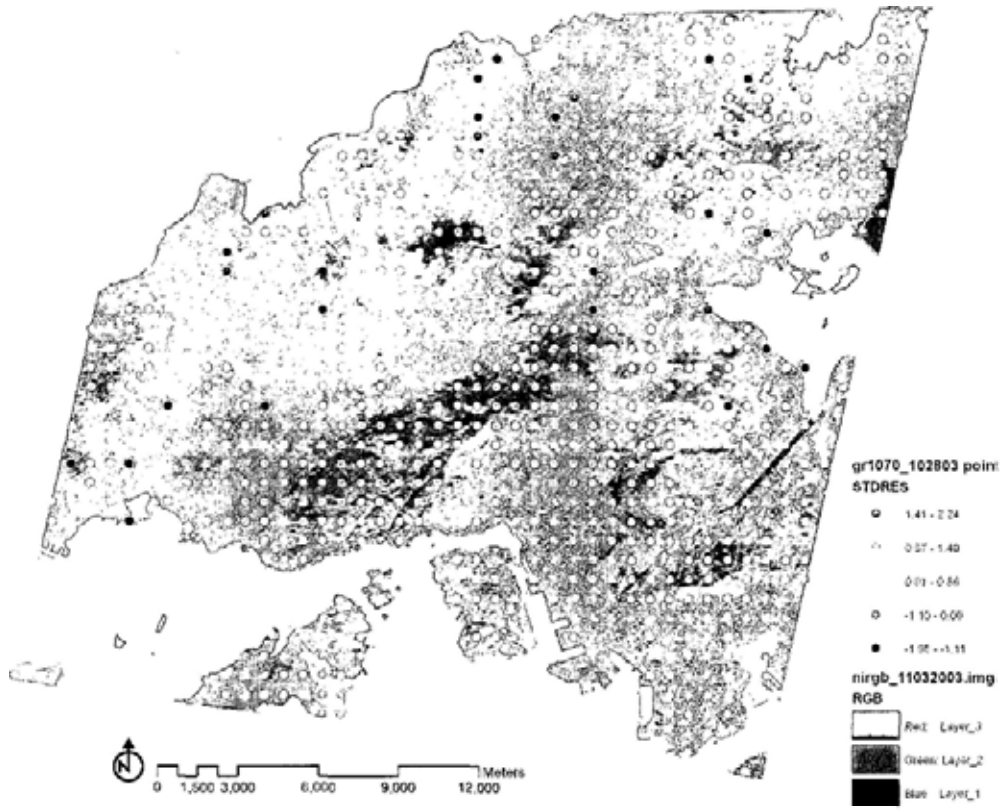

Figure A6.23 Standardized residual distribution of nighttime model 10/28/03

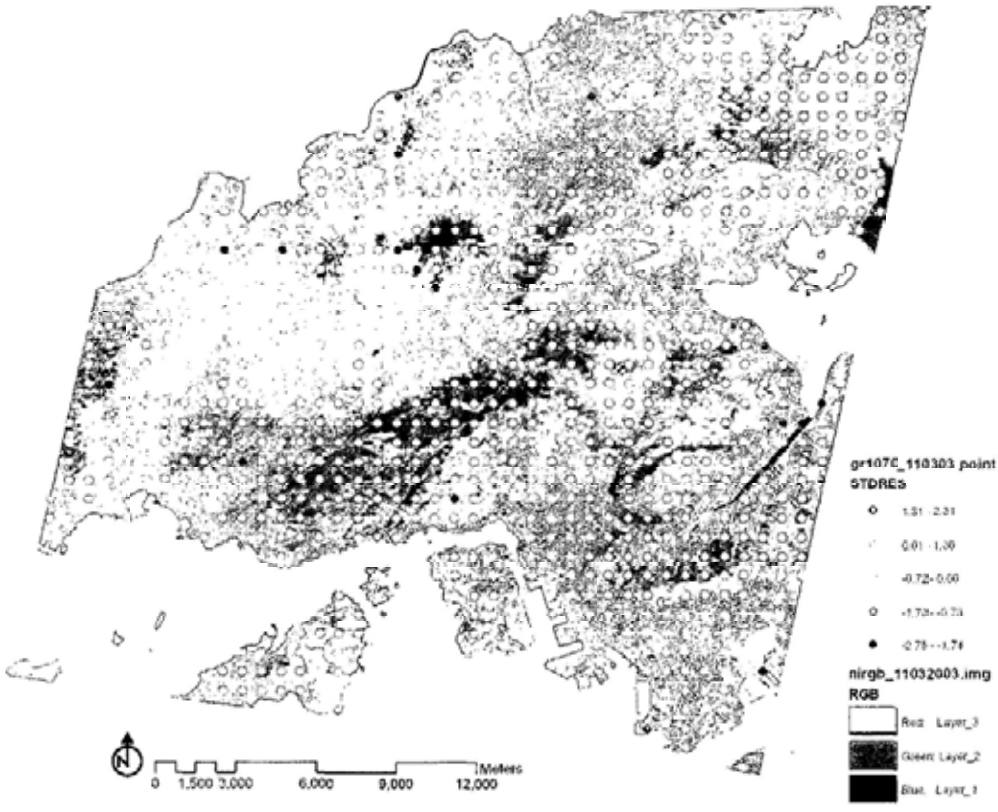

Figure A6.24 Standardized residual distribution of daytime model 11/03/03

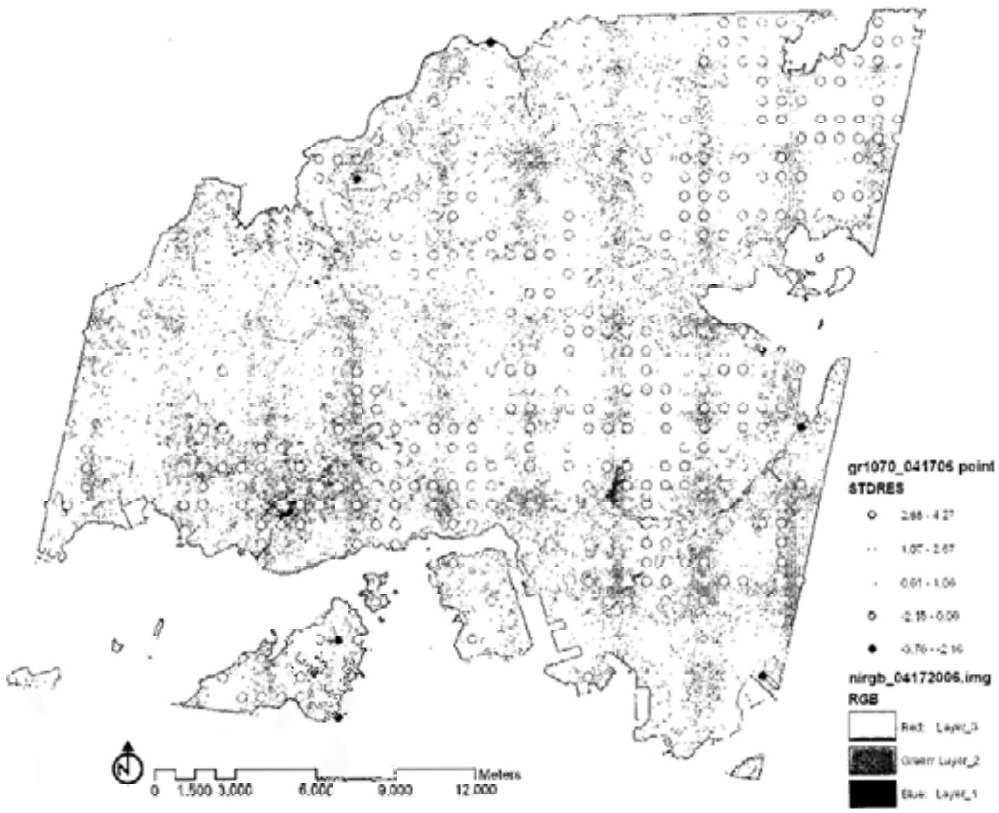

Figure A6.25 Standardized residual distribution of daytime model 04/17/06

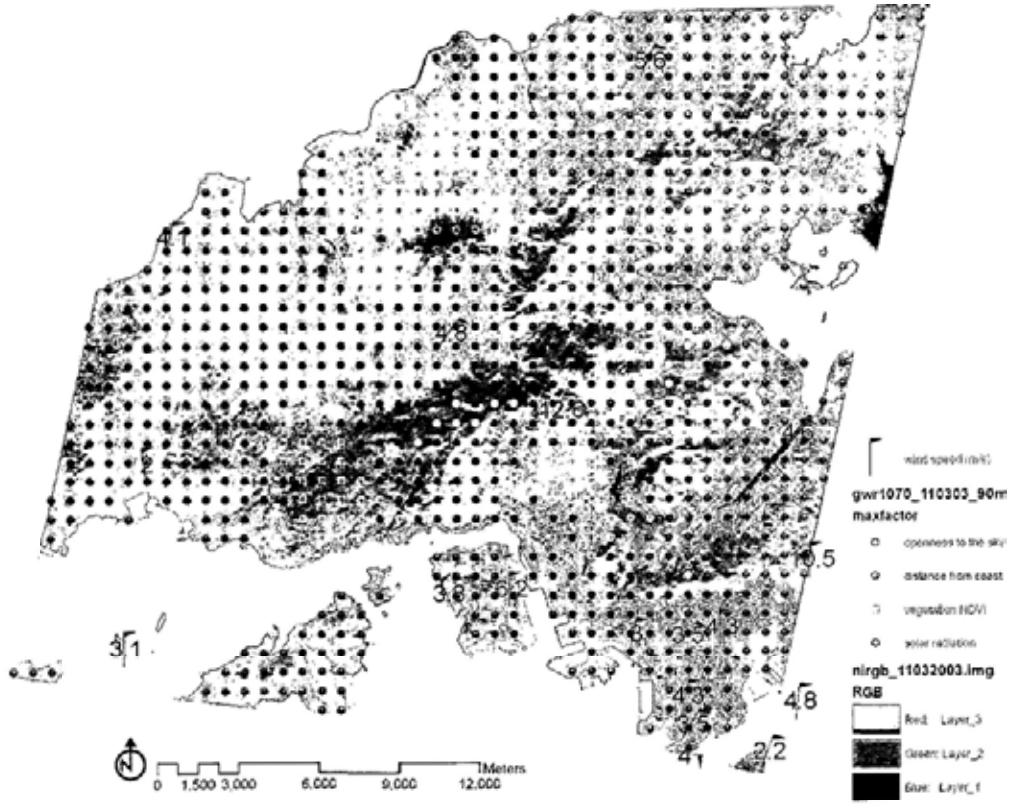

Figure A6.26 Local dominant factor to LST variation in daytime model 11/03/03

REFERENCES

Anderson, R. Local Government and Urban Heat Island Mitigation. Available at http://ist-socrates.berkeley.edu/~es196/projects/2000final/anderson.pdf

Arnfield, A. J. (1982). An Approach to the Estimation of the Surface Radiative Properties and Radiation Budgets of Cities. *Physical Geography*, 3(2), 97-122.

ASTER User Handbook. Available at http://asterweb.jpl.nasa.gov/content/03_data/04_Documents/aster_user _guide_v2.pdf, pp 25-26.

Balling, R. C. (1992). *The Heated Debate*. Pacific Research Institute for Public Policy, SanFransisco, CA, pp57-59.

Balling, R. C. and Brazell, S. W. (1988). High Resolution Surface Temperature Patterns in a Complex Urban Terrain. *Photogramm. Eng. Remote Sen.* 54, 1289–1293.

Becker, F. and Li, Z. L. (1990). Towards A Local Split Window Method Over Land Surface Temperature from a Satellite. *International Journal of Remote Sensing*, 11, 369-394.

Becker, F., and Li, Z. L. (1995). Surface Temperature and Emissivity at Different Scales: Definition, Measurement and Related Problems. *Remote Sensing Reviews*, 12, 225-253.

Benedict, M.A. and McMahon, E.T. (2002). Green Infrastructure: Smart Conservation for the 21st Century. *Renewable Resources Journal,* 20(3), 12-17.

Belsley, D.A, Kuh, E., and Welsch, R.E. (1980) .Regression *diagnostics: Identifying influential data and sources of collinearity.* New York: John Wiley & Sons.

Bitter, C., Mulligan, G.F. and Sandy, D. (2007). Incorporating Spatial Variation in Housing Attribute Prices: A Comparison of Geographically Weighted Regression and the Spatial Expansion Method. *Journal of Geographical Systems*, 9, 7-27.

Bonan, G. (2008). *Ecological Climatology*. Chapter 14, 2nd edition, Cambridge University Press, p.6.

Borruso, G. (2003). Network Density and the Delimitation of Urban Areas. *Transactions in GIS*, 7 (2), 177–191.

Borruso, G. (2005).Network Density Estimation: Analysis of Point Patterns over a Network. *Lecture Notes in Computer Science*, 3482, 126-132.

Brazel, A.J. and Johnson, D.M. (1980). Land Use Effects on Temperature and Humidity in the Salt River Valley, Arizona. *Journal of the Arizona-Nevada Academy of Science*, 15(2), 54-61.

Brest, C.L. (1987). Seasonal Albedo of an Urban/Rural Landscape from Satellite Observations. *J. Appl. Meteorol.*, 26, 1169–1187.

Bornstein, R.D. (1968). Observations of the Urban Heat Island Effect in New York. *City. J. Appl. Metero.*, 7, 575-582.

Brown, R.D. and Gillespie, T.J. (1995). *Microclimate Landscape Design: Creating Thermal Comfort and Energy Efficiency*. Chichester: John Wiley & Sons.

Brown University. (2004). Enhancing Rhode Island's Urban/Suburban Forest. From http://envstudies.brown.edu/classes/es201/2003/Forestry/heatislands.htm

Brunsdon, C, Fotheringham S. and Charlton, M. (1996). Geographically Weighted Regression: A Method for Exploring Spatial Nonstationarity. *Geographical Analysis*, 28, 281-298

Brunsdon, C., Fotheringham, S. and Charlton, M. (1998). Geographically Weighted Regression-Modelling Spatial Non-stationarity. *The Statistician*, Vol. 47, No. 3, 431-443.

Brunsdon, C., Fotheringham, A. S. and Charlton, M. E. (2002).Geographically Weighted Summary Statistics: A Framework for Localized Exploratory Data Analysis. *Computers, Environment and Urban Systems*, 26, 501–524.

Burt, J.E., O'Rourke, P.A., and Terjung, W.H. (1982). The Relative Influence of Urban Climates on Outdoor Human Energy Budgets and Skin Temperature I. Modeling Considerations. *International Journal of Biometerology*, 26(1),3-23.

Byrne, G.F., Kalma, J.D. and Streten, N.A. (1984). On The Relation between HCMM Satellite Data and Temperatures from Standard Meteorological Sites in Complex Terrain. *Int. J. Remote Sens.*, 5, 56–77.

Carlson, T.N., Augustine, J.A., and Boland, F.E. (1977). Potential Application of Satellite Temperature Measurements in the Analysis of Land Use over Urban Areas. *Bulletin of the American Meteorological Society,* 58(12), 1301-1303.

Carlson, T.N., Dodd, J.K., Benjamin, S.G. and Cooper, J.N. (1981). Satellite Estimation of the Surface-Energy Balance, Moisture Availability and Thermal Inertia. *Journal of Applied Meteorology* 20(1), 67-87.

Carnahan,W. H. and Larson, R. C. (1990). An Analysis of an Urban Heat Sink. *Remote Sens. Environ.,* 33, 65–71.

Carrão, H. and Caetano, M. (2002).The Effect of Scale on Landscape Metrics. http:www.igeo.pt/gdr/pdf/Carrao2002c.pdf (last accessed Dec 22.2007).

Caselles, V., Garcia, M.J. Lopez, Melia, J. and Cueva, A.J. Perez (1991). Analysis of the Heat-Island Effect of the City Of Valencia, Spain, Through Air

Temperature Transects and NOAA Satellite Data. *Theor. Appl. Climatol.*, 43, 195–203.

Cassetti, E. (1972). The Expansion Method. *Geogr.Anal.*, 4,432-449.

Chan, Andy T. and Yeung, Victor C. H. (2005).Implementing Building Energy Codes In Hong Kong: Energy Savings, Environmental Impacts and Cost. *Energy and Buildings*, 37(6), 631-642.

Charlton, M., Fotheringham, S. and Brunsdon, C. *Geographically Weighted Regression, Version 2.x, User's Manual and Installation Guide*. Available at: http://www.geog.ubc.ca/courses/geog471/labs/The_GWR_Manual.htm

Chandler, T.J. (1967). Night Time Temperatures in Relation to Leicester's Urban Form. *Meteorological Mangzine*, 96,244-250.

Chen, Y., Li, X., Li, J. (2004).*Remote Sensing Analysis of Urban Thermal Environment-Pattern, Process, Simulation and Effect*. Beijing: Science press (in Chinese).

Condeso, T. E. and Meentemeyer, R. K. (2007). Effects of Landscape Heterogeneity on the Emerging Forest Disease Sudden Oak Death. *Journal of Ecology*, 1-12.

Coret, L., Briottet, X., Kerr, Y. H., and Chehbouni, A. (2004). Simulation Study of View Angle Effects on Thermal Infrared Measurements over Heterogeneous Surfaces. *IEEE Transactions on Geoscience and Remote Sensing*, 42 (3), 664-672.

Craig, C.D. and Lowry, W.P. (1972). Reflections on the Urban Albedo. Preprints Conf. on Urban Environment and Second Conf. on Bio-meteorology, Philadelphia, Amer.Meteor.Soc., 159-164

Dash, P., Gottsche, F. M., Olesen, F. S. and Fischer, H. (2002). Land Surface Temperature and Emissivity Estimation from Passive Data: Theory and Practice- Current Trends. *International Journal of Remote Sensing*, 23, 2563-2594.

Desjardins, R., Gray, J. and Bonn, F. (1990). Atmospheric Corrections for Remotely Sensed Thermal Data in a Cool Humid Temperate Zone. *International Journal of Remote Sensing*, 118, 1369-1389.

Easterling, D.R., Horton, B., Jones, P.D., Peterson, T.C., Karl, T.R., Parker, D.E., Salinger, M.J., Razuvayev, V., Plummer, N., Jamason, P., and Folland, C.K.(1997). Maximum and Minimum Temperature Trends for the Globe, *Science*, 277, 364-367.

Eliasson I. (1996). Urban Nocturnal Temperatures, Street Geometry and Land Use. *Atmos. Environ.*, 30, 379-392.

Eliasson, I. (2000). The Use of Climate Knowledge in Urban Planning. *Landscape and Urban Planning*, 48(1-2), 31-44.

Eliasson, I. and Svensson, M.K. (2003). Spatial Air Temperature Variations and Urban Land Use-A Statistical Approach. *Meteorol. Appl.*, 10,135-149.

Emmanuel, R. (1997). *Summertime Heat Island Effects of Urban Design Parameters*. Ph.D. Thesis. The University of Michigan.

ESRI, (2006). *ArcGIS 9.2 Desk Help*. Available at: http://webhelp.esri.com/arcgisdesktop/9.2/index.cfm?TopicName=Points_Solar_Radiation

Forman, R. T. T. and Godron, M. (1986). *Landscape Ecology*. New York: John Wiley and Sons Ltd.

Fotheringham, A.S., Brunsdon, C. and Charlton, M. (1998). Geographically

Weighted Regression: A Natural Evolution of the Expansion Method for Spatial Data Analysis. *Environment and Planning A,* 30: 1905-1927

Fotheringham, A.S., Brunsdon, C. and Chartlon, M. (2002). *Geographically Weighted Regression: the analysis of spatially varying relationships*. England: John Wiley & Sons Ltd.

Franca, G. B. and Cracknell, A.P. (1994). Retrival of Land and Sea Surface Temperature Using NOAA-11 AVHRR Data in North-Eastern Brazil. *International Journal of Remote Sensing*, 15, 1695-1712.

Francois, C. and Ottle, C. (1996). Atmospheric Corrections in the Thermal Infrared: Global and Water Vapor Dependent Split-Window Algorithm: Applications to ATSR and AVHRR Data. *IEEE Transactions on Geoscience and Remote Sensing*, 34,457-469.

Frohn, R. C. (1998).*Remote Sensing for Landscape Ecology – New Metric Indicators for Monitoring, Modeling, and Assessment of Ecosystems*, Department of Geography, University of Cincinnati, Cincinnati, Ohio, pp. 99.

Foukal, P. et al. (2006). Variations in Solar Luminosity and Their Effect on the Earth's Climate. *Nature*, 443,161.

Fu, P. and Rich, P.M., HEMI (2000). *The Solar Analyst, User Manual*. USA.

Gallo, K.P., McNab, A.L., Karl, T.R., Brown, J.F., Hood, J.J. and Tarpley, J.D. (1993a).The Use of a Vegetation Index for Assessment of the Urban Heat Island Effect. *Int. J. Remote Sens.*, 14, 2223–2230.

Gallo, K. P., McNab, A. L., Karl, T. R., Brown, J. F., Hood, J. J. and Tarpley, J. D.(1993b). The Use of NOAA AVHRR Data for Assessment of the Urban Heat Island Effect. *J. Appl. Meteorol.*, 32, 899–908.

Gallo, K. P., Tarpley, J. D., McNab, A. L. and Karl, T. R. (1995).Assessment of Urban Heat Islands: A Satellite Perspective. *Atmospheric Research*, 37(1-3), 37-43.

Geoghegan, J., Pritchard, L., Orgneva-Himmelberger, Y., Chowdhury, R. R., Sanderson, S., and Turner, B. L. II. (1998). "Socializing the Pixel" and "Pixelizing the Social" in Land-Use and Land-Cover Change. In D. Liverman, E. F. Moran, R. R. Rindfuss, and P. C. Stern (Eds.) *People and Pixels-linking Remote Sensing and Social Science*, (pp:51-69). Washing D. C.: National Academy Press.

George, L.A. and Becker, W. G. (2003). Investigating the Urban Heat Island Effect with a Collaborative Inquiry Project. *Journal of Geoscience Education*, 51(2), 237-43.

Gill, S., Handley, J., Ennos, R. and Pauleit, S. (2007). Adapting Cities for Climate Change: The Role of the Green Infrastructure. *Built Environment, Climate Change and Cities*, 33(1), 115-133.

Gillespie, A., Rokugawa, S., Matsunaga, T., Cothern, J., Hook, S. and Kahle, A. (1998). A Temperature and Emissivity Separation Algorithm for Advanced Space-Borne Thermal Emission and Reflection Radiometer (ASTER) Images. *IEEE Transactions on Geoscience and Remote Sensing*, 36, 1113-1126.

Gillespie, A., Rokugawa, S., Hook, S.J., Matsunaga, T., and Kahle, A. (1999). *Temperature/ Emissivity Separation Algorithms Theoretical Basis Document, version 2.4.*

Giridharan, R., Ganesan, S., and Lau, S. S. Y. (2004). Daytime Urban Heat Island Effect in High-Rise and High-Density Residential Development in Hongkong. *Energy and Buildings*, 36: 525-534.

Givoni, B. (1998). *Climate Considerations in Building and Urban Design.* John Wiley and Sons. New York.

Golden, J. (2005). An Academic-Industry-Government Partnership to Mitigate Urban Climate Impacts via Engineering Innovations. *Urban Climatology and Its Applications.* Cambridge.

Goldstein, H. (1987).*Multilevel Models in Educational and Social Research.* Oxford: Oxford University Press.

Goh, K. C. and Chang, C. H. (1999).The Relationship between Height to Width Ratios and the Heat Island Intensity at 22:00 H for Singapore. *International Journal of Climatology*, Volume 19, Issue 9, 1011 – 1023.

Gorr,W.L. and Olligschlaeger, A.M.(1994).Weighted Spatial Adaptive Filtering: Monte Carlo Studies and Application to Illicit Drug Market Modeling.*Geogr.Anal.*,26,67-87.

Goward, S.N. (1981). Thermal Behavior of Urban Landscapes and the Urban Heat Island. *Physical Geography*, 2(1), 19-33.

Graves, H. M. and Phillipson, M.C. (2000). *Potential Implications of Climate Change in the Built Environment.* East Kilbride: BRE, Centre for Environmental Engineering.

Graves, H. M., Watkins, R., Westbury, P. and Littlefair, P. J. (2001). *Cooling Buildings in London.* London: BR 431, CRCLtd,

Griffith, J.A., Martinko, E.A., Price, K.P. (2000). Landscape Structure Analysis of Kansas at Three Scales. *Landscape and Urban Planning*, 52 (1), 45-61.

Gustafson, E.J. (1998). Quantifying Landscape Spatial Pattern: What Is the State of the Art? *Ecosystems*, 1, 143–156.

Hall, G., Huemmrich, K., Goetz, S., Sellers, P., and Nickeson, J. (1992). Satellite Remote Sensing of Surface Energy Balance: Success, Failure and Unresolved Issues in FIFE. *Journal of Geophysical Research*, 97, 19061-19089.

Hardegree, L. C. (2006). *Spatial Characteristics of the Remotely-Sensed Surface Urban Heat Island in Baton Rouge, LA: 1988-2003.* Ph.D Dissertation.

Hargis, C.D., Bissonette, J.A. and David, J.L. (1998). The Behavior of Landscape Metrics Commonly Used In the Study of Habitat Fragmentation. *Landscape Ecology*, 13, 167–186.

Harris, R., Jen, M., Kilham, D., Thomas, E., Brunsdon, C., and Jarvis, C. (2006). Developing Grid Enabled Spatial Regression Models, Published in *the Proceedings of the 2nd International Conference on e-Social Science*, Manchester, 28 - 30 June 2006.

Henry, J.A. and Dicks, S.E. (1987). Association of Urban Temperatures with Land Use and Surface Materials. *Landscape and Urban Planning*, 14, 21-29.

Henry, J.A., Dicks, S.E. and Marotz, G.A. (1985). Urban and Rural Humidity Distributions: Relationships to Surface Materials and Land Use. *Journal of Climatology* ,5,53-62.

Henry, J. A., Dicks, S. E., Wetterqvist, O. F., and Roguski, S. J. (1989). Comparison of Satellite, Ground- Based, And Modeling Techniques for Analyzing the Urban Heat Island. *Photogrammetric Engineering and Remote Sensing*, 55 (1), 69-76.

Herzog, F. and Lausch, A. (2001). Supplementing Land-Use Statistics With Landscape Metrics: Some Methodological Considerations. *Environmental Monitoring and Assessment,* 72(1), 37–50.

Hinkel, K. M., Nelson, F. E., Klene, A. E., Bell, J. H. (2003). The Urban Heat Island in winter at Barrow, Alaska. *International Journal of Climatology*, 23(15), 1889–1905.

Hofierka, J. and Suri, M. (2002). The Solar Radiation Model for Open Source GIS: Implementation and Applications. *Proceedings of the Open Source GIS - GRASS Users Conference,* 2002. pp.1-19.

Holt, J. B. and Lo, C. P. (2008). The Geography of Mortality in the Atlanta Metropolitan Area. *Computers, Environment and Urban Systems*, 32(2), 149-164

Hong Kong Observatory, (2004).Technical Note No.107.

Hook, S., Gabell, A., Green, A., and Kealy, P. (1992). A Comparison of Techniques for Extracting Emissivity Information from Thermal Infrared Data for Geological Studies. *Remote Sensing Environment*, 42, 123-135.

Horner, M. W. (2002). Extensions to the Concept of Excess Commuting. *Environment and Planning,* 34, 543–566.

Huang, Y. (2000). *Regional Economic Development in Yangtze River Delta since 1978: Jiangsu Province as a Particular Case*. PHD thesis,CUHK.

Huang, Y. and Leung, Y. (2002). Analyzing Regional Industrialization in Jiangsu Province Using Geographically Weighted Regression. *Journal of Geographical Systems*, 4, 233-249.

Hui, S. C. M. (2000). Low Energy Building Design in High Density Urban Cities. *World Renewable Energy Congress*, Brighton, United Kingdom.

Hui, S. C. M. (2003). Energy Efficiency and Environmental Assessment for Buildings in Hong Kong. *the MECM LEO Seminar - Advances on Energy*

Efficiency and Sustainability in Buildings, 21-22 January 2003, Kuala Lumpur, Malaysia.

Hsu, S. (1984). Variation of an Urban Heat Island in Phoenix. *Professional Geographer*, 36(2), 196-200.

IPCC, (2007a). Climate change 2007: The Physical Scientific Basis (Summary for Policymakers). *Contribution of Working Group I to the Fourth Assessment Report of the Intergovernmental Panel on Climate Change*, 18pp.

IPCC, (2007b). Climate Change 2007: Mitigation of Climate Change (Summary for Policymakers). *Working Group III Contribution to the Intergovernmental Panel on Climate Change Fourth Assessment Report*, 36pp.

Irfan, N., Zahoor, A., Khan, N. U. (2001).Minimizing the Urban Heat Island Effect through Landscaping. *Journal of Architecture and Planning, Townscapes, 1.*

Isaac, A. M. (2001). Settlement Patterns and Site Planning, In Arvind Krishan, Nick Baker, Simos Yannas, S V Szokolay (Eds.) *Climate Responsive Architecture: A Design Handbook for Energy Efficient Buildings*, New Delhi: Tata McGraw-Hill Publishing Company Limited.

Jenks, M., Burton, E. and Williams, K. (1996).*The Compact City-A Sustainable Urban Form?*. Spon, London.

Jones, K. (1991). Specifying and Estimating Multilevel Models for Geographical Research. *Trans.Inst.Br.Geogr.*, 16,148-159.

Jones, P.Y. Groisman, Coughlan, M., Plummer, N., Wangl, W.C. and Karl, T.R. (1990). Assessment of Urbanization Effects in Time Series of Surface Air Temperatures Over Land. *Nature*, 347(6289), 169-172.

Jusuf, S. K., Wong, N.H., Hagen, E., Anggoro, R. and Hong, Y. (2007).The Influence of Land Use on the Urban Heat Island in Singapore. *Habitat International*, 31(2), 232-242.

Karl, T.R., Diaz, H.F. and Kukla, G. (1988). Urbanization: Its Detection and Effect in the United States Climate Record. *Journal of Climate*, 1, 1099-1123.

Kealy, P. and Hook, S. (1993). Separating Temperature and Emissivity in Thermal Infrared Multispectral Scanner Data: Implication for Recovering Land Surface Temperatures. *IEEE Transactions on Geoscience and Remote Sensing*, 31, 1155-1164.

Kerr, Y.H., Lagouarade, J.P. and Imbernon, J. (1992). Accurate Land Surface Temperature Retrieval from Avhrr Data with Use of an Improved Split Window Algorithm. *Remote Sensing of Environment*, 41, 197-209.

Kidder, S.Q. and Essenwanger, O.M. (1995). The Effect of Clouds and Wind on the Difference in Nocturnal Cooling Rates between Urban and Rural Areas. *Journal of Applied Meteorology* ,34, 2440-2448.

Kidder, S. Q. and Wu, H. T. (1987). A Multispectral Study of the St. Louis Area under Snow-Covered Conditions Using NOAA-7 AVHRR Data. *Remote Sens. Environ.*, 22, 159–172.

Kim, H. H. (1992). Urban Heat Island. *Int. J. Remote Sensing*, 13, 2319–2336.

Kinouchi, T. and Yoshitani, J. (2001). Simulation of Urban Heat Island in Tokyo with Future Possible Increases of Authropogenic Heat, Vegetation Cover and Water Surface. *Proceedings of the 2001 international symposium on environment hydraulics*.

Kukla, G., Gavin, J. and Karl, T.R. (1986).Urban Warming. *J. Climate Appl. Meteorol.*, 25, 1265–1270.

Lam, K. K. and Hui, J. (2001). Highlights and Prospects of Energy Consumption in Hong Kong. *Symposium 2001 on Towards Environmental Sustainability,* HongKong, November, 2001.

Landsberg, H.E. (1970). Man-Made Climatic Changes. *Science*, 170, 1265-1274.

Landsberg, H.E. (1976). *Weather, Climate and Human Settlements*. World Meteorological Organization, Publication 448, Special Environmental Report 7, pp. 45

Landsberg, H.E. (1981). *The Urban Climate*. Academic Press. New York, NY.

Lantsberg, A. Sustainable Urban Energy Planning: A Roadmap for Research and Funding. Available at http:www.energy.ca.gov/2005publications/ CEC-500-2005-102/CEC-500-2005-102.PDF, accessed Dec 5 2007.

Landsberg, H.E. and Maisel, T.N. (1972). Micrometeorological Observations in an Area of Urban Growth. *Boundary Layer Meteorology*, 2, 365-70.

Lee, W. L. and Yik, F. W. H. (2002).Regulatory And Voluntary Approaches for Enhancing Energy Efficiencies of Buildings in Hong Kong. *Applied Energy*, 71(4), 251-274.

Li, H. and Reynolds, J.F. (1995). On Definition and Quantification of Heterogeneity. *Oikos*, 73, 280–284.

Li, H. and Wu, J. (2004). Use and Misuse of Landscape Indices. *Landscape Ecology*, 19, 389–399.

Li, W.J., Putra, Y. Simon, Yang, P.J. Perry (2004). GIS Analysis for the Climatic Evaluation of 3D Urban Geometry: The Development of GIS Analytical Tools for Sky View Factor. *Seventh International Seminar on GIS in Developing Countries (GISDECO 2004).*

Liang, S. (2004). *Quantitative Remote Sensing of Land Surfaces*. First ed. Wiley, New York, NY.

Liang, S. (1997). Retrieval of Land Surface Temperature and Water Vapor Content from AVHRR Thermal Imagery Using an Artificial Neural Network. *Proc. IGARSS*.4, 1959-1961.

Lim, Y. K., Cai, M., Kalnay, E., and Zhou, L. (2005). Observational Evidence of Sensitivity of Surface Climate Changes to Land Types and Urbanization. *Geophys. Res. Lett.*, 32, L22712.

Lo, C. P., Quattrochi, D. A. and Luvall, J. C. (1997).Application of High-Resolution Thermal Infrared Remote Sensing and GIS to Assess the Urban Heat Island Effect. *International Journal of Remote Sensing*, 18(2), 287-304.

Lyon, R.J.P. (1965). Analysis of Rocks by Spectral Infrared Emission (8 to 25 micron). *Econ. Geol.*, 60,715-736.

Malaret, E., Bartolucci, L.A., Lozano, D. F., Anuta, P.E., and McGillen, C.D. (1985). Thematic Mapper Data Quality Analysis. *Photogrammetric Engineering & Remote Sensing*, 51(9), 1407-1416.

Matson, M., McClain, E.P., McGinnis, D.F., Pritchard, Jr. and J.A. (1978). Satellite Detection of Urban Heat Islands. *Mon. Weather Rev.*, 106, 1725–1734.

Matzarakis, A., Mayer, H. and Iziomon, M.(1999). Applications of a Universal Thermal Index: Physiological Equivalent Temperature. *International Journal of Biometeorology*, 43, 76-84.

McGarigal, K., Cushman, S.A., Neel, M.C. and Ene, E. (2002).FRAGSTATS: Spatial Pattern Analysis Program for Categorical Maps. Computer software program produced by the authors at the University of Massachusetts, Amherst. Available at: www.umass.edu/landeco/research/fragstats/fragstats.html.

McGarigal, K. and Marks, B.J. (1995). FRAGSTATS: Spatial Pattern Analysis Program for Quantifying Landscape Structure. *Gen.Tech.Rep. PNW-GTR-351,* US Dep. Agric. For. Serv. Pacific Northwest Research Station, Portland, OR, USA, pp 1-122.

McGarigal, K. and McComb, W.C. (1995). Relationships between Landscape Structure and Breeding Birds in the Oregon Coast Range. *Ecological Monographs*, 65, 235–260.

McGarigal, K. and Marks, B.J. (1994). *Fragstats: Spatial Pattern Analysis Program for Quantifying Landscape Structure (Vesion 2.0).*Corvallis: Forest Science Department, Oregon State University.

Meir, I. A. (2001). Settlement Patterns and Site Planning, In Arvind Krishan, Nick Baker, Simos Yannas, S V Szokolay (Eds.) *Climate Responsive Architecture: A Design Handbook for Energy Efficient Buildings*, New Delhi: Tata McGraw-Hill Publishing Company Limited.

Mennis, J. and Jordan, L. (2005). The Distribution of Environmental Equity: Exploring Spatial Nonstationarity in Multivariate Models of Air Toxic Releases. *Annals of the Association of American Geographers*, 95(2), 249–268.

Mennis, J. (2006). Mapping the Results of Geographically Weighted Regression. *The Cartographic Journal*, 43(2), 171–179.

Milaka, K. and Photis, Y. (2004). Defining a Geographically Weighted Regression Model of Urban Evolution. Application to the City of Volos, Greece. *ERSA Conference,* Available at http://www.ersa.org/ersaconfs/ersa04/PDF/507.pdf

Miller, P. C., Stoner, W. A. and Tieszen, L. L. (1976). A Model of Stand Photosynthesis for the Wet Meadow Tundra at Barrow, Alaska. *Ecology*, Vol.

57, No. 3, 411-430.

Morgan, D., Myrup, L., Rogers, D., and Baskett, R. (1977). Microcliamtes with an Urban Area. *Annals of the Association of American Geographers*, 67(1), 55-65.

Niachou, A., Papakonstantinou, K., Santamouris, M., Tsangrassoulis, A., Mihalakakou, G. (2001). Analysis of the Green Roof Thermal Properties and Investigation of Its Energy Performance. *Energy and Buildings*, 33(7), 719-729.

Nichol, J. E. (1994). A GIS-Based Approach to Microclimate Monitoring in Singapore's High-Rise Housing Estates. *Photogrammetric Engineering & Remote Sensing*, 60 (10), 1225-1232.

Nichol, J. E. (1996). High-Resolution Surface Temperature Patterns Related to Urban Morphology in a Tropical City: A Satellite-Based Study. *J. Appl. Meteorol.* 35(1), 135–146.

Nichol, J.E. (2003). Heat Island Studies in Third World Cities Using GIS and Remote Sensing. In V. Mesev (Ed.), *Remotely Sensed Cities* (pp. 243–264), Taylor and Francis, London.

Nichol, J., Law, K. and Au-Yeung, W. (2002). A Comparison of Daytime and Night-Time Thermal Satellite Images of Hong Kong for Urban Climate Studies. *Proceedings of Map Asia 2002, Asian Conference on GIS, GPS Aerial Photography and Remote Sensing*, 7-9 August, 2002, Bangkok, Thailand, p.85

Nichol, J. and Lee, C.M. (2005). Urban Vegetation Monitoring in Hong Kong Using High Resolution Multispectral Images. *International Journal of Remote Sensing*, 26(5), 903-918.

Nichol, J. and Wong, M. S. (2005). Modeling Urban Environmental Quality in a Tropical City. *Landscape and Urban Planning*, 73(1), 49-58.

Norman, J. M. and Becker, F. (1995). Terminology in Thermal Infrared Remote Sensing of Natural Surfaces. *Agricultral and Forest Meterology*, 77, 153-166.

Nunez, M., Eliasson, I. and Lindgren, J. (2001). Spatial Variations of Longwave Radiation in Göteborg, Sweden. *Theoretical and Applied Climatology*, 67, 181-192.

Nunez, M. and Oke, T.R. (1980). Modeling the Daytime Urban Surface Energy Balance. *Geographical Analysis*, 12(4), 373-386.

Ochi, S., Uchihama, D., Takeuchi, W., and Yasuoka, Y. (2002).Monitoring Urban Heat Environment Using MODIS Data from Main Cities in East Asia. *Proceedings of the Asian Conference on GIS, GPS, Aerial Photography and Remote Sensing*, 07-09 August, Bangkok, Tailand, pp.84.

Oke, T.R. and Fuggle, R.F. (1972). Comparison of Urban/Rural Counter and Net Radiation at Night. *Boundary Layer Meteorology* 2, 290-307.

Oke, T.R. (1973). City Size and the Urban Heat Island. *Atmospheric Environment* 7(8), 769-779.

Oke, T.R. (1976). The Distinction between Canopy and Boundary- Level Heat Islands. *Atmosphere,* 14, 268-277.

Oke, T. R. (1978).*Boundary Layer Climates*, Methuen, London.

Oke, T.R. (1979). *Review of Urban Climatology, 1973-1976.* World Meteorological Organization, Publication 539, Technical Note 169, pp. 100.

Oke, T.R. (1981). Canyon Geometry and the Nocturnal Urban Heat Island: Comparison of Scale Model and Field Observations. *J.Climatol.*. 1, 237-254.

Oke, T.R. (1982). The Energetic Basis of the Urban Heat Island. *Quarterly Journal of Royal Meteorology Society*, 108, 1-24.

Oke, T.R. (1987a). *Boundary Layer Climatology*. London, Methuen, pp. 435

Oke, T.R. (1988a). The Urban Energy Balance. *Progress in Physical Geography* ,12, 471-508.

Oke, T.R. (1988b). Street Design and Urban Canopy Layer Climate. *Energy and Buildings* ,11,103-113.

Oke, T.R., Johnson, G.T., Steyn, D.G., Watson, I.D. (1991).Simulation of Surface Urban Heat Islands under Ideal Conditions at Night. 2. Diagnosis of causation. *Boundary-Layer Meteorol.*, 56, 339-358.

Oke, T.R. (1995). The Heat Island Characteristics of the Urban Boundary Layer: Characteristics, Causes and Effects. In J.E. Cermak, A.G. Davenport, E.J. Plate, and D.X. Viegas (Ed.). *Wind Climate in Cities* (pp. 81–107). Netherlands: Kluwer Academic.

Oke, T.R. (1997a). Urban Climates and Global Change. In Perry, A. and Thompson, R. (eds). *Applied Climatology: Principles and Practices* (pp. 273–287). London: Routledge.

Oke, T.R. (1997b). Urban Environments. In W.G.Bailey, T.R.Oke and W.R.Rouse (eds),*The surface climates of Canada* (pp.303-327), McGill-Queen's University Press, Montreal.

Oke, T.R., Johnson, G.T., Steyn, D.G., and Waston, I.D. (1991).Simulation of Surface Urban Heat Islands Under 'Ideal' Conditions at Night: Part 2: Diagnosis of Causation. *Boundary layer Meterology*, 56, 339-358.

Oke, T.R., Spronken-Smith, A., Jauregui, E., and Grimmond, C.S.B. (1999). The

Energy Balance of Central Mexico City during the Dry Season. *Atmospheric Envirionment,* 33(24-25), 3919-3930.

O'Neill, R.V., Jones, K.B., Riitters, K.H., Wickham, J.D., Goodman, I.A. (1994). *Landscape Monitoring and Assessment Research Plan*, Environmental Protection Agency, U.S. EPA 620/R-94/009, pp. 53.

O'Neill, R. V., Krummel, J. R., Gardner, R. H., Sucihara, G., Jackson, B., DeAngelis, D. L., Milne, B. T., Turner, M. G., Zygmunt, B., Christensen, S. W., Dale, V. H., Graham, R. L. (1988). Indices of Landscape Pattern. *Landscape Ecology,* 1(3), 153 – 162.

Onmura, S., Matsumoto, M. and Hokoi, S. (2001). Study on Evaporative Cooling Effect of Roof Lawn Gardens. *Energy and Buildings,* 33(7), 653-666.

Osmond, P. (2004). Rooftop "Greening" As an Option for Microclimate Amelioration in a High-Density Building Complex. *Fifth Conference on Urban Environment.* Available at http://ams.confex.com/ams/ AFAPURBBIO/techprogram/session_17390.htm

Papadakis, G., Tsamis, P. and Kyritsis, S. (2001). An Experimental Investigation of the Effect of Shading with Plants for Solar Control of Buildings. *Energy and Buildings,* 33(8), 831-836.

Pauleit, S. and Duhme, F. (2000). Assessing the Environmental Performance of Land Cover Types for Urban Planning. *Landscape and Urban Planning,* 52(1), 1-20.

Pauleit, S., Ennos, R. and Golding, Y. (2005). Modeling the Environmental Impacts of Urban Land Use and Land Cover Change - A Study in Merseyside, UK. *Landscape and Urban Planning,* 71(2-4), 295-310.

Pease, R. W., Lewis, J.E., and Outcalt, S.I. (1976). Urban Terrain Climatology and Remote Sensing. *Annals of the Association of American Geographers*, 66(4), 557-569.

Planning Department, HKSAR, (2001). Consultancy Study to Analyze Broad Land Use Pattern of Hong Kong. Available at http://www.pland.gov.hk/p_study/comp_s/lup/index_e.htm.

Roth, M., Oke, T.R., and Emery, W.J. (1989). Satellite-Derived Urban Heat Islands from Three Coastal Cities and the Utilization of Such Data in Urban Climatology. *International Journal of Remote Sensing*, 10, 1699–1720.

Piringer, M., Grimmond, C.S.B., Joffre, S.M., Mestayer, P., Middleton, D.R., Rotach, M.W., Baklanov, A., De Ridder, K., Ferreira, J., Guilloteau, E., Karppinen, A., Martilli, A., Masson, V., Tombrou, M. (2002). Investigating the Surface Energy Balance in Urban Areas – Recent Advances and Future Needs. *Water, Air, & Soil Pollution: Focus*, 2(5-6), 1-16.

Pongracz, R., Bartholy, J. and Dezso Z. (2006). Remotely Sensed Thermal Information Applied to Urban Climate Analysis. *Advances in Space Research*, 37(12), 2191-2196.

Prata, A.J. (1993). Land Surface Temperature Derived from the Advanced Very High Resolution Radiometer and the Along-Track Scanning Radiometer 1, Theory. *J. Geophys. Res.*, 98, 16689-16702.

Prata, A. J., Caselles, V., Coll, C., Sobrino, J.A., and Ottle, C. (1995). Thermal Remote Sensing of Land Surface Temperature from Satellites: Current Status and Future Prospects. *Remote Sensing Review*, 12, 175-224.

Prata, A. J. and Platt, C.M.R. (1991). Land Surface Temperature Measurements from the AVHRR. *Proc. 5th AVRHH User Meet*, 433-438.

Price, J.C. (1979). Assessment of the Urban Heat Island Effect through the Use of Satellite Data. *Mon. Weather Rev.*, 107, 1554–1557.

Price, J.C. (1984). Land Surface Temperature Measurements from the Split Window Channels of the NOAA-7/AVHRR. *Journal of Geophysical Research*, 89, 7231-7237.

Qin, Z., and Karnleli, A. (1999). Progress in Remote Sensing of Land Surface Temperature and Ground Emissivity Using NOAA-AVHRR Data. *International Journal of Remote Sensing*, 20, 2367-2393.

Quattrochi, D. A. and Luvall, J. C. (1999a). *High Spatial Resolution Airborne Multispectral Thermal Infrared Data to Support Analysis and Modeling Tasks in the EOS IDS Project ATLANTA.* Available at: http://wwwghcc.msfc.nasa.gov/atlanta/, Global Hydrology and Climate Center, NASA, Huntsville, Alabama (last date accessed: 26 June 2005).

Quattrochi, D.A and Luvall, J.C. (1999b). Thermal Infrared Remote Sensing for Analysis of Landscape Ecological Processes: Methods and Applications. *Landscape Ecology* 14(6), 577-598.

Quattrochi, D. A. and Luvall, J. C. (2004). *Thermal Remote Sensing in Land Surface Processes*, Publisher Boca Raton,CRC Press.

Quattrochi, D. A. and Ridd, M. K. (1994). Measurement and Analysis of Thermal Energy Responses from Discrete Urban Surfaces Using Remote Sensing Data. *International Journal of Remote Sensing*, 15(10), 1991–2022.

Quattrochi, D.A. and Ridd, M.K. (1998). Analysis of Vegetation within a Semi-Arid Urban Environment Using High Spatial Resolution Airborne Thermal Infrared Remote Sensing Data. *Atmospheric Environment*, 32(1), 19-33.

Outcalt, S.I. (1972). A Reconnaissance Experiment in Mapping and Modeling the Effect of Land Use on Urban Thermal Regimes. *Journal of Applied Meteorology*, 11(8), 1369-1373.

Rao, P.K. (1972). Remote Sensing of Urban Heat Islands from an Environmental Satellite. *Bulletin of American Meteorological Society*, 53, 647-648.

Rayner, J.N. (1984). Simulation Models in Climatology. In G.L.Gaile and C.J.Willmott (Eds.), *Spatial Statistics and Models* (pp.417-442), Dordrecht: D.Reidel Publishing.

Reckie, R. F. (1972). *Design in the Built Environment*. Edward Arnold (Publishers) Limited, London.

Riitters, K. H., O'Neill, R. V., Hunsaker, C. T., Wickham, J. D., Yankee, D. H., Timmins, S. P., Jones, K. B., Jackson, B. L. (1995). A Factor Analysis of Landscape Pattern and Structure Metrics. *Landscape Ecology*, 10(1), 23–39.

Roth, M., Oke, T.R. and Emery, W.J. (1989). Satellite Derived Urban Heat Islands from Three Coastal Cities and the Utilization of Such Data in Urban Climatology. *International Journal of Remote Sensing*, 10(11), 1699-1720.

Samuels, R. Urban Heat Islands. *Report Submit to Sustainable Cities 2025 Inquiry*. Available at http://www.aph.gov.au/house/committee/environ/cities/subs/sub34.pdf

Scafetta, N. and West, B. J. (2006). Phenomenological Solar Contribution to the 1900–2000 Global Surface Warming. *Geophysical Research Letters*, 33 (5), L05708. Retrieved on 2007-05-08.

Seng, S. B., Chong, A. K. and Moore, A. (2005).Geostatistical Modeling, Analysis and Mapping of Epidemiology of Dengue Fever in Johor State, Malaysia. *SIRC 2005 – The 17th Annual Colloquium of the Spatial Information*

Research Centre University of Otago, Dunedin, New Zealand, November 24th-25th 2005.

Sobrino, J. A., Coll, C. and Casselles, V. (1991). Atmospheric Corrections for Land Surface Temperature Using AVHRR Channels 4 and 5. *Remote Sensing of Environment*, 38, 19-34.

Sobrino, J. A., Li, Z., Stoll, M. and Becker, F. (1994). Improvements in the Split Window Technique for Land Surface Temperature Determination. *IEEE Transactions on Geoscience and Remote Sensing*, 32,243-253.

Song, Y. (2003). *Impacts of Urban Growth Management on Urban Form: A Comparative Study of Portland, Oregon, Orange County, Florida and Montgomery County, Maryland.* National Center for Smart Growth Research and Education.

Souza, L. C. L., Rodrigues, D. S., Mendes, J. F. G. (2003). Sky View Factors Estimation Using a 3d-Gis Extension. *Eighth International IBPSA Conference.*

Souza, L. C. L., Pedrotti, F. S. and Leme, F. T. (2004). Urban Geometry and Electrical Energy Consumption in a Tropical City. *Fifth Conference on Urban Environment.* http://ams.confex.com/ams/AFAPURBBIO/techprogram/session_17390.htm

Steemers, K. (2003). Cities, Energy and Comfort: A PLEA 2000 Review. *Energy and Buildings,* 35(1), 1-2.

Stewart, I. D. (2007). Landscape Representation and the Urban-Rural Dichotomy. In *Empirical Urban Heat Island Literature,*1950-2006. Available at http:www.sci.u-szeged.hu/eghajlattan/akta07/111-121.pdf, last accessed Dec.18 2007.

Stone, B. Jr. and Rodgers, M. O. (2001). Urban Form and Thermal Efficiency: How the Design of Cities Influence the Urban Heat Island Effect. *Journal of the American Planning Assosiation, 67 (2)*, 186-198.

Stott, P. A. et al. (2003). Do Models Underestimate the Solar Contribution to Recent Climate Change? *Journal of Climate*, 16 (24), 4079–4093.

Streutker, D. R. (2002). A Remote Sensing Study of the Urban Heat Island of Houston, Texas. *International Journal of Remote Sensing*, 23, 2595–2608.

Streutker, D. R. (2003). Satellite-Measured Growth of the Urban Heat Island of Houston, Texas. *Remote Sens. Environ.*, 85, 282–289.

Sturman, A.P. (1998). Applied Climatology. *Progress in Physical Geography*, 22(4), 1, 558-565.

Su, B. S., Chong, A. K., Moore, A. (2005). Geostatistical Modeling, Analysis and Mapping of Epidemiology of Dengue Fever in Johor State, Malaysia. Paper Presented at SIRC 2005 – The 17th Annual Colloquium of the Spatial Information Research Centre, University of Otago, Dunedin, New Zealand, November 24th-25th 2005.

Svensson, M. K. (2004). Sky View Factor Analysis – Implications for Urban Air Temperature Differences. *Meteorol. Appl.*, 11, 201–211.

Svensson, M.K. and Eliasson, I. (2002). Diurnal Air Temperatures in Built-Up Areas in Relation to Urban Planning. *Landscape and Urban Planning*, 61(1), 37-54.

Tang, J.M. (2007).*The Analysis of Spatial-Temporal Dynamics of Urban Landscape Structure: A Comparison of Two Petroleum-Oriented Cities*. Ph.D Dissertation.

Takeuchi, W., Worakanchana, K.,Yasuoka, Y. and Phonekeo, V. (2007). Comparative Analysis and Monitoring of Urban Heat Island Intensity in Asian Mega Cities by MODIS. *6th International Symposium on new technologies for urban safety of mega cities in Asia (USMCA)*, Dhaka, Bangladesh, Dec. 10.2007.

Terjung, W.H. and Louie, S.S.F. (1973). Solar Radiation and Urban Heat Islands. *Annals of the Association of American Geographers*, 66(2), 181-207.

Terjung, W.H. (1974). A Climate Model of Urban Energy Budgets. *Geographical Analysis*, 6(4), 341-367.

Terjung, W.H. (1976). Climatology of Geographers. *Annals of the Association of American Goegraphers*, 66(2), 199-222.

Terjung, W.H. and O'Rourke, P.A. (1980). Simulating the Causal Elements of Urban Heat Islands. *Boundary-layer Meteorology*, 19(1), 93-118.

Tobler, W.R. (1970). A Computer Movie Simulating Urban Growth in the Detroit Region. *Economic Geography* ,46(2), 234-240.

Toutin, T. (2004).Geometric Processing of Remote Sensing Images: Models, Algorithms and Methods. *International Journal of Remote Sensing*, 25 (10), 1893-1924.

Tuller, S.E. (1975). The Energy Budget of Man: Variations with Aspect in a Downtown Urban Environment. *International Journal of Biometeorology*, 19(1), 2-13.

Turner, M. G. (1987). Spatial Simulation of Landscape Changes in Georgia: A Comparison of 3 Transition Models. *Landscape Ecology 1*, 1, 29-36.

Turner, M G and Gardner, R. H. E. (1991). *Quantitative Methods in Landscape*

Ecology (pp. 536). Springer, New York.

Ulivieri C., Castronuovo, M. M., Francioni, R. and Cardillo, A. (1994). A Split Window Algorithm for Estimating Land Surface Temperature from Satellites. *Advances in Space Research*, 14, 59-65.

Upmanis, H., Eliasson, I. and Lindqvist, S. (1998). The Influence of Green Areas on Nocturnal Temperatures in a High Latitude City (Goteborg, Sweden). *International Journal of Climatology*, 18, 681-700.

Voogt, J.A. (EPA presentation). How Researchers Measure Urban Heat Islands. From http://www.epa.gov/heatisland/resources/pdf/EPA_How_to_measure_a_UHI.pdf

Voogt, J. A. (2002). Urban Heat Island. *Encyclopedia of Global Environment Change: Volume 3, Causes and Consequences of Global Environmental Change* (pp.660-666). John Wiley & Sons, Ltd, Chichester.

Voogt, J.A. (2004). Urban Heat Islands: Hotter Cities. Available at: http://www.actionbioscience.org/environment/voogt.html.

Voogt, J.A. and Oke, T. R. (1997). Complete Urban Surface Temperatures. *Journal of Applied Meteorology*, 36, 1117-1132.

Voogt, J. A. and Oke, T. R. (2003). Thermal Remote Sensing of Urban Climates. *Remote Sensing of Environment*, 86 (3), 370-384.

Wagner, H.H. and Fortin, M. (2005). Spatial Analysis of Landscapes: Concepts and Statistics. Special Feature. *Ecology*, 86, 1975–1987.

Wan, Z. and Dozier, J. (1996). A Generalized Split-Window Algorithm for Retrieving Land Surface Temperature Measurement from Space. *IEEE Transactions on Geoscience and Remote Sensing*, 34, 892-905.

Wan, Z. and Li, Z.L. (1997). A Physics-Based Algorithm for Retrieving Land Surface Emissivity and Temperatures from EOS/MODIS Data. *IEEE Transactions on Geoscience and Remote Sensing*, 35, 980-996.

Weng, Q. (2001). A Remote Sensing- GIS Evaluation of Urban Expansion and Its Impact on Surface Temperature in the Zhujiang Delta, China. *International Journal of Remote Sensing* 22(10), 1999-2014.

Weng. Q. (2003). Fractal Analysis of Satellite-Detected Urban Heat Island Effect. *Photogramm. Eng. Remote Sensing,* 69, 555–566.

Weng, Q., Lu, D. and Schubring, J. (2004). Estimation of Land Surface Temperature-Vegetation Abundance Relationship for Urban Heat Island Studies. *Remote Sens. Environ.*, 89(4), 467–483.

Weng, Q. and Quattrochi, D. A. (2006). Thermal Remote Sensing of Urban Areas: An Introduction to the Special Issue. *Remote Sensing of Environment*, 104, 119–122.

Weng, Q. and Yang, S. (2004). Managing the Adverse Thermal Effects of Urban Development in a Densely Populated Chinese City. *Journal of Environmental Management,* 70(2), 145-156.

Weng, Q. and Yang, S. (2006).Urban Air Pollution Patterns, Land Use, and Thermal Landscape: An Examination of the Linkage Using GIS. *Environmental Monitoring and Assessment*, 117, 463–489.

Whitford, V., Ennos, A.R. and Handley, J.F. (2001). "City Form and Natural Process" - Indicators for the Ecological Performance of Urban Areas and Their Application to Merseyside, UK. *Landscape and Urban Planning,* 57(2), 91-103.

Yee, F. W. (2004). Provision of Service for Characterizing the Climate Change

Impact in Hong Kong. *Final report submitted to the HKSAR – Environmental Protection Department, Tender AM02 – 316.*

Yu, D. Geographically Weighted Regression. Available at http://pages.csam.montclair.edu/~yu/GISDay_GWR.ppt

Yue, T. X., Haber, W., Herzog, F., Cheng, T., Zhang, H. Q. and Wu, Q. H. (1998). Models for Dlustrategy and Their Applications. *Elológia (Bratislava),* 17, Suppl. 1, 118–128.